Cancer-immune system interplay in the tumor microenvironment

Stefania Di Blasio

The research presented in this thesis was performed at the Department of Tumor Immunology, Radboud Institute for Molecular Life Sciences, Nijmegen, in collaboration with the Department of Dermatology of the Radboud university medical center, Nijmegen, The Netherlands. Printing of this thesis was financed by the Radboud university medical center, Nijmegen, The Netherlands.

ISBN: 978-94-6182-774-6

Cover design: Theodora Kotsi-Felici and Stefania Di Blasio
Layout and Printing: Off Page, Amsterdam

Cancer-immune system interplay in the tumor microenvironment

Proefschrift

ter verkrijging van de graad van doctor

aan de Radboud Universiteit Nijmegen

op gezag van de rector magnificus prof. dr. J.H.J.M. van Krieken,

volgens besluit van het college van decanen

in het openbaar te verdedigen op dinsdag 18 april 2017

om 14.30 uur precies

door

Stefania Di Blasio

Geboren op 8 november 1985

te Pesaro, Italië

Promotoren

Prof. dr. C.G. Figdor

Prof. dr. I.J.M. de Vries

Copromotoren

Dr. S.V. Hato

Dr. E.H. van den Bogaard

Manuscriptcommissie

Prof. dr. A. Cambi

Prof. dr. J.A. Jansen

Dr. T.K. van den Berg (Sanquin, Amsterdam)

Cancer-immune system interplay in the tumor microenvironment

Doctoral Thesis

to obtain the degree of doctor

from Radboud University Nijmegen

on the authority of the Rector Magnificus prof. dr. J.H.J.M. van Krieken,

according to the decision of the Council of Deans

to be defended in public on Tuesday, April 18, 2017

at 14.30 hours

by

Stefania Di Blasio

born on November 8, 1985

in Pesaro, Italy

Supervisors

Prof. dr. C.G. Figdor

Prof. dr. I.J.M. de Vries

Co-supervisors

Dr. S.V. Hato

Dr. E.H. van den Bogaard

Doctoral Thesis Committee

Prof. dr. A. Cambi

Prof. dr. J.A. Jansen

Dr. T.K. van den Berg (Sanquin, Amsterdam)

"Starting a new journey may scare us.
But with each new step, we realize
how dangerous it would have been to stand still"

"Iniziare un nuovo cammino spaventa.
Ma dopo ogni passo che percorriamo
ci rendiamo conto di come era pericoloso rimanere fermi"

Roberto Benigni

Preface

The goal of the immune system is to protect the body from invaders, such as cancer cells. In an ideal situation, tumors would constitute a target for the activated patient host immune response. However, by engaging in dynamic interactions with the healthy host cells and multiple components of the local tumor microenvironment (TME), cancer cells can eventually escape this detection.

Dendritic cells (DCs) are central in controlling effective induction of anti-tumor immunity. Success of this stimulation hinges upon the activation status of DCs. Defective or impaired DC activation facilitates tolerance towards cancer cells, while fully functional DCs strongly promote cytotoxic T cell activation. Growing knowledge on the immunosuppressive mechanisms that accompany tumor progression indicates that the TME is the main artificer of the defective activation of DCs. In this line, the first objective of this thesis was to broaden our knowledge on the impact of tumor-driven immunosuppression on human DCs; and to study two distinct anti-cancer strategies that have the potential to restore DC activation.

Because of the lack of physiological complexity of two-dimensional (2D) cell monolayers, the second part of this thesis aims at exploring novel techniques that will contribute to our understanding of the complexity of in vivo tissues. In particular, I exploited the power of three-dimensional (3D) human skin melanoma models, to mimic the cell biological context and the heterotypic crosstalk of the TME, while having the benefit of the controlled lab environment that supports cell function. Moreover, I applied an innovative imaging technique, to accurately assess immune cell infiltrates in human primary melanomas.

Contents

CHAPTER 1

General introduction and scope of this thesis

Partially published in modified form in:

Clinical Implications of Co-Inhibitory Molecule Expression in the Tumor Microenvironment for DC Vaccination: A Game of Stop and Go.
*Angela Vasaturo #, **Stefania Di Blasio** #, Deborah G. Peeters, Coco C. de Koning, I. Jolanda M. de Vries, Carl G. Figdor, Stanleyson V. Hato.*
Front Immunol. 2013 Dec 3;4:417. doi: 10.3389/fimmu.2013.00417. Review.

Tumor-dendritic cell interplay in cancer: immunogenic DAMPs and their receptors
***Stefania Di Blasio**, Dorian A. Stolk, Nienke de Haas, Carl G. Figdor, Stanleyson V. Hato.*
Submitted. Review.

 # equal contribution

Dendritic cells: key players in anti-cancer response

The goal of the immune system is to protect the body from invaders: external invaders, such as pathogens or viruses, but also internal invaders, such as cancer cells. The immune system can be distributed across two basic components: the innate and the adaptive immune system. Dendritic cells (DCs) are the most potent antigen presenting cells (APCs) and provide a functional link between innate and adaptive immune responses [1,2]. This requires a number of discrete steps. Firstly, in their immature state, DCs must take up take up and process tumor proteins into antigens (Ags), which can be encountered *in situ* or delivered to the DCs *ex vivo* as part of a therapeutic vaccine [3]. This has to be coupled to an activation or maturation signal to the DC. Next, these matured, tumor-antigen presenting DCs migrate towards the lymphoid organs, where they induce antigen-specific T cell responses that target the tumor (Figure 1) [4,5].

Priming of naïve T cells into antigen-specific effector T cells by DCs requires four signals: (I) engagement of a T cell receptor (TCR) with a peptide-major-histocompatibility complex (MHC) on the DC, and (II) the right balance between expression of co-stimulatory molecules on the DC surface (such as CD40, CD80 and CD86) that activate T cell proliferation; and co-inhibitory molecules that attenuate T cell activation. Co-inhibitory molecules are expressed both on T cells, such as the receptors programmed cell death-1 (PD-1) and the cytotoxic T lymphocyte-associated antigen-4 (CTLA-4), and on DCs, such as the ligands PD-ligand 1 (PD-L1) and PD-ligand 2 (PD-L2) [4,6-12]. (III) A third signal is provided by cytokines secreted by the DCs, which regulate the differentiation of naïve T cells into different subsets of effector T cells, in particular $CD4^+$ T helper cells. This process results in the differentiation towards a Th1, Th2, Th9, Th17 or regulatory T cell (Treg) phenotype [13]. Lastly (IV), environmental cues from the DCs, such as DC-processed metabolites, provide T cells with a signal to home and migrate to certain tissues [14]. Efficient anti-tumor responses are believed to require $CD8^+$ cytotoxic (killer) T cells but recent data indicate that induction of $CD4^+$ T helper cells also aid in clinical efficacy [15]. Conversely, DCs may also trigger antibody- and natural killer (NK) cell responses, which may also contribute to anti-tumor immunity [16,17].

Dendritic cell subsets

DCs encompass very heterogeneous cell populations [18-20]. This level of heterogeneity relates to their origin, anatomical localization, phenotype and function. There are two major types of DCs in humans and mice: lymphoid-derived or plasmacytoid DCs ($CD11c^-$, pDCs) and myeloid-derived DCs ($CD11c^+$, mDCs) [11,21,22]. In steady state, pDCs reside in the blood and in lymphoid organs (bone marrow, spleen,

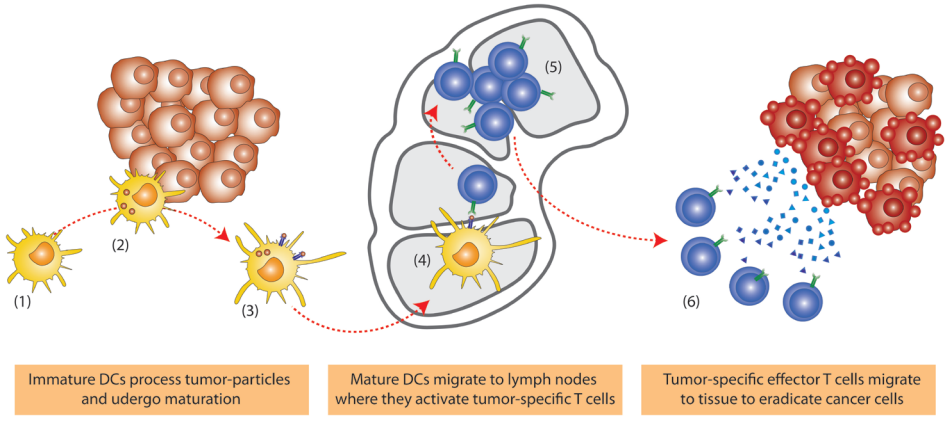

Figure 1. Dendritic cells have the potential to stimulate anti-tumor immunity. (1) Tissue-resident immature dendritic cells (DCs) patrol the environment for signs of danger, such as tumor cells. (2) DCs engulf tumor-derived particles and process them into antigens (ags) for presentation on MHC molecules (3). Following ag-processing, (4) DCs undergo maturation and migrate towards the lymph node, where they induce the activation of tumor-specific T lymphocytes. (5) Activated effector T cells disseminate and home to pheripheral tissue to kill cancer cells and eradicate the tumor.

lymph nodes). In response to inflammation and release of 'danger' signals, pDCs accumulate in peripheral tissues at the site of damage. pDCs are central in anti-viral immunity, as they produce high amounts of type I interferons in response to viral infection [21,23]. The other class of DCs, mDCs, comprises several DC subsets. In human skin, the epidermis contains Langerhans cells (LCs), whereas the dermis hosts $CD1a^+$ DCs and $CD14^+$ DCs. In humans, $CD16^+$ DCs, $CD1c^+$ (BDCA1) DCs and $CD141^+$ (BDCA3) DCs are found circulating in the blood. Human $CD1c^+$ DCs and $CD141^+$ DCs share homology with mouse $CD11c^+$ DCs, expressing either CD11b or CD8/CD103, respectively [11,22,24,25].

Tumors engineer an immunosuppressive microenvironment that hampers their eradication by the immune system

In an ideal situation, cancer cells would constitute a target for the activated patient host immune response. Recent studies indicate that early tumors can be eliminated or contained by the immune system; however, by a process involving immunoediting, tumor cells can eventually escape this detection [26]. They do so by:

1. hiding from immune surveillance (upregulation of CD47 and downregulation of MHC molecules)

2. inhibiting immune cell function and inducing tolerance to the tumor (immunosuppressive cytokines secretion; expression of inhibitory molecules, such as PD-L1)
3. recruiting suppressive immune cells that hamper T cell function (including Tregs)
4. producing tumor growth enhancing factors (such as vascular endothelial growth factor, VEGF)
5. modulating the activity of ECM-modifying enzymes that facilitate tumor dissemination (matrix metalloproteases, MMPs) [27-31].

These acquired functional capabilities allow cancer cells to survive, proliferate and metastasize [27-31]. With this intricate picture in mind, researchers have started to describe tumors as "aberrant" organs, whose complexity is comparable to that of normal healthy tissues. Thus, in order to unravel the biology of cancer, researches need to comprehend the primary role of the tumor microenvironment (TME). The TME is the dynamic milieu of cellular and acellular components that comprise the tumor exists. The TME consists of tumor cells, recruited normal cells (such as fibroblasts, endothelial cells and infiltrating immune cells) embedded in an extracellular matrix (ECM) that provides functional and structural support for tumor growth (Figure 2).

Evidence shows that infiltrating immune cells can be either beneficial or detrimental to patients, depending on their nature. Indeed, immune infiltrates are heterogeneous and vary between tumor types and from patient to patient. Different immune cell types can be found infiltrating a tumor, including macrophages, DCs, distinct T lymphocytes subsets, B cells and NK cells.

The presence of tumor infiltrating lymphocytes (TILs) has been associated with improved survival of patients with prostate, breast, colorectal, ovarian cancer or melanoma [32-36]. This can be attributed to the secretion of chemokines, by tumor cells and other infiltrating immune cells in the TME, which attract relevant immune cells into the tumor. Chemokines, such as CX3CL1 (also known as fractalkine), CCL5, CXCL9 and CXCL10 are associated with infiltration of memory T cells and effector T cells into the tumor, as well as prolonged disease-free survival and overall survival. By contrast, recruitment of immunosuppressive immune cell types, such as Tregs, myeloid-derived suppressor cells (MDSCs) and tumor-associated macrophages (TAMs), hampers anti-tumor immunity and is associated with decreased survival of cancer patients [37-39]. These cells produce cytokines with anti-inflammatory activities, such as IL-10 and TGFβ, which inhibit the function of effector immune cells and pro-angiogenic effects, including VEGF, to promote metastatic dissemination.

Because of the complexity of the TME, understanding the heterotypic interactions that occur at the tumor site is of utmost importance. These interactions are in fact key regulators of tumorigenesis and escape of immune surveillance, which are in

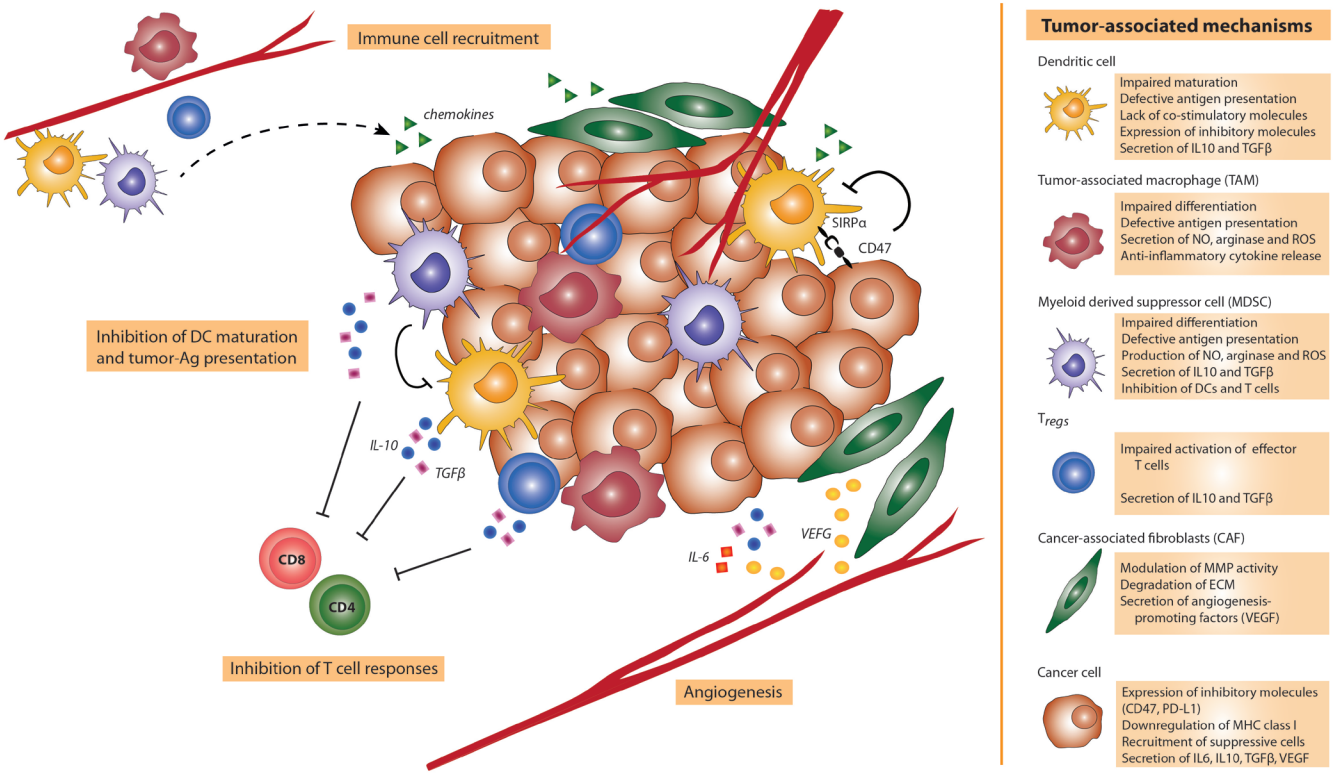

Figure 2. Tumors engineer an immunosuppressive microenvironment that hampers their eradication by the immune system. Established cancers consist of a wide range of immune cells that contribute to the tumor stroma of a growing malignancy. In addition to malignant cells, tumors consist of infiltrating cells, including dendritic cells (DCs), tumor-associated macrophages (TAMs), myeloid derived suppressor cells (MDSCs), regulatory T cells (Tregs) and cancer associated fibroblasts (CAFs). These cells co-ordinately form a complex regulatory network that fosters tumor growth by creating an environment that enables cancers to evade immune surveillance and destruction.

turn an essential requirement for tumor progression. Amongst a variety of tumor-mediated inhibitory mechanisms, signalling through the surface protein CD47 has recently received considerable attention. Part of this thesis aims at investigating the effects of CD47 expression on tumor cells and its ability to interfere with DC function, as a strategy for immunosurveillance escape.

Inhibitory signalling through CD47: a "don't eat me" alert for immunoevasion

CD47 (also known as integrin associated protein, IAP) is a 50kDa cell surface protein belonging to the immunoglobulin (Ig) superfamily. It comprises a glycosylated N-terminal domain, a pentaspanin transmembrane domain and a cytoplasmic tail. CD47 was first identified on erythrocytes as an important regulator of homeostasis. Newly developed erythrocytes that enter blood circulation express high levels of CD47 on the cell membrane. This prevents these young healthy red blood cells (RBCs) from being cleared from the bloodstream by phagocytes. As they age, erythrocytes lose CD47 expression, which facilitates RBCs turnover, as cells lacking CD47 are rapidly engulfed by macrophages and DCs[40,41].

Inhibition of phagocytosis is mediated by CD47-engagement to signal regulatory protein alpha (SIRPα) receptor on the surface of professional and non-professional phagocytes [42-44]. SIRPα (also known as SHPS-1 and CD172a) belongs to the Ig family of cell surface glycoproteins and is highly expressed on myeloid DCs, macrophages, fibroblasts, endothelial cells and neurons. In steady state, the binding of CD47 to SIRPα, is an important mechanism for maintenance of homeostasis. Hence, by preventing clearance of healthy normal cells by phagocytes, CD47/SIRPα interaction contributes to keeping DC activation under control [42,45,46]. Lack of CD47 expression in murine RBCs ($CD47^{-/-}$ RBCs), or SIRPα blockade with monoclonal antibodies, were sufficient to make RBCs a target for engulfment by DCs. This subsequently stimulated DC maturation and activated an adaptive immune response [41]. Surprisingly, mice lacking CD47 or its receptor, SIRPα, were protected from autoimmune diseases. This seemed to be explained by the fact that absence of signalling through SIRPα causes chronic activation of DCs, which eventually culminates in their exhaustion and clearance from the body [42,47].

Despite initial evidence as a removal marker of aged RBCs, CD47 exerts this distinct "don't eat me" function on virtually all cells in the body. Particularly, malignant cells from solid and hematopoietic tumors express higher levels of CD47 than their normal counterparts [48]. Additionally, increased CD47 expression on tumor lesions appears to be an independent, poor prognostic predictor for survival and tumor refractoriness in distinct haematological or solid malignancies [48-51]. In accordance with this notion, subcutaneous injection of malignant cells, expressing high levels

of CD47, resulted in tumor growth and metastasis formation; whereas absence of CD47 dramatically reduced tumor volume and risk of dissemination [48,52]. Researchers have therefore hypothesized that the "don't eat me" CD47/SIRPα interaction is a common strategy that enables cancer cells to elude immune recognition, through evasion of phagocytosis (Figure 3). This hypothesis was confirmed by the finding

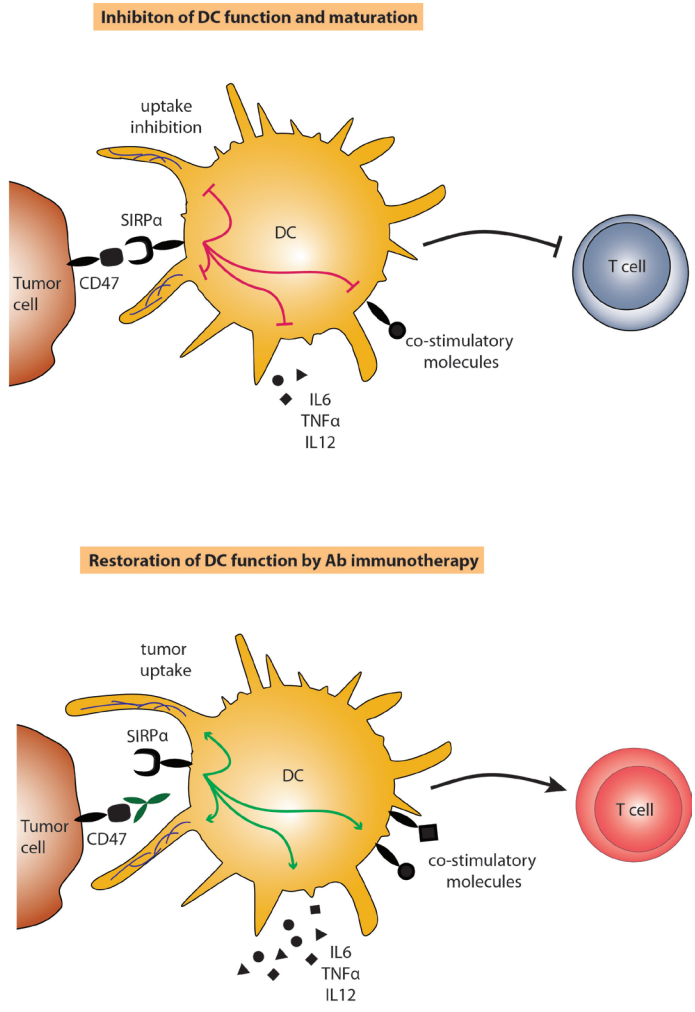

Figure 3. "Don't eat me" signal CD47 contributes to immunosuppression. Upregulation of the "don't eat me" signal CD47 on tumor cells inhibits dendritic cell (DC) function. In particular, by engaging its receptor on DCs, SIRPα, CD47 blocks tumor-cell engulfment by DCs. This hampers DC maturation and impedes the activation of effector anti-tumor specific T cells *(top)*. Blockade of CD47/SIRPα pathway, using monoclonal antibodies targeting either CD47 or SIRPα, restores tumor uptake by DCs, DC maturation and stimulation of T cells for tumor eradication.

that targeting of CD47 by monoclonal antibodies abrogated tumor cell uptake by macrophages [43,49,53]. Similarly, blockade of SIRPα on macrophages increased phagocytosis of CD47^{high} leukemia cells to a level comparable to that of CD47-lacking cells[52].

Altogether, these observations suggest that the inhibitory CD47/SIRPα axis may play a critical role in supporting cancer progression. Thus, interfering with this interaction may prove to be a powerful tool in the treatment of various tumors.

The three dimensions of cancer

In the previous sections, we discussed the complex nature of cancer. Within the TME, malignant cells are in continuous dynamic interactions with the healthy host tissue cells and the ECM. These tight connections are meticulously coordinated by intrinsic signalling crosstalk between cancer cells, as well as extrinsic interactions with other cell types and multiple components of the TME. Tumor niches have been increasingly recognized as influencing cancer cell resistance to therapies. Nevertheless, our knowledge on the intricate network of mechanisms of the TME is still scarce. Unravelling this interplay is essential for understanding, and eventually reversing, tumor-mediated immunosuppression, thus realizing the goal of targeted cancer treatments.

Life isn't flat: the need for complexity in cancer research

Over the past decades, a vast array of cancer model systems has been devised to study the TME, each presenting unique strengths and flaws. These models range from two-dimensional cell monolayers (2D) to animal models.

Culture of human primary cells and immortalized tumor cell lines in 2D have greatly contributed to our knowledge about cancer, are easy to expand and require limited handling. Nevertheless, 2D models lack tissue specific architecture, mechanical and biochemical cues, as well as cell-cell and cell-matrix communications, as found in *in vivo* tissues (Table 1). This may trigger false findings by forcing cells to adapt to an artificial, flat and rigid surface and lead to biased conclusions [54].

On the other side of the coin, animal models seem an advantageous system in which to mimic disease complexity. However, there are many ethical considerations related to animal testing and they sometimes fail to reflect human biology [55,56]. Many forms of cancer lack a validated animal model, including skin cancer, such as melanoma [57,58]. The most striking issue related to animal use in the development of anti-tumor therapies relates to the fact that such animal models only poorly predict human immune response. Indeed, anticancer drugs, entering preclinical phases for investigating mode of action and risk assessment, often fail to reach clinical trials [59].

Table 1. Advantages and limitations of culture models 'at a glance'

Culture model	Advantages	Limitations
2D	• Accessibility of human immortalized cell lines and primary cells of different origins • Easy to expand, require limited handling • Possibility of co-culturing two different cell types	• Lack of specific tissue architecture • Absence of mechanical and biochemical cues, as well as cell-cell and cell-matrix interactions • Lack of physiological relevance of cell culture supports (i.e. plastic flasks or glass supports)
3D	• Providing dimensional and architectural complexity that is highly similar to that of the *in vivo* tissue • Platforms for co-culture of three (or more) different cell types • Possibility to titrate cell number and ratio • Supplying sites for studying cell-cell/cell-matrix interactions and effects of the stromal environment • Time and cost effective alternatives to the use of lab animals (also related to ethical issues)	• "Technical hurdles" Defined culture period: a maximum of a few weeks (as compared to *in vivo* studies). Difficult handling of constructs. Limited supply of human biopsies to isolate cellular and matrix tissue components • Lack of blood flow and, in general, immune compartment

Together, these limitations strongly indicate the necessity for improved models for cancer research. These models should, on the one hand, be in line with the 3Rs guidelines (reduction, refinement and replacement of animals in experiments); and, on the other hand, offer the complexity of real human tissues [60,61].

Three-dimensional (3D) human tissue culture models

The potential power of a human culture system that faithfully mimics the *in vivo* situation, while having the benefit of the controlled lab environment that supports cell function, has inspired researchers to develop three-dimensional (3D) human tissue culture models (also referred to as engineered tissue models, tissue equivalents or organotypic models).

One of the main advantages of 3D cultures is the possibility to study cells in their "original" environment (Table 1). The ECM that embeds cells under natural conditions stabilizes the structure of the tissue, but it also represents a framework for cells, allowing cellular communication, growth and propagation into all three dimensions. Therefore, culture of cells on 2D culture dishes or in 3D matrices directly affects cellular development, migration profile, shape and function. Growth of ovarian epithelial cells in 3D induces histological morphology that is reminiscent of the tumor type from which they are derived. These characteristics are lost when the same cells are cultured in 2D [62]. Additionally, cells cultured in 3D display distinct gene expression profiles when compared to the exact same cells grown

in monolayers [63,64]. Specific cell-cell, cell-ECM interactions and biological factor (oxygen/nutrients/waste) gradients drive changes in intracellular signal transduction. These changes eventually reflect diversities in phenotype, proliferation rates, cell migration and metabolic functions [54,65,66]. In turn, genetic and functional changes occurring within a cell can cause an intercellular feedback to the other cells present in the microenvironment. So far, the mechanisms regulating these feedback loops have been mostly investigated in 2D co-culture systems, with obvious limitations to their applicability [67]. A notable benefit offered by the advent of 3D culture technology is the possibility to create a multi-cellular environment, with potentially no restraints in the amount and type of cells used.

Besides those advantages, 3D culture systems also present some limitations. Handling of such models requires advanced technical skills, and long-term optimization is compulsory for developing tissue equivalents that closely mimic *in vivo* microenvironment. Just as importantly, some technical hurdles have to be overtaken, like human leukocyte antigen (HLA) matching and the lack of a blood and lymphatic systems. HLA matching is especially important when studying the activation of T lymphocytes by antigen-presenting cells, expressing MHC molecules for (tumor) antigen-presentation. In order to overcome the lack of circulation, attempts have been made to engineer collagen matrices containing a microvasculature network of endothelial cells [68]. Additionally, 3D models that are built using matrix components and primary cells isolated from tissue, are reliant on a regular supply of fresh human biopsies (obtained as surgical waste material) of adequate size. This obviously limits the applicability of 3D engineered tissue cultures as high-throughput platforms for drug testing.

Despite those restrictions, such models represent a unique tool for prolonged dynamic investigation of "living" tissues and cell interactions. Currently, the use of 3D models is being explored in many fields for *in vitro* assessment of disease biology, ranging from dermatological research to infectious diseases and cancer [69-74]. Among those, human tissue equivalents of skin have received great attention. The skin is the largest organ in the body and the first line of defense against pathogens. Therefore, development of 3D models of human skin may bring remarkable progresses in treatment of skin disorders, including the most aggressive form of skin cancer, melanoma. State-of-the-art of skin- and melanoma-engineered models is summarized in the following paragraph.

State-of-the-art of human 3D engineered tissue models of skin biology and cancer

Over the past thirty years, protocols for generating 3D human skin equivalents have been refined and optimized, paving the way for advances in the investigation of skin

biology, disease pathology and therapeutics [75-77,93,99] .These 3D human skin models resemble the basic architecture of real skin. They consist of a dermal compartment, providing structural support to the reconstructed skin, and an epidermal compartment, containing epidermal cells (keratinocytes) and other skin-associated cells, such as melanocytes or their malignant counterpart (melanoma cells) (Table 2).

Table 2. An overview of 3D models of human skin, pre-malignant skin and melanoma

	Dermal compartment	Cellular components	Limitations of the model	Ref.
Models of human skin	Rat-tail or bovine collagen type I	KCs Fibroblasts	Animal-derived collagen matrix.	[86,143-145]
		Mo-LCs[143] Mo-DDCs[143] (immune cells co-seeded with KCs)	Fibroblasts deposit collagen IV (BM components), however it is not uniform. Refs. [86,145]: no immune cells.	
		RAW264.7 murine macrophages[144] (in a co-culture transwell system)	Ref [139]: murine-human co culture.	
	Superimposed fibroblast-derived sheets	KCs Fibroblasts	Fibroblast-deposition of collagen requires 35 days of culture. No immune cells.	[146]
	Artificial scaffold embedded in agarose-fibronectin gel	KCs Fibroblasts Mo-DCs	Artificial scaffold, not representative of real tissue.	[147]
	DED	KCs Fibroblasts[86]	Ref [86]: No immune cells.	[86,87]
		CD4+ T lymphocytes[87]	Ref [87]: No stromal compartment.	
Models of skin with melanocytes	Rat-tail or bovine collagen type I	KCs Fibroblasts Melanocytes	Ref [143]: Poor epidermal differentiation (absence of *Stratum Granulosum* and *Stratum Corneum*). No immune cells.	[79,148]
	DED	KCs Fibroblasts Melanocytes	No immune cells. Ref [91]: No stromal compartment.	[91,95]

Table 2. *Continued*

	Dermal compartment	Cellular components	Limitations of the model	Ref.
Models of melanoma	Rat-tail or bovine collagen type I	KCs Fibroblasts Melanoma cell lines	Animal-derived collagen matrix. No immune cells	70,79,98
	Superimposed fibroblast-derived sheets	KCs Fibroblasts Endothelial cell line (HUVEC) Melanoma cell lines	Fibroblast-deposition of collagen requires 35 days of culture. No immune cells	83
	Alvetex scaffold embedded in fibroblast-secreted matrix	KCs Fibroblasts Melanoma cell lines	Artificial scaffold, not representative of real tissue. No immune cells	80
	DED	KCs Fibroblasts[93] Melanoma cell lines	No immune cells	93,96

BM, basal membrane; DCs, dendritic cells; DED, de-epidermized extracellular dermis; KCs, keratinocytes; mo-DCs, monocyte-derived dendritic cells; mo-LCs, monocyte-derived Langerhans cells.

Many 3D skin models were generated using bovine or rat-tail collagen type I as dermal substrates [78]. These matrices were soon after enriched with stromal cells, such as fibroblasts. The presence of fibroblasts in the dermal compartment, where they secrete large amounts of growth factors, was shown to be crucial for proper proliferation and differentiation of skin cells [79]. However, these collagen matrices are not suitable for long-term cultures, due to their predisposition for contraction. Moreover, they are not representative of the "real" human skin microenvironment, as they introduce non-human ECM components and do not retain a native BM structure [80]. Fibroblasts cultured for several weeks, under specific conditions, can secrete their own ECM, as well as a basal membrane (BM) equivalent (consisting of collagen IV and laminin) [81-83]. Therefore, fibroblast sheets can be stacked to build layers of dermis[83]. The major drawback of these procedures is, however, the long culture period (up to four weeks) required to obtain a fibroblast-derived dermis [80]. In order to have a more physiological skin substitute, attempts were made to generate skin equivalents using *ex vivo* dermis [84]. The use of *ex vivo* or de-epidermized dermis (DED) to grow keratinocytes was first described by Ponec *et al* [85]. DED is obtained

from skin isolated from patients undergoing corrective breast or abdominal wall surgery. Following separation of the dermis from the epidermis, further processing eliminates cellular components from the dermal compartment. This human acellular DED maintains intact the structural and biological characteristics of human ECM. It consists of proteoglycan and fibrous proteins, which include collagen, elastin, fibronectin and laminin. DED preserves basal membrane (BM) proteins and can be manipulated to include stromal and immune cells [86,87].

The possibility of manipulating enginereed skin models to include different cell types makes them a powerful platform to investigate many disorders that affect human skin. Organotypic skin models with patient-derived keratinocytes have been extensively used for studying molecular mechanisms controlling inflammatory diseases, such as psoriasis or dermatitis [71,74,88-90].

Primary immune cells, isolated from blood or tissues, have a limited lifespan when cultured *in vitro.* For this reason, organotypic skin models that encompasses stromal- and immunocompetence are scarce. *In vitro*-derived human dendritic cells and Langerhans cells, embedded in artificial matrices, were shown to acquire migratory properties upon UV irradiation or treatment with the skin sensitizer, dinitrochlorobenzene (DNCB), suggesting a functional activity in response to stress stimuli. Thus far, the most advanced model of inflammatory skin diseases, reports the effective cross-talk between keratinocytes and T lymphocytes. This epidermal-immune cell interaction resulted in a psoriasiform inflammation, which was mediated by the release of soluble factors by activated $CD4^+$ T cells. Inflammation could be reverted by addition of anti-inflammatory drugs, targeting either keratinocytes (trans-retinoic acids) or T cells (Cyclosporin A) [71].

The potential of such models can also be translated to the field of cancer research, for investigation of the malignant transformation of melanocytes, the melanin pigment-producing cells of the skin; as well as for unraveling mechanisms that control melanoma progression and escape from immunesurveillance.

In skin reconstructs, melanocytic cells from different stages of progression (normal to metastatic) show remarkable consistency in their physical distribution, growth and migration patterns, as would be expected from healthy skin and patients with melanoma. Normal melanocytes home to the basement membrane, where they are found located within the basal keratinocytes without apparent proliferation [91]. Moreover, normal melanocytes retain the ability to undergo pigmentation in response to ultraviolet irradiation [92]. Organotypic melanoma models mimic different stages of melanoma progression and confirm clinical observations: early radial growth phase (RGP) primary melanomas proliferate predominantly in the suprabasal area of the epidermis; whereas, vertical growth phase (VGP) and metastatic melanomas (MM) disrupt basal membrane components and invade into the dermis [78,80,93-98].

Initial dissemination of melanoma cells occurs through entry into the vasculature and colonization at distal sites. Additionally, the uncontrolled proliferation of malignant cells requires increased supply of nutrients and oxygen from the blood flow. In order to study the angiogenic potential of melanoma cells in a physiologically relevant context, researchers have established a microvascular network using HUVEC cells in Fb-derived matrices. Tumor cell lines derived by metastatic sites secreted high levels of vascular endothelia growth factor (VEGF) and displayed a potent proangiogenic effect, as compared to cells derived from primary sites [83]. The microvasculature network formed in the presence of MM was more complex, branched and dense. Moreover, they could also observe proximity of tumor cells and endothelial cells.

Altogether, these observations reinforce the hypothesis that organotypic skin models have the power to mimic the (tumor) microenvironment because of their three-dimensionality and multiparametric tailorability. Moreover, those studies demonstrate the applicability of such models to study the pathogenesis of skin inflammation and cancer. We believe that addition of stromal and immune compartments within 3D melanoma models will be pivotal for uncovering the importance of the TME in cancer development, control and treatment.

Dying the "right way" for inducing anti-tumor responses

During the past decade, studies have highlighted how cancer cells modulate the immune system in their local microenvironment. This is a requirement for tumor progression, as it allows the tumor to hide from or evade immune responses. Despite this escape from immunosurveillance, ample evidence shows that it is possible to induce specific anti-tumor immune responses either naturally (spontaneous) or therapeutically. Therefore, the aim of anti-cancer treatments is to activate, or reactivate, the immune system in cancer patients for therapeutic benefit. Recent studies have described the beneficial effects of chemotherapy-induced immunogenic cell death (ICD), and have shed new light on the mechanisms of action that determine the efficacy of chemotherapeutic drugs.

Chemotherapy induces immunogenic cell death

Cancer is commonly considered a disease driven by genetic changes that cause uncontrolled proliferation and invasion of malignant cells[29]. A recently discovered defining requirement for cancer initiation and progression is evasion of anti-tumor immune responses. Nonetheless, most conventional anti-cancer therapies, such as chemotherapy, aim at the rapid destruction of dividing tumor cells, by targeting mechanisms important for cell division [99]. This leads to apoptosis of transformed cells,

a process initially thought to be immunologically-silent [99]. However, recent studies have shown that in mice with a functional immune system, chemotherapeutic drugs are more effective in eradicating tumors than in mice lacking a functional immune system [100,101]. This immunological effect relies on the ability of certain anti-cancer therapeutics to evoke cellular stress, which eventually culminates in the induction of an immunogenic form of apoptosis, also known as ICD (Figure 4) [102-104]. The term 'immunogenicity' describes the capacity of an agent, be it a cell or a pathogen, to induce an immune response and relies on the combination of two factors: antigenicity and adjuvanticity [105,106]. Expression of tumor specific Ags (antigenicity), that differ from their normal counterparts, per se is not sufficient to initiate a robust anti-tumor response [105]. Cells undergoing ICD are characterized by the release of 'danger' signals during and after cell death, referred to as damage associated molecular patterns (DAMPs) [107,108]. These DAMPs are normally sequestered within living cells, but once secreted or exposed on the cell surface, they stimulate inflammatory responses (adjuvanticity) [103,108]. In the original landmark studies, ICD was defined by three types of 'danger' signals: secretion of ATP, exposure of calreticulin (CRT), and release of high mobility group protein-1 (HMGB1) [103,104]. These ICD-associated DAMPs serve different purposes in modulation of the immune system and can

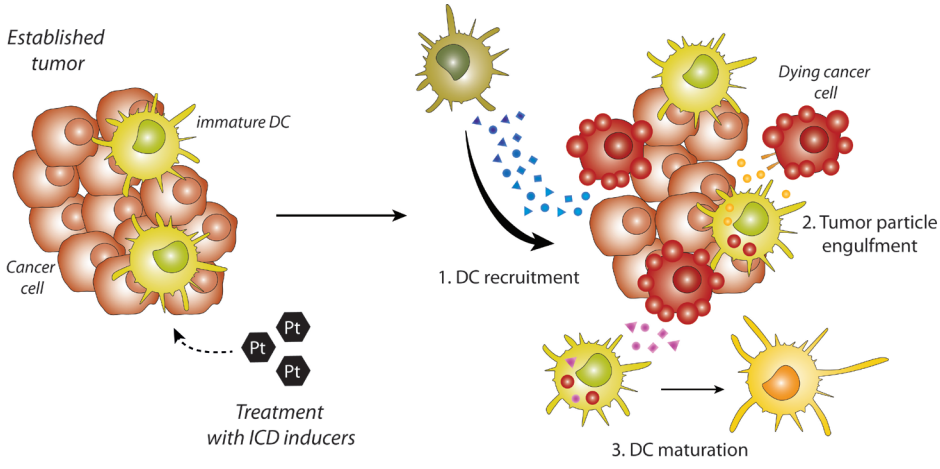

Figure 4. Effects of immunogenic cell death induction on dendritic cells. Treatment with immunogenic cell death (ICD) inducers, such as platinum-based chemotherapeutics, activates an ER-mediated stress response in cancer cells that culminates with immunogenic apoptosis. Dying cancer cells emit 'danger' signals that can (1) recruit dendritic cells (DCs) to the site of inflammation, (2) mediate engulfment of tumor-derived particles by DCs, (3) stimulate DC activation. Together, all these events eventually result in DC maturation that elicits potent anti-tumor immune responses. DC, dendritic cell; Pt, platinum.

be grouped in 'recruitment' (ATP), 'engulfment' (CRT) and 'activating' (HMGB1) signals [109,110]. Accumulating preclinical evidence suggests that release of DAMPs is crucial for the induction of effective anti-tumor immune responses. These DAMPs exert their functions by engaging pattern recognition receptors (PRRs), expressed on the surface of APCs, in particular DCs [111]. As proposed by Tesniere *et al.,* ICD-related DAMPs act as "keys" on the "locks" (DC receptors) that stimulate DC maturation, for unlocking effective anti-tumor immune responses [85]. Maturation of DCs is a multistep process that requires three distinct events. Secretion of 'recruitment' molecules by cells undergoing ICD has a chemoattractant effect, facilitating DC influx into the site of tissue damage [111]. Subsequently, 'engulfment' signals direct Ag uptake by DCs [112]. The process of ICD is further characterized by the passive release of 'activating' signals, which stimulate DC maturation [113]. Following Ag uptake and processing, mature DCs migrate to lymph nodes. Here, they present captured Ags via MHC-I molecules to naïve $CD8^+$ T cells leading to the induction of Ag-specific cytotoxic responses [104].

Sensing danger signals: ATP recruits DCs

Nucleotides serve as a universal source for intracellular energy transfer. Under stressful conditions (such as inflammation, mechanical or ischaemic injury, apoptosis, or necrosis), cells can release nucleotides from the intracellular compartment to the extracellular milieu [114]. When released into the extracellular space, the triphosphonucleotide ATP, no longer acts as an energy carrier, rather it functions as a chemotactic agent and signalling molecule, by interacting with specific membrane-bound nucleotide receptors [114]. Passive release of ATP during necrosis or its active secretion in immunogenic apoptosis thus functions as a "find me" signal, regulating immune cell recruitment to the site of damage and contributing to inflammation [114-116]. Recognition of ATP by DCs is mediated by the purinergic class 2 receptor (P2R) subtypes, P2YRs and P2XRs [114,117,118]. Human and mouse studies identified PY2Rs as the main sensors for immature, but not mature, DC recruitment mediated by ATP; P2XRs on the other hand played a minor role [103,107-111]. This could be explained by the observation that signalling via the two best-characterized receptors, P2Y2 and P2X7, is dependent on the extracellular concentration of ATP. P2Y2 receptors have a higher affinity for low (nanomolar) concentrations of extracellular ATP, whereas P2X7 receptors only respond to high (micromolar) ATP doses [119]. This difference suggested that P2 receptors mediate chemoattraction in two ways. In the early stages of apoptosis, where the cell membrane is still intact and about 2% of the cellular ATP is released, P2Y2 receptors regulate attraction of tissue-resident immune cells. This ATP-mediated recruitment of immune cells may act as a positive feedback loop for immune stimulation. Activation of purinergic receptor

signalling on local immune cells by ATP can, in turn, induce these cells to release high amounts of ATP, which leads to recruitment of distant cells towards the site of inflammation [117,120] By contrast, P2X7 receptors play a minor role in chemoattraction, but are mainly involved in regulation of DC activation. In particular, the ATP-P2X7 axis might induce release of pro-inflammatory cytokines by DCs recruited to or located in close proximity to damaged cells, where higher ATP concentrations can be detected in the extracellular space [112].

Clearing the threat: Calreticulin, an "eat me" signal that mediates cell engulfment by DCs

Calreticulin is an endoplasmic reticulum (ER)-associated multi-functional chaperone molecule, which regulates protein folding, maturation and trafficking [121]. Moreover, it also plays a central role in intracellular calcium homeostasis [122]. Under certain specific forms of cell damage or cell death, endogenous calreticulin (endo-CRT) translocates to the cell surface (ecto-CRT) [123]. The presence of ecto-CRT on the surface of damaged or dying cells flags them for uptake by APCs and is a classic 'hallmark' of ICD [123]. Certain chemotherapeutic drugs, such as anthracyclines, oxaliplatin and bortezomib, were shown to augment ecto-CRT expression [123,124]. Antracycline-treated murine CT26 cells, exposing ecto-CRT, were efficiently taken up by moDCs. In contrast, inhibition of CRT/receptor interaction (via blocking antibodies or transcript knock down), abolished the phagocytosis of dying tumor cells by murine moDCs [123]. Human primary effusion lymphoma cells, killed with the anticancer drug bortezomib, were taken up more efficiently by human immature moDCs, compared to live cells [125]. Similar observations were found in an *in vitro* study using various tumor cell lines and primary tumor cells, treated with a panel of chemotherapeutics [126,127]. APCs express several receptors capable of recognizing ecto-CRT, one of these being the low-density lipoprotein receptor-related protein 1 (LRP1), also known as CD91 [128,129,130]. CD91 is a type 1 transmembrane protein and regulates cell signalling processes, by binding to multiple proteins (up to 40 ligands have been identified so far) [131]. The exact binding site(s) for ectoCRT within CD91 have not been identified yet [132].

Launching the immune system: ATP and HMGs, triggers for DC activation

In addition to the chemoattractant role described earlier, extracellular ATP can act as a regulator of immune responses, by modulating DC phenotype and function [133]. ATP may indeed initiate a Th1 immune response upon cellular damage and also curtail severe inflammation by promoting Th2 responses or tolerance. In particular, *in vitro* stimulation of moDCs with millimolar (1-5mM) ATP concentrations skewed the immune reaction towards a Th1 response, by enhancing secretion of IL-1β,

TNFα and IL-12 by DCs [134,135]. On the other hand, micromolar (up to 500μM) ATP concentrations impaired functional DC maturation in favor of a Th2 or tolerogenic immune, by increasing surface expression of the co-stimulatory molecules, CD80, CD83, CD86, but inhibiting pro-inflammatory cytokines release [134-136]. Additionally, potentiation of cytokine production, in particular of IL-12, was observed as long as IL-12 concentrations, under ATP stimulation, remained below a specific threshold value; while inhibition was observed when more IL-12 was released [137]. Although evidence exists on the effects on P2XRs and P2Y11Rs on DC maturation, given the number of purinergic receptor subtypes expressed by DCs and the lack of specific agonists or inhibitors for each subtype, it has been difficult to unequivocally identify which receptors are involved in a given cellular response.

Another class of molecules involved in DC stimulation upon induction of ICD is represented by the small chromosomal high mobility group (HMG) proteins. HMG proteins bind to DNA strands and in doing so increase flexibility, facilitate remodeling and ensure proper transcriptional regulation, by recruiting transcription factors and endowing chromosomes with nuclease sensitivity [138]. Despite their nuclear localization, components of the HMGB and HMGN families can be passively released into the extracellular environment at later stages of cell death; whereas cells undergoing non-immunogenic apoptosis retain HMGB1 and HMGN1 inside cell membranes [139,140]. When released in the extracellular milieu, HMGB1 and HMGN1 facilitate activation of APCs and the onset of an inflammatory response [139]. HMGB1 and HMGN1 are ligands of toll-like receptor 4 (TLR4), a PPR broadly expressed on human DCs [22,23,139,141,130]. During anti-cancer chemotherapy, the HMGB1/TLR4 signaling pathway is crucial for cross presentation of dying tumor cells by DCs and the efficacy of anti-cancer chemotherapy in mice [141]. In line with this notion, the loss-of-function Asp299Gly polymorphism of TLR4 in breast cancer patients was associated with a faster relapse after anthracycline-based chemotherapy, as compared to patients carrying the wild type TLR4 allele [141,142]. HMGN1 was also shown to activate DCs and thus stimulate immune responses. The HMGN1/TLR4 pathway activated the NF-κB–dependent production of the pro-inflammatory cytokines IL-6, IL-1β and TNF by mouse bone-marrow derived DCs. Also, *in vitro* incubation of human moDCs with HMGN1 upregulated the expression of co-stimulatory molecules (CD80, CD83 and CD86) and MHC antigen-presentation complexes [139].

A lot of effort has been devoted into increasing our understanding of the molecular parameters that govern ICD. However, we are just beginning to characterize the complex interactions of immunogenic DAMPs with their receptors that lead to robust antitumor immunity. For most of the "non-classical"-ICD DAMPs, evidence is based on a relatively limited number of studies, mostly performed with murine APCs or with human monocytes or *in vitro* generated moDCs. Definitely,

more research is needed to clearly define the role of those, as well as other DAMPs in ICD-mediated induction of anti-tumor immunity. Understanding the molecular pathways of ICD-DAMP interplay in DCs, is pivotal to the exploitation of these principles in order to increase the efficacy of immunogenic inducers, and to develop new strategies for cancer therapy.

Scope of this thesis

Tumor progression and resistance to anti-cancer therapies require interplay between cancer cells, host tissue cells and the EMC, within the tumor microenvironment. As a result, cancer cells can elude antitumor immunity or induce tolerogenic responses. Some of the key events that lead to immunosuppression originate from the interaction of tumor cells with DCs. DCs are master switches of immunity and tolerance. Hence, signals provided by DCs, upon interaction with cancer cells, dictate the fate of an anti-tumor response. Following uptake of tumor particles, DCs can exhibit a malfunctioning phenotype. These "defective" DCs are no longer available to alert the immune system to cancer. A promising strategy to support DC function involves the switch of an immunosuppressive state into an immunostimulatory state.

The **first aim** of my thesis was to study the interplay between tumor cells and human naturally-occurring DC subsets; and to explore potential strategies to revert tumor-mediated immunosuppression.

The **second aim** of my thesis was to investigate DC-tumor cell interaction in a 3D model that mimics the *in vivo* tumor microenvironment. To this aim I developed an *in vitro* 3D skin model of human melanoma as a tumor model for studying this interaction. This model is amenable to titration of different cellular components and to application for many *in vitro* investigative approaches. Using this model, tumor growth, immune cell function as well as tumor-immune cell interactions can be studied.

Thesis outline

An increasing number of conventional chemotherapeutic compounds were recently found to possess immunostimulatory properties. In **Chapter 2,** I explored the effect of two of the most used platinum compounds, oxaliplatin and cisplatin, in the induction of an immunostimulatory form of cancer cell death, also known as immunogenic cell death (ICD). Next, I assessed whether platinum-induced ICD affected phenotype and function of human naturally occurring DC subsets. Interestingly, I show that human DCs differ in their capacity to respond to ICD signals and eventually stimulate T cell responses. In **Chapter 3,** I expanded these observations, hypothesizing that the combination of platinum-induced ICD with blocking of inhibitory mechanisms, by antibody-based immunotherapy, might cooperate and overcome tumor-mediated immunosuppression. In particular, I set out to investigate the effect of shifting the balance between inhibitory "don't eat me" signals, by means of CD47 signaling, while enhancing ICD-induced "eat me" signals (such as Calreticulin) on tumor cells. To study cancer-host cell interactions under

conditions that mimic the *in vivo* situation, I developed an immunocompetent 3D human melanoma model, of which the details are described in **Chapter 4**. My results demonstrate that this novel 3D model is a promising tool for direct observation of the interplay between melanoma cells and DCs. Moreover, in **Chapter 5,** I exploited multispectral imaging to assess immune cell infiltrates in human primary melanomas. This innovative imaging technique combines imaging with spectroscopy to obtain accurate information about quantitative expression data and tissue distribution of different cell types within the TME. Finally, in **Chapter 6,** the findings of this thesis are discussed and future perspectives are outlined.

References

1. Bakdash, G., Schreurs, I., Schreibelt, G. & Tel, J. Crosstalk between dendritic cell subsets and implications for dendritic cell-based anticancer immunotherapy. *Expert review of clinical immunology* **10**, 915-926, doi:10.1586/1744666x.2014.912561 (2014).
2. Banchereau, J., Briere, F., Caux, C. *et al.* Immunobiology of dendritic cells. *Annual review of immunology* **18**, 767-811, doi:10.1146/annurev.immunol.18.1.767 (2000).
3. Figdor, C. G., de Vries, I. J. M., Lesterhuis, W. J. & Melief, C. J. Dendritic cell immunotherapy: mapping the way. *Nature medicine* **10**, 475-480 (2004).
4. Bakdash, G., Sittig, S. P., van Dijk, T., Figdor, C. G. & de Vries, I. J. M. The nature of activatory and tolerogenic dendritic cell-derived signal II. *Frontiers in immunology* **4** (2013).
5. Palucka, K. & Banchereau, J. Cancer immunotherapy via dendritic cells. *Nature Reviews Cancer* **12**, 265-277 (2012).
6. Bhardwaj, N., Friedman, S. M., Cole, B. C. & Nisanian, A. Dendritic cells are potent antigen-presenting cells for microbial superantigens. *The Journal of experimental medicine* **175**, 267-273 (1992).
7. Benencia, F., Sprague, L., McGinty, J., Pate, M. & Muccioli, M. Dendritic cells the tumor microenvironment and the challenges for an effective antitumor vaccination. *BioMed Research International* **2012** (2012).
8. Shen, Z., Reznikoff, G., Dranoff, G. & Rock, K. L. Cloned dendritic cells can present exogenous antigens on both MHC class I and class II molecules. *The Journal of Immunology* **158**, 2723-2730 (1997).
9. Cahalan, M. D. & Parker, I. in *Seminars in immunology.* 442-451 (Elsevier).
10. Schuurhuis, D. H., Laban, S., Toes, R. E. *et al.* Immature Dendritic Cells Acquire Cd8+ Cytotoxic T Lymphocyte Priming Capacity upon Activation by T Helper Cell–Independent or–Dependent Stimuli. *The Journal of experimental medicine* **192**, 145-150 (2000).
11. Ziegler-Heitbrock, L., Ancuta, P., Crowe, S. *et al.* Nomenclature of monocytes and dendritic cells in blood. *Blood* **116**, e74-80, doi:10.1182/blood-2010-02-258558 (2010).
12. Schreiber, R. D., Old, L. J. & Smyth, M. J. Cancer Immunoediting: Integrating Immunity's Roles in Cancer Suppression and Promotion. *Science* **331**, 1565-1570, doi:10.1126/science.1203486 (2011).
13. Zhu, J. & Paul, W. E. Peripheral CD4+ T-cell differentiation regulated by networks of cytokines and transcription factors. *Immunol Rev* **238**, 247-262, doi:10.1111/j.1600-065X.2010.00951.x (2010).
14. Sigmundsdottir, H. & Butcher, E. C. Environmental cues, dendritic cells and the programming of tissue-selective lymphocyte trafficking. *Nature immunology* **9**, 981-987, doi:10.1038/ni.f.208 (2008).
15. Schreibelt, G., Bol, K. F., Aarntzen, E. H. *et al.* Importance of helper T-cell activation in dendritic cell-based anticancer immunotherapy. *OncoImmunology* **2**, e24440 (2013).
16. Lee, S. C., Srivastava, R. M., López-Albaitero, A., Ferrone, S. & Ferris, R. L. Natural killer (NK): dendritic cell (DC) cross talk induced by therapeutic monoclonal antibody triggers tumor antigen-specific T cell immunity. *Immunol Res* **50**, 248-254, doi:10.1007/s12026-011-8231-0 (2011).
17. Douagi, I., Gujer, C., Sundling, C. *et al.* Human B cell responses to TLR ligands are differentially modulated by myeloid and plasmacytoid dendritic cells. *J Immunol* **182**, 1991-2001, doi:10.4049/jimmunol.0802257 (2009).

18. Bonasio, R. & von Andrian, U. H. Generation, migration and function of circulating dendritic cells. *Current opinion in immunology* **18**, 503-511, doi:10.1016/j.coi.2006.05.011 (2006).
19. MacDonald, K. P., Munster, D. J., Clark, G. J. *et al.* Characterization of human blood dendritic cell subsets. *Blood* **100**, 4512-4520, doi:10.1182/blood-2001-11-0097 (2002).
20. Collin, M., McGovern, N. & Haniffa, M. Human dendritic cell subsets. *Immunology* **140**, 22-30, doi:10.1111/imm.12117 (2013).
21. Liu, K., Victora, G. D., Schwickert, T. A. *et al.* In vivo analysis of dendritic cell development and homeostasis. *Science* **324**, 392-397, doi:10.1126/science.1170540 (2009).
22. Piccioli, D., Tavarini, S., Borgogni, E. *et al.* Functional specialization of human circulating CD16 and CD1c myeloid dendritic-cell subsets. *Blood* **109**, 5371-5379, doi:10.1182/blood-2006-08-038422 (2007).
23. Tel, J., Schreibelt, G., Sittig, S. P. *et al.* Human plasmacytoid dendritic cells efficiently cross-present exogenous Ags to CD8+ T cells despite lower Ag uptake than myeloid dendritic cell subsets. *Blood* **121**, 459-467, doi:10.1182/blood-2012-06-435644 (2013).
24. Nizzoli, G., Krietsch, J., Weick, A. *et al.* Human CD1c+ dendritic cells secrete high levels of IL-12 and potently prime cytotoxic T-cell responses. *Blood* **122**, 932-942, doi:10.1182/blood-2013-04-495424 (2013).
25. Osugi, Y., Vuckovic, S. & Hart, D. N. Myeloid blood CD11c(+) dendritic cells and monocyte-derived dendritic cells differ in their ability to stimulate T lymphocytes. *Blood* **100**, 2858-2866, doi:10.1182/blood.V100.8.2858 (2002).
26. Schreiber, R. D., Old, L. J. & Smyth, M. J. Cancer immunoediting: integrating immunity's roles in cancer suppression and promotion. *Science* **331**, 1565-1570, doi:10.1126/science.1203486 (2011).
27. Pickup, M. W., Mouw, J. K. & Weaver, V. M. The extracellular matrix modulates the hallmarks of cancer. *EMBO Reports* **15**, 1243-1253, doi:10.15252/embr.201439246 (2014).
28. Hanahan, D. & Weinberg, Robert A. Hallmarks of Cancer: The Next Generation. *Cell* **144**, 646-674, doi:http://dx.doi.org/10.1016/j.cell.2011.02.013 (2011).
29. Hanahan, D. & Weinberg, R. A. The Hallmarks of Cancer. *Cell* **100**, 57-70, doi:http://dx.doi.org/10.1016/S0092-8674(00)81683-9 (2000).
30. Pietras, K. & Östman, A. Hallmarks of cancer: Interactions with the tumor stroma. *Experimental Cell Research* **316**, 1324-1331, doi:http://dx.doi.org/10.1016/j.yexcr.2010.02.045 (2010).
31. Colotta, F., Allavena, P., Sica, A., Garlanda, C. & Mantovani, A. Cancer-related inflammation, the seventh hallmark of cancer: links to genetic instability. *Carcinogenesis* **30**, 1073-1081, doi:10.1093/carcin/bgp127 (2009).
32. Conejo-Garcia, J. R., Benencia, F., Courreges, M. C. *et al.* Letal, A tumor-associated NKG2D immunoreceptor ligand, induces activation and expansion of effector immune cells. *Cancer Biol Ther* **2**, 446-451 (2003).
33. DeNardo, D. G. & Coussens, L. M. Inflammation and breast cancer. Balancing immune response: crosstalk between adaptive and innate immune cells during breast cancer progression. *Breast Cancer Res* **9**, 212, doi:10.1186/bcr1746 (2007).
34. Talmadge, J. E., Donkor, M. & Scholar, E. Inflammatory cell infiltration of tumors: Jekyll or Hyde. *Cancer and Metastasis Reviews* **26**, 373-400 (2007).
35. Waldner, M., Schimanski, C. C. & Neurath, M. F. Colon cancer and the immune system: the role of tumor invading T cells. *World J Gastroenterol* **12**, 7233-7238 (2006).

36. Vasaturo, A., Halilovic, A., Bol, K. F. *et al.* T cell landscape in a primary melanoma predicts the survival of patients with metastatic disease after their treatment with dendritic cell vaccines. *Cancer Research*, doi:10.1158/0008-5472.can-15-3211 (2016).
37. Gabrilovich, D. I. & Nagaraj, S. Myeloid-derived suppressor cells as regulators of the immune system. *Nature Reviews Immunology* **9**, 162-174 (2009).
38. Gabrilovich, D. I., Ostrand-Rosenberg, S. & Bronte, V. Coordinated regulation of myeloid cells by tumours. *Nature Reviews Immunology* **12**, 253-268 (2012).
39. Teng, M. W., Ritchie, D. S., Neeson, P. & Smyth, M. J. Biology and clinical observations of regulatory T cells in cancer immunology. *Curr Top Microbiol Immunol* **344**, 61-95, doi:10.1007/82_2010_50 (2011).
40. Oldenborg, P.-A., Zheleznyak, A., Fang, Y.-F. *et al.* Role of CD47 as a Marker of Self on Red Blood Cells. *Science* **288**, 2051-2054, doi:10.1126/science.288.5473.2051 (2000).
41. Yi, T., Li, J., Chen, H. *et al.* Splenic Dendritic Cells Survey Red Blood Cells for Missing Self-CD47 to Trigger Adaptive Immune Responses. *Immunity* **43**, 764-775, doi:http://dx.doi.org/10.1016/j.immuni.2015.08.021 (2015).
42. Barclay, A. N. & van den Berg, T. K. The Interaction Between Signal Regulatory Protein Alpha (SIRPα) and CD47: Structure, Function, and Therapeutic Target. *Annual Review of Immunology* **32**, 25-50, doi:10.1146/annurev-immunol-032713-120142 (2014).
43. Chao, M. P., Weissman, I. L. & Majeti, R. The CD47-SIRPα Pathway in Cancer Immune Evasion and Potential Therapeutic Implications. *Current Opinion in Immunology* **24**, 225-232, doi:10.1016/j.coi.2012.01.010 (2012).
44. Oldenborg, P.-A. CD47: A Cell Surface Glycoprotein Which Regulates Multiple Functions of Hematopoietic Cells in Health and Disease. *ISRN Hematology* **2013**, 614619, doi:10.1155/2013/614619 (2013).
45. Braun, D., Galibert, L., Nakajima, T. *et al.* Semimature Stage: A Checkpoint in a Dendritic Cell Maturation Program That Allows for Functional Reversion after Signal-Regulatory Protein-α Ligation and Maturation Signals. *The Journal of Immunology* **177**, 8550-8559, doi:10.4049/jimmunol.177.12.8550 (2006).
46. Latour, S., Tanaka, H., Demeure, C. *et al.* Bidirectional Negative Regulation of Human T and Dendritic Cells by CD47 and Its Cognate Receptor Signal-Regulator Protein-α: Down-Regulation of IL-12 Responsiveness and Inhibition of Dendritic Cell Activation. *The Journal of Immunology* **167**, 2547-2554, doi:10.4049/jimmunol.167.5.2547 (2001).
47. van den Berg, Timo K. & van Bruggen, R. Loss of CD47 Makes Dendritic Cells See Red. *Immunity* **43**, 622-624, doi:http://dx.doi.org/10.1016/j.immuni.2015.09.008 (2015).
48. Willingham, S. B., Volkmer, J.-P., Gentles, A. J. *et al.* The CD47-signal regulatory protein alpha (SIRPa) interaction is a therapeutic target for human solid tumors. *Proceedings of the National Academy of Sciences of the United States of America* **109**, 6662-6667, doi:10.1073/pnas.1121623109 (2012).
49. Chao, M. P., Alizadeh, A. A., Tang, C. *et al.* Therapeutic Antibody Targeting of CD47 Eliminates Human Acute Lymphoblastic Leukemia. *Cancer Research* **71**, 1374-1384, doi:10.1158/0008-5472.can-10-2238 (2011).
50. Majeti, R., Chao, M. P., Alizadeh, A. A. *et al.* CD47 is an adverse prognostic factor and therapeutic antibody target on human acute myeloid leukemia stem cells. *Cell* **138**, 286-299, doi:10.1016/j.cell.2009.05.045 (2009).
51. Xu, J.-F., Pan, X.-H., Zhang, S.-J. *et al. CD47 blockade inhibits tumor progression human osteosarcoma in xenograft models.* (2015).

52. Jaiswal, S., Jamieson, C. H. M., Pang, W. W. *et al.* CD47 is up-regulated on circulating hematopoietic stem cells and leukemia cells to avoid phagocytosis. *Cell* **138**, 271-285, doi:10.1016/j.cell.2009.05.046 (2009).
53. Feng, M., Chen, J. Y., Weissman-Tsukamoto, R. *et al.* Macrophages eat cancer cells using their own calreticulin as a guide: Roles of TLR and Btk. *Proceedings of the National Academy of Sciences of the United States of America* **112**, 2145-2150, doi:10.1073/pnas.1424907112 (2015).
54. Brohem, C. A., da Silva Cardeal, L. B., Tiago, M. *et al.* Artificial Skin in Perspective: Concepts and Applications. *Pigment cell & melanoma research* **24**, 35-50, doi:10.1111/j.1755-148X.2010.00786.x (2011).
55. de Vries, R. B. M., Leenaars, M., Tra, J. *et al.* The potential of tissue engineering for developing alternatives to animal experiments: a systematic review. *Journal of Tissue Engineering and Regenerative Medicine* **9**, 771-778, doi:10.1002/term.1703 (2015).
56. Davis, M. M. Immunology Taught by Humans. *Science translational medicine* **4**, 117fs112-117fs112, doi:10.1126/scitranslmed.3003385 (2012).
57. Cekanova, M. & Rathore, K. Animal models and therapeutic molecular targets of cancer: utility and limitations. *Drug Design, Development and Therapy* **8**, 1911-1922, doi:10.2147/DDDT.S49584 (2014).
58. Kuzu, O. F., Nguyen, F. D., Noory, M. A. & Sharma, A. Current State of Animal (Mouse) Modeling in Melanoma Research. *Cancer Growth and Metastasis* **8**, 81-94, doi:10.4137/CGM.S21214 (2015).
59. Mak, I. W. Y., Evaniew, N. & Ghert, M. Lost in translation: animal models and clinical trials in cancer treatment. *American Journal of Translational Research* **6**, 114-118 (2014).
60. Graham, M. L. & Prescott, M. J. The multifactorial role of the 3Rs in shifting the harm-benefit analysis in animal models of disease. *European Journal of Pharmacology* **759**, 19-29, doi:10.1016/j.ejphar.2015.03.040 (2015).
61. Katt, M. E., Placone, A. L., Wong, A. D., Xu, Z. S. & Searson, P. C. In Vitro Tumor Models: Advantages, Disadvantages, Variables, and Selecting the Right Platform. *Frontiers in Bioengineering and Biotechnology* **4**, 12, doi:10.3389/fbioe.2016.00012 (2016).
62. Myungjin Lee, J., Mhawech-Fauceglia, P., Lee, N. *et al.* A three-dimensional microenvironment alters protein expression and chemosensitivity of epithelial ovarian cancer cells in vitro. *Lab Invest* **93**, 528-542, doi:10.1038/labinvest.2013.41 (2013).
63. Ghosh, S., Spagnoli, G. C., Martin, I. *et al.* Three-dimensional culture of melanoma cells profoundly affects gene expression profile: A high density oligonucleotide array study. *Journal of Cellular Physiology* **204**, 522-531, doi:10.1002/jcp.20320 (2005).
64. Zschenker, O., Streichert, T., Hehlgans, S. & Cordes, N. Genome-Wide Gene Expression Analysis in Cancer Cells Reveals 3D Growth to Affect ECM and Processes Associated with Cell Adhesion but Not DNA Repair. *PLoS ONE* **7**, e34279, doi:10.1371/journal.pone.0034279 (2012).
65. Bellis, A. D., Bernabé, B. P., Weiss, M. S. *et al.* Dynamic Transcription Factor Activity Profiling in 2D and 3D Cell Cultures. *Biotechnology and bioengineering* **110**, 563-572, doi:10.1002/bit.24718 (2013).
66. Mazzoleni, G., Di Lorenzo, D. & Steimberg, N. Modelling tissues in 3D: the next future of pharmaco-toxicology and food research? *Genes & Nutrition* **4**, 13-22, doi:10.1007/s12263-008-0107-0 (2009).
67. Li, L., Dragulev, B., Zigrino, P., Mauch, C. & Fox, J. W. The invasive potential of human melanoma cell lines correlates with their ability to alter fibroblast gene expression in vitro

and the stromal microenvironment in vivo. *International Journal of Cancer* **125**, 1796-1804, doi:10.1002/ijc.24463 (2009).

68. Rouwkema, J. & Khademhosseini, A. Vascularization and Angiogenesis in Tissue Engineering: Beyond Creating Static Networks. *Trends in Biotechnology* **34**, 733-745, doi:http://dx.doi.org/10.1016/j.tibtech.2016.03.002 (2016).
69. Villasante, A. & Vunjak-Novakovic, G. Tissue-engineered models of human tumors for cancer research. *Expert opinion on drug discovery* **10**, 257-268, doi:10.1517/17460441.2015.1009442 (2015).
70. Syed, D. N., Chamcheu, J.-C., Khan, M. I. *et al.* Fisetin inhibits human melanoma cell growth through direct binding to p70S6K and mTOR: findings from 3-D melanoma skin equivalents and computational modeling. *Biochemical pharmacology* **89**, 349-360, doi:10.1016/j.bcp.2014.03.007 (2014).
71. van den Bogaard, E. H., Bergboer, J. G. M., Vonk-Bergers, M. *et al.* Coal tar induces AHR-dependent skin barrier repair in atopic dermatitis. *The Journal of Clinical Investigation* **123**, 917-927, doi:10.1172/JCI65642 (2013).
72. Popov, L., Kovalski, J., Grandi, G., Bagnoli, F. & Amieva, M. R. Three-Dimensional Human Skin Models to Understand Staphylococcus aureus Skin Colonization and Infection. *Frontiers in Immunology* **5**, 41, doi:10.3389/fimmu.2014.00041 (2014).
73. Dongari-Bagtzoglou, A. & Kashleva, H. Development of a highly reproducible three-dimensional organotypic model of the oral mucosa. *Nature protocols* **1**, 2012-2018, doi:10.1038/nprot.2006.323 (2006).
74. Jean, J., Lapointe, M., Soucy, J. & Pouliot, R. Development of an in vitro psoriatic skin model by tissue engineering. *Journal of Dermatological Science* **53**, 19-25, doi:http://dx.doi.org/10.1016/j.jdermsci.2008.07.009 (2009).
75. Shen, J., van den Bogaard, E. H., Kouwenhoven, E. N. *et al.* APR-246/PRIMA-1(MET) rescues epidermal differentiation in skin keratinocytes derived from EEC syndrome patients with p63 mutations. *Proceedings of the National Academy of Sciences of the United States of America* **110**, 2157-2162, doi:10.1073/pnas.1201993110 (2013).
76. van den Bogaard, E. H., Rodijk-Olthuis, D., Jansen, P. A. M. *et al.* Rho Kinase Inhibitor Y-27632 Prolongs the Life Span of Adult Human Keratinocytes, Enhances Skin Equivalent Development, and Facilitates Lentiviral Transduction. *Tissue Engineering Part A.* **18**, 1827-1836, doi:doi:10.1089/ten.tea.2011.0616 (2012).
77. Regnier, M., Prunieras, M. & Woodley, D. Growth and differentiation of adult human epidermal cells on dermal substrates. *Frontiers of Matrix Biology* **9**, 4-35 (1981).
78. Li, L., Fukunaga-Kalabis, M. & Herlyn, M. The Three-Dimensional Human Skin Reconstruct Model: a Tool to Study Normal Skin and Melanoma Progression. *Journal of Visualized Experiments : JoVE*, 2937, doi:10.3791/2937 (2011).
79. Meier, F., Nesbit, M., Hsu, M.-Y. *et al.* Human Melanoma Progression in Skin Reconstructs : Biological Significance of bFGF. *The American Journal of Pathology* **156**, 193-200 (2000).
80. Hill, D. S., Robinson, N. D. P., Caley, M. P. *et al.* A Novel Fully Humanized 3D Skin Equivalent to Model Early Melanoma Invasion. *Molecular Cancer Therapeutics* **14**, 2665-2673, doi:10.1158/1535-7163.mct-15-0394 (2015).
81. El Ghalbzouri, A., Commandeur, S., Rietveld, M. H., Mulder, A. A. & Willemze, R. Replacement of animal-derived collagen matrix by human fibroblast-derived dermal matrix for human skin equivalent products. *Biomaterials* **30**, 71-78, doi:http://dx.doi.org/10.1016/j.biomaterials.2008.09.002 (2009).

82. El Ghalbzouri, A., Jonkman, M. F., Dijkman, R. & Ponec, M. Basement Membrane Reconstruction in Human Skin Equivalents Is Regulated by Fibroblasts and/or Exogenously Activated Keratinocytes. *Journal of Investigative Dermatology* **124**, 79-86, doi:http://dx.doi.org/10.1111/j.0022-202X.2004.23549.x (2005).
83. Gibot, L., Galbraith, T., Huot, J. & Auger, F. A. Development of a tridimensional microvascularized human skin substitute to study melanoma biology. *Clinical & Experimental Metastasis* **30**, 83-90, doi:10.1007/s10585-012-9511-3 (2013).
84. Prunieras, M., Regnier, M. & Schlotterer, M. [New procedure for culturing human epidermal cells on allogenic or xenogenic skin: preparation of recombined grafts]. *Annales de Chirurgie Plastique Esthétique* **24**, 375-362 (1979).
85. Ponec, M. Reconstruction of human epidermis on de-epidermized dermis: Expression of differentiation-specific protein markers and lipid composition. *Toxicology in Vitro* **5**, 597-606, doi:http://dx.doi.org/10.1016/0887-2333(91)90100-R (1991).
86. El Ghalbzouri, A., Lamme, E. & Ponec, M. Crucial role of fibroblasts in regulating epidermal morphogenesis. *Cell and Tissue Research* **310**, 189-199, doi:10.1007/s00441-002-0621-0 (2002).
87. van den Bogaard, E. H., Tjabringa, G. S., Joosten, I. *et al.* Crosstalk between Keratinocytes and T Cells in a 3D Microenvironment: A Model to Study Inflammatory Skin Diseases. *Journal of Investigative Dermatology* **134**, 719-727, doi:http://dx.doi.org/10.1038/jid.2013.417 (2014).
88. Tjabringa, G., Bergers, M., van Rens, D. *et al.* Development and Validation of Human Psoriatic Skin Equivalents. *The American Journal of Pathology* **173**, 815-823, doi:10.2353/ajpath.2008.080173 (2008).
89. Niehues, H., Schalkwijk, J., van Vlijmen-Willems, I. M. J. J. *et al.* Epidermal equivalents of filaggrin null keratinocytes do not show impaired skin barrier function. *Journal of Allergy and Clinical Immunology*, doi:http://dx.doi.org/10.1016/j.jaci.2016.09.016.
90. Kamsteeg, M., Bergers, M., de Boer, R. *et al.* Type 2 Helper T-Cell Cytokines Induce Morphologic and Molecular Characteristics of Atopic Dermatitis in Human Skin Equivalent. *The American Journal of Pathology* **178**, 2091-2099, doi:10.1016/j.ajpath.2011.01.037 (2011).
91. Rehder, J., Souto, L. R. M., Issa, C. M. B. M. & Puzzi, M. B. Model of human epidermis reconstructed in vitro with keratinocytes and melanocytes on dead de-epidermized human dermis. *Sao Paulo Medical Journal* **122**, 22-25 (2004).
92. Bessou, S., SurlÈVe-Bazeille, J.-E., Sorbier, E. & TaÏEb, A. Ex Vivo Reconstruction of the Epidermis With Melanocytes and the Influence of UVB. *Pigment Cell Research* **8**, 241-249, doi:10.1111/j.1600-0749.1995.tb00670.x (1995).
93. Eves, P., Katerinaki, E., Simpson, C. *et al.* Melanoma invasion in reconstructed human skin is influenced by skin cells – investigation of the role of proteolytic enzymes. *Clinical & Experimental Metastasis* **20**, 685-700, doi:10.1023/B:CLIN.0000006824.41376.b0 (2003).
94. Commandeur, S., Sparks, S. J., Chan, H.-L. *et al.* In-vitro melanoma models: invasive growth is determined by dermal matrix and basement membrane. *Melanoma Research* **24**, 305-314 (2014).
95. Eves, P., Layton, C., Hedley, S. *et al.* Characterization of an in vitro model of human melanoma invasion based on reconstructed human skin. *British Journal of Dermatology* **142**, 210-222, doi:10.1046/j.1365-2133.2000.03287.x (2000).
96. Van Kilsdonk, J. W. J., Bergers, M., Van Kempen, L. C. L. T., Schalkwijk, J. & Swart, G. W. M. Keratinocytes drive melanoma invasion in a reconstructed skin model. *Melanoma Research* **20**, 372-380, doi:10.1097/CMR.0b013e32833d8d70 (2010).

97. Berking, C. & Herlyn, M. Human skin reconstruct models: a new application for studies of melanocyte and melanoma biology. *Histology and Histopathology* **16**, 669-674 (2001).
98. Vörsmann, H., Groeber, F., Walles, H. *et al.* Development of a human three-dimensional organotypic skin-melanoma spheroid model for in vitro drug testing. *Cell Death & Disease* **4**, e719, doi:10.1038/cddis.2013.249 (2013).
99. Chabner, B. A. & Roberts, T. G. Chemotherapy and the war on cancer. *Nat Rev Cancer* **5**, 65-72 (2005).
100. Tesniere, A., Schlemmer, F., Boige, V. *et al.* Immunogenic death of colon cancer cells treated with oxaliplatin. *Oncogene* **29**, 482-491, doi:http://www.nature.com/onc/journal/v29/n4/suppinfo/onc2009356s1.html (2009).
101. Zitvogel, L., Galluzzi, L., Smyth, Mark J. & Kroemer, G. Mechanism of Action of Conventional and Targeted Anticancer Therapies: Reinstating Immunosurveillance. *Immunity* **39**, 74-88, doi:http://dx.doi.org/10.1016/j.immuni.2013.06.014 (2013).
102. Kono, K., Mimura, K. & Kiessling, R. Immunogenic tumor cell death induced by chemoradiotherapy: molecular mechanisms and a clinical translation. *Cell Death Dis* **4**, e688, doi:10.1038/cddis.2013.207 (2013).
103. Hato, S. V., Khong, A., de Vries, I. J. & Lesterhuis, W. J. Molecular pathways: the immunogenic effects of platinum-based chemotherapeutics. *Clinical cancer research : an official journal of the American Association for Cancer Research* **20**, 2831-2837, doi:10.1158/1078-0432.ccr-13-3141 (2014).
104. Kroemer, G., Galluzzi, L., Kepp, O. & Zitvogel, L. Immunogenic cell death in cancer therapy. *Annual review of immunology* **31**, 51-72, doi:10.1146/annurev-immunol-032712-100008 (2013).
105. Matzinger, P. Tolerance, Danger, and the Extended Family. *Annual Review of Immunology* **12**, 991-1045, doi:doi:10.1146/annurev.iy.12.040194.005015 (1994).
106. Galluzzi, L., Buqué, A., Kepp, O., Zitvogel, L. & Kroemer, G. Immunological Effects of Conventional Chemotherapy and Targeted Anticancer Agents. *Cancer Cell* **28**, 690-714, doi:10.1016/j.ccell.2015.10.012.
107. Tesniere, A., Panaretakis, T., Kepp, O. *et al.* Molecular characteristics of immunogenic cancer cell death. *Cell Death Differ* **15**, 3-12, doi:10.1038/sj.cdd.4402269 (2008).
108. Krysko, D. V., Garg, A. D., Kaczmarek, A. *et al.* Immunogenic cell death and DAMPs in cancer therapy. *Nat Rev Cancer* **12**, 860-875, doi:http://www.nature.com/nrc/journal/v12/n12/suppinfo/nrc3380_S1.html (2012).
109. Chao, M. P., Jaiswal, S., Weissman-Tsukamoto, R. *et al.* Calreticulin is the dominant pro-phagocytic signal on multiple human cancers and is counterbalanced by CD47. *Science translational medicine* **2**, 63ra94, doi:10.1126/scitranslmed.3001375 (2010).
110. Hochreiter-Hufford, A. & Ravichandran, K. S. Clearing the Dead: Apoptotic Cell Sensing, Recognition, Engulfment, and Digestion. *Cold Spring Harbor Perspectives in Biology* **5**, a008748, doi:10.1101/cshperspect.a008748 (2013).
111. Akira, S., Uematsu, S. & Takeuchi, O. Pathogen recognition and innate immunity. *Cell* **124**, 783-801, doi:10.1016/j.cell.2006.02.015 (2006).
112. Ravichandran, K. S. Beginnings of a good apoptotic meal: the find-me and eat-me signaling pathways. *Immunity* **35**, 445-455, doi:10.1016/j.immuni.2011.09.004 (2011).
113. Tesniere, A., Apetoh, L., Ghiringhelli, F. *et al.* Immunogenic cancer cell death: a key-lock paradigm. *Current Opinion in Immunology* **20**, 504-511, doi:http://dx.doi.org/10.1016/j.coi.2008.05.007 (2008).

114. Idzko, M., Ferrari, D. & Eltzschig, H. K. Nucleotide signalling during inflammation. *Nature* **509**, 310-317, doi:10.1038/nature13085 http://www.nature.com/nature/journal/v509/n7500/abs/nature13085.html#supplementary-information (2014).
115. Bours, M. J. L., Swennen, E. L. R., Di Virgilio, F., Cronstein, B. N. & Dagnelie, P. C. Adenosine 5'-triphosphate and adenosine as endogenous signaling molecules in immunity and inflammation. *Pharmacology & Therapeutics* **112**, 358-404, doi:http://dx.doi.org/10.1016/j.pharmthera.2005.04.013 (2006).
116. Martins, I., Tesniere, A., Kepp, O. *et al.* Chemotherapy induces ATP release from tumor cells. *Cell Cycle* **8**, 3723-3728, doi:10.4161/cc.8.22.10026 (2009).
117. Junger, W. G. Immune cell regulation by autocrine purinergic signalling. *Nat Rev Immunol* **11**, 201-212, doi:10.1038/nri2938 (2011).
118. Jacobson, K. A., Balasubramanian, R., Deflorian, F. & Gao, Z. G. G protein-coupled adenosine (P1) and P2Y receptors: ligand design and receptor interactions. *Purinergic signalling* **8**, 419-436, doi:10.1007/s11302-012-9294-7 (2012).
119. Trautmann, A. *Extracellular ATP in the Immune System: More Than Just a "Danger Signal"*. Vol. 2 (2009).
120. Cekic, C. & Linden, J. Purinergic regulation of the immune system. *Nat Rev Immunol* **16**, 177-192, doi:10.1038/nri.2016.4 (2016).
121. Jiang, Y., Dey, S. & Matsunami, H. Calreticulin: Roles in Cell-Surface Protein Expression. *Membranes* **4**, 630-641, doi:10.3390/membranes4030630 (2014).
122. Arnaudeau, S., Frieden, M., Nakamura, K. *et al.* Calreticulin Differentially Modulates Calcium Uptake and Release in the Endoplasmic Reticulum and Mitochondria. *Journal of Biological Chemistry* **277**, 46696-46705, doi:10.1074/jbc.M202395200 (2002).
123. Obeid, M., Tesniere, A., Ghiringhelli, F. *et al.* Calreticulin exposure dictates the immunogenicity of cancer cell death. *Nat Med* **13**, 54-61, doi:http://www.nature.com/nm/journal/v13/n1/suppinfo/nm1523_S1.html (2007).
124. Panaretakis, T., Kepp, O., Brockmeier, U. *et al.* Mechanisms of pre-apoptotic calreticulin exposure in immunogenic cell death. *The EMBO journal* **28**, 578-590, doi:10.1038/emboj.2009.1 (2009).
125. Cirone, M., Di Renzo, L., Lotti, L. V. *et al.* Primary effusion lymphoma cell death induced by bortezomib and AG 490 activates dendritic cells through CD91. *PLoS One* **7**, e31732, doi:10.1371/journal.pone.0031732 (2012).
126. Fucikova, J., Kralikova, P., Fialova, A. *et al.* Human Tumor Cells Killed by Anthracyclines Induce a Tumor-Specific Immune Response. *Cancer Research* **71**, 4821-4833, doi:10.1158/0008-5472.can-11-0950 (2011).
127. Fucikova, J., Moserova, I., Truxova, I. *et al.* High hydrostatic pressure induces immunogenic cell death in human tumor cells. *International Journal of Cancer* **135**, 1165-1177, doi:10.1002/ijc.28766 (2014).
128. Gonias, S. L. & Campana, W. M. LDL Receptor–Related Protein-1. *The American Journal of Pathology* **184**, 18-27, doi:10.1016/j.ajpath.2013.08.029.
129. Gardai, S. J., McPhillips, K. A., Frasch, S. C. *et al.* Cell-surface calreticulin initiates clearance of viable or apoptotic cells through trans-activation of LRP on the phagocyte. *Cell* **123**, 321-334, doi:10.1016/j.cell.2005.08.032 (2005).
130. Basu, S., Binder, R. J., Ramalingam, T. & Srivastava, P. K. CD91 Is a Common Receptor for Heat Shock Proteins gp96, hsp90, hsp70, and Calreticulin. *Immunity* **14**, 303-313, doi:http://dx.doi.org/10.1016/S1074-7613(01)00111-X (2001).

131. Franchini, M. & Montagnana, M. in *Clinical Chemistry and Laboratory Medicine* Vol. 49 967 (2011).
132. Lillis, A. P., Van Duyn, L. B., Murphy-Ullrich, J. E. & Strickland, D. K. The low density lipoprotein receptor-related protein 1: Unique tissue-specific functions revealed by selective gene knockout studies. *Physiological reviews* **88**, 887-918, doi:10.1152/physrev.00033.2007 (2008).
133. Jacob, F., Novo, C. P., Bachert, C. & Van Crombruggen, K. Purinergic signaling in inflammatory cells: P2 receptor expression, functional effects, and modulation of inflammatory responses. *Purinergic Signalling* **9**, 285-306, doi:10.1007/s11302-013-9357-4 (2013).
134. Wilkin, F., Duhant, X., Bruyns, C. *et al.* The P2Y11 Receptor Mediates the ATP-Induced Maturation of Human Monocyte-Derived Dendritic Cells. *The Journal of Immunology* **166**, 7172-7177, doi:10.4049/jimmunol.166.12.7172 (2001).
135. Ferrari, D., La Sala, A., Chiozzi, P. *et al.* The P2 purinergic receptors of human dendritic cells: identification and coupling to cytokine release. *The FASEB Journal* **14**, 2466-2476, doi:10.1096/fj.00-0031com (2000).
136. la Sala, A., Ferrari, D., Corinti, S. *et al.* Extracellular ATP Induces a Distorted Maturation of Dendritic Cells and Inhibits Their Capacity to Initiate Th1 Responses. *The Journal of Immunology* **166**, 1611-1617, doi:10.4049/jimmunol.166.3.1611 (2001).
137. Wilkin, F., Stordeur, P., Goldman, M., Boeynaems, J.-M. & Robaye, B. Extracellular adenine nucleotides modulate cytokine production by human monocyte-derived dendritic cells: dual effect on IL-12 and stimulation of IL-10. *European Journal of Immunology* **32**, 2409-2417, doi:10.1002/1521-4141(200209)32:9<2409::AID-IMMU2409>3.0.CO;2-H (2002).
138. Štros, M. HMGB proteins: Interactions with DNA and chromatin. *Biochimica et Biophysica Acta (BBA) - Gene Regulatory Mechanisms* **1799**, 101-113, doi:http://dx.doi.org/10.1016/j.bbagrm.2009.09.008 (2010).
139. Yang, D., Postnikov, Y. V., Li, Y. *et al.* High-mobility group nucleosome-binding protein 1 acts as an alarmin and is critical for lipopolysaccharide-induced immune responses. *The Journal of Experimental Medicine* **209**, 157-171, doi:10.1084/jem.20101354 (2012).
140. Hock, R., Furusawa, T., Ueda, T. & Bustin, M. HMG chromosomal proteins in development and disease. *Trends in Cell Biology* **17**, 72-79, doi:http://dx.doi.org/10.1016/j.tcb.2006.12.001 (2007).
141. Apetoh, L., Ghiringhelli, F., Tesniere, A. *et al.* Toll-like receptor 4-dependent contribution of the immune system to anticancer chemotherapy and radiotherapy. *Nat Med* **13**, 1050-1059, doi:10.1038/nm1622 (2007).
142. Apetoh, L., Tesniere, A., Ghiringhelli, F., Kroemer, G. & Zitvogel, L. Molecular interactions between dying tumor cells and the innate immune system determine the efficacy of conventional anticancer therapies. *Cancer research* **68**, 4026-4030, doi:10.1158/0008-5472.can-08-0427 (2008).
143. Bechetoille, N., Dezutter-Dambuyant, C., Damour, O. *et al.* Effects of Solar Ultraviolet Radiation on Engineered Human Skin Equivalent Containing Both Langerhans Cells and Dermal Dendritic Cells. *Tissue Eng* **13**, 2667-2679, doi:doi:10.1089/ten.2006.0405 (2007).
144. Chung, E., Choi, H., Lim, J. E. & Son, Y. Development of skin inflammation test model by co-culture of reconstituted 3D skin and RAW264.7 cells. *Tissue Engineering and Regenerative Medicine* **11**, 87-92, doi:10.1007/s13770-013-1113-x (2014).
145. Zhang, T., Somasundaram, R., Berencsi, K. *et al.* Migration of cytotoxic T lymphocytes toward melanoma cells in three-dimensional organotypic culture is dependent on CCL2 and CCR4. *European Journal of Immunology* **36**, 457-467, doi:10.1002/eji.200526208 (2006).

146. Pouliot, R., Larouche, D., Auger, F. *et al. Reconstructed human skin produced in vitro and grafted on athymic mice1,2*, <http://ovidsp.ovid.com/ovidweb.cgi?T=JS&PAGE=reference&D=ovftf&NEWS=N&AN=00007890-200206150-00010> (2002).
147. David, Y. S. C., Claire, J., Sheila, M., John, W. H. & Amir, M. G. The development of a 3D immunocompetent model of human skin. *Biofabrication* **5**, 035011 (2013).
148. Souto, L. R. M., Rehder, J., Vassallo, J. *et al.* Model for human skin reconstructed in vitro composed of associated dermis and epidermis. *Sao Paulo Medical Journal* **124**, 71-76 (2006).

CHAPTER 2

Human CD1c$^+$ DCs are critical cellular mediators of immune responses induced by immunogenic cell death

Stefania Di Blasio[1], Inge M.N. Wortel[1,#], Diede A. G. van Bladel[1,*], Laura E. de Vries[1,#], Tjitske Duiveman-de Boer[1], Kuntal Worah[1], Nienke de Haas[1], Sonja I. Buschow[1,†], I. Jolanda M. de Vries[1,2], Carl G. Figdor[1], Stanleyson V. Hato[1]

[#]Equal contribution

[1]Department of Tumor Immunology, Radboud Institute for Molecular Life Sciences, Radboud University Medical Center, Nijmegen, the Netherlands

[2]Department of Medical Oncology, Radboud University Medical Center, Nijmegen, the Netherlands

[†]Current address: Department of Gastroenterology and Hepatology, Erasmus MC University Medical Center, Rotterdam, the Netherlands

Abstract

Chemotherapeutics, including the platinum compounds oxaliplatin (OXP) and cisplatin (CDDP), are standard care of treatment for cancer. Although chemotherapy has long been considered immunosuppressive, evidence now suggests that certain cytotoxic agents can efficiently stimulate anti-tumor responses, through the induction of a form of apoptosis, called immunogenic cell death (ICD). ICD is characterized by exposure of calreticulin and heat shock proteins (HSPs), secretion of ATP and release of high mobility group box 1 (HMGB1). Proper activation of the immune system relies on the integration of these signals by dendritic cells (DCs). Studies on the crucial role of DCs, in the context of ICD, have been performed using mouse models or human *in vitro*-generated monocyte-derived DCs, which do not fully recapitulate the *in vivo* situation.

Here, we explore the effect of platinum-induced ICD on phenotype and function of human blood circulating DCs. Tumor cells were treated with OXP or CDDP and induction of ICD was investigated. We show that both platinum drugs triggered translocation of calreticulin and HSP70, as well as the release of ATP and HMGB1. Platinum treatment increased phagocytosis of tumor fragments by human blood DCs and enhanced phenotypic maturation of blood myeloid and plasmacytoid DCs. Moreover, upon interaction with platinum-treated tumor cells, $CD1c^+$ DCs efficiently stimulated allogeneic proliferation of T lymphocytes. Together, our observations indicate that platinum-treated tumor cells may exert an active stimulatory effect on human blood DCs. In particular, these data suggest that $CD1c^+$ DCs are critical mediators of immune responses induced by ICD.

Introduction

Platinum-based chemotherapy is currently approved as first-line treatment for several malignancies, including colon and testicular cancer [1]. Besides a direct cytotoxic effect on tumor cells, some chemotherapeutic compounds are now recognized to have beneficial effects on the immune system, which may contribute to their clinical effectiveness [2-7]. Accordingly, a number of anti-cancer drugs, including the platinum-based compound oxaliplatin (OXP), were shown to be more effective against tumors established in immunocompetent, as opposed to immunodeficient mice [5]. This was predicated on the ability of these drugs to induce a form of cell death that activated the immune system and promoted anti-tumor immune responses. As such, these agents are referred to as immunogenic cell death (ICD)-inducers [8].

ICD-inducers cause severe cell stress, which activates distinct molecular pathways that can result in the induction of apoptosis [4]. Classically, ICD requires three molecular events, which may or may not be linked. First is the translocation of chaperone molecule calreticulin from the lumen of the endoplasmic reticulum (ER) to the cell surface (ecto-CRT) [9, 10]. Ecto-CRT serves as an "eat me" signal that marks tumor cells for engulfment by phagocytic cells [9]. Second is the active secretion of ATP into the extracellular environment, which acts as a chemoattractant for immune cells and directs the differentiation of myeloid precursors into inflammatory cells [11, 12]. Thirdly, release of high mobility group box 1 (HMGB1) into the extracellular milieu, which is required for optimal induction of T cell-mediated anti-tumor responses [13]. Other than the three 'hallmarks' of ICD, the ER-resident chaperones, heat shock proteins (Hsp) Hsp70 and Hsp90, are exposed on the membrane of cells undergoing severe stress. These molecules are not included in the canonical definition of ICD, nevertheless they also act as danger signals and might contribute to the stimulation of antigen-presenting cells (APCs) [14].

Induction of a systemic tumor-specific immune response by ICD requires the recognition and integration of these separate signals (ecto-CRT, ATP and HMGB1) into one command that drives T cell activation. Dendritic cells (DCs) are one of the main cell types that serve this role. They are the main APCs that link innate and adaptive immunity. DCs can encounter tumor cells in two ways. Firstly, the chemoattractants ATP and HMGB1 induce intratumoral recruitment of DCs [11]. Secondly, tumor cells that have detached from the tumor bulk are likely to enter blood circulation, facilitating their spread to distant locations in the body [15]. In the blood stream, these circulating tumor cells (CTCs) can encounter blood-circulating DCs. Platinum-induced exposure of ICD-markers might contribute to make CTCs "visible" and more sensitive to DC recognition. Indeed, treatment with well-known ICD-inducers, anthracyclines, induced ecto-CRT expression on CTCs *in*

vivo [16]. Chemotherapy treated-tumor cells are engulfed by immature DCs, which then undergo maturation. Mature DCs process and present tumor antigens to naïve cytotoxic lymphocytes, prompting anti-tumor responses[7, 16] . Accordingly, perturbation of key elements of adaptive immunity, such as *in vivo* depletion of dendritic cells (DCs), or knockout of DC receptors, resulted in failure to prime an anti-tumor response in chemotherapy-treated mouse models [5, 13, 17].

There are two major DC subsets circulating in human peripheral blood, myeloid DCs (mDCs) and plasmacytoid DCs (pDCs) [18]. Classically, myeloid DCs are subdivided into $CD16^+$, $CD1c^+$ and $CD141^+$ DCs, based on the expression of specific surface molecules [19]. However, genome-wide expression profile analysis recently suggested that $CD16^+$ DCs may represent a particular subset of monocytes, with DC-like properties [20]. For simplicity we will refer to them as $CD16^+$ DCs. Transcriptional, phenotypic and functional studies highlight significant differences between human blood DCs, suggesting a biological specialization of these DC subsets [21, 22]. Despite the great interest that ICD has gained in the past decade, the role of naturally occurring human DCs, especially for DCs that circulate in the blood, in this process is poorly understood, as most studies have been performed in murine models or with *in vitro* generated monocyte-derived DCs (moDCs) [11, 23]. Here we study induction of ICD in human tumor cells by two of the most widely used platinum compounds, OXP and cisplatin (CDDP), and how that affects human DC subsets. We report that, at clinically relevant concentrations, both compounds induced apoptosis of tumor cells, which was accompanied by the expression and release of ICD-associated molecules. Exposure of tumor cells to platinum drugs resulted in increased uptake of tumor fragments by naturally occurring blood DCs and stimulated DC maturation. Surprisingly, only $CD1c^+$ DCs were subsequently able to drive T cell proliferation.

Materials & Methods

Cell culture, transduction and stable cell line

Cells were cultured at 37°C, 5% CO_2. Human testicular carcinoma (2102EP and 833KE) and murine colon carcinoma (CT26) cell lines were cultured in RPMI 1640 (Gibco, Thermo Fisher Scientific, catalog# 42401-018), supplemented with 10% fetal calf serum (FCS, Greiner bio-one) and Ultra-glutamine (Lonza, catalog# BE17-605E/U1). Human melanoma (BLM and BLM-GFP) and colorectal adenocarcinoma (Caco-2) cells were cultured in Dulbecco's modified Eagle's medium (DMEM, Gibco, 31966-021), with 5% or 20% FCS, respectively. The Lenti6/Block-iT-shScramble (GFP) vector was a kind gift of Prof. Peter Friedl (RIMLS, The Netherlands). The specific scramble shRNA sequence has no homology to

any known mammalian gene. BLM cells were infected with lentiviral vector and (10µg/ml) polybrene and incubated at 37°C, 5% CO_2, overnight. Then medium was refreshed and cells were analyzed after 72h of treatment. Stable cell line was selected with 5µg/ml blasticidin.

Cell death induction and quantification

Tumor cells were treated with oxaliplatin (OXP, lot# R01730), cisplatin (cis-diamminedichloroplatinum(II), CDDP, lot# PR00202) (both Accord) or mitoxantrone (MTX, Sandoz, lot# D50333A) to induce cell death. Cell death was assessed by double staining with annexin V fluorescein isothiocyanate-FITC (AnnV-FITC, BD Bioscience, catalog# C34554) and DAPI (Sigma-Aldrich, catalog# 32670). Briefly, cells were collected, washed with PBS and incubated with AnnV-FITC (1:40), $CaCl_2$ (1M, 1:666) in PBS on ice, in the dark for 15min. An equal volume of DAPI in PBS (final concentration 1:2000) was added immediately prior measurement by flow cytometry.

Flow cytometric analysis of ecto-CRT and ecto-HSP70

$6x10^4$ tumor cells were let adhere in 24-well plates and treated with OXP or CDDP for 24 or 48 hours. Subsequently, cells were harvested with cold TEN buffer (40 mM Tris, 150 mM NaCl, 10 mM EDTA, pH 7.8), transferred to a 96-well plate and washed twice with PBA. After incubation with a Fc-receptor blocking buffer (2% human or murine serum in PBS, 15min at 4°C) cells were stained for 30min at 4°C with a primary antibody in PBA, followed by extensive washing and incubation with an Alexa488-conjugated monoclonal secondary antibody (Goat-anti-Mouse IgG1, Life Technologies, catalo#A-21121) in PBA for 20min at 4°C. Isotype-matched IgG antibodies were used as control. Surface expression of CRT (anti-CRT, clone ab2907, Abcam, catalog# ab2907; anti-CRT-PE, clone FMC 75, Enzo Life Sciences, catalog# ADI-SPA-601PE-F) and Hsp70 (anti-HSP70, clone C92F3A-5, Enzo Life Sciences, catalog# ADI-SPA-810-D) was analyzed by flow cytometry (Suppl. Table 1).

Detection of ATP and HMGB1 release

Tumor cells ($6x10^4$) were adhered in 24-well plates in 1ml of heat-inactivated complete medium and treated with OXP or CDDP for 24h or 48h. Supernatants were collected, dying floating cells removed by centrifugation and supernatants frozen immediately. ATP secretion was measured with the ENLITEN ATP Assay (Promega, catalog# FF2000) according to the manufacturer's protocol. HMGB1 release was assessed by enzyme-linked immunosorbent assay (ELISA, IBL International, catalog# ADI-SPA-810-D) according to manufacturer's instructions.

Isolation of human blood immune cells

Peripheral blood mononuclear cells (PBMCs) were isolated from buffy coats obtained from healthy volunteers (Sanquin) and purified via centrifugation over a ficoll density gradient (Axis-Shield) in SepMate tubes (Stemcell technologies). Isolation of human blood DC subsets was achieved by a sequence of negative and positive selection steps using magnetic beads (Human CD16+ Monocyte Isolation Kit, catalog# 130-091-765; Human CD1c+ (BDCA-1) Dendritic Cell Isolation Kit, catalog# 130-090-506; Human CD304+ (BDCA-4/Neuropilin-1) MicroBead Kit, catalog# 130-090-512; all Miltenyi Biotec). DC purity was assessed by staining with primary labeled antibodies (see also Suppl. Table 1): anti-CD1c-PE (Miltenyi biotec, clone AD5-8E7, catalog# 130-090-508), anti-CD11c-APC (Miltenyi biotec, clone MJ4-27G12, catalog# 130-092-412), anti-CD20-APC (eBioscience, clone 2H7, catalog# 17-0209), anti-CD15-FITC (Miltenyi biotec, clone VIMC6, catalog# 130-081-101), anti-CD56-PE (IQ Products, clone MOC-1, catalog# IQP-114R), anti-CD123-APC (Miltenyi biotec, clone AC145, catalog# 130-090-901) and anti-CD303-PE (Miltenyi biotec, clone AC144, catalog# 130-090-511). Purity levels higher than 98% were achieved, determined by flow cytometry. Peripheral blood leukocytes (PBLs) were isolated from PBMCs by depletion of monocytes via adherence to plastic culture flasks (1 hour at 37°C). Floating cells (PBLs) were collected and resuspended in X-VIVO-15 medium (Lonza, catalog# BE04-418Q) supplemented with 2% human serum (HS, Sanquin).

Microarray data

For the analysis publically available affymetrix, CEL files containing expression data of resting human pDCs, $CD1c^+$ and $CD16^+$ were downloaded from ArrayExpress (accession: E-TABM-34). Data have been published by others [50]. Raw files were processed in the R programming environment and intensity values across the different datasets were normalized using the RMA normalization function of the affy package [51]. Specific annotation packages for human were used to map array probe identifiers to corresponding species specific gene symbols. In case of redundant probes, the probes with highest summed intensity of all samples were considered. The normalized log2 transformed datasets was z-scored (setting the data to a mean=0 and a variance=1) and heat maps were generated using freely availably GeneE program (http://www.broadinstitute.org/).

Immunofluorescence

For evaluation of CRT expression, BLM cells were cultured on glass coverslips and treated overnight with 50μM OXP, 66μM CDDP, 1uM MTX or left untreated. Cells were washed, fixed in 0.25% paraformaldehyde (PFA) in PBS for 5min at RT. Cells were blocked and subsequently incubated with wheat germ agglutinin-biotinylated

(WGA) for 45min at 4°C. After extensive wash, cells were stained with primary anti-CRT antibody (Abcam, clone ab2907, Suppl. Table 1) in cold confocal laser scanning microscope (CLSM) buffer (3% bovine serum albumin, 50mM Glycine in PBS) for 30min at RT, followed by incubation with secondary Alexa conjugates in cold CLSM blocking buffer, for 20min at RT. Cells were then fixed in 4% PFA/PBS for 20min at RT. Nuclei were stained with DAPI (1:3000) in CLSM for 5min at RT. Samples were imaged with an Olympus FV1000 Confocal Laser Scanning Microscope. Images were analyzed using the open source-imaging platform, Fiji (imageJ 64 Bit for Windows).

Co-cultures and uptake assays

Tumor cells were stained with 2μM of the fluorescent probe 5(6)-Carboxyfluorescein diacetate N-succinimidyl ester (CFSE, Invitrogen, Thermo Fisher Scientific, catalog# C34554), according to manufacturer's instructions. Fluorescently–labelled (CFSE or GFP) tumor cells were seeded in T75 flasks (Corning), adhered and treated with OXP or CDDP. After treatment, tumor cells ($5x10^5$ cells, target) and DCs ($5x10^5$ cells, effector) were cocultured at a 1:1 ratio in Falcon tubes (BD Falcon) in X-VIVO-15 supplemented with 2% HS (final concentration $1x10^6$/ml). Co-cultures were stained with an APC-labeled primary antibody recognizing a specific DC surface marker (CD11c for CD1c$^+$ and CD16$^+$ DCs, CD123 for pDCs; see also Suppl. Table 1) and analyzed by flow cytometry. Extent of phagocytosis was determined as the percentage of double positive events (i.e. CD11c$^+$ or CD123$^+$-APC/GFP$^+$ or CFSE$^+$). For blocking experiments, tumor cells were pre-incubated (30min at 4°C) with blocking agents or negative controls: CRT blocking peptide (20 μg/mL, MBL International, catalog# JM-3077BP-50), irrelevant gp100 peptide$_{272\text{-}300}$ (20 μg/mL, JPT), anti-CD91 (20 μg/mL, Thermo Fisher Scientific, clone 8G1, catalog# MA1-27198) or IgG1,k (20 μg/mL, Biolegend, clone MG1-45). Extra volume blocking agents or matched controls were added to co-cultures at same final concentration.

Flow cytometric analysis of DC maturation

Phenotypical assessment of DC maturation after 48h of coculture with tumor cells was performed by flow cytometry. Briefly, cells were washed in PBA, incubated with Fc-receptor blocking buffer (2% HS in PBS, 15min at 4°C) and subsequently stained with primary antibodies in PBA (30min at 4°C). Monoclonal directly labeled anti-human antibodies used were (Suppl. Table 1): anti-CD11c-APC (Miltenyi biotec, clone MJ4-27G12, catalog# 130-092-412), anti-CD123-APC (Miltenyi biotec, clone AC145, catalog# 130-090-901), anti-CD80-PECy7 (BD Pharmingen, clone L307.4, catalog# 561135), anti-CD86-PECy7 (BD Pharmingen, clone 2331, catalog# 561128), anti-HLA-ABC-PE (BD Pharmingen, clone G46-2.6, catalog# 555553) and anti-HLA-DR-PE (BD Pharmingen, clone G46-6, catalog# 555812). Appropriate isotype controls

were included. Geometric mean fluorescence intensity (GeoMFI) of maturation markers was assessed on CD11c$^+$ (for CD1c$^+$ and CD16$^+$ DCs) or CD123$^+$ (for pDCs) populations. As a positive control, DCs were stimulated with poly I:C (CD1c$^+$ and CD16$^+$ DCs, 2 µg/mL, Enzo Life Science, catalog# ALX-746-021-M005) or R848 (pDCs, 4 µg/mL, Enzo Life Science, catalog# ALX-420-038-M025). To improve *in vitro* pDC viability, IL-3 (10 ng/mL, Cellgenix, catalog# 1002-050) was added to culture medium.

Cytokine quantification

Supernatants from tumor cell-DC cocultures (18 hours) were collected, dying floating cells removed by centrifugation and supernatants frozen immediately for detection of secreted cytokines. Human Th1/Th2 cytokines (IFN-γ, IL-2, IL-4, IL-5, IL-10, IL-12 (p70), TNF-α and TNF-β) were quantified with a multiplex FlowCytomix kit (eBioscience, BMS810FF) according to the manufacturer's instructions.

DC sorting and Mixed Lymphocyte Reaction (MLR)

Tumor-DC co-cultures were established as described above. After wash in cold wash buffer (PBS/0.1% BSA/5mM EDTA) and incubation in Fc-receptor blocking buffer (2% HS in wash buffer, 15min at 4°C), cells were stained with sterile primary antibodies in wash buffer (20min at 4°C). The following antibodies were used (Suppl. Table 1): anti-HLA-DR-PECy7 for all subsets (BD Biosciences, clone L243, catalog# 335813), anti-CD1c-PE for CD1c$^+$ DCs (Miltenyi biotec, clone AD5-8E7, catalog# 130-090-508), anti-CD16-APC for CD16$^+$ DCs (Miltenyi biotec, clone VEP13, catalog# 130-098-101) and anti-CD304-PE for pDCs (Miltenyi biotec, clone AD5-17F6, catalog# 130-090-533). Sorting of DCs was performed using a Fluorescence Activated Cell Sorter Aria (FACSAria, BD Bioscience), based on FSC/SSC properties and positivity for DC markers (Suppl. Fig 5). Allogeneic PBLs were stained with 5µM CFSE (Invitrogen), according to manufacturer's instructions and added to the sorted DCs at a ratio of 5:1 (Lymphocytes:DCs), for an additional period of 5 days, in 2% HS X-VIVO-15. After 5 days, co-cultures were stained with a primary anti-CD3-BV421 antibody (BD Horizon, clone SK7, catalog# 563798) and analyzed by flow cytometry. The percentage of proliferating T cells (CD3$^+$) was determined by assessing CFSE dilution in the fraction of CD3$^+$ cells.

Statistical analysis

Unless otherwise indicated, experiments were performed at least three times, yielding comparable results. Data were analyzed by means of Prism v. 5.03 (GraphPad Software). Statistical significance was assessed by One-way Anova, followed by a Dunnett's post-test or Two-way Anova, followed by a Bonferroni's post-test, as appropriate. *P*-values <0.05 were considered as statistically significant.

Results

Cisplatin and oxaliplatin induce a form of cancer cell death consistent with ICD

Up till now most studies on induction of ICD by platinum compounds, OXP and CDDP were performed in mouse models and little is known about the ability of platinum compounds to induce ICD in human tumor cells[5, 9]. We investigated the molecular hallmarks of platinum-induced cancer cell death *in vitro*. We treated human colon (Caco2), testicular (833KE and 2102EP) and melanoma (BLM) cell lines with increasing, clinically relevant doses of OXP or CDDP and studied cell death using Annexin V and DAPI staining. Both OXP and CDDP decreased viability of BLM cells in a time- and dose-dependent manner (Fig 1a,b), as indicated by increased phosphatidylserine exposure and stronger nuclear DAPI staining. Similar cytotoxicity was observed for 833KE, 2102EP and Caco-2 cells (data not shown). Given the chemosensitivity of testicular carcinoma cells, 833KE and 2102EP cell lines were treated with lower drug concentrations, compared to the other cell lines studied. Despite sharing similar mechanisms of action, OXP, but not CDDP, was previously described to trigger exposure of ecto-CRT on the murine colon cancer cell line CT26 [5]. Surprisingly, we observed similar, if not stronger translocation of ecto-CRT after BLM and Caco-2 cells were exposed to CDDP compared to OXP (Fig 1c,d; Suppl. Fig 1b). Analysis of expression kinetics on BLM cells showed that ecto-CRT was detected as early as 1 hour after treatment and its exposure was dose- and concentration dependent (Fig 1c, Suppl. Fig 1a). On the other hand, OXP and CDDP had less marked effects on the translocation of ecto-CRT in 833KE, 2102EP and CT26 cell lines, at time and dosage tested (Fig 1d,e; Supp. Fig 1b,c).

In order to simulate the pharmacokinetics of platinum treatment, which is administered intravenously and remain in the body for a few hours [24], we exposed cells to OXP or CDDP for 8 hours, washed away the drug and cultured the cells for an additional 40 hours under drug-free conditions. This short-term drug exposure to OXP or CDDP dose-dependently decreased viability of BLM cells and induced ecto-CRT expression (Fig 1f,g), similar to long-term (48 hours) treatment (Fig 1b,c).

Next, we measured the expression of Hsp70, ATP and HMGB1 on different tumor cell lines treated with platinum drugs. Both OXP and CDDP induced translocation of Hsp70 (ecto-Hsp70) to the cell surface of human BLM, 833KE and 2102EP cells, as well as the murine CT26 cell line as observed using flow cytometry (Fig 2a-c, Suppl. Fig. 2a,d). Concurrent with increased ecto-HSP70, we observed increased secretion of ATP (Fig 2d-f, Suppl. Fig. 2b) and HMGB1 (Fig 2g-i, Suppl. Fig. 2c,e) in the supernatant of platinum-treated tumor cells. In all, we show that both OXP and CDDP cause apoptosis of human tumor cells, with the concomitant translocation

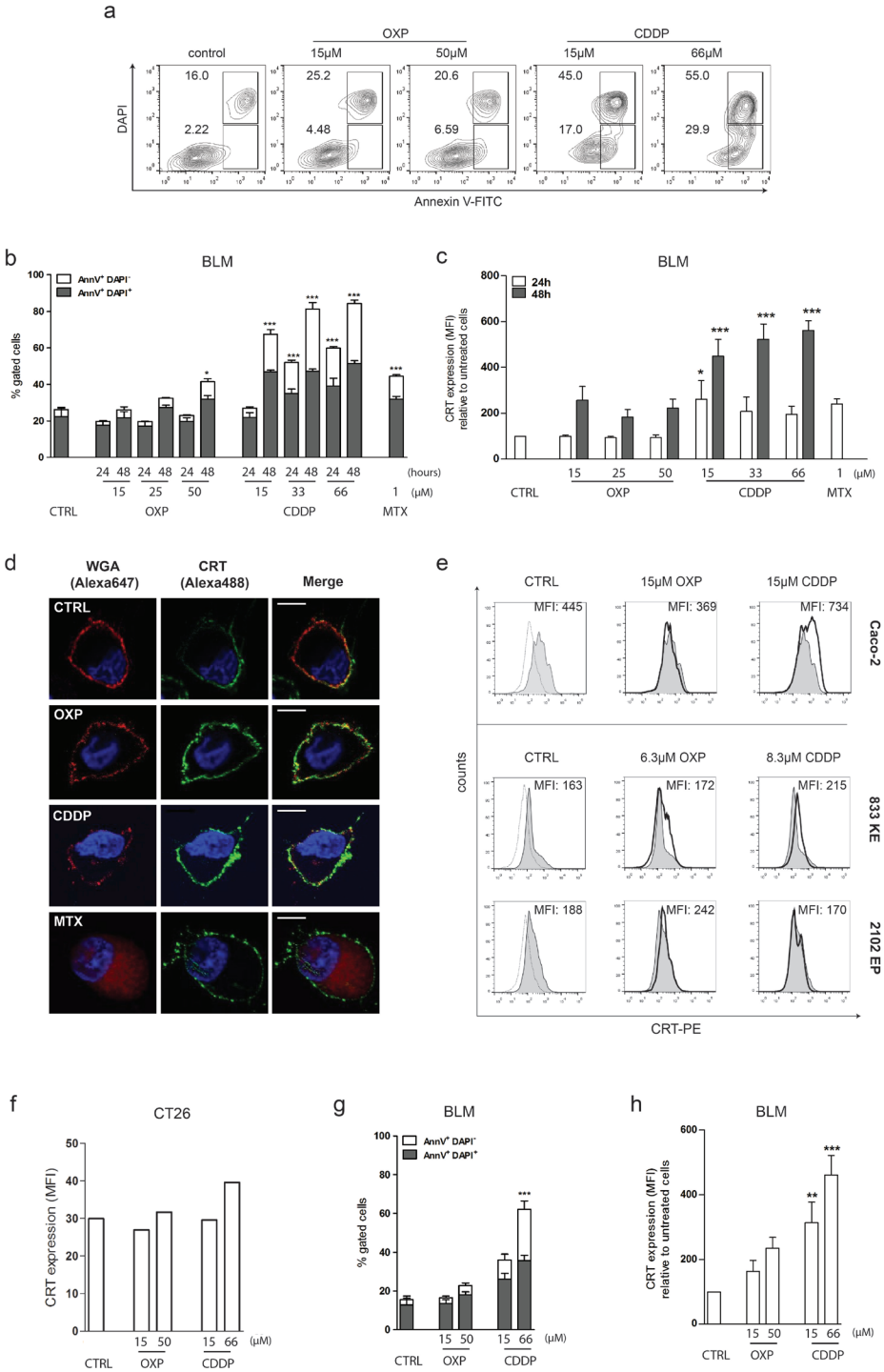
a
control
OXP
15μM
50μM
CDDP
15μM
66μM
16.0
2.22
25.2
4.48
20.6
6.59
45.0
17.0
55.0
29.9
DAPI
Annexin V-FITC
b
BLM
AnnV+ DAPI-
AnnV+ DAPI+
% gated cells
24 48 24 48 24 48 24 48 24 48 24 48 (hours)
15 25 50 15 33 66 1 (μM)
CTRL
OXP
CDDP
MTX
c
BLM
24h
48h
CRT expression (MFI) relative to untreated cells
15 25 50 15 33 66 1 (μM)
CTRL
OXP
CDDP
MTX
d
WGA (Alexa647)
CRT (Alexa488)
Merge
CTRL
OXP
CDDP
MTX
e
CTRL
15μM OXP
15μM CDDP
MFI: 445
MFI: 369
MFI: 734
Caco-2
CTRL
6.3μM OXP
8.3μM CDDP
MFI: 163
MFI: 172
MFI: 215
833 KE
MFI: 188
MFI: 242
MFI: 170
2102 EP
counts
CRT-PE
f
CT26
CRT expression (MFI)
15 50 15 66 (μM)
CTRL
OXP
CDDP
g
BLM
AnnV+ DAPI-
AnnV+ DAPI+
% gated cells
15 50 15 66 (μM)
CTRL
OXP
CDDP
h
BLM
CRT expression (MFI) relative to untreated cells
15 50 15 66 (μM)
CTRL
OXP
CDDP

of ecto-CRT and ecto-HSP and the extracellular release of ATP and HMGB1. These results suggest that both platinum compounds induce a form of cell death that fulfils the requirements for immunogenic apoptosis.

Human DCs preferentially phagocytose platinum-treated tumor cells in a CRT-dependent manner

We investigated whether platinum-induced ecto-CRT had an effect on the recognition and uptake of tumor cells by human blood DCs [9]. First, we examined whether treatment with platinum drugs led to increased interaction between tumor cells and human blood DCs using confocal microscopy. For this experiment, the human melanoma cell line BLM was modified to stably express the fluorescent protein GFP (hereafter referred to as BLM-GFP). Untreated BLM and BLM-GFP showed no difference in surface expression of calreticulin (CRT). Furthermore, platinum-treatment induced comparable upregulation of CRT on both BLM and BLM-GFP (Suppl. Fig 3a). Tumor cells were left untreated or treated with OXP or CDDP for 48 hours and then co-cultured with $CD1c^+$ DCs for 3 hours. We observed increased interaction between DCs and tumor cells treated with CDDP or OXP compared to untreated cells (Fig 3a, b). Based on the fact that tumor cells are several orders of magnitude larger than blood DCs, we hypothesized that DCs, in contrast to macrophages, do not ingest whole tumor cells but only subcellular fragments of these cells. To evaluate whether fragments of platinum-treated cells are preferentially

◀ **Figure 1. Sensitivity of tumor cell lines to platinum drugs and platinum-mediated exposure of ecto-CRT. (A, B)** Frequency of apoptotic (Annexin V^+ $DAPI^-$) and secondary necrotic (Annexin V^+ $DAPI^+$) BLM cells after treatment with OXP or CDDP. Human melanoma BLM cells were cultured with platinum drugs or left untreated, for 24h or 48h. Cells were stained with Annexin-V-FITC and DAPI and analyzed by flow cytometry. Data are presented as representative contour plot (A) or mean±SEM (at least *n*=2, performed in duplicates) (B). **(C, E, F)** CRT exposure was assessed on Annexin V^+ $DAPI^-$ cells after treatment with OXP or CDDP by flow cytometry. BLM cells were treated as described above. Data are relative mean±SEM (at least *n*=3, in duplicates) (C). Representative histograms show CRT expression (MFI) on human colon (Caco-2) and testicular (833KE and 2102EP) cancer cell lines following 24h of treatment with OXP or CDDP. Caco-2 were treated with 15μM of OXP or CDDP; 833KE and 2102EP were treated with 6.3μM OXP or 8.3μM CDDP. Isotype (grey line), control (grey filled histogram), treatment (black thick line) (E). Exposure of CRT on murine colon cancer CT26 cells was assessed after 24h of treatment with 15μM of OXP or CDDP. Data are means of duplicates of one representative experiment (F). (D) CRT expression was confirmed by confocal microscopy. BLM cells were stained with an anti-CRT antibody and the membrane marker, wheat germ agglutinin (WGA). Scale bar 10 μm. **(G, H)** Frequency of apoptotic *vs.* necrotic cells (G) and CRT exposure (H) on BLM cells, after short-term (8h) drug exposure to OXP or CDDP, at indicated doses. Results are mean±SEM (*n*=3 in duplicates). Significance was determined with One-way ANOVA, *P < 0.05, ***P < 0.001, as compared to control (CTRL) cells.

taken up by the three human DC subsets examined in this study, we established *in vitro* co-cultures of platinum-treated tumor cells and DCs. Tumor cells were exposed to OXP or CDDP. Concentration and duration of treatment with platinum drugs were specifically chosen for each cell line in order to maximize induction of ICD hallmarks, while maintaining cell viability at the start of the co-culture. Fluorescently labelled-tumor cells were co-cultured with DCs for 24 or 48 hours. Uptake of untreated versus OXP- or CDDP-treated tumor cells was assessed by flow cytometry (Fig 3c-f, Suppl. Figure 3). In order to distinguish between binding of tumor cells fragments to the cell membrane of DCs and active uptake, we performed co-culture experiments at 4°C *versus* 37°C, respectively. As shown in Figure 3c, DCs are capable of taking up (37°C) fragments of tumor cells. In contrast, there is a low level of binding (4°C) of tumor fragments to DCs, which did not increase upon treatment (Fig 3c, Suppl. Fig 3c). Furthermore, while there was a considerable increase in the uptake of platinum treated cells between 24 and 48 hours of co-culture, uptake of control cells was not markedly increased in time (Fig 3d).

Distinct DC subsets have different capacities to phagocytose soluble and cell-associated tumor antigens[22]. We therefore tested the capacity of $CD1c^+$ DCs, $CD16^+$ DCs and pDCs to take up OXP- or CDDP-treated tumor cells. Treatment of BLM cells with CDDP led to a significant increase in the uptake of tumor fragments by all DC subsets. Plasmacytoid DCs were the least efficient DC subset in engulfing tumor-derived particles, whereas $CD1c^+$ and $CD16^+$ DCs were more proficient (Fig 3e). These results were consistent across different cell lines (833KE, 2102EP and Caco2) used in the co-culture with $CD1c^+$ and $CD16^+$ DCs (Fig 3f). OXP was less potent than CDDP in inducing uptake of BLM cells (Fig 3e), in contrast to the other cell lines tested, for which OXP was slightly more potent than CDDP (Fig 3f). These differences might be due to differences in drug uptake in the different cell lines.

We wondered whether uptake of tumor fragments was solely dependent on CRT expression and thus performed the uptake experiment in the presence of a CRT-blocking peptide [25, 26]. An irrelevant peptide (derived from gp100) or a mouse isotype antibody were used as negative controls (Fig 4a, Suppl. Fig 3d). As expected, the irrelevant peptide, as well as, the non-specific IgG control, did not affect phagocytic ability of $CD1c^+$ DCs. However, engagement of ecto-CRT with a CRT-blocking peptide completely abolished uptake of tumor cells, including those treated with platinum drugs. This observation confirmed the crucial role played by CRT in directing tumor cell fragment uptake. The most commonly described receptor for ecto-CRT is the low-density lipoprotein receptor-related protein 1 (LRP1), also known as CD91 [27]. The expression of CD91 on distinct human blood circulating DC subsets has not been characterized before, thus we analyzed CD91 expression on $CD1c^+$ DCs, $CD16^+$ DCs and pDCs by flow cytometry. Monocytes ($CD14^+$) were previously

shown to express CD91 and were used as a positive control (Fig 4b) [28]. Both CD1c$^+$ and CD16$^+$ DCs, as well as monocytes, clearly expressed the ecto-CRT receptor. On the other hand, and consistent with the low uptake of chemotherapeutically induced tumor cell fragments, pDCs showed little-to-no expression of CD91. We observed a similar trend looking at the transcriptomes of these DC subsets (Fig 4c). mRNA levels of CD91 were highest in CD16$^+$ and CD1c$^+$ DCs, whereas pDCs showed the lowest expression. Subsequent blocking of CD91 on CD1c$^+$ DCs, with a specific anti-CD91 blocking antibody, however, did not affect phagocytosis of tumor cells, despite its high expression levels (Fig 4d). To complement this analysis, we also investigated the expression of alternative receptors for ecto-CRT. Both the scavenger

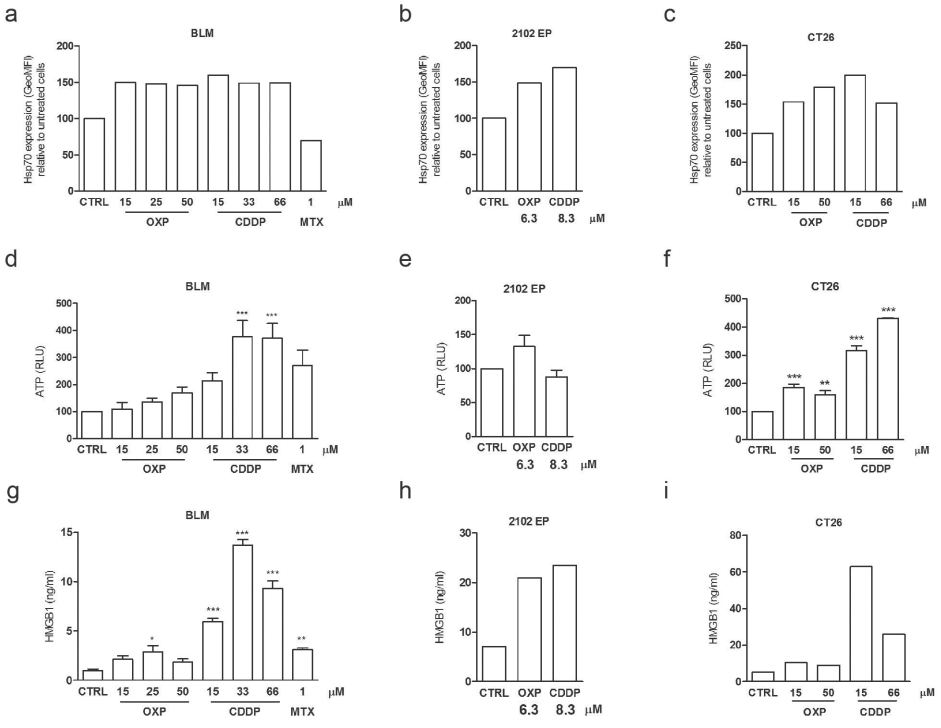

Figure 2. Platinum drugs induce release of immunogenic signals for DCs stimulation. (A, B, C) Surface expression of Hsp70 on BLM (A), 2102EP (B) and CT26 (C) cells, after platinum treatment, was assessed on Annexin V$^+$ DAPI$^-$ cells by flow cytometry. Cells were cultured with OXP or CDDP at indicated doses, for 24h (2102EP and CT26) or 48h (BLM). Data are presented as mean (n=2). (D, E, F) Extracellular ATP was measured by luciferase assay, in supernatants of cells cultured as described above. Results represent relative means±SEM (at least n=2, done in duplicates). (G, H, I) Elisa detection of HMGB1 release in supernatant of cells cultured as described above. Data are means±SEM (at least n=2). Significance was determined with One-way ANOVA, *P < 0.05, **P < 0.01, ***P < 0.001, as compared to control (CTRL) cells.

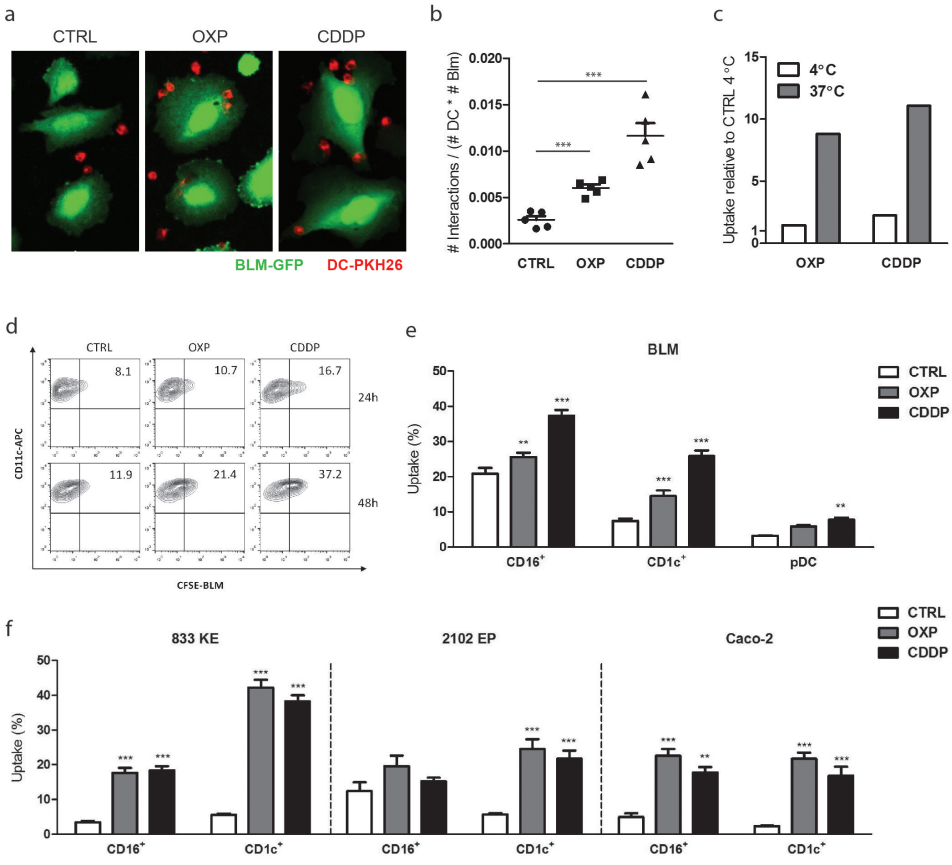

Figure 3. Platinum-treatment increases phagocytosis of tumor cells by human DC subsets. (A, B) BLM-GFP cells were treated with 15μM OXP or CDDP for 48h and co-cultured with CD1c$^+$ DCs (pre-labeled with PKH26) for 3h. Representative confocal image (A) and quantification (B) of BLM-DC interactions. A total of 5 images per sample were taken and the number of interactions was normalized over the number of DC and BLM cells present in the image. Data represent mean±SEM of 1 representative experiment. (C) Percentage of uptake (48h co-culture, 37°C, grey bar) of 15μM OXP or CDDP treated-BLM cells by CD1c$^+$ DCs *versus* binding (4°C, white bar). Values are relative to binding of control (CTRL) BLM cells and show mean (n=2). (D) Representative contour plot of control (CTRL) or platinum treated-BLM cells uptake by CD1c$^+$ DCs upon 24 or 48 hours of co-culture. (E, F) Percentage of phagocytosis of BLM (E), 833 KE, 2102 EP, Caco2 (F) human tumor cell lines by different DC subsets (CD16$^+$, CD1c$^+$ and pDCs). BLM and Caco-2 were treated with 15μM of OXP or CDDP for 48h; 833KE and 2102EP were treated with 6.3μM OXP or 8.3μM CDDP for 24h. CTRL (white bar) or treated tumor cells (grey or black bars) were co-cultured with DCs for 48h and extend of uptake was assessed by flow cytometry. The graph shows the mean±SEM (at least n=2, in duplicate). Significance was determined by Two-way ANOVA, **P < 0.01, ***P < 0.001, as compared to CTRL cells.

receptor class-A (SR-A, also known as CD204) and the scavenger receptor expressed by endothelial cell-1 (SREC-I) were reported to bind ecto-CRT[29, 30]. Transcriptomic analysis of SR-A and SREC-I revealed that these receptors are variably expressed on blood DC subsets, with CD1c+ DCs again showing the highest expression (Fig 4c). Taken together, our data demonstrate that blood DCs take up platinum-treated tumor cells more efficiently than untreated cells and this uptake is strictly dependent

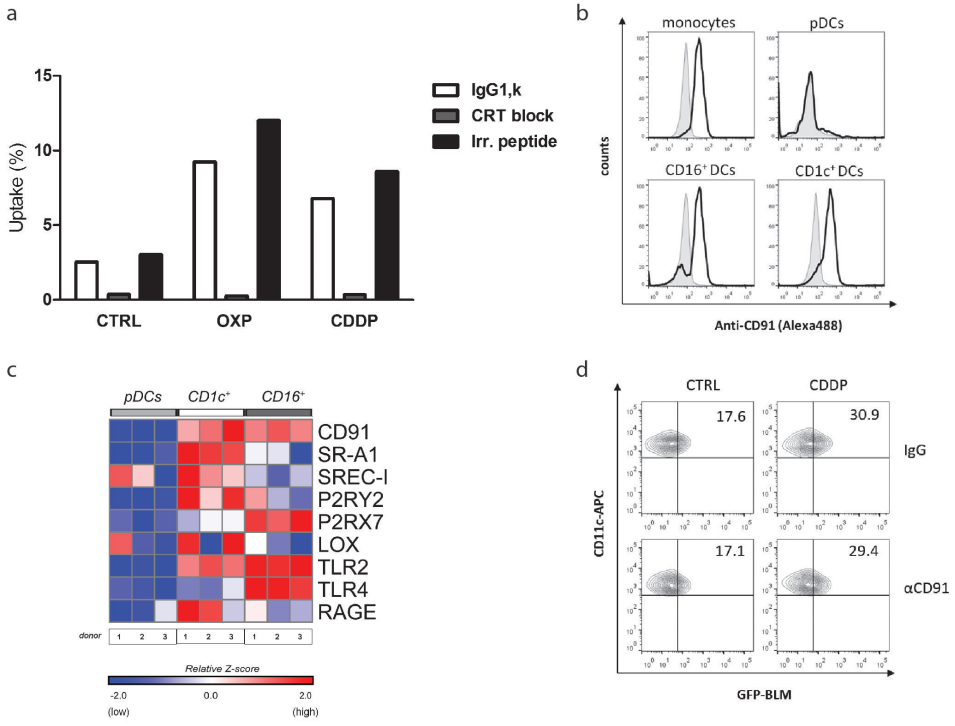

Figure 4. Human DCs take up platinum-treated tumor cells in a CRT-dependent manner. (A) Percentage of uptake of 15μM OXP or CDDP treated-BLM cells by CD1c+ DCs. Control or treated tumor cells were co-cultured with DCs in the presence of isotype (white bar), CRT blocking peptide (grey bar) or irrelevant tumor antigen (gp100) peptide (black bar) for 2h. Extent of uptake was assessed by flow cytometry. Data show means of duplicates of one representative experiment. **(B)** Representative histograms showing CD91 expression on human monocytes (CD14+) and DCs (CD16+, CD1c+ and pDCs). Isotype (grey filled histogram), anti-CD91 (black thick line). **(C)** Heatmap of relative mRNA expression levels of genes in human DC subsets. Heatmap shows the normalized expression of genes (Z-scores) in CD16+, CD1c+ and pDCs. Data are represented from 3 healthy donors. **(D)** Representative contour plot of CTRL or CDDP (15μM, 48h) treated-BLM cells uptake by CD1c+ DCs upon functional blocking of CD91 on DCs. BLM cells and DCs were co-cultured overnight in the presence of isotype control or CD91-blocking antibody. Percentage of phagocytosis was assessed by flow cytometry.

on CRT exposure. Additionally, while we observed uptake of tumor fragments by all DC subsets, they differentially express receptors capable of binding ecto-CRT.

Phagocytosis of platinum-treated tumor cells induces maturation of human DC subsets

Next, we investigated whether the CRT-mediated uptake of tumor cells fragments may lead to DC maturation. The transcriptomes of DCs for receptors that sense danger signals released by dying tumor cells were assessed. $CD1c^+$ DCs showed the highest mRNA expression levels of the P2RY2 (recognizing ATP), LOX-1 (HSPs) and RAGE (HMGB1) receptors; as well as, of the common receptors for HSPs and HMGB1 (TLR2) (Fig 4c). Exceptions were P2RX7 (ATP) and TLR4 (HSPs and HMGB1), for which $CD16^+$ DCs had higher mRNA expression levels (Fig 4c). On the other hand, pDCs showed the lowest expression of all these receptors on mRNA level (Fig 4c).

Following co-culture with platinum treated tumor cells, we measured surface expression of several markers on DCs, involved in antigen presentation and co-stimulation (Fig 5). As a positive control, DCs were stimulated with TLR ligands (poly I:C (pI:C) or R848). Co-culture of DCs with platinum-treated BLM cells induced a significant upregulation of co-stimulatory molecules, CD80 and CD86. Although pDCs were less efficient in taking up tumor fragments (Fig 3e), upregulation of co-stimulatory molecules (CD80 and CD86) was more prominent in pDCs than $CD1c^+$ or $CD16^+$ DCs (Fig 5a), despite the lower expression of receptors recognising the dying cell fragments on these cells. In addition, we analyzed the expression of major histocompatibility complex (MHC) classes I and II, required for antigen presentation to T cells. Platinum-treatment only moderately influenced MHC I and II expression on DC subsets (Fig 5b). We observed similar effects of platinum treatment for 2102EP (Fig 6a,b) and 833KE (Fig 6c,d) cells co-cultured with $CD1c^+$ or $CD16^+$ DCs.

In addition to phenotypical maturation, we tested cytokine secretion in the supernatant of tumor-DC co-cultured overnight upon induction of ICD (Fig 5c,d). $CD1c^+$ DCs markedly increased the production of the proinflammatory cytokine, TNF-α, as well as the anti-inflammatory cytokine, IL-10, in response to interaction with both OXP- and CDDP treated BLM cells. On the other hand, $CD16^+$ DCs and pDCs showed no significant response to platinum-treated tumor cells. Furthermore, we could not detect any IL-2, IL-4, IL-5, IL-12, TNF-β and IFN-γ (data not shown).

Platinum-treated tumor cells stimulate human $CD1c^+$ DCs to induce a T cell response

Co-culture of DCs with different platinum-treated tumor cell lines (BLM, 2102 EP and 833KE) led to uptake of tumor cells and subsequent maturation of DC. Next, we investigated the ability of these mature DCs to stimulate allogeneic T cell

proliferation. Proliferation of CD3+ T cells was quantified by measuring CFSE dilution in a Mixed Lymphocyte Reaction (MLR) (Fig 7a, Suppl. Fig 5). As shown in Fig 7b,

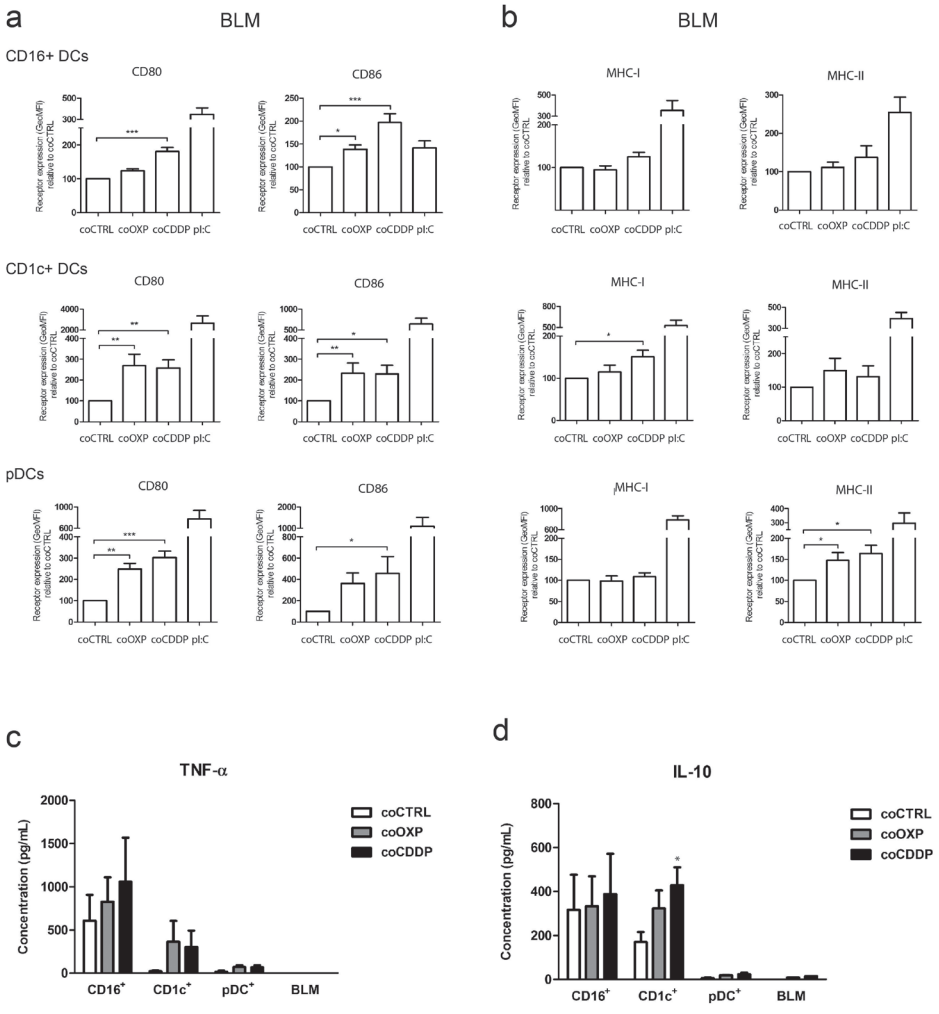

Figure 5. Phagocytosis of platinum-treated BLM cells induces maturation of human DC subsets. (A, B) The expression of maturation markers on DC subsets (CD16+, CD1c+ and pDCs) following 48h of co-culture with control or platinum treated BLM cells. DC stimulated with TLR ligands (4µg/ml R848 for pDCs and 2µg/ml poli(I:C) for CD16+ and CD1c+) were used as positive controls. The expression levels were determined by flow cytometry and depicted as GeoMFI values, relative to those of the co-culture with control tumor cells (coCTRL). The graphs show the mean±SEM (*n*=7). Significance was determined by One-way ANOVA, * *P*< .05, **P < 0.01, ***P < 0.001. (C, D) TNF-α and IL-10 production was analyzed in supernatants of overnight co-cultured pre treated-BLM and DCs by a multiplex FlowCytomix kit. Significance was determined by two-tailed *t*-test, * *P*< .05.

CD16+ DCs were not able to induce significant T cell proliferation in any of the conditions tested. On the other hand CD1c+ DCs co-cultured with OXP- or CDDP-treated tumor cells, showed a significant increase in T cell proliferation compared to untreated cells. Plasmacytoid DCs were able to induce allogeneic T cell proliferation but there was no difference between pDCs co-cultured with untreated cells or

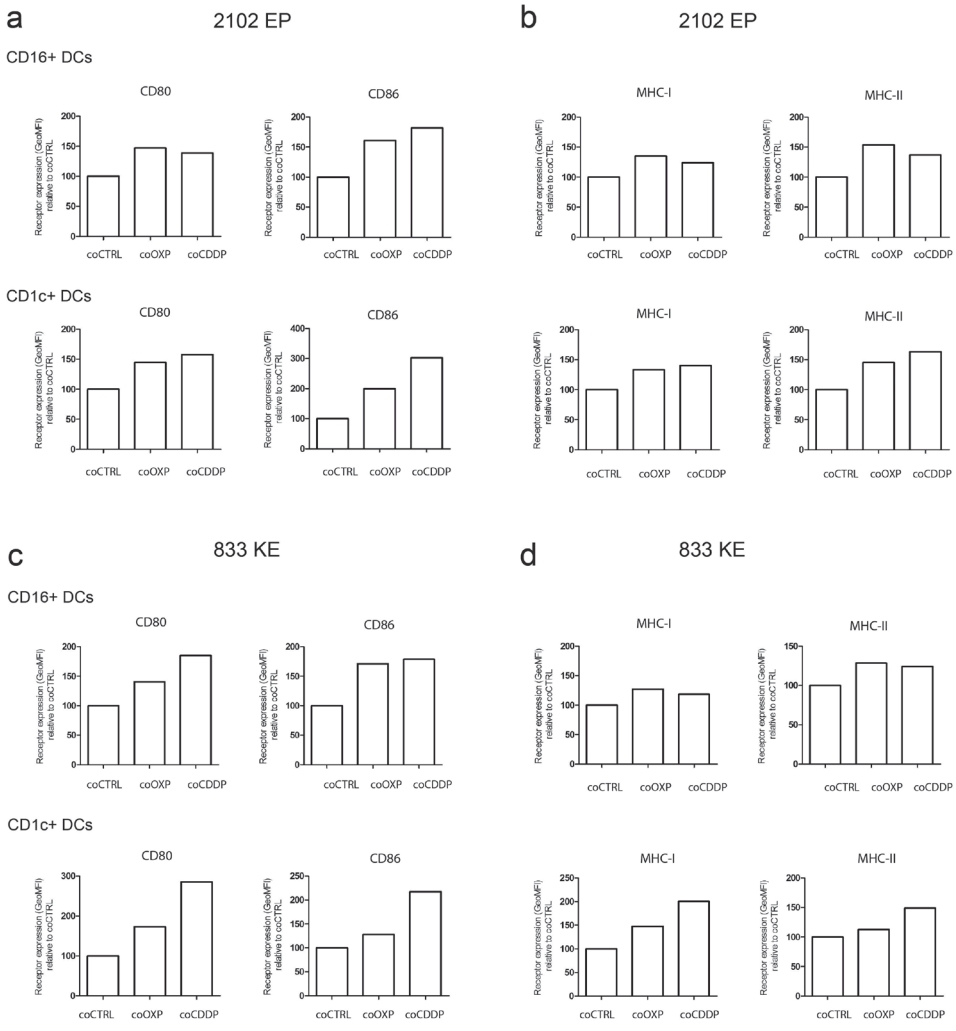

Figure 6. Phagocytosis of platinum-treated testicular cancer cells induces maturation of human DC subsets. The expression of maturation markers on DC subsets (CD16+, CD1c+ and pDCs) following 48h of co-culture with control or platinum treated 2102EP (A, B) or 833KE (C, D) cells. The expression levels were determined by flow cytometry and depicted as GeoMFI values, relative to those of the co-culture with control tumor cells (coCTRL). The graphs show the mean (*n*=2).

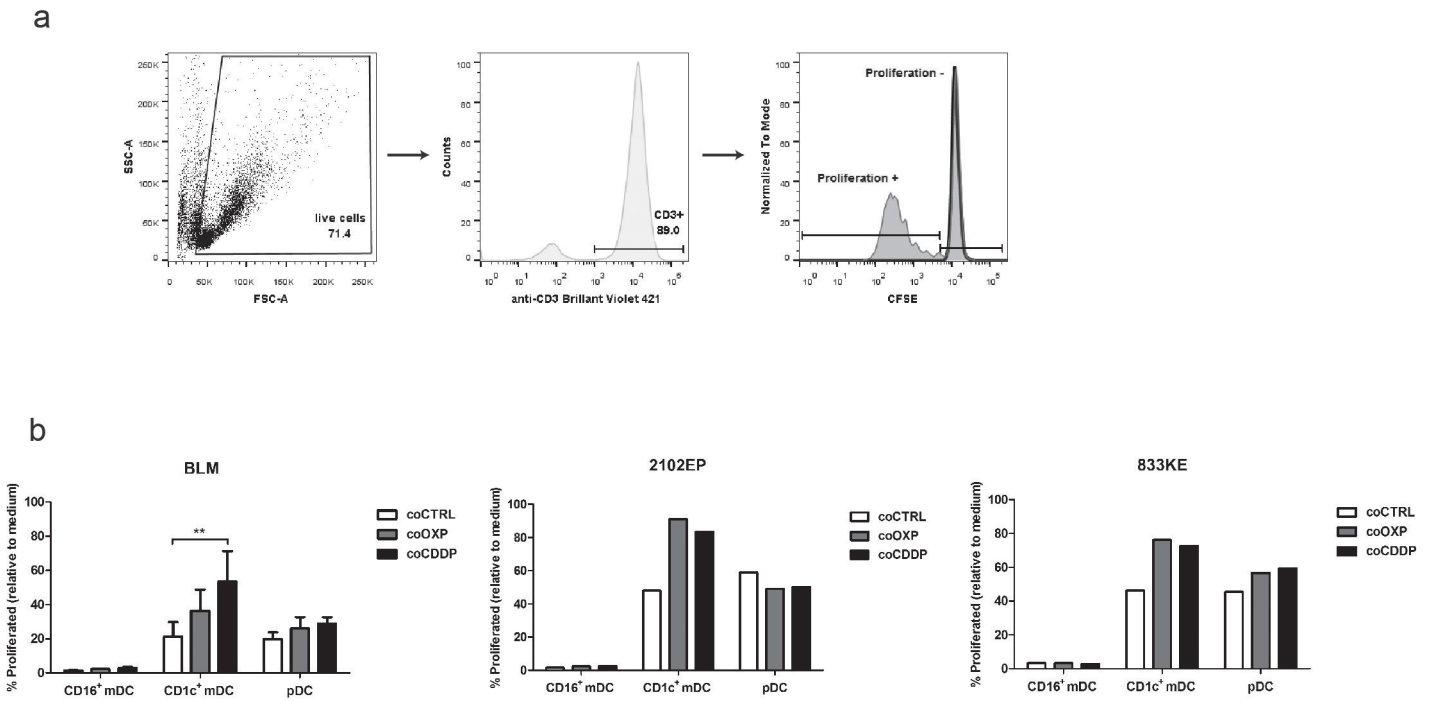

Figure 7. Human CD1c⁺ DCs mediate T cell activation against chemotherapy treated-tumor cells. The ability of CD16⁺, CD1c⁺ and pDCs to induce T cell proliferation upon co-culture with control (white), OXP (grey) or CDDP (black) treated-tumor cells was determined in a Mixed lymphocyte reaction. FACS sorted DCs were co-cultured with allogeneic CFSE-labeled peripheral blood lymphocytes (PBLs) for 5 days. (A) PBL proliferation was measured as the percentage of CD3⁺ cells showing CFSE dilution and expressed relative to CD3⁺ cells cultured in medium. (B) Percentage of proliferated CD3⁺ cells. Data are mean±SEM of at least triplicates of *n*=3 (BLM) or 1 representative (833KE and 2102EP) experiments. Significance was determined by Two-way ANOVA, **P < 0.01.

platinum-treated cells. Altogether these results seem to suggest that CD1c$^+$ DCs are most effectively activated by tumor cells undergoing ICD and might have the potency to drive subsequent immune responses.

Discussion

The human immune system plays a fundamental role in tumor recognition and control [31]. Recent advances, including the discovery of immunogenic cell death (ICD) and its contribution to clinical efficacy, suggest that durable clinical responses to chemotherapy require the presence of a functional immune system[3, 32, 33]. DCs are the key cells in this scenario, as they are required to kick-start effective adaptive immune responses [34-36].

Here, we study the function of the three most abundant human blood circulating DCs (CD1c$^+$ DCs, CD16$^+$ DCs and pDCs) in ICD induced by the platinum drugs oxaliplatin (OXP) and cisplatin (CDDP). We observed that, contrary to previous reports, both drugs were able to induce expression of the three hallmarks of ICD: CRT exposure, secretion of ATP and release of HMGB1. Furthermore, we show that all three DC subsets preferentially take up fragments derived from platinum-treated tumor cells and subsequently undergo phenotypical maturation.

Although the first compounds discovered to initiate an immunogenic form of apoptosis were structurally similar and all belonged to the class of the anthracyclines, the list of ICD inducers has since been expanded [5, 37-40]. Previously, Tesniere et al. found that the platinum drug CDDP fails to initiate ICD by itself, despite its similarity in structure and function to the ICD-inducer OXP [4, 5]. Nonetheless, CDDP was converted into an ICD inducer by exogenous co-administration of Cxcl2 (ortholog of the human pro-inflammatory cytokine/chemokine IL-8) [41]. Here we show that CDDP, as well as OXP, could upregulate exposure of ecto-CRT and induce release of ATP and HMGB1 in human tumor cells of distinct origins. Our observation that the human melanoma cell line BLM secretes high amounts of IL-8 (data not shown) could be a possible explanation for the discrepancy between our study and the results of Tesniere et al. This suggests that different cell lines may have distinct intrinsic potentials to emit immunogenic signals. In apparent accordance with this notion, UV irradiation has been described to induce ICD in murine models, yet it failed to do so in human cancer cell lines tested in another study [23, 40].

In addition to the three ICD hallmarks described above, surface translocation of the heat shock protein Hsp70 could expand the general definition of ICD [23, 39]. We here report that both OXP and CDDP were able to upregulate expression of Hsp70 in various human tumor cell lines.

Treatment of human tumor cells with OXP or CDDP increased uptake of tumor fragments by all three human DC subsets. As previously reported [22], CD1c$^+$ and

CD16+ DCs efficiently phagocytosed cell fragments, whereas pDCs showed lower uptake capacity. This uptake was dependent on ecto-CRT, however blocking of the CRT receptor did not abrogate tumor cell fragment uptake, suggesting that other receptors might be involved. The multi-ligand scavenger receptors SR-A (CD204) and scavenger receptor expressed by endothelial cell-1 (SREC-I), have been proposed to be involved in ecto-CRT binding [29, 30]. Our transcriptome analysis of blood DC subsets confirms that SR-A and SREC-I are expressed on distinct human DCs [42]. The presence of these alternative receptors might explain why blocking of CD91 did not diminish the uptake. Furthermore, we cannot exclude the possibility that there may be more receptors involved in ecto-CRT binding and that these have yet to be described. More research is required to reveal which receptor is responsible for CRT mediated uptake on human DC-subsets.

The human DC population is characterized by high degree of heterogeneity that reflects their phenotypical and functional properties, as well as their location in the body[43]. Consequently, DCs can interact with tumor cells in multiple ways. Immature DCs populate peripheral tissues and organs, where they are committed to (tumor) antigen capture[43]. In addition, myeloid and plasmacytoid DC subsets are found circulating in the blood, where they may encounter CTCs that have detached from the primary tumor and entered into the bloodstream[18]. Furthermore, DCs can home to and infiltrate tumors. As an example, inflammatory dendritic cells (inflDCS), were described as a distinct subset of DCs originating from *in situ* differentiation of monocytes recruited to the site of inflammation[44]. In mice, monocytes were recruited into the tumor bed within 12 hours following mitoxantrone treatment, and differentiated into inflDCs. Addition of a neutralizing antibody against CD11b abrogated activation of tumor-specific CD8+ T cells, indicating that DCs play a central role in ICD-mediated initiation of anti-tumor responses [11]. In this perspective, distinct DC subsets might be relevant as cellular mediators of ICD. Among blood DC populations, CD141+ DCs are also equipped with the potent ability to cross-prime cytotoxic T lymphocytes [22]. However, their scarce frequency represents a major hurdle in investigating their role in many aspects of DC biology.

Stimulation of an effective T cell response is determined by several critical steps. These involve (tumor) antigen uptake, processing and (cross)-presentation, as well as phenotypical and functional maturation of DCs [45, 46]. Murine DCs were reported to upregulate maturation-associated markers upon phagocytosis of bortezomib-treated colon cancer cells [47]. Similar effects were observed for human moDCs that were co-cultured with Idarubicin- or Bortezomib-treated tumor cell lines [23, 39]. Accordingly, we showed that interaction of OXP- or CDDP-treated tumor cells with blood DC subsets induced phenotypical maturation of DCs, observed as upregulation of co-stimulatory molecules (CD80 and CD86). In line with previous observations [22], although pDCs were

less able to take up antigens from their environment than other subsets, they efficiently matured and induced high levels of co-stimulation. Despite strong phagocytic ability and induction of maturation, CD16$^+$ DCs appeared to be the least efficient inducers of T cell responses, probably due to their minimal cross-presenting capacity [22]. This seems to be in accordance with the hypothesis that CD16$^+$ DCs may share some biological functions with DCs, yet they are more similar to monocytes, based on the comparison of their gene expression profiles [20]. The most effective response was observed for CD1c$^+$ DCs. Notably, CD1c$^+$ DCs were the only DC subset that, in response to interaction with platinum-treated tumor cells, secreted TNF-α and IL-10, cytokines typically induced upon exposure to different maturation stimuli[48,49]. This myeloid DC population was capable of engulfing platinum-treated tumor cells, responding to activatory signals and inducing T cell proliferation. In support of the functional observations, our transcriptomic analysis revealed that CD1c$^+$ DCs had higher expression of DC receptors sensing danger signals released by dying tumor cells, on mRNA levels as compared to the other two DC subsets. Appropriately, deficiency or loss-of-function mutations of genes encoding these receptors, was shown to compromise the efficacy of anti-cancer chemotherapy, stressing their crucial role in ICD [5, 13, 17].

In summary, we have investigated for the first time the role of the three most abundant human blood DC populations (CD1c$^+$ DCs, CD16$^+$ DCs and pDCs) in the context of ICD and show that only CD1c$^+$ DCs were capable of inducing allogeneic T cell response *in vitro*. Moreover, we expanded the list of ICD inducers, showing that - similarly to OXP - CDDP induces a form of tumor cell death consistent with ICD. Together, these observations point towards an active stimulatory effect of platinum-treated tumor cells on DCs that naturally occur in the human body and may contribute to the translation of current knowledge on ICD into clinical settings.

Acknowledgments

This work was supported by a grant from the Dutch Cancer Society and Alpe deHuZes foundation to S.V.H. (KUN2013-5958) and Dutch Cancer Society grant (KUN2009-4402). CGF received an NWO Spinoza award and ERC Adv Grant PATHFINDER (269019). IJMdV received NWO Vici Grant 918.14.655.

Author contribution

SDB, SVH and CGF conceived the study. SDB, IMNW, DAGvB and LEdV performed the experiments and analyzed the data. TDB and NdH helped performing the experiments. KW and SIB provided microarray data. SDB wrote the manuscript. All authors revised and approved the final version of the manuscript.

References

1. Chabner BA, Roberts TG. Chemotherapy and the war on cancer. Nat Rev Cancer 2005; 5:65-72.
2. Zitvogel L, Apetoh L, Ghiringhelli F, Kroemer G. Immunological aspects of cancer chemotherapy. Nat Rev Immunol 2008; 8:59-73.
3. Lesterhuis WJ, Haanen JBAG, Punt CJA. Cancer immunotherapy – revisited. Nat Rev Drug Discov 2011; 10:591-600.
4. Hato SV, Khong A, de Vries IJM, Lesterhuis WJ. Molecular Pathways: The Immunogenic Effects of Platinum-Based Chemotherapeutics. Clinical Cancer Research 2014; 20:2831-7.
5. Tesniere A, Schlemmer F, Boige V, Kepp O, Martins I, Ghiringhelli F, Aymeric L, Michaud M, Apetoh L, Barault L, et al. Immunogenic death of colon cancer cells treated with oxaliplatin. Oncogene 2009; 29:482-91.
6. Lesterhuis WJ, Punt CJA, Hato SV, Eleveld-Trancikova D, Jansen BJH, Nierkens S, Schreibelt G, de Boer A, Van Herpen CML, Kaanders JH, et al. Platinum-based drugs disrupt STAT6-mediated suppression of immune responses against cancer in humans and mice. The Journal of Clinical Investigation 2011; 121:3100-8.
7. Nowak AK, Lake RA, Marzo AL, Scott B, Heath WR, Collins EJ, Frelinger JA, Robinson BWS. Induction of Tumor Cell Apoptosis In Vivo Increases Tumor Antigen Cross-Presentation, Cross-Priming Rather than Cross-Tolerizing Host Tumor-Specific CD8 T Cells. The Journal of Immunology 2003; 170:4905-13.
8. Kepp O, Senovilla L, Kroemer G. Immunogenic cell death inducers as anticancer agents. Oncotarget 2014; 5:5190-1.
9. Obeid M, Tesniere A, Ghiringhelli F, Fimia GM, Apetoh L, Perfettini J-L, Castedo M, Mignot G, Panaretakis T, Casares N, et al. Calreticulin exposure dictates the immunogenicity of cancer cell death. Nature medicine 2007; 13:54-61.
10. Panaretakis T, Kepp O, Brockmeier U, Tesniere A, Bjorklund AC, Chapman DC, Durchschlag M, Joza N, Pierron G, van Endert P, et al. Mechanisms of pre-apoptotic calreticulin exposure in immunogenic cell death. The EMBO Journal 2009; 28:578-90.
11. Ma Y, Adjemian S, Mattarollo Stephen R, Yamazaki T, Aymeric L, Yang H, Portela Catani João P, Hannani D, Duret H, Steegh K, et al. Anticancer Chemotherapy-Induced Intratumoral Recruitment and Differentiation of Antigen-Presenting Cells. Immunity 2013; 38:729-41.
12. Elliott MR, Chekeni FB, Trampont PC, Lazarowski ER, Kadl A, Walk SF, Park D, Woodson RI, Ostankovich M, Sharma P, et al. Nucleotides released by apoptotic cells act as a find-me signal to promote phagocytic clearance. Nature 2009; 461:282-6.
13. Apetoh L, Ghiringhelli F, Tesniere A, Obeid M, Ortiz C, Criollo A, Mignot G, Maiuri MC, Ullrich E, Saulnier P, et al. Toll-like receptor 4-dependent contribution of the immune system to anticancer chemotherapy and radiotherapy. Nature medicine 2007; 13:1050-9.
14. Wiersma VR, Michalak M, Abdullah TM, Bremer E, Eggleton P. Mechanisms of translocation of ER chaperones to the cell surface and immunomodulatory roles in cancer and autoimmunity. Frontiers in Oncology 2015; 5.
15. Wong SY, Hynes RO. Lymphatic or Hematogenous Dissemination: How Does a Metastatic Tumor Cell Decide? Cell cycle (Georgetown, Tex) 2006; 5:812-7.
16. Chaput N, De Botton S, Obeid M, Apetoh L, Ghiringhelli F, Panaretakis T, Flament C, Zitvogel L, Kroemer G. Molecular determinants of immunogenic cell death: surface exposure of calreticulin makes the difference. J Mol Med 2007; 85:1069-76.

17. Ghiringhelli F, Apetoh L, Tesniere A, Aymeric L, Ma Y, Ortiz C, Vermaelen K, Panaretakis T, Mignot G, Ullrich E, et al. Activation of the NLRP3 inflammasome in dendritic cells induces IL-1[beta]-dependent adaptive immunity against tumors. Nature medicine 2009; 15:1170-8.
18. MacDonald KPA, Munster DJ, Clark GJ, Dzionek A, Schmitz J, Hart DNJ. Characterization of human blood dendritic cell subsets. Blood 2002; 100:4512-20.
19. Piccioli D, Tavarini S, Borgogni E, Steri V, Nuti S, Sammicheli C, Bardelli M, Montagna D, Locatelli F, Wack A. Functional specialization of human circulating CD16 and CD1c myeloid dendritic-cell subsets. Blood 2007; 109:5371-9.
20. Robbins SH, Walzer T, Dembélé D, Thibault C, Defays A, Bessou G, Xu H, Vivier E, Sellars M, Pierre P, et al. Novel insights into the relationships between dendritic cell subsets in human and mouse revealed by genome-wide expression profiling. Genome Biology 2008; 9:R17-R.
21. Schreibelt G, Tel J, Sliepen KEWJ, Benitez-Ribas D, Figdor C, Adema G, de Vries IJ. Toll-like receptor expression and function in human dendritic cell subsets: implications for dendritic cell-based anti-cancer immunotherapy. Cancer Immunol Immunother 2010; 59:1573-82.
22. Tel J, Schreibelt G, Sittig SP, Mathan TSM, Buschow SI, Cruz LJ, Lambeck AJA, Figdor CG, de Vries IJM. Human plasmacytoid dendritic cells efficiently cross-present exogenous Ags to CD8+ T cells despite lower Ag uptake than myeloid dendritic cell subsets. Blood 2013; 121:459-67.
23. Fucikova J, Kralikova P, Fialova A, Brtnicky T, Rob L, Bartunkova J, Špíšek R. Human Tumor Cells Killed by Anthracyclines Induce a Tumor-Specific Immune Response. Cancer Research 2011; 71:4821-33.
24. Cullen JW. Pharmacokinetics of Chemotherapy. Journal of Pediatric Oncology Nursing 1989; 6:21-2.
25. Chao MP, Jaiswal S, Weissman-Tsukamoto R, Alizadeh AA, Gentles AJ, Volkmer J, Weiskopf K, Willingham SB, Raveh T, Park CY, et al. Calreticulin is the dominant pro-phagocytic signal on multiple human cancers and is counterbalanced by CD47. Science translational medicine 2010; 2:63ra94-63ra94.
26. Pang WW, Pluvinage JV, Price EA, Sridhar K, Arber DA, Greenberg PL, Schrier SL, Park CY, Weissman IL. Hematopoietic stem cell and progenitor cell mechanisms in myelodysplastic syndromes. Proceedings of the National Academy of Sciences of the United States of America 2013; 110:3011-6.
27. Basu S, Binder RJ, Ramalingam T, Srivastava PK. CD91 Is a Common Receptor for Heat Shock Proteins gp96, hsp90, hsp70, and Calreticulin. Immunity 2001; 14:303-13.
28. Hart JP, Gunn MD, Pizzo SV. A CD91-Positive Subset of CD11c+ Blood Dendritic Cells: Characterization of the APC that Functions to Enhance Adaptive Immune Responses against CD91-Targeted Antigens. The Journal of Immunology 2004; 172:70-8.
29. Berwin B, Hart JP, Rice S, Gass C, Pizzo SV, Post SR, Nicchitta CV. Scavenger receptor-A mediates gp96/GRP94 and calreticulin internalization by antigen-presenting cells. The EMBO Journal 2003; 22:6127-36.
30. Berwin B, Delneste Y, Lovingood RV, Post SR, Pizzo SV. SREC-I, a Type F Scavenger Receptor, Is an Endocytic Receptor for Calreticulin. Journal of Biological Chemistry 2004; 279:51250-7.
31. de Visser KE, Eichten A, Coussens LM. Paradoxical roles of the immune system during cancer development. Nat Rev Cancer 2006; 6:24-37.
32. Eggermont AMM, Kroemer G, Zitvogel L. Immunotherapy and the concept of a clinical cure. European Journal of Cancer 2013; 49:2965-7.

33. Rios-Doria J, Durham N, Wetzel L, Rothstein R, Chesebrough J, Holoweckyj N, Zhao W, Leow CC, Hollingsworth R. Doxil Synergizes with Cancer Immunotherapies to Enhance Antitumor Responses in Syngeneic Mouse Models. Neoplasia 2015; 17:661-70.
34. Blachère NE, Darnell RB, Albert ML. Apoptotic Cells Deliver Processed Antigen to Dendritic Cells for Cross-Presentation. PLoS Biol 2005; 3:e185.
35. Jung S, Unutmaz D, Wong P, Sano G-I, De los Santos K, Sparwasser T, Wu S, Vuthoori S, Ko K, Zavala F, et al. In Vivo Depletion of CD11c+ Dendritic Cells Abrogates Priming of CD8+ T Cells by Exogenous Cell-Associated Antigens. Immunity 2002; 17:211-20.
36. Martin K, Schreiner J, Zippelius A. Modulation of APC function and anti-tumor immunity by anti-cancer drugs. Frontiers in Immunology 2015; 6.
37. Casares N, Pequignot MO, Tesniere A, Ghiringhelli F, Roux S, Chaput N, Schmitt E, Hamai A, Hervas-Stubbs S, Obeid M, et al. Caspase-dependent immunogenicity of doxorubicin-induced tumor cell death. The Journal of Experimental Medicine 2005; 202:1691-701.
38. Schiavoni G, Sistigu A, Valentini M, Mattei F, Sestili P, Spadaro F, Sanchez M, Lorenzi S, D'Urso MT, Belardelli F, et al. Cyclophosphamide Synergizes with Type I Interferons through Systemic Dendritic Cell Reactivation and Induction of Immunogenic Tumor Apoptosis. Cancer Research 2011; 71:768-78.
39. Spisek R, Charalambous A, Mazumder A, Vesole DH, Jagannath S, Dhodapkar MV. Bortezomib enhances dendritic cell (DC)–mediated induction of immunity to human myeloma via exposure of cell surface heat shock protein 90 on dying tumor cells: therapeutic implications. Blood 2007; 109:4839-45.
40. Obeid M, Panaretakis T, Joza N, Tufi R, Tesniere A, van Endert P, Zitvogel L, Kroemer G. Calreticulin exposure is required for the immunogenicity of [gamma]-irradiation and UVC light-induced apoptosis. Cell Death Differ 2007; 14:1848-50.
41. Sukkurwala AQ, Martins I, Wang Y, Schlemmer F, Ruckenstuhl C, Durchschlag M, Michaud M, Senovilla L, Sistigu A, Ma Y, et al. Immunogenic calreticulin exposure occurs through a phylogenetically conserved stress pathway involving the chemokine CXCL8. Cell Death Differ 2014; 21:59-68.
42. Jin J-O, Park H-Y, Xu Q, Park J-I, Zvyagintseva T, Stonik VA, Kwak J-Y. Ligand of scavenger receptor class A indirectly induces maturation of human blood dendritic cells via production of tumor necrosis factor-α. Blood 2009; 113:5839-47.
43. Collin M, McGovern N, Haniffa M. Human dendritic cell subsets. Immunology 2013; 140:22-30.
44. Segura E, Amigorena S. Inflammatory dendritic cells in mice and humans. Trends in immunology 2013; 34:440-5.
45. Bakdash G, Sittig SP, van Dijk T, Figdor CG, de Vries IJM. The nature of activatory and tolerogenic dendritic cell-derived signal II. Frontiers in Immunology 2013; 4:53.
46. Ikeda H, Chamoto K, Tsuji T, Suzuki Y, Wakita D, Takeshima T, Nishimura T. The critical role of type-1 innate and acquired immunity in tumor immunotherapy. Cancer Science 2004; 95:697-703.
47. Demaria S, Santori FR, Ng B, Liebes L, Formenti SC, Vukmanovic S. Select forms of tumor cell apoptosis induce dendritic cell maturation. Journal of Leukocyte Biology 2005; 77:361-8.
48. Sköld AE, van Beek JJP, Sittig SP, Bakdash G, Tel J, Schreibelt G, de Vries IJM. Protamine-stabilized RNA as an ex vivo stimulant of primary human dendritic cell subsets. Cancer Immunology, Immunotherapy 2015; 64:1461-73.

49. Sittig SP, Bakdash G, Weiden J, Sk, #xf6, ld AE, Tel J, Figdor CG, de Vries IJM, Schreibelt G. A Comparative Study of the T Cell Stimulatory and Polarizing Capacity of Human Primary Blood Dendritic Cell Subsets. Mediators of Inflammation 2016; 2016:11.
50. Lindstedt M, Lundberg K, Borrebaeck CAK. Gene Family Clustering Identifies Functionally Associated Subsets of Human In Vivo Blood and Tonsillar Dendritic Cells. The Journal of Immunology 2005; 175:4839-46.
51. Gautier L, Cope L, Bolstad BM, Irizarry RA. affy—analysis of Affymetrix GeneChip data at the probe level. Bioinformatics 2004; 20:307-15.

Supplementary materials

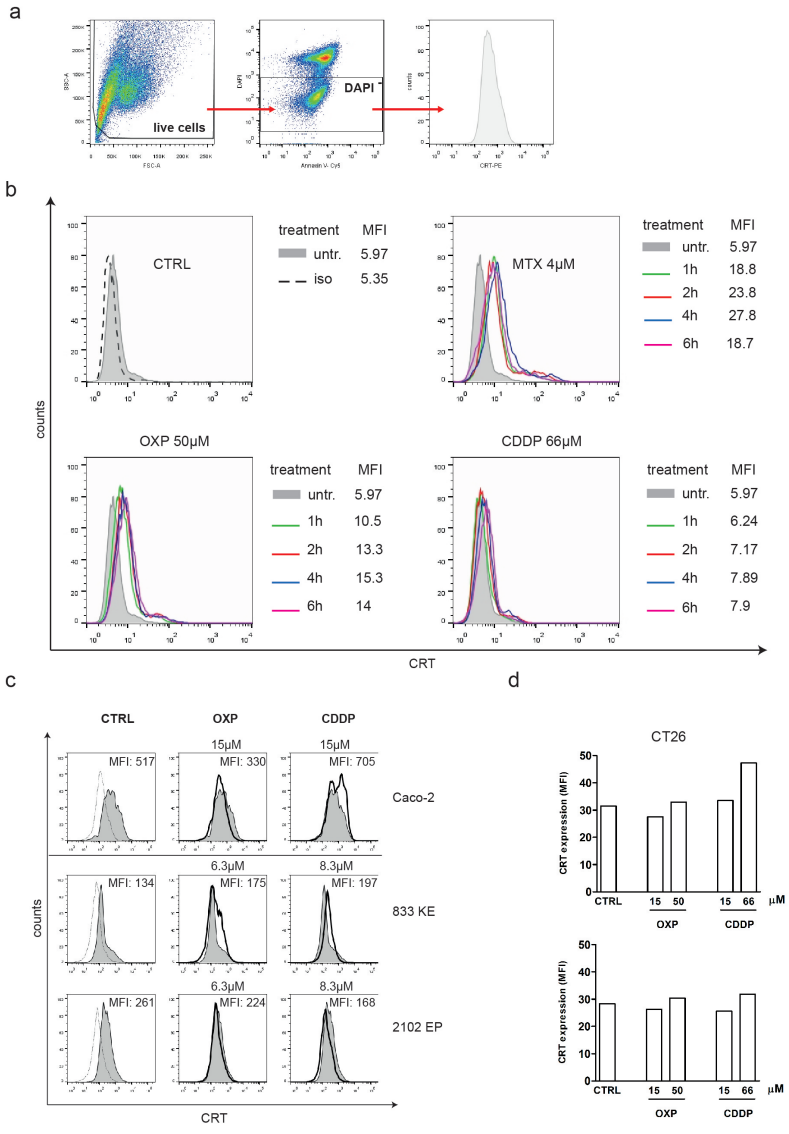

Supplementary Figure 1. Platinum-treatment increases exposure of ecto-CRT on tumor cells. (A) Gating strategy for assessment of cell viability and expression of surface DAMPs (CRT and Hsp70). Cells were gated on live cells. Ecto-CRT and Hsp70 expression was assessed on DAPI$^-$ cells. (B) Representative flow cytometry histogram of the kinetics of the expression of ecto-CRT on BLM cells after treatment with OXP, CDDP or MTX. (C) Representative replicate histograms showing CRT expression (MFI) on human colon (Caco-2) and testicular (833KE and 2102EP) cancer cell lines, following 24h of treatment with OXP or CDDP. Isotype (grey line), control (grey filled histogram), treatment (black thick line) (D). Exposure of CRT on murine colon cancer CT26 cells was assessed after 24h of treatment with OXP or CDDP. Data show duplicates of one representative experiment.

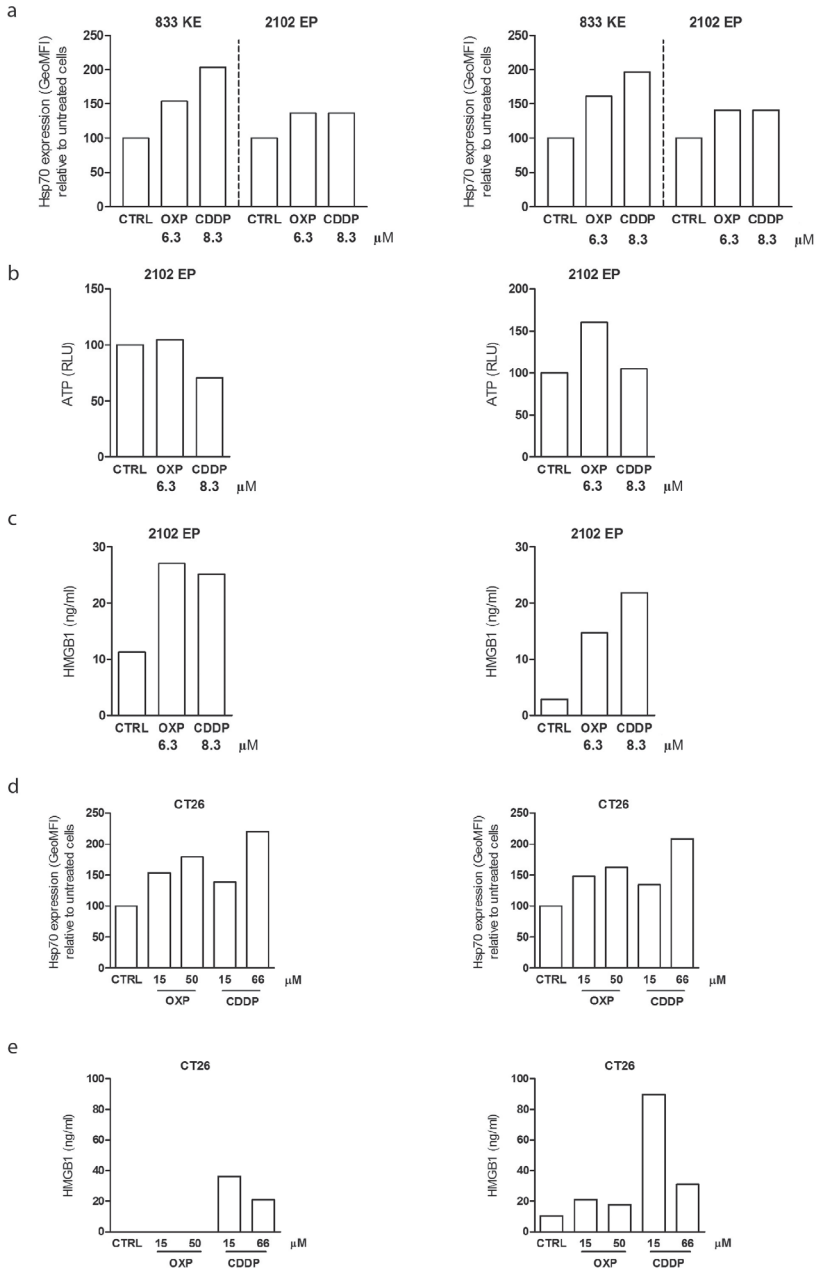

Supplementary Figure 2. Detection of immunogenic DAMPs released by melanoma, testicular and colon cancer cells upon platinum-treatment. (A, B, C) Surface expression of Hsp70 on BLM, 2102EP and CT26 cells, after platinum treatment, was assessed by flow cytometry on AnnexinV^{+}/DAPI^{-} cells. (D, E, F) Extracellular ATP and HMGB1 release in supernatants of platinum-treated cells. Histograms show separate replicates (A-C, E, F) or mean of duplicates (D) of independent experiments.

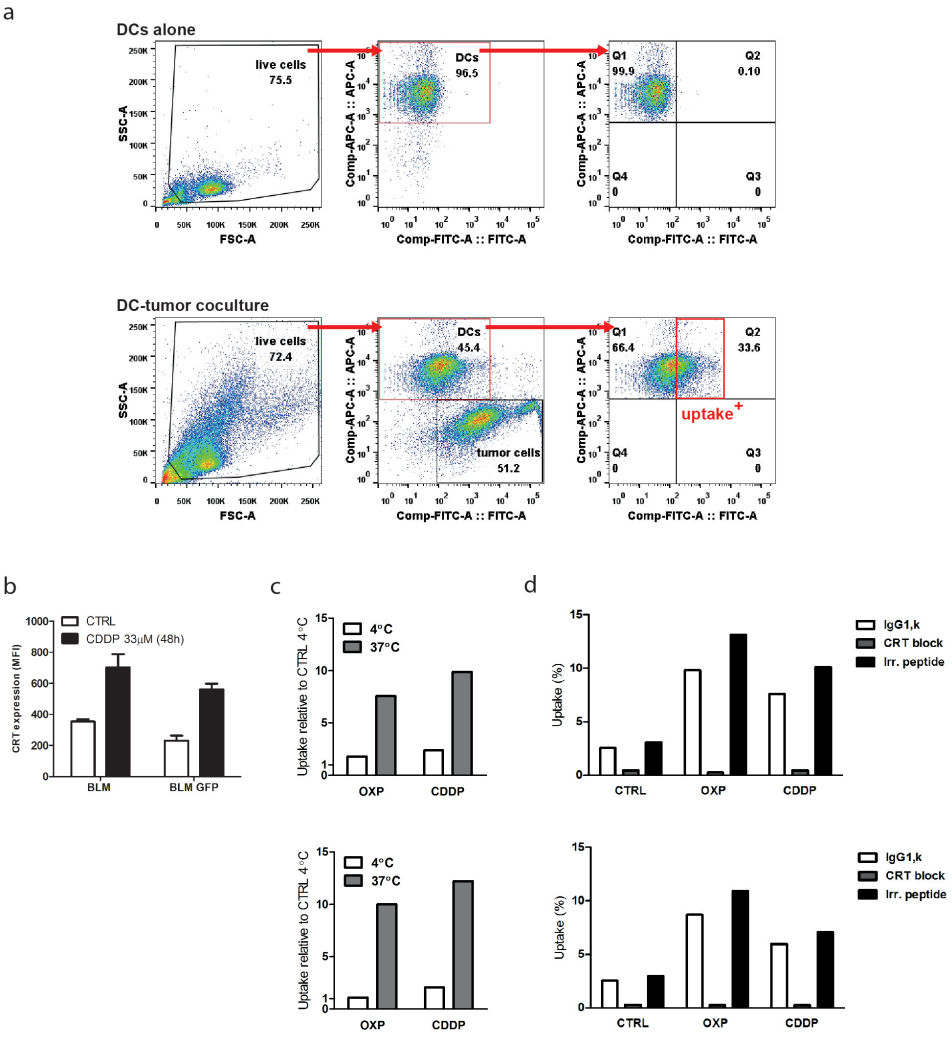

Supplementary Figure 3. Dendritic cells actively take up tumor-derived fragments. (A) Gating strategy for tumor cell binding and uptake. Tumor cells, prelabeled with CFSE or expressing the fluorescent protein GFP, were co-cultured with DC subsets. Before assessment of binding/uptake, DCs were incubated with antibodies recognizing CD11c (APC), for CD16$^+$ and CD1c$^+$ DCs, or CD123 (APC), for pDCs. Extent of binding/uptake was assessed by gating on DCs and analyzing the percentage of APC$^+$CFSE$^+$ (or GFP$^+$) double positive events. (B) Expression of CRT on BLM *versus* BLM-GFP cells, as assessed by flow cytometry. Cells were left untreated or treated with CDDP for 48h. (C) DCs actively take up tumor-fragments as shown by percentage of uptake (37°C, grey bar) of platinum treated-BLM cells by CD1c$^+$ DCs *versus* binding (4°C, white bar). Histograms show values relative to binding of control (CTRL) BLM cells of 2 independent experiments. (D) Control or platinum-treated BLM cells were co-cultured with CD1c$^+$ DCs in the presence of isotype (white bar), CRT blocking peptide (grey bar) or irrelevant tumor antigen (gp100) peptide (black bar) for 2h and percentage of uptake was assessed by flow cytometry. Data show separate duplicates of one experiment.

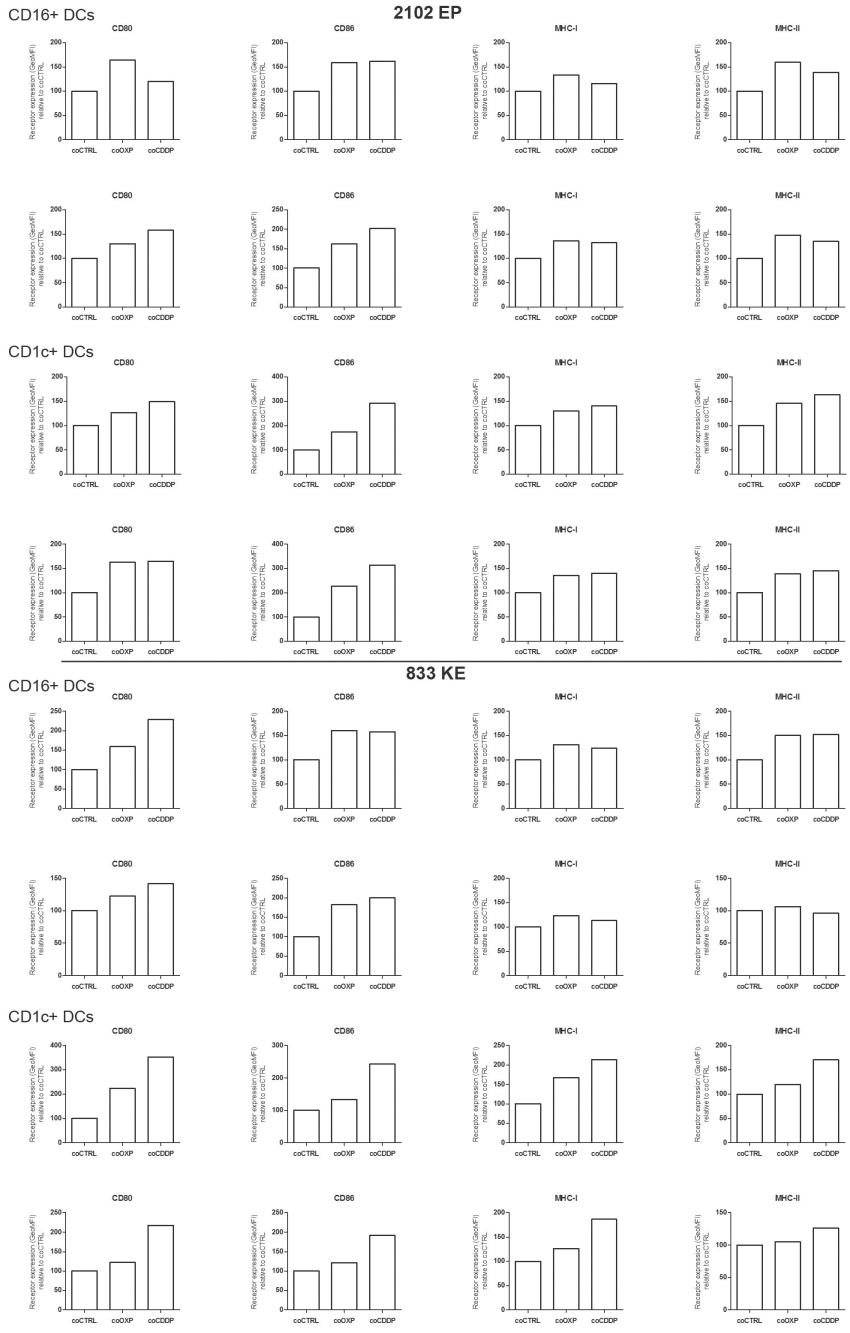

Supplementary Figure 4. Maturation of CD16⁺ DCs and CD1c⁺ DCs following phagocytosis of platinum-treated testicular cancer cells. The expression of maturation markers on CD16⁺ DCs and CD1c⁺ DCs following 48h of co-culture with control or platinum-treated 2102EP or 833KE cells. Histograms show separate duplicates of independent experiments.

a

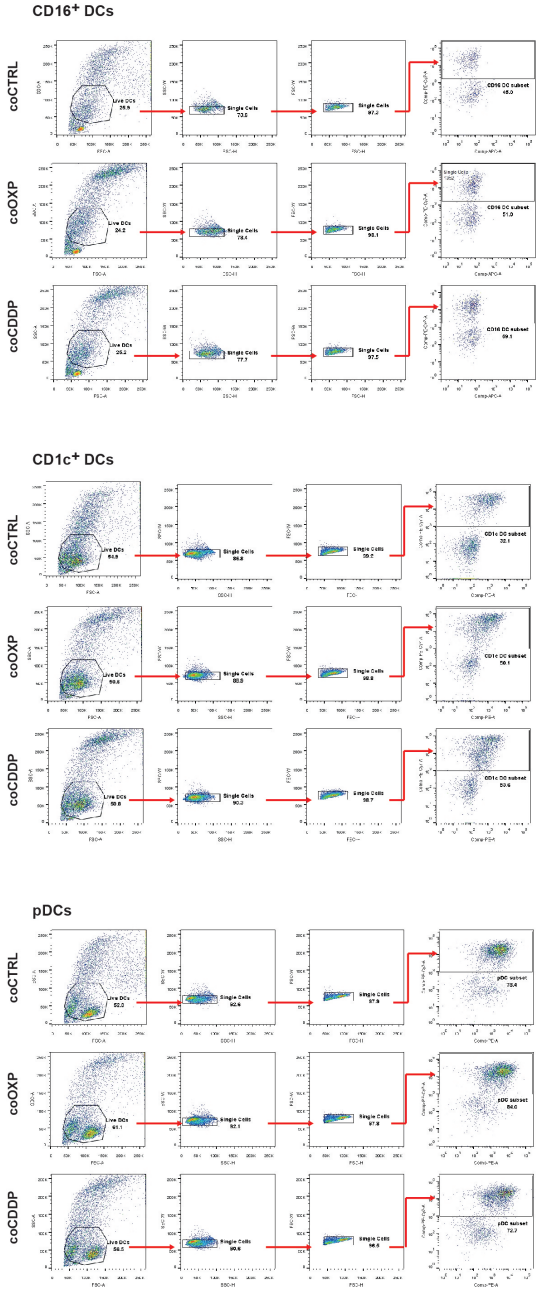

b

Yield of FACS sorted DCs

DC subset	Condition	# sorted DCs (*10^6)	% total
CD16	coCTRL	0.075	6.9
CD16	coOXP	0.071	6.8
CD16	coCDDP	0.051	5.1
CD1c	coCTRL	0.086	6.9
CD1c	coOXP	0.113	13.9
CD1c	coCDDP	0.100	15.5
pDC	coCTRL	0.108	28
pDC	coOXP	0.092	36
pDC	coCDDP	0.089	27.7

Supplementary Figure 5. Gating strategy for the sorting of human blood DC subsets. (A) Before Fluorescence-activated cell sorting (FACS), co-cultures of tumor cells and DCs were incubated with antibodies recognizing HLA-DR (PE-Cy7), CD16 (APC), CD1c (PE), CD304 (PE). DCs were sorted from tumor cells based on the expression of HLA-DR in addition to CD16, CD1c and CD304 to obtain CD16$^+$ DCs, CD1c$^+$ DCs and pDCs, respectively. (B) Yield and percentage of isolated cells from one representative experiment are shown.

Supplementary Table 1. List of antibodies (listed following order of appearance in M&M)

Antibody	Clone	Supplier	Cat no.	Dilution (Application)
anti-CRT	ab2907	Abcam	ab2907	1:100 (FACS) 1:50 (Confocal)
anti-CRT-PE	FMC 75	Enzo Life Science	ADI-SPA-601PE-F	1:100 (FACS)
anti-HSP 70	C92F3A-5	Enzo Life Science	ADI-SPA-810-D	1:100 (FACS)
anti-CD1c-PE	AD5-8E7	Miltenyi biotec	130-090-508	1:100 (FACS; Sorting)
anti-CD11c-APC	MJ4-27G12	Miltenyi biotec	130-092-412	1:25 (FACS)
anti-CD20-APC	2H7	eBioscience	17-0209	1:25 (FACS)
anti-CD15-FITC	VIMC6	Miltenyi biotec	130-081-101	1:25 (FACS)
anti-CD56-PE	MOC-1	IQ Products	IQP-114R	1:25 (FACS)
anti-CD123-APC	AC145	Miltenyi biotec	130-090-901	1:25 (FACS)
anti-CD303-PE	AC144	Miltenyi biotec	130-090-511	1:25 (FACS)
anti-CD91α	A2MRα-2	Invitrogen	37-3800	1:50 (FACS)
anti-CD80-PECy7	L307.4	BD Pharmingen	561135	1:12 (FACS)
anti-CD86-PECy7	2331	BD Pharmingen	561128	1:48 (FACS)
anti-HLA-ABC-PE	G46-2.6	BD Pharmingen	555553	1:8 (FACS)
anti-HLA-DR-PE	G46-6	BD Pharmingen	555812	1:8 (FACS)
anti-HLA-DR-PECy7	L243	BD Biosciences	335813	1:100 (Sorting)
anti-CD16-APC	VEP13	Miltenyi biotec	130-098-101	1:66 (Sorting)
anti-CD304-PE	AD5-17F6	Miltenyi biotec	130-090-533	1:66 (Sorting)
anti-CD3-BV421	SK7	BD Horizon	563798	1:50 (FACS)

CHAPTER 3

Cooperation between CD47 blockade and platinum treatment can potentially revert tumor-mediated immunosuppression through human CD1c$^+$ DCs

Stefania Di Blasio[1], Laura E. de Vries[1], Inge M.N. Wortel[1], Diede A. G. van Bladel[1], I. Jolanda M. de Vries[1,2], Carl G. Figdor[1,#], Stanleyson V. Hato[1]

[1]Department of Tumor Immunology, Radboud Institute for Molecular Life Sciences, Radboud University Medical Center, Nijmegen, the Netherlands. [2]Department of Medical Oncology, Radboud University Medical Center, Nijmegen, the Netherlands

Manuscript in preparation

Abstract

Tumor progression is dependent on the ability of tumor cells to either elude anti-tumor immunity or induce tolerance against the tumor. Some of the key events that lead to subversion of anti-cancer immune responses originate from the interaction of tumor cells with host immune cells, in particular dendritic cells (DCs). DCs are master regulators of tolerance and immunity. Hence, signals provided by DCs, upon interaction with cancer cells, dictate the fate of an anti-tumor response. Interaction between DCs and tumor cells lead to uptake of tumor-derived fragments, after which DCs can display a "defective" phenotype resulting in induction of tolerance rather than effective anti-tumor immunity. Tumor cell uptake by DCs is regulated by the balance of "don't eat me" (e.g. CD47) versus "eat me" (e.g. Calreticulin, CRT) signals expressed on cancer cells. In this study, we set out to investigate the effect of shifting this balance by inhibiting "don't eat me" signals, while enhancing "eat me" signals on tumor cells. We measured uptake of tumor material by the naturally occurring human blood DC subset, $CD1c^+$ DCs and assessed DC maturation. We demonstrated that either CD47 blockade or CRT upregulation by platinum drugs increased tumor cell uptake by DCs. Consequently, the uptake of these treated cells induced phenotypical $CD1c^+$ DC maturation, measured by upregulation of the co-stimulatory molecule CD86 and major histocompatibility complex class II (MHC II). Moreover, we observed that blocking of CD47 cooperates with platinum-treatment in increasing CD86 expression on $CD1c^+$ DCs compared to either treatment alone, albeit tumor uptake was not markedly enhanced. We therefore suggest that combining CD47 blockade with chemotherapy might contribute to reverting tumor-mediated suppression of DC maturation, eventually restoring DC activation and induction of T cell proliferation.

Introduction

Cancer development and progression is dependent on the ability of tumor cells to either elude antitumor immunity or induce a tolerogenic response[1]. Tumor-mediated subversion of immune responses can occur at different levels. The establishment of a tumor microenvironment (TME) can inhibit antigen presentation, halt immune cell activity and recruit suppressive immune cells, such as myeloid-derived suppressor cells (MDSCs) or tumor-associated macrophages[2]. Moreover, it is now evident that the failure of the immune system, to build protection against tumor cells, strongly depends on the signals provided by antigen presenting cells (APCs) to effector immune cells[3,4].

Dendritic cells (DCs) are the main professional APCs and they are necessary to control and balance tolerance and immunity. Immature DCs patrol peripheral tissues, sample antigens and undergo a series of phenotypical and functional changes, which can convert immature DCs into efficient stimulators of naïve T cells, favoring the development of Th1 responses. Alternatively, phenotypically or functionally-impaired DCs can induce tolerogenic mechanisms[4,5]. DCs encompass a heterogeneous class of immune cells that differ in phenotype, localization and functional specialization[6]. Human blood contains two major DC subtypes, myeloid (mDCs) and plasmacytoid (pDCs) DCs[7]. pDCs are the principal mediators of antiviral immunity as they produce large amounts of type I interferons (IFNs) in response to viral stimuli. Myeloid DCs can be subdivided into $CD16^+$ DCs, $CD1c^+$ DCs and $BDCA3^+$ DCs, and have been well characterized as efficient antigen-presenting cells and inducers of adaptive immunity[8].

DCs in the TME are found in immature state, characterized by low level of surface expression of co-stimulatory molecules, as well as, altered cytokine profiles[3,5]. There are two main mechanisms that hamper efficient DC function in the TME. Firstly, a suppressive cytokine milieu characterized by the production of VEGF, IL-10, IL-6, TGF-β, which contribute to blockade of DC activation and/or desensitization of mature DCs[3,9]. Secondly, engagement of inhibitory receptors (e.g. signal regulatory protein α (SIRPα) on DCs[10-13]. Upon SIRPα ligation, both murine and human DCs displayed a distinct immature phenotype, characterized by down-regulation of co-stimulatory molecules and impaired cytokine production. Moreover, these "defective" DCs were unable to stimulate T cell responses[10-13].

SIRPα is a type I transmembrane receptor of the IgG superfamily, expressed on neurons, endothelial cells and professional phagocytes (monocytes, macrophages and DCs)[14] and binds to the ubiquitous transmembrane protein CD47 (also known as integrin-associated protein, IAP)[15]. CD47 is expressed on all hematopoietic cells, where it prevents cell clearance by phagocytes and as a result is often referred to

as a "don't eat me" signal[16,17]. However, CD47 was also found markedly upregulated in solid and hematopoietic tumors, representing a potential mechanism of escape from immunosurveillance[18].

CD47-SIRPα interaction regulates DC function by activating two distinct downstream signalling pathways. SIRPα generates a negative signal via its two intracellular immunoreceptor-based inhibition motifs (ITIMs) and the recruitment of SRC homology 2 domain-containing phosphatases (SHP-1 and/or SHP-2), which ultimately cause inhibition of phagocytosis[16,19,20]. Alternatively, SIRPα physically associates with JAK2 and phosphorylated-STAT3, resulting in the activation of the JAK/STAT signaling cascade and subsequent down-regulation of inflammatory immune responses[21-23].

Besides "don't eat me" signals, cells (especially dying cells) can also express "eat me" signals such as calreticulin (CRT), which flags these cell for engulfment by phagocytes[24,25]. Whether a cell is taken up by phagocytes or not depends on the balance between these "eat me" and "don't eat me" signals. CRT is a chaperone molecule residing in the lumen of the endoplasmic reticulum (ER)[26,27]. Under conditions that cause extensive ER stress, CRT translocates and become exposed on the cell surface (ecto-CRT)[26,27]. Viable cells can also express low amounts of ecto-CRT, but this is not sufficient to overcome CD47 expression and induce cellular uptake[25]. Upregulation of ecto-CRT is one of the "hallmarks" (in addition to heat shock proteins (HSPs), ATP and high mobility group box 1, HMGB1) that defines a form of immunologically active apoptosis, known as immunogenic cell death (ICD)[28].

Anti-cancer therapies inducing ICD include treatment with the platinum chemotherapeutics, oxaliplatin (OXP) and cisplatin (cis-diamminedichloroplatinum, CDDP)[27,29]. We recently reported that after treatment with OXP or CDDP human tumor cells were engulfed more efficiently by human blood DCs. Increased uptake was dependent on upregulation of ecto-CRT on tumor cell surface, as demonstrated by complete abrogation of phagocytosis upon CRT blockade. Following uptake of platinum-treated tumor cells, all tested DC subsets underwent phenotypical maturation, however $CD1c^+$ DCs showed to be the most efficient blood DC subtype in promoting T cell proliferation in the context of ICD (Chapter 2 of this thesis).

Based on these observations, we aimed at exploring the effect of blocking the inhibitory "don't eat me" signal CD47, while enhancing the expression of the activating "eat me" signal ecto-CRT, on tumor cells. Thus, we investigated whether changes in the balance between "eat me" and "don't eat me" signals would affect phenotype and function of naturally occurring blood $CD1c^+$ DCs. We report that, functional blockade of CD47, with the monoclonal antibody B6H12 on live tumor cells, was able to promote melanoma cell engulfment by $CD1c^+$ DCs. Additionally, we

show that CD47 blockade has the potential to revert tumor-mediated suppression of DC maturation. Similar effects were observed when CD1c$^+$ DCs were co-cultured with platinum-treated tumor cells, known to express high levels of ecto-CRT. Finally, combination of CD47 blockade with platinum treatment displayed a synergistic effect on DC-mediated tumor cell uptake and upregulation of the maturation marker, CD86 on CD1c$^+$ DCs. Taken together, our findings suggest that blocking CD47 in the context of chemotherapy-induced ICD might potentiate activation of CD1c$^+$ DCs and eventually result in a stronger stimulation of anti-tumor immunity.

Materials & Methods

Cell culture, transduction and stable cell line

Human melanoma cells, BLM and BLM-GFP, were cultured in Dulbecco's modified Eagle's medium (DMEM, Gibco), supplemented with 5% fetal calf serum and 5% CO_2 humidified air at 37°C. The Lenti6/Block-iT-shScramble (GFP) vector was a kind gift of Prof. Peter Friedl (RIMLS, The Netherlands). The sequence of this construct does not match any known mammalian genes. BLM cells were infected with lentiviral vector and (10µg/ml) polybrene and incubated at 37°C, 5% CO_2, overnight. Then medium was refreshed and cells were analyzed after 72h of treatment. Stable cell line was selected with 5µg/ml blasticidin.

Isolation of human blood immune cells and generation of moMfs and moDCs

Peripheral blood mononuclear cells (PBMCs) were isolated from buffy coats obtained from healthy volunteers (Sanquin) and purified via centrifugation over a ficoll density gradient (Axis-Shield) in SepMate tubes (Stemcell technologies). Isolation of human blood DC subsets was achieved by a sequence of negative and positive selection steps using magnetic beads (Human CD1c$^+$ (BDCA-1) Dendritic Cell Isolation Kit, Miltenyi Biotec). DC purity was assessed by staining with primary labeled antibodies: anti-CD1c-PE (Miltenyi biotec, clone AD5-8E7), anti-CD11c-APC (Miltenyi biotec, clone MJ4-27G12) and anti-CD20-APC (eBioscience, clone 2H7). Purity levels higher than 98% were achieved, determined by flow cytometry. Monocyte-derived macrophages (moMFs) and monocyte-derived DCs (moDCs) were obtained as follow. Monocytes were isolated by adherent selection of PBMCs and cultured in RPMI 10% FCS, supplemented with GM-CSF and IL-4 (moDCs) or GM-CFS (moMfs) for 5 days. Peripheral blood leukocytes (PBLs) were isolated from PBMCs by depletion of monocytes via adherence to plastic culture flasks (1 hour at 37°C). Floating cells (PBLs) were collected and resuspended in X-VIVO-15 medium (Lonza) supplemented with 2% human serum (HS, Sanquin).

Co-cultures and uptake assays

Tumor cells were stained with 2 μM of the fluorescent dye 5(6)-Carboxyfluorescein diacetate N-succinimidyl ester (CFSE, Invitrogen, Thermo Fisher Scientific), according to manufacturer's instructions. Tumor cells and APCs (blood CD1c+ DCs, moMfs or moDCs) were co-cultured at either 1:1 or 1:4 ratio in Falcon tubes (BD Falcon) in X-VIVO-15 supplemented with 2% HS (final concentration $1x10^6$ cells/ml). Co-cultures were stained with an APC-labelled anti-CD11c antibody and analyzed by flow cytometry. Extent of phagocytosis was determined as the percentage of double positive events (i.e. $CD11c^+$-APC/GFP^+ or $CD11c^+$-APC/$CFSE^+$). For blocking experiments, tumor cells were pre-incubated (30min at 4°C) with blocking agents or negative controls: anti-CD47 blocking (B6H12) and non-blocking (2D3) antibodies, 20 μg/mL, both eBioscience) or IgG1,k (20 μg/mL, Biolegend). Extra volume of blocking agents or matched controls were added to co-cultures at same final concentration.

Flow cytometry

Phenotypical assessment of DC maturation after co-culture with tumor cells was performed by flow cytometry. Briefly, cells were washed in PBA, incubated with Fc-receptor blocking buffer (2% HS in PBS, 15min at 4°C) and subsequently stained with primary antibodies in PBA (30min at 4°C). Monoclonal directly labeled anti-human antibodies used were: anti-CD11c-APC (Miltenyi biotec), anti-CD80-PECy7 (BD Pharmingen), anti-CD86-APC (BD Pharmingen), anti-MHC I-PE (BD Pharmingen) and anti-MHC II-APC (BD Pharmingen). Appropriate isotype controls were included.

For detection of surface expression of CD47 on human melanoma cells and SIRP-α on $CD1c^+$ DCs, moMfs and moDCs, cells were stained with an anti-CD47 antibody (B6H12, eBioscience) and an anti-CD172a (Biolegend), respectively, as described above. Following incubation with primary antibodies and extensive wash, cells were incubated with Goat-anti-mouse Alexa488 or Goat-anti-mouse Alexa674 secondary antibodies.

DC sorting and Mixed lymphocyte reaction (MLR)

Tumor-DC co-cultures were established as described above. After wash in cold wash buffer (PBS/0.1% BSA/5mM EDTA) and incubation in Fc-receptor blocking buffer (2% HS in wash buffer, 15min at 4°C), cells were stained with sterile primary antibodies in wash buffer (20min at 4°C). The following antibodies were used: anti-MHC II-PECy7 (BD Biosciences, clone L243), anti-CD1c-PE (Miltenyi biotec, clone AD5-8E7). Sorting of DCs was performed using a Fluorescence Activated

Cell Sorter Aria (FACSAria, BD Bioscience), based on FSC/SSC properties and positivity for DC markers. Allogeneic PBLs were stained with 5 μM CFSE (Invitrogen), according to manufacturer's instructions and added to the sorted DCs at a ratio of 5:1 (Lymphocytes:DCs), for an additional period of 5 days, in 2% HS X-VIVO-15. After 5 days, co-cultures were stained with a primary anti-CD3-BV421 antibody (BD Horizon, clone SK7) and analyzed by flow cytometry. The percentage of proliferating T cells ($CD3^+$) was determined by assessing CFSE dilution in the fraction of $CD3^+$ cells.

Cytokine quantification

Supernatants from tumor cell-DC co-cultures (18 hours) were collected, dying/floating cells were removed by centrifugation and supernatants frozen immediately for detection of secreted cytokines. Human cytokines were quantified with a multiplex FlowCytomix kit (eBioscience, BMS810FF) according to the manufacturer's instructions.

Platinum treatment of tumor cells

Fluorescently–labelled (CFSE or GFP) tumor cells were seeded in T75 flasks (Corning), adhered and treated with oxaliplatin (OXP) or cisplatin (cis-diamminedichloroplatinum(II), CDDP) (both Accord).

Confocal microscopy

CFSE-labelled BLM cells were co-cultured with PKH26-labelled CD1c+DCs as described above, in the presence of IgG or blocking anti-CD47 (B6H12) antibody, at a final concentration of 20μg/ml. After 2h of incubation, DC-BLM cultures were let adhere on poly-L-lysine coated glass slides for 1h, carefully washed and fixed with 4% paraformaldehyde (PBS) in PBS. Uptake of CFSE-BLM-derived particles by $CD1c^+$ DCs was analyzed with a Laser Scanning Confocal microscope (Olympus). A total of 6 images per sample were taken and the number of DCs engulfing tumor-fragments was normalized over the number of DCs present in the image.

Statistical analysis

Unless otherwise indicated, experiments were performed at least three times, yielding comparable results. Data were analyzed using Prism v. 5.03 (GraphPad Software). Statistical significance was assessed by paired t-test. *P*-values <0.05 were considered as statistically significant.

Results

Melanoma cells suppress maturation and activation of CD1c$^+$ DCs

Tumor cells can affect DC maturation and function, both via secretion of inhibitory soluble factors and via contact-dependent mechanisms[9,17,24,30,31]. The majority of the studies that investigated tumor-mediated DC suppression have utilized either murine DCs or human *in vitro*-differentiated monocytes-derived DCs (moDCs). These models have some limitations as they lack many characteristics of human DCs found *in vivo*[25]. Therefore, we aimed to investigate the influence of human melanoma cells on phenotype and function of human CD1c$^+$ DCs, *in vitro*. We co-cultured freshly-isolated CD1c$^+$ DCs with melanoma BLM cancer cells, at different DC-to-tumor cell ratios (1:1 and 1:4) for 48 hours, and measured the extent of DC maturation by flow cytometry (Fig 1a). The co-culture with melanoma cells caused a drastic down-regulation of co-stimulatory (CD80, CD86) and major histocompatibility complex class I and II (MHC-I, MHC-II) molecules on CD1c$^+$ DCs. This marked inhibitory effect of tumor cells on DC maturation was observed already at the lowest DC-to-tumor cell ratio (1:1) tested, suggesting a high suppressive potency of BLM cells (Fig 1a).

Next, we evaluated the effect of co-culture with BLM cells on pro- and anti-inflammatory cytokine secretion by CD1c$^+$ DCs, represented by the secretion of TNF-α and IL-10 respectively (Fig 1b). Consistent with the inhibition of DC maturation, melanoma cells suppressed the production of the pro-inflammatory cytokine TNF-α and induced a minor but significant increase in IL-10 secretion. Furthermore, we could not detect any IL-2, IL-4, IL-5, IL-12, TNF-β and IFN-γ (data not shown). Because an altered activation status of DCs is often responsible for impaired T cell stimulatory activity, we tested whether CD1c$^+$ DCs co-cultured alone or with BLM melanoma cells, had different capacity to induce T cell proliferation. Proliferation of CD3$^+$ T cells was quantified by measuring CFSE dilution in a mixed lymphocyte reaction (MLR) (Fig 1c). As expected, interaction between melanoma cells and DCs markedly suppressed the capacity of CD1c$^+$ DCs to induce allogeneic T cell activation. Collectively, these data demonstrate that melanoma cells are capable of altering DC activation status and restrain functional ability of CD1c$^+$ DCs.

CD47 blockade enhances uptake of live tumor cells by CD1c$^+$ DCs and restores DC maturation

Overexpression of CD47 by tumor cells has been suggested as a possible mechanism of immune evasion in general and impaired DC function in particular[10,11,23]. We wondered whether this mechanism might be involved in the immunosuppressive

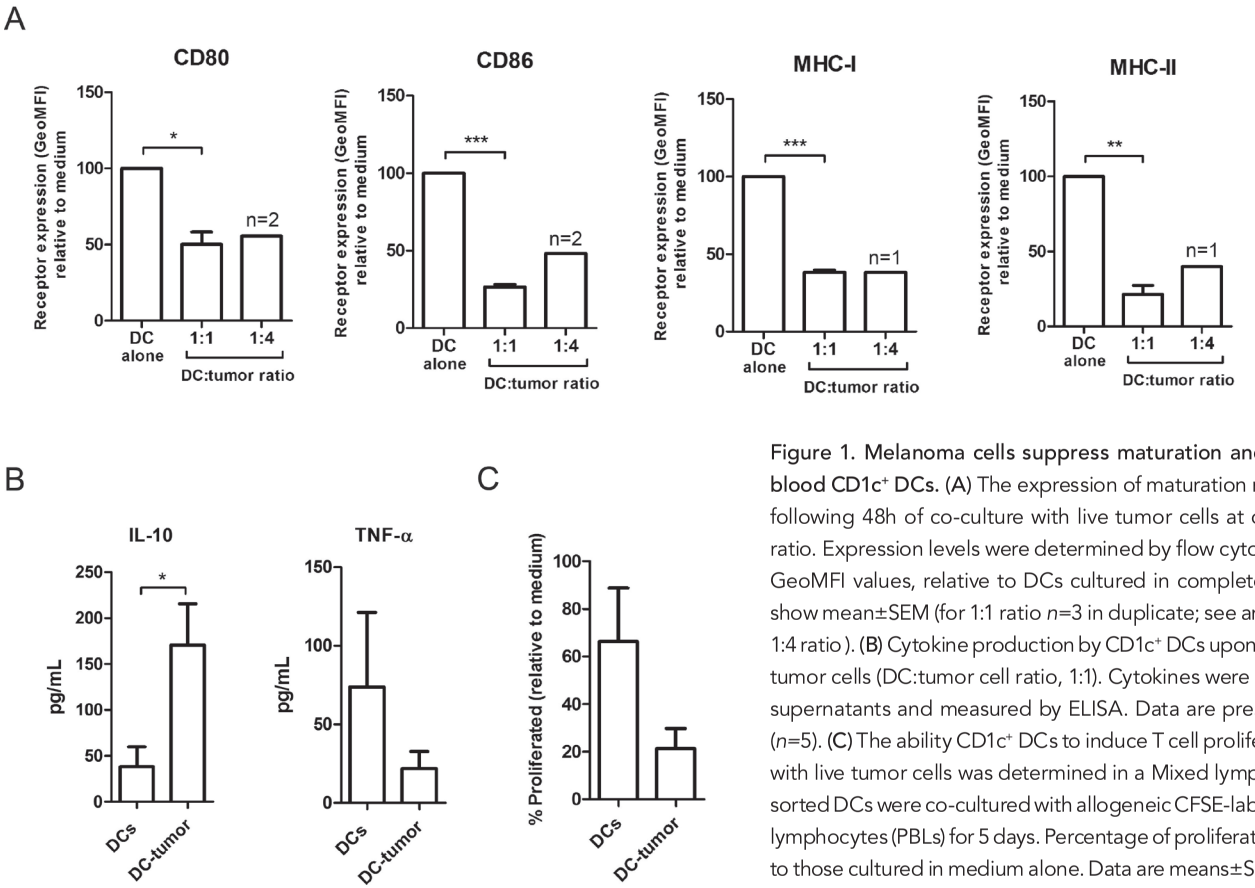

Figure 1. Melanoma cells suppress maturation and activation of human blood CD1c$^+$ DCs. (A) The expression of maturation markers on CD1c$^+$ DCs, following 48h of co-culture with live tumor cells at different DC:tumor cell ratio. Expression levels were determined by flow cytometry and depicted as GeoMFI values, relative to DCs cultured in complete medium. The graphs show mean±SEM (for 1:1 ratio *n*=3 in duplicate; see annotations on graph for 1:4 ratio). (B) Cytokine production by CD1c$^+$ DCs upon 18h co-culture with live tumor cells (DC:tumor cell ratio, 1:1). Cytokines were detected in cell culture supernatants and measured by ELISA. Data are presented as means±SEM (*n*=5). (C) The ability CD1c$^+$ DCs to induce T cell proliferation upon co-culture with live tumor cells was determined in a Mixed lymphocyte reaction. FACS sorted DCs were co-cultured with allogeneic CFSE-labeled pheripheral blood lymphocytes (PBLs) for 5 days. Percentage of proliferated CD3$^+$ T cells, relative to those cultured in medium alone. Data are means±SEM of at least triplicates of *n*=3. Significance was determined with paired *t*-test.*P < 0.05, **P < 0.01, ***P < 0.001, as compared to DCs cultured in medium.

effect we observed in our BLM melanoma - CD1c$^+$ DCs co-cultures. We started by screening several human melanoma cell lines for their CD47 surface expression, using flow cytometry analysis. All melanoma cell lines tested expressed high levels of CD47 (Fig 2a). BLM cells had the highest CD47 expression and were used in subsequent experiments.

CD47 was reported to exert its inhibitory effects by engaging SIRPα on APCs[27]. We measured surface expression of SIRPα on CD1c$^+$ DCs, as well as on *in* vitro monocyte-derived macrophages (moMfs) and moDCs (Fig 2b).

If CD47-SIRPα interaction is one of the immune-evasive mechanisms responsible for the inhibition of DC activation, we hypothesized that addition of a blocking antibody would, at least partially, rescue DC immunosuppression. We therefore established co-cultures of BLM melanoma cells and CD1c$^+$ DCs, in the presence of a CD47 blocking mAb (B6H12) or isotype IgG1,k control (Fig 3). We tested the

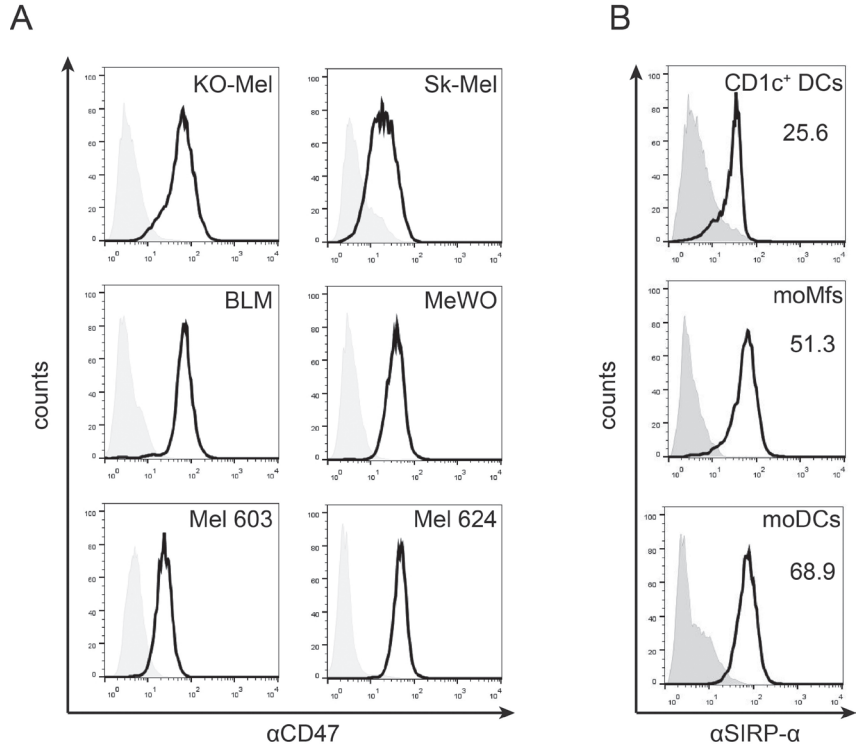

Figure 2. Expression of CD47 and SIRPα. **(A)** Representative histograms showing surface expression of CD47 on different human melanoma cell lines (KO-Mel, SK-Mel, BLM, MeWO, Mel603 and Mel624). **(B)** Representative histograms showing surface expression of SIRPα on blood CD1c$^+$ DCs, moMfs and moDCs). Isotypes (grey filled histogram), anti-CD47 or anti-SIRPα antibody (black line).

effect of CD47 blockade on the capacity of human APCs to engulf CFSE–labeled BLM-derived fragments. The positive effect of CD47 blockade has been previously described for macrophages and *in vitro* differentiated DCs[13,31,32], human moMfs or moDCs were included as additional controls (Fig 3a). We confirmed that moMfs have the highest ability to take up $CFSE^+$-tumor fragments at baseline (in the presence of control antibody IgG1,k, which does not block CD47-SIRPα interaction). Lower phagocytosis rate than moMfs was observed for $CD1c^+$ DCs and moDCs, which were equally potent phagocytes at baseline. Interestingly, CD47 blockade with the B6H12 mAb, led to a higher increase in $CD1c^+$ DC mediated uptake of $CFSE^+$-tumor fragments, indicating that these naturally circulating blood DCs had captured BLM-derived particles with more efficiency (Fig 3a), when compared to moDCs and moMfs. Increased engulfment of $CFSE^+$ BLM-derived fragments by $CD1c^+$ DCs, upon blocking of CD47, was confirmed by confocal microscopy (Fig 3b). To further verify that CD47-SIRPα interaction negatively regulates $CD1c^+$ DCs function, we used an additional mAb (2D3) directed against CD47, but which is known not to block CD47-SIRPα interaction, and measured tumor cell uptake and DC maturation by flow cytometry (Fig 3c,d). As shown in Fig 3c and 3d, disruption of CD47-SIRPα interaction counteracted the inhibitory pathway regulated by SIRPα and resulted in significantly higher uptake and increased surface expression of the co-stimulatory molecule CD86, as compared to isotype IgG1,k control or non-blocking 2D3 antibody. Notably, the expression level of CD86 upon CD47 blockade was almost as high as the expression measured on DC cultured alone, thus not exposed to the immunosuppressive effect of BLM cells (Fig 3d). Although less prominent, the beneficial effect of CD47 blockade was also observed for MHC-II (Fig 3d).

Altogether, our findings demonstrate that functional blocking of CD47 on tumor cells increased their engulfment by human $CD1c^+$ blood DCs. This was accompanied by high expression of DC maturation markers, supporting the observation that disruption of CD47-SIRPα interaction counteracts the immunosuppression induced by melanoma cells.

Platinum treatment rescues DC maturation and function

We previously reported that tumor cell death induced by treatment with the platinum chemotherapeutics, oxaliplatin and cisplatin, was characterized by the surface upregulation of CRT molecule on BLM cells, as well as the release of the inflammatory mediators, HSPs, ATP and HMGB1. Moreover, we showed that enhanced interaction of platinum-treated BLM melanoma cells and $CD1c^+$ DCs, and subsequent engulfment of tumor fragments, were dependent on ecto-CRT expression. In turn, platinum-mediated ICD of BLM cells, induced upregulation of

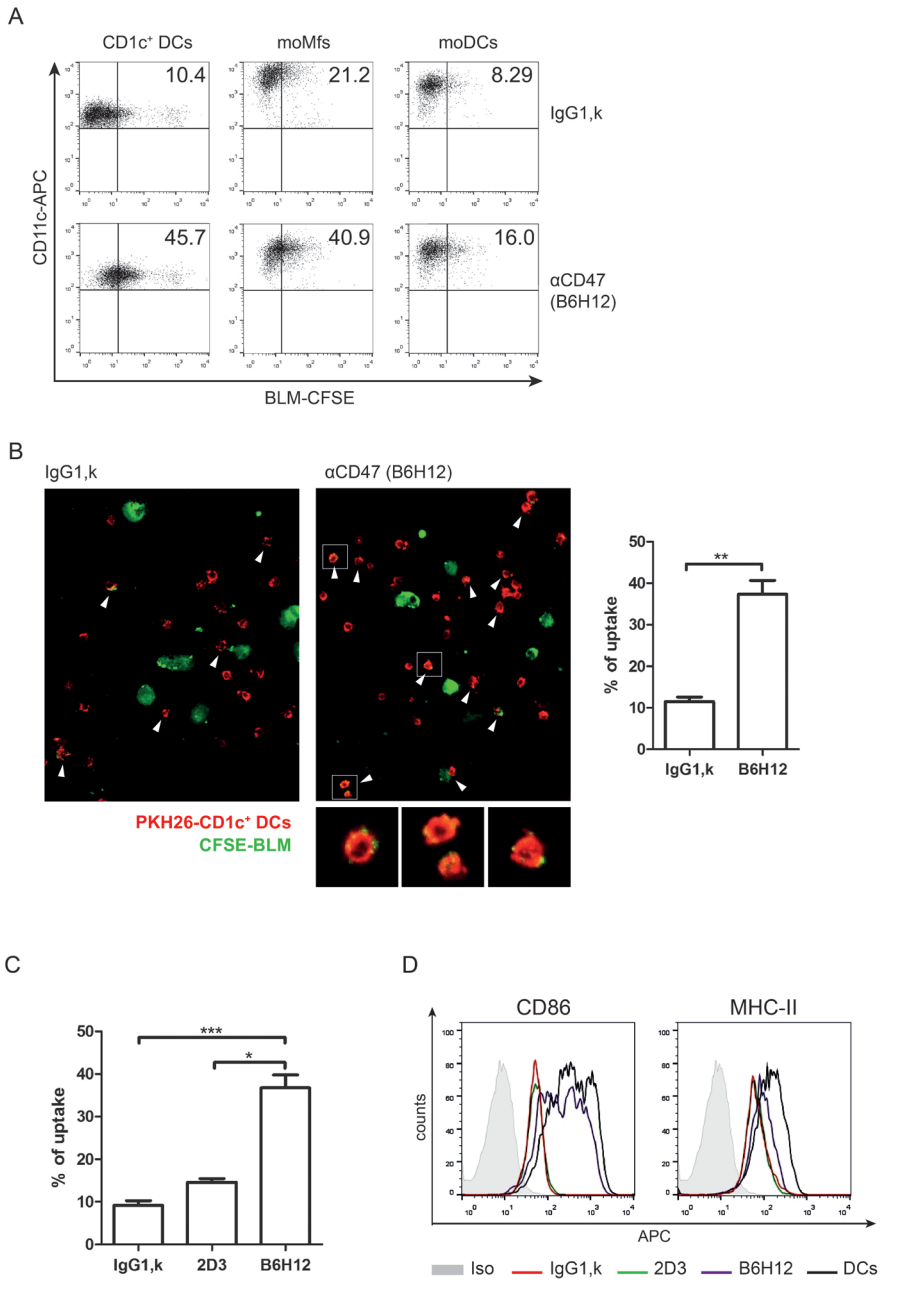

Figure 3. CD47 blockade enhances uptake of live tumor cells by CD1c⁺ DCs and restores DC maturation. CFSE-labeled BLM cells and different APCs were co-cultured for 2 hours in the presence of isotype control (IgG1,k) or anti-CD47 (B6H12) blocking antibody (final concentration 20μg/ml). **(A)** Representative dot plot of live BLM cells uptake by CD1c⁺ DCs, moMFs and moDCs upon functional blocking of CD47 on tumor cells. Percentage of phagocytosis was assessed by flow ▶

co-stimulatory molecules and functional activation of blood CD1c$^+$ DCs (Chapter 2 of this thesis). Given the ability of OXP and CDDP to induce ICD, we hypothesized that co-culture of DCs with platinum-treated BLM cells might shift the balance between 'eat me' and 'don't eat me' signals and thus reverting the immunosuppressive effects induced by the interaction with live tumor cells. We pre-treated BLM cells with clinical relevant concentrations of OXP or CDDP for 48 hours. We aimed at investigating the sole role of platinum treatment on tumor cells, excluding any direct effect of the chemotherapeutics on DCs. To this purpose, we removed any excess of drugs by extensive washing and fed untreated, OXP- or CDDP-treated BLM cells to blood CD1c$^+$ DCs for 48 hours (Fig 4). Platinum treatment induced upregulation of ecto-CRT on BLM cells (Fig 4a) and enhanced tumor-fragment uptake by blood CD1c$^+$ DCs (not shown). We then analyzed the surface expression of co-stimulatory (CD80, CD86) and major histocompatibility complex class I and II (MHC-I, MHC-II) molecules on blood CD1c$^+$ DCs (Fig 4b). As shown in Fig 1a, live tumor cells had a dramatic effect on the activation status of DCs. However, induction of ICD by platinum treatment reversed this suppression, with a notable effect at the level of co-stimulation (CD80 and CD86) (Fig 4b). The effect of platinum-treatment observed for MHC-I and MHC-II was less strong, yet it indicates that interfering with the activation of tumor-mediated immunoevasive mechanisms has beneficial consequences on DC maturation.

Furthermore, we checked how platinum treatment affected DC-mediated T cell proliferation (Fig 4c). We established blood CD1c$^+$ DCs-allogeneic CD3$^+$ T cells co-cultures and performed an MLR assay, as described in Fig 1c. Blood CD1c$^+$ DCs were pre-cultured with untreated or platinum-treated BLM cells, or alone in culture medium, for 48 hours, prior addition to CD3$^+$ T cells. Treatment of melanoma cells with either OXP or CDDP, restored DC-mediated T cell proliferation, counteracting the inhibition caused by live tumor cell-DC interaction.

▶ cytometry. (**B**) Representative confocal image (magnification 40X). Arrowheads indicate uptake of CFSE-BLM-derived particles by CD1c$^+$ DCs (pre-labeled with PKH26). A total of 6 images per sample were taken and the number of DCs engulfing tumor-fragments was normalized over the number of DCs present in the image. Data represent means of triplicates±SEM of 1 representative experiment. (**C**) Percentage of uptake of BLM-CFSE cells by CD1c$^+$ DCs (2h co-culture), in the presence of IgG1,k, non-blocking anti-CD47 (2D3) or blocking anti-CD47 (B6H12) mAbs. Final concentration 20μg/ml. The graph shows the means±SEM ($n \geq 2$ triplicate samples). (**D**) Representative histograms showing surface expression of maturation markers, CD86 and MHC-II on CD1c$^+$ DCs co-cultured with BLM cells for 24h.. Isotype (light grey filled histogram), IgG1,k (red), anti-CD47 (2D3, green), anti-CD47 (B6H12, purple), DCs alone (black). Significance was determined with paired *t*-test.*P < 0.05, **P < 0.01, ***P < 0.001.

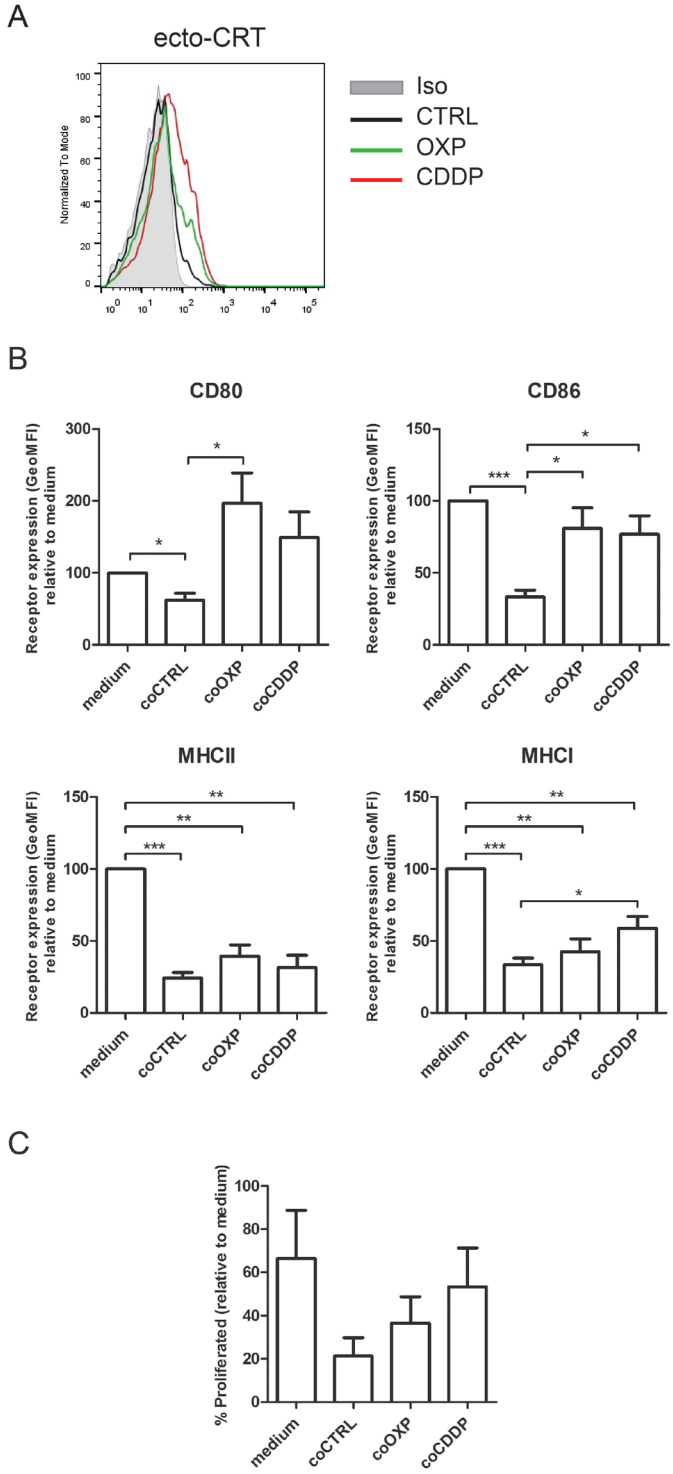
A
ecto-CRT
Normalized To Mode
Iso
CTRL
OXP
CDDP
B
CD80
CD86
MHCII
MHCI
Receptor expression (GeoMFI) relative to medium
medium
coCTRL
coOXP
coCDDP
C
% Proliferated (relative to medium)

Potential cooperation of CD47 blockade and platinum treatment

We showed that tumor-mediated immunosuppression could be subverted either by blocking of CD47 on live BLM cells or upregulating 'eat me' signals like ecto-CRT by inducing immunogenic tumor cell death. We therefore hypothesized that combination of these two therapeutic approaches might cooperate and potentiate their beneficial effects on DC stimulation. Firstly, we checked whether platinum treatment could influence CD47 expression on melanoma cells. BLM cells were treated with 15μM OXP or CDDP for 24 hours and surface CD47 expression was analysed by flow cytometry. Surprisingly, we observed that OXP and CDDP were equally capable to upregulate CD47 expression on tumor cells (Fig 5a). We previously reported that CDDP was more potent than OXP in triggering uptake of BLM cells. Here, we compared the ability of $CD1c^+$ DCs to engulf live (CTRL) or CDDP-treated BLM cells in the presence of a blocking anti-CD47 (B6H12) mAb or isotype control, *in vitro* (Fig 5b). We confirmed that CDDP-treated BLM cells were taken up more efficiently by $CD1c^+$ DCs when CD47 was not functionally blocked, as compared to CTRL cells. Similarly, CD47 blockade facilitated phagocytosis of live BLM cells, in comparison to IgG1,k. Interestingly, CD47 blockade in combination with CDDP treatment strengthened, albeit not dramatically, tumor cell engulfment by $CD1c^+$ DCs, as compared to either therapy alone (Fig 5b). Moreover, flow cytometry analysis of DC maturation showed that, functional blockade of CD47 in combination with chemotherapy markedly increased the expression of the co-stimulatory molecule CD86 (Fig 5c).

◀ **Figure 4. Platinum treatment rescues DC maturation and function.** (**A**) Representative histogram showing surface expression of ecto-CRT on BLM cells treated with OXP or CDDP for 48h. Isotype (light grey filled histogram), untreated (CTRL, black), OXP (green), CDDP (red). (**B**) Expression of maturation markers on $CD1c^+$ DCs following 48h of co-culture with untreated or platinum-treated BLM cells. Expression levels were determined by flow cytometry and depicted as GeoMFI values, relative to DCs cultured in medium. The graphs show mean±SEM (*n*=5). (**C**) Mixed lymphocyte reaction to determine T cell proliferation induced by $CD1c^+$ DCs upon co-culture with (un)treated tumor cells. FACS sorted DCs were co-cultured with allogeneic CFSE-labeled pheripheral blood lymphocytes (PBLs) for 5 days. Percentage of proliferated $CD3^+$ T cells, relative to those cultured in medium alone. Data are means±SEM of at least triplicates of *n*=3. Significance was determined with paired *t*-test.*P < 0.05, **P < 0.01, ***P < 0.001, as compared to DCs cultured in medium.

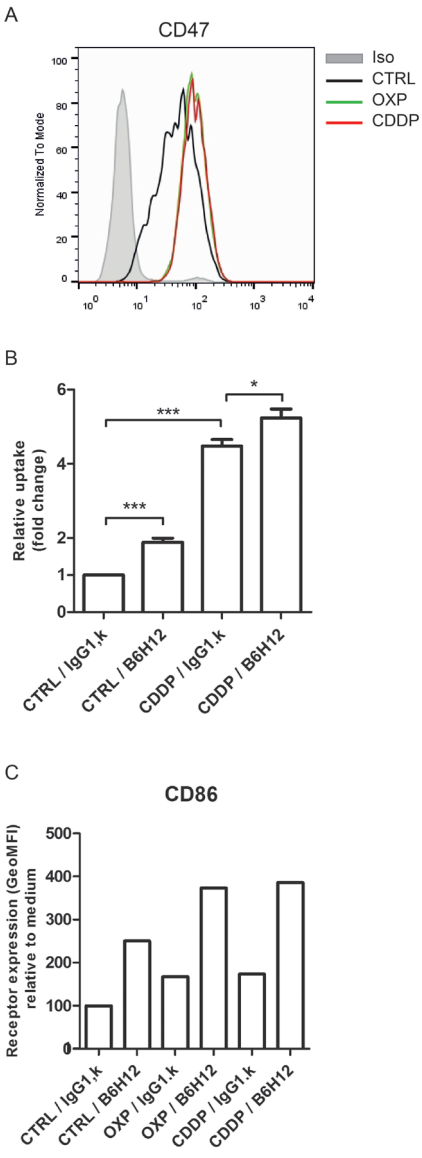

Figure 5. Potential synergistic effects of CD47 blockade and platinum treatment. (A) Representative histogram showing surface expression of CD47 on BLM cells treated with OXP or CDDP for 24h. Isotype (light grey filled histogram), untreated (CTRL, black), OXP (green), CDDP (red). (B) Relative uptake of BLM-GFP cells by CD1c$^+$ DCs (48h co-culture), in the presence of IgG1,k or blocking anti-CD47 (B6H12) mAbs. Final concentration 20µg/ml. The graph shows the means±SEM (*n*=2 duplicate samples). (C) Expression of CD86 on CD1c$^+$ DCs in co-culture with untreated or platinum-treated BLM cells. Expression levels were determined by flow cytometry and depicted as GeoMFI values, relative to DCs cultured with untreated (CTRL) BLM cells in the presence of IgG1,k. One representative experiment is shown. Significance was determined with paired *t*-test.*P < 0.05, **P < 0.01, ***P < 0.001.

Discussion

Dendritic cells play a key role in the regulation of the immune system[5] The nature of signals delivered by DCs, upon encounter with (tumor) antigens, determines the fate of the immune response. Molecular mechanisms responsible for initiating immune reactions or inducing tolerance are tightly interconnected and may be considered

two sides of the same coin[4,5,28]. Tumor cells have developed several mechanisms to evade immunosurveillance, including taking advantage of regulatory signalling pathways, to evade phagocytosis and possibly halt initiation of anti-tumor responses[3].

Here, we investigated the interaction between melanoma cells and human CD1c$^+$ DCs naturally circulating in the blood. We observed that, co-culture with live tumor cells affected expression of co-stimulatory molecules and function of CD1c$^+$ DCs. Phenotypical and functional changes on DCs resulted in diminished capacity to drive T cell proliferation. Our observations are in accordance with other studies performed on human *in vitro*-generated moDCs or murine DCs[9,23,24,31]. Co-culture of moDCs with primary cells or tumor cell lines caused an immature phenotype in DCs, stimulated IL-10 production and inhibited TNF-α secretion, eventually causing T cell unresponsiveness[23,31]. Similarly, maturation and activation of murine splenic DCs were impaired by culture with melanoma cells[24].

A putative mechanism responsible for tumor-mediated DC suppression relies on the interaction between CD47 on live tumor cells and SIRPα on DCs[12]. Engagement of SIRPα by CD47 was suggested to activate two distinct downstream signaling pathways. CD47-SIRPα can signal through the ITIM-SHP-1 complex that transmit an anti-phagocytic signal; in addition, it can also trigger STAT3 phosphorylation that is linked to an immature APC phenotype and secretion of IL-10[23,33]. The dual role of CD47-SIRPα interaction is mediated by two adjacent but distinct binding regions for CD47 on SIRPα[34]. Whether the boosting of tumor fragments uptake by CD47 blocking mAb (B6H12), interferes with the activation of only one or both SIRPα-downstream mechanisms remains unclear[23]. In our study, we confirmed that engagement of CD47 by the B6H12 mAb, but not by a matched isotype control or the non-blocking anti-CD47 (2D3) mAb, restored engulfment of tumor cell fragments by different human APCs, such as moMfs, moDCs and naturally-occurring blood CD1c$^+$ DCs. Moreover, only functional disruption of the CD47-SIRPα interaction using the B6H12 mAb, reversed tumor-mediated inhibition of CD1c$^+$ DCs maturation. Activation of the STAT3 signalling pathway is known to be involved in regulation of CD86 and MHC-II expression[33]. Tumor-mediated CD86 down-regulation was fully rescued by the addition in co-culture of the blocking B6H12 mAb. Upregulation of MHC class II molecule was also enhanced, albeit to a lesser extent. This difference might be dependent on the kinetics of expression of the two maturation markers and analysis of DC phenotype at a later time point would help clarifying this point.

CD47 is a marker of self for all hematopoietic cells. Therefore, it is not surprising that, human APCs co-express SIRPα and CD47[10,35]. In our co-culture experiments, melanoma cells were pre-incubated with CD47 blocking mAb. After CD47 blocking, melanoma cells were fed to CD1c$^+$ DCs, and extra volume of anti-CD47 mAbs or isotype controls were added to tumor-DC co-cultures, at the same final concentration. Binding of mAbs to

specific cellular receptors is a dynamic process. Thus, it is likely that CD47 on DCs could compete with CD47 on tumor cells for the binding of anti-CD47 unbound molecules. Engagement of CD47 on human moDCs, by blocking mAb or CD47-FC fusion protein, was reported to negatively regulate moDC maturation and IL-12 production[12,35]. For this reason, we can suggest that knockdown of CD47 on tumor cells or SIRPα on DCs, would further support the hypothesis that CD47-SIRPα interaction is one of the crucial mechanisms regulating tumor-mediated suppression of $CD1c^+$ DCs.

Phagocytosis relies on the balance between anti-phagocytic ("don't eat me") and pro-phagocytic ("eat me") signals on target cells. The inhibitory action of CD47 is counterbalanced by ecto-CRT, translocated to the surface of tumor cells upon ER stress. We recently reported that platinum-treatment upregulated ecto-CRT on the surface of melanoma cells and enhanced tumor-cell uptake by blood $CD1c^+$ mDCs. Moreover, interaction with platinum-treated tumor cells induced $CD1c^+$ DCs activation and T cell proliferation. Here we show that, in a similar way to CD47 blockade, platinum-treatment rescued tumor-mediated suppression of DC maturation, which in turn restored induction of $CD3^+$ T cells by DCs proliferation. Although crucial to facilitate cellular uptake by phagocytes, ecto-CRT alone is not sufficient to stimulate DC maturation and function[36]. Additional activating signals expressed on or released by tumor cells are required to strengthen DC stimulation. In our previous report, we showed that both OXP and CDDP led to upregulation of HSPs, as well as passive release of ATP and secretion of HMGB1[REF]. We believe that induction of ICD is likely to be strong enough to overcome the suppressive mechanisms employed by tumor cells, thus explaining the beneficial effect of platinum treatment observed.

In contrast to the favourable impact of CD47 blockade or chemotherapy alone on DC-mediated phagocytosis, we showed that addition of the blocking (B6H12) anti-CD47 mAb, to co-culture of DCs with platinum-treated BLM cells, did not potentiate the chemotherapic effect on BLM uptake by $CD1c^+$ DCs. We postulate that increased expression of ecto-CRT on dying tumor cells dominates over the blockade of CD47. Consequently, combination of the two therapeutic approaches did not lead to increased uptake. We observed a higher expression of CD47 on cells treated with platinum drugs; however, this effect alone does not indicate whether CD47 is still able to engage SIRPα. On live cells, in fact, CD47 is evenly distributed, whereas it clusters into patches on apoptotic cells[37-39]. Clustering per se does not seem to affect binding to SIRPα, but it is proposed that CD47 loses its ability to activate SIRPα, thereby preventing uptake of apoptotic cells[38]. The mechanisms governing redistribution and functional inactivation have not been elucidated yet.

Studies performed on xenograft mouse models of hepatocellular carcinoma or leukemia, suggested that combination of CD47 blockade and treatment with chemotherapeutic drugs (sorafenib, doxorubicin or cytarabine), might exert synergistic

effects on suppression of tumor growth, as compared to either therapies alone[40,41,42]. When designing combination therapies, sequence and doses of both anti-CD47 and chemotherapeutics have to be carefully determined, in order to prevent undesired effects on the immune response. Researchers showed that *in vivo* administration of chemotherapy, following anti-CD47 blockade had deleterious effect on the host immune response to the tumor. In contrast, when chemotherapy treatment was given prior to anti-CD47 mAbs, this preserved host memory response against relapsing tumors[43]. These observations seem to be in line with our results, showing a marked upregulation of CD86 on the surface of blood CD1c$^+$ DCs upon interaction with BLM cells pre-treated with platinum drugs, in addition to functional blocking of CD47.

Altogether, we report that interaction with tumor cells transmits a negative signal to naturally circulating human blood CD1c$^+$ DCs that have impaired ability to establish adaptive responses. Evidence suggests that SIRPα-engagement by CD47 might be responsible for the immunosuppressive effect observed[10,13,23]. In addition we show that shifting the balance between inhibitory "don't eat me" and activating "eat me" signals via CD47 blockade, either alone or in combination with chemotherapy, has the potential to revert tumor-mediated immunosuppression. This might contribute to enhance the immunogenicity of melanoma cells and promote activation of CD1c$^+$ DCs, in favour of the induction of a robust anti-tumor immune response.

Aknowledgments

This work was supported by a grant from the Dutch Cancer Society and Alpe deHuZes foundation to S.V.H. (KUN2013-5958) and Dutch Cancer Society grant (KUN2009-4402). CGF received an NWO Spinoza award and ERC Adv Grant PATHFINDER (269019). IJMdV received NWO Vici Grant 918.14.655.

Author contribution

SDB, SVH and CGF conceived the study. SDB, LEdV, IMNW and DAGvB performed the experiments and analyzed the data. SDB wrote the manuscript. All authors revised and approved the final version of the manuscript.

References

1. Zitvogel, L., Tesniere, A. & Kroemer, G. Cancer despite immunosurveillance: immunoselection and immunosubversion. *Nat Rev Immunol* **6**, 715-727 (2006).
2. Kerkar, S. P. & Restifo, N. P. Cellular Constituents of Immune Escape within the Tumor Microenvironment. *Cancer Research* **72**, 3125-3130, doi:10.1158/0008-5472.can-11-4094 (2012).
3. Gabrilovich, D. Mechanisms and functional significance of tumour-induced dendritic-cell defects. *Nat Rev Immunol* **4**, 941-952 (2004).
4. Karthaus, N., Torensma, R. & Tel, J. Deciphering the Message Broadcast by Tumor-Infiltrating Dendritic Cells. *The American Journal of Pathology* **181**, 733-742, doi:http://dx.doi.org/10.1016/j.ajpath.2012.05.012 (2012).
5. Dudek, A. M., Martin, S., Garg, A. D. & Agostinis, P. Immature, Semi-mature and Fully mature Dendritic Cells: Towards a DC-cancer cells interface that augments anticancer immunity. *Frontiers in Immunology* **4**, doi:10.3389/fimmu.2013.00438 (2013).
6. Klechevsky, E. in *Crossroads Between Innate and Adaptive Immunity V* (eds P. Stephen Schoenberger, D. Peter Katsikis, & Bali Pulendran) 43-54 (Springer International Publishing, 2015).
7. Bakdash, G., Schreurs, I., Schreibelt, G. & Tel, J. Crosstalk between dendritic cell subsets and implications for dendritic cell-based anticancer immunotherapy. *Expert review of clinical immunology* **10**, 915-926, doi:10.1586/1744666x.2014.912561 (2014).
8. MacDonald, K. P. A. *et al.* Characterization of human blood dendritic cell subsets. *Blood* **100**, 4512-4520, doi:10.1182/blood-2001-11-0097 (2002).
9. Ghiringhelli, F. *et al.* Tumor cells convert immature myeloid dendritic cells into TGF-β–secreting cells inducing CD4(+)CD25(+) regulatory T cell proliferation. *The Journal of Experimental Medicine* **202**, 919-929, doi:10.1084/jem.20050463 (2005).
10. Latour, S. *et al.* Bidirectional Negative Regulation of Human T and Dendritic Cells by CD47 and Its Cognate Receptor Signal-Regulator Protein-α: Down-Regulation of IL-12 Responsiveness and Inhibition of Dendritic Cell Activation. *The Journal of Immunology* **167**, 2547-2554, doi:10.4049/jimmunol.167.5.2547 (2001).
11. Braun, D. *et al.* Semimature Stage: A Checkpoint in a Dendritic Cell Maturation Program That Allows for Functional Reversion after Signal-Regulatory Protein-α Ligation and Maturation Signals. *The Journal of Immunology* **177**, 8550-8559, doi:10.4049/jimmunol.177.12.8550 (2006).
12. Schäkel, K. *et al.* Human 6-Sulfo LacNAc-Expressing Dendritic Cells Are Principal Producers of Early Interleukin-12 and Are Controlled by Erythrocytes. *Immunity* **24**, 767-777, doi:http://dx.doi.org/10.1016/j.immuni.2006.03.020 (2006).
13. Yi, T. *et al.* Splenic Dendritic Cells Survey Red Blood Cells for Missing Self-CD47 to Trigger Adaptive Immune Responses. *Immunity* **43**, 764-775, doi:http://dx.doi.org/10.1016/j.immuni.2015.08.021 (2015).
14. Adams, S. *et al.* Signal-Regulatory Protein Is Selectively Expressed by Myeloid and Neuronal Cells. *The Journal of Immunology* **161**, 1853-1859 (1998).
15. Matozaki, T., Murata, Y., Okazawa, H. & Ohnishi, H. Functions and molecular mechanisms of the CD47–SIRPα signalling pathway. *Trends in Cell Biology* **19**, 72-80, doi:http://dx.doi.org/10.1016/j.tcb.2008.12.001 (2009).
16. Oldenborg, P.-A. *et al.* Role of CD47 as a Marker of Self on Red Blood Cells. *Science* **288**, 2051-2054, doi:10.1126/science.288.5473.2051 (2000).

17. Seo, M. J. *et al.* Interactions of dendritic cells with cancer cells and modulation of surface molecules affect functional properties of CD8+ T cells. *Molecular Immunology* **48**, 1744-1752, doi:http://dx.doi.org/10.1016/j.molimm.2011.04.018 (2011).
18. Willingham, S. B. *et al.* The CD47-signal regulatory protein alpha (SIRPa) interaction is a therapeutic target for human solid tumors. *Proceedings of the National Academy of Sciences of the United States of America* **109**, 6662-6667, doi:10.1073/pnas.1121623109 (2012).
19. Kharitonenkov, A. *et al.* A family of proteins that inhibit signalling through tyrosine kinase receptors. *Nature* **386**, 181-186 (1997).
20. Veillette, A., Thibaudeau, E. & Latour, S. High Expression of Inhibitory Receptor SHPS-1 and Its Association with Protein-tyrosine Phosphatase SHP-1 in Macrophages. *Journal of Biological Chemistry* **273**, 22719-22728, doi:10.1074/jbc.273.35.22719 (1998).
21. Stofega, M. R., Argetsinger, L. S., Wang, H., Ullrich, A. & Carter-Su, C. Negative Regulation of Growth Hormone Receptor/JAK2 Signaling by SIRPα. *Journal of Biological Chemistry*, doi:10.1074/jbc.M004238200 (2000).
22. Alblas, J. *et al.* Signal Regulatory Protein α Ligation Induces Macrophage Nitric Oxide Production through JAK/STAT- and Phosphatidylinositol 3-Kinase/Rac1/NAPDH Oxidase/H(2)O(2)-Dependent Pathways. *Molecular and Cellular Biology* **25**, 7181-7192, doi:10.1128/MCB.25.16.7181-7192.2005 (2005).
23. Toledano, N., Gur-Wahnon, D., Ben-Yehuda, A. & Rachmilewitz, J. Novel CD47: SIRPα Dependent Mechanism for the Activation of STAT3 in Antigen-Presenting Cell. *PLoS ONE* **8**, e75595, doi:10.1371/journal.pone.0075595 (2013).
24. Hargadon, K. M. *et al.* Melanoma-derived factors alter the maturation and activation of differentiated tissue-resident dendritic cells. *Immunol Cell Biol* **94**, 24-38, doi:10.1038/icb.2015.58 (2016).
25. Klarquist, J. S. & Janssen, E. M. Melanoma-infiltrating dendritic cells: Limitations and opportunities of mouse models. *Oncoimmunology* **1**, 1584-1593, doi:10.4161/onci.22660 (2012).
26. Barclay, A. N. & van den Berg, T. K. The Interaction Between Signal Regulatory Protein Alpha (SIRPα) and CD47: Structure, Function, and Therapeutic Target. *Annual Review of Immunology* **32**, 25-50, doi:10.1146/annurev-immunol-032713-120142 (2014).
27. Chao, M. P., Weissman, I. L. & Majeti, R. The CD47-SIRPα Pathway in Cancer Immune Evasion and Potential Therapeutic Implications. *Current Opinion in Immunology* **24**, 225-232, doi:10.1016/j.coi.2012.01.010 (2012).
28. Hargadon, K. M. Tumor-Altered Dendritic Cell Function: Implications for Anti-Tumor Immunity. *Frontiers in Immunology* **4**, 192, doi:10.3389/fimmu.2013.00192 (2013).
29. Oldenborg, P.-A., Gresham, H. D. & Lindberg, F. P. Cd47-Signal Regulatory Protein α (Sirpα) Regulates Fcγ and Complement Receptor–Mediated Phagocytosis. *The Journal of Experimental Medicine* **193**, 855-862 (2001).
30. Gur-Wahnon, D., Borovsky, Z., Beyth, S., Liebergall, M. & Rachmilewitz, J. Contact-dependent induction of regulatory antigen-presenting cells by human mesenchymal stem cells is mediated via STAT3 signaling. *Experimental Hematology* **35**, 426-433, doi:http://dx.doi.org/10.1016/j.exphem.2006.11.001 (2007).
31. Gur-Wahnon, D., Borovsky, Z., Liebergall, M. & Rachmilewitz, J. The Induction of APC with a Distinct Tolerogenic Phenotype via Contact-Dependent STAT3 Activation. *PLoS ONE* **4**, e6846, doi:10.1371/journal.pone.0006846 (2009).

32. Tseng, D. *et al.* Anti-CD47 antibody–mediated phagocytosis of cancer by macrophages primes an effective antitumor T-cell response. *Proceedings of the National Academy of Sciences* **110**, 11103-11108, doi:10.1073/pnas.1305569110 (2013).
33. Yu, H., Kortylewski, M. & Pardoll, D. Crosstalk between cancer and immune cells: role of STAT3 in the tumour microenvironment. *Nat Rev Immunol* **7**, 41-51 (2007).
34. Lee, W. Y. *et al.* Novel Structural Determinants on SIRPα that Mediate Binding to CD47. *The Journal of Immunology* **179**, 7741-7750, doi:10.4049/jimmunol.179.11.7741 (2007).
35. Demeure, C. E. *et al.* CD47 Engagement Inhibits Cytokine Production and Maturation of Human Dendritic Cells. *The Journal of Immunology* **164**, 2193-2199, doi:10.4049/jimmunol.164.4.2193 (2000).
36. Tesniere, A. *et al.* Immunogenic cancer cell death: a key-lock paradigm. *Current Opinion in Immunology* **20**, 504-511, doi:http://dx.doi.org/10.1016/j.coi.2008.05.007 (2008).
37. Gardai, S. J. *et al.* Cell-surface calreticulin initiates clearance of viable or apoptotic cells through trans-activation of LRP on the phagocyte. *Cell* **123**, 321-334, doi:10.1016/j.cell.2005.08.032 (2005).
38. Nilsson, A. & Oldenborg, P.-A. CD47 promotes both phosphatidylserine-independent and phosphatidylserine-dependent phagocytosis of apoptotic murine thymocytes by non-activated macrophages. *Biochemical and Biophysical Research Communications* **387**, 58-63, doi:http://dx.doi.org/10.1016/j.bbrc.2009.06.121 (2009).
39. Lv, Z. *et al.* Loss of Cell Surface CD47 Clustering Formation and Binding Avidity to SIRPα Facilitate Apoptotic Cell Clearance by Macrophages. *The Journal of Immunology* **195**, 661-671, doi:10.4049/jimmunol.1401719 (2015).
40. Lo, J. *et al.* Nuclear factor kappa B–mediated CD47 up-regulation promotes sorafenib resistance and its blockade synergizes the effect of sorafenib in hepatocellular carcinoma in mice. *Hepatology* **62**, 534-545, doi:10.1002/hep.27859 (2015).
41. Lo, J. *et al.* Anti-CD47 antibody suppresses tumour growth and augments the effect of chemotherapy treatment in hepatocellular carcinoma. *Liver International*, n/a-n/a, doi:10.1111/liv.12963 (2015).
42. Wang, Y., Yin, C., Feng, L., Wang, C. & Sheng, G. Ara-C and anti-CD47 antibody combination therapy eliminates acute monocytic leukemia THP-1 cells in vivo and in vitro. *Genetic and molecular research* **14**, 5630-5641, doi:10.4238/2015 (2015).
43. Liu, X. *et al.* CD47 blockade triggers T cell-mediated destruction of immunogenic tumors. *Nat Med* **21**, 1209-1215, doi:10.1038/nm.3931
44. http://www.nature.com/nm/journal/v21/n10/abs/nm.3931.html#supplementary-information (2015).
45. Lindstedt, M., Lundberg, K. & Borrebaeck, C. A. K. Gene Family Clustering Identifies Functionally Associated Subsets of Human In Vivo Blood and Tonsillar Dendritic Cells. *The Journal of Immunology* **175**, 4839-4846, doi:10.4049/jimmunol.175.8.4839 (2005).
46. Gautier, L., Cope, L., Bolstad, B. M. & Irizarry, R. A. affy—analysis of Affymetrix GeneChip data at the probe level. *Bioinformatics* **20**, 307-315, doi:10.1093/bioinformatics/btg405 (2004).

CHAPTER 4

Taking the tumor microenvironment to the third dimension: visualization of CD1c$^+$ DCs migration and function in a novel human melanoma skin model

Stefania Di Blasio[1], Angela Vasaturo[1], Marcella Tazzari[1], Irene Stefanini[2], Gert-Jan Bakker[4], Joost Schalkwijk[3], Stanleyson V. Hato[1], Ellen H. van den Bogaard[3], Carl G. Figdor[1]

[1]Department of Tumor Immunology, Radboud Institute for Molecular Life Sciences, Radboud University Medical Center, Nijmegen, The Netherlands; [2]Istituto Agrario di San Michele All'Adige (IASMA), Fondazione Edmund Mach, Department of Computational Biology, San Michele All'Adige, Italy; [3]Department of Dermatology, Radboud University Medical Center, Nijmegen, The Netherlands; [4]Department of Cell Biology, RIMLS, St. Radboud UMC, Nijmegen, Netherlands.

Manuscript in preparation

Abstract

Melanoma is the most aggressive form of skin cancer. Due to the ability to build a microenvironment that supports tumor progression, melanoma cells are capable of evading the immune system. Pre-clinical mouse models and conventional *in vitro* two-dimensional (2D) studies have shed light on important aspects of melanoma immunobiology. However, standard cultures fail to capture the complexity of the real tissue architecture. Besides, given the ethical concerns and the questionable translational character of murine models to human biology, a more physiologically relevant model, that closely resembles the *in vivo* features of human melanoma, is required. Here, we present a novel human three-dimensional (3D) immuno-competent engineered skin model of melanoma. This model is based on the co-culture of different cell types using a deepidermized acellular dermis (DED) as an extracellular matrix scaffold. In order to reconstitute the skin melanoma tissue microenvironment, primary keratinocytes are co-seeded with melanoma cells onto the DED. Keratinocytes differentiate into a fully developed epidermis and tumor cells emulate melanoma invasion in the underneath dermal compartment. Primary fibroblasts and $CD1c^+$ dendritic cells were incorporated into the acellular dermis to expand the organotypic model into a functional melanoma microenvironment. The repopulated DED provides an adequate support that guarantees cell survival, migration and function of all cell types. Histological analysis demonstrated that the reconstructed microenvironment displays morphological features of primary melanoma and showed the correct spatial cell distribution. Two-photon imaging revealed that the dendritic cells are able to actively migrate, interact with tumor cells and sample tumor-derived microparticles. These results highlight the applicability of our 3D reconstructed human melanoma microenvironment to explore the interplay between malignant, non-malignant cells and the immune system. We propose that our 3D melanoma skin model has the potential to provide a unique tool for generating "living" skin melanoma tissue, and may play an instrumental role in the identification of new therapeutic targets for immunotherapy.

Introduction

Progressive tumor growth and development of metastases are dynamic processes, which rely upon the establishment of complex interactions between malignant cancer cells and the non-transformed host cells of the tumor microenvironment [1, 2]. Communication of malignant cells with the normal tissue cellular and extracellular components plays a critical role in determining the fate of tumor progression and activation of an effective antitumor immunity [1]. Accordingly, pre-clinical and clinical observations demonstrated that cancer cells foster a 'tolerizing' microenvironment, characterized by chronic inflammation, recruitment and infiltration of immune cells, and the activation of a plethora of immunosuppressive mechanisms [1]. These mechanisms not only impede effective anti-tumor immunity, but also are responsible for tumor resistance to chemo- and immunotherapy [3].

Melanoma is amongst the most lethal types of tumor of the skin [4]. This form of skin cancer is caused by the malignant transformation of melanocytes, the epidermal cells responsible for the production of melanin pigment [4]. Although in the past decades we have seen a remarkable progress in the understanding of melanoma immunobiology, knowledge on the intricate network of mechanisms that regulate tumor-mediated immunosuppression is still lacking [3].

Most of the studies that aimed at dissecting melanoma-host immune cell interactions were performed using *in vitro* two-dimensional (2D) co-culture of cells in monolayers. These studies provided insights into many aspects of the mechanisms regulating the fate of immune response to the tumor, however the 2D nature of these models ignores the relevant structural and functional complexity of *in vivo* tissues [5]. In fact, monolayer systems are limited by the lack of a large number of contacts between cell types and by the absence of a physiologically relevant extracellular matrix (ECM), which affects cell function and response to microenvironmental stimuli [6]. Thus, conventional studies are hampered by the difficulties in culturing cells in 2D and extrapolating these findings to the three-dimensional tumor microenvironment (3D TME).

To identify determinants of melanoma progression in a more physiologically relevant system, researchers have relied on mouse models. However, there are considerable obstacles that complicate the use of these *in vivo* models for melanoma research [7]. Besides the ethical issue of using animals for the investigation of tumor biology, both the histological and immunological differences between rodent and human skin often challenge the interpretation of data obtained by *in vivo* studies [7]. Therefore, *in vitro* systems that provide organizational complexity that is between the 2D (co-)culture of cells and organ cultures *in vivo* have attracted considerable attention in the research field [8, 9].

In vitro tissue-engineered skin models or human skin equivalents (HSEs) are informative and manipulable systems, which can bring together melanoma cells with other relevant cells of the tissue microenvironment, in a context that recapitulates the characteristics of human skin cancer lesions [10]. In these models, human epidermal cells and melanoma cell lines, with different invasive capacities, are seeded onto fibroblasts-enriched, animal-derived collagen matrices [11-13]. Others have developed organotypic models based on acellular, de-epidermized human dermis (DED) or self-assembled living sheets made with human fibroblasts secreting their own ECM, to obtain a model that more closely resembles the multifaceted skin tissue[14-17]. Despite the substantial contribution in the field, currently available melanoma skin equivalents are lacking in one important aspect: the immune compartment [18]. Melanoma is considered one of the most immunogenic cancer types. Thus, any model intending to investigate melanoma progression in the context of the tumor microenvironment should also consider the involvement of the immune system.

We have successfully adapted an existing *in vitro* 3D model of melanoma[17], which lacked stromal and immune components, into an immunocompetent tissue-engineered melanoma skin equivalent. This model is build from primary human keratinocytes and immortalized human melanoma cells seeded onto a de-epidermized human dermis (DED). Primary human dermal fibroblasts and immune cells, such as $CD1c^+$ dendritic cells (DCs), were incorporated into the acellular dermal compartment. Histological analysis of tissue sections showed the correct spatial distribution of the cells within the reconstructed tissue microenvironment, demonstrating that melanoma model closely recapitulates tumor growth as observed in human lesions. Live imaging with two-photon microscopy revealed that the reconstructed environment supports cell survival, migration and function of both malignant and immune cells of the TME.

We here present, for the first time to our knowledge, a novel human immunocompetent 3D melanoma engineered skin tissue that has the potential to provide a unique tool for generating "living" skin melanoma tissue, for the investigation of cellular interplays within the TME. Unraveling these complex intra- and intercellular communications may ultimately pave the way to the identification of new therapeutic targets for immunotherapy.

Materials & Methods

Cell culture, transduction and stable cell line development

Human melanoma cells, BLM and BLM-GFP, were cultured in Dulbecco's modified Eagle's medium (DMEM, Gibco), supplemented with 5% fetal calf serum and 5%

CO_2 humidified air at 37°C. The Lenti6/Block-iT-shScramble (GFP) vector was a kind gift of Prof. Peter Friedl (RIMLS, The Netherlands). The sequence of this construct does not match any known mammalian genes. BLM cells were infected with lentiviral vector and (10µg/ml) polybrene and incubated at 37°C, 5% CO_2, overnight. Then medium was refreshed and cells were analyzed after 72h of treatment. A stable cell line was selected with 5µg/ml blasticidin.

Isolation of cellular and extracellular matrix human skin components

Generation of de-epidermized dermis (DED) and isolation of human primary keratinocytes from human abdominal skin, derived from donors who underwent surgery for abdominal wall correction, was performed as previously described [19]. Briefly, human skin was incubated for five to ten minutes in phosphate-buffered saline (PBS) at 56°C to allow separation of the epidermis from the dermis. DED was obtained by incubating the dermis for one month in PBS containing gentamicin (0.5 mg/ml; Life Technologies, Inc.) and antibiotic/antimycotic (Life Technologies, Inc.) at 37°C. Continuous cycles of freezing and thawing ensured the depletion of all living cells in the dermis. Punches were prepared from this DED using a 8-mm biopter and frozen for further use. IHC staining of heparan sulfate and collagen type IV, two typical basal layer components, demonstrated that DED still contained an intact basal membrane [20]. Keratinocytes were isolated from the epidermal layer by trypsin treatment for 16 to 20 hours at 4°C, and then cultured in the presence of irradiated (3295 cGy for 4.10 minutes) mouse fibroblasts 3T3 cells. 3T3 cells were seeded at a concentration of $3x10^4$ cells per cm^2 in Greens medium, which consisted of two parts Dulbecco's modified Eagle's medium (Life Technologies), one part of Ham's F12 medium (Life Technologies), 10% fetal bovine serum (Hyclone), L-glutamine (4 mmol/L; Life Technologies, Inc.), penicillin/streptomycin (50 IU/ml; Life Technologies, Inc.), adenine (24.3 µg/ml; Calbiochem, San Diego, CA), insulin (5 µg/ml; Sigma, St. Louis, MO), hydrocortisone (0.4 µg/ml; Merck, Darmstadt, Germany), triiodothyronine (1.36 ng/ml, Sigma), cholera toxin (10^{-10} mol/L, Sigma). The next day keratinocytes were added at a concentration of $5x10^4$ cells per cm^2. Keratinocytes-3T3 cells co-cultures were maintained for three days in Greens medium. Thereafter, medium was replaced by Greens medium containing epidermal growth factor (EGF, 10 ng/ml; Sigma), cells were expanded until 90% confluence and stored in the liquid nitrogen. Keratinocytes were used at passage one or two in the model. Adult human dermal fibroblasts were purchased by ATCC and maintained in Fibroblast medium (3:1 DMEM: Ham's F12 Nutrient Mixture, Gibco) supplemented with 10% FCS, and expanded until 80% confluence. Passages three to nine were used for the experiments.

Isolation of human blood immune cells Peripheral blood mononuclear cells (PBMCs) were isolated from buffy coats obtained from healthy volunteers (Sanquin) and purified via centrifugation over a ficoll density gradient (Axis-Shield) in SepMate tubes (Stemcell technologies). Isolation of human blood DC subsets was achieved by a sequence of negative and positive selection steps using magnetic beads (Human $CD1c^+$ (BDCA-1) Dendritic Cell Isolation Kit, Miltenyi Biotec). DC purity was assessed by staining with primary labeled antibodies: anti-CD1c-PE (Miltenyi biotec, clone AD5-8E7), anti-CD11c-APC (Miltenyi biotec, clone MJ4-27G12) and anti-CD20-APC (eBioscience, clone 2H7). Purity levels higher than 98% were achieved, determined by flow cytometry. Before injection into the dermal compartment of the melanoma skin equivalent for microscopy assessment, $CD1C^+$ DCs were labeled with the membrane dyes PKH26 or CFSE (2uM, Sigma) according to manufacturers' protocols and resuspended in X-VIVO-15 medium (Lonza) supplemented with 2% human serum (HS, Sanquin).

Generation of three-dimensional human skin melanoma model

Human melanoma skin equivalent was generated as described before with minor modifications [17]. Briefly, 8mm punch biopsy of decellularized deepidermized dermis (DED) was seeded with human primary keratinocytes, dermal fibroblasts and myeloid $CD1C^+$ DCs and melanoma cells from the human metastatic BLM cell line (Fig 1). Fibroblasts were incorporated in the DED using the centrifugal seeding procedure. The DED was placed carefully basal membrane side down on a transwell insert in a 24-well plate (24-wells ThinCert, Greiner Bio-One) and $0.15x10^6$ fibroblasts were seeded onto the reticular side of the DED in Fibroblast complete medium. The plate was centrifuged for one hour at 500rpm. After centrifugation, DED was maintained in Fibroblast complete medium for three days at 37°C, to allow fibroblast distribution and migration into the reticular and papillary dermal layers. After three days of culture, the DED was turned basal membrane side up in the transwell insert and seeded with different ratios of keratinocytes and BLM cells (KC:BLM = 5:1, 10:1, 25:1 and 50:1). The melanoma skin equivalent was cultured submerged for three days in PONEC medium containing 5% serum (PONEC 5% medium), to allow proliferation of keratinocytes and tumor cells. PONEC 5% medium consists of two parts Dulbecco's modified Eagle's medium (Life Technologies, Inc.), one part of Ham's F12 medium (Life Technologies, Inc.), 5% calf serum (Hyclone), L-glutamine (4 mmol/L; Life Technologies, Inc.), penicillin/streptomycin (50 IU/ml; Life Technologies, Inc.), adenine (24.3 µg/ml; Calbiochem, San Diego, CA), insulin (0.2 µmol/l; Sigma, St. Louis, MO), hydrocortisone (1 µmol/l; Merck, Darmstadt, Germany), triiodothyronine (1.36 ng/ml, Sigma), cholera toxin (10^{-10} mol/L, Sigma), ascorbic acid (50µg/ml; Sigma). Thereafter, the skin equivalent

was shifted to the air-liquid interface and cultured for seven days in PONEC medium without serum, supplemented with keratinocyte and epidermal growth factors (PONEC 0% medium), during which a fully differentiated epidermal layer is formed. PONEC 0% medium consists of two parts Dulbecco's modified Eagle's medium (Life Technologies, Inc.), one part of Ham's F12 medium (Life Technologies, Inc.), L-glutamine (4 mmol/L; Life Technologies, Inc.), penicillin/streptomycin (50 IU/ml; Life Technologies, Inc.), adenine (24.3 µg/ml; Calbiochem, San Diego, CA), L-serine (1mg/ml; Sigma), L-carnitine (2 µg/ml, sigma), bovine serum albumin lipid mix (palmitic acid 25 µmol/l; arachidonic acid 7 µmol/l; linoleic acid 15µmol/l; vitamin E 0.4µg/ml; all from Sigma), insulin (0.1 µmol/l; Sigma, St. Louis, MO), hydrocortisone (1 µmol/l; Merck, Darmstadt, Germany), triiodothyronine (1.36 ng/ml, Sigma), cholera toxin (10^{-10} mol/L, Sigma), ascorbic acid (50 µg/ml; Sigma), keratinocyte growth factor (5 ng/ml, Sigma), epidermal growth factor (2 ng/ml, Sigma). After culturing the skin equivalent air-exposed for seven days, $0{,}1x10^6$ PKH26-labeled $CD1C^+$ DCs were microinjected into the dermis using glass microneedles. Glass microneedles were prepared by pulling 1mm OD glass capillaries (World precision instruments, Inc.) with a vertical needle pipette puller (Kopf), which reproducibly pulls needles with desired geometries according to programmable parameters. Needles were broken open with a razor blade just behind their tip and filled from the distal end with 12µl cell suspension using microloader tips (Eppendorf). Microneedles were attached to a needle holder, which was connected via an air tubing system to a manual syringe pump (BD). Microinjection was performed using air pressure. Care was taken not to allow the broken glass microneedle to rupture the dermis. Incorporation of fluorescently labeled $CD1c^+$ DCs was immediately confirmed by observing the injected dermis under a fluorescent microscope. Immunocompetent melanoma skin equivalents were cultured for additional 48 hours at 37°C in PONEC 0% medium.

Immunohistochemistry

Formalin fixed human skin equivalents were processed for routine histology. Sections were stained with hematoxilin-eosin (H&E) or processed for immunohistochemical staining. Following antigen retrieval with EDTA, sections were stained with primary antibody incubation (anti-CD45, Dako); staining was developed using a DAB staining kit.

Image acquisition

Epifluorescent images of whole skin models were acquired, at fixed distances in depth (z-step size=10µm), using an automated brightfield multi-color epifluorescence microscope (Leica DMI6000B, Leica , Germany). Immunohistochemical staining of whole tissue slides were imaged using Vectra Intelligent Slide Analysis System (Version 2.0.8, PerkinElmer Inc.). All time-lapse experiments were performed using

a multiparameter multiphoton microscope (TriMScope-II, LaVision BioTec, Bielefeld, Germany) on a temperature-controlled stage (37°C). 4D time-lapse recordings were acquired by sequential scanning with 950 nm (eGFP and PKH26) and 1090 nm (SHG), with a sampling rate of 1 frame/2min over periods of 2-4h.

Image processing

Images were analyzed using the open source-imaging platform, Fiji (imageJ 64 Bit for Windows). Mosaic images were stitched using the Stitch Grid/Collection plugin. Z-volumes containing DCs were quantified using individual slices of epifluorescent images acquired at 10µm z-resolution. For DC motility and DC-tumor cell interactions, drifts in time-lapse recordings were corrected using the Correct 3D drift plugin. If necessary, images were scaled and adjusted for brightness and contrast to enhance visualization. Immunohistochemical images, taken at the Vectra sytem, were analyzed with the image analysis software, InForm (Version 2.1, PerkinElmer Inc.).

Statistical analysis

Significance between groups is established using T-test performed in Graphpad Prism.

Results

Skin melanoma model displays morphological features of primary human melanoma

Generation of the human skin melanoma model is depicted in Fig. 1a. Primary human fibroblasts (Fbs) are seeded onto the reticular dermal side (opposite to papillary side and basal membrane) of an acellular, de-epidermized dermis (DED) via centrifugal force (day 1). This is followed by a 3-days culture to allow Fbs migration and distribution through the collagen fibers of the DED (Suppl. Fig 1a). In order to reconstitute melanoma in a fully developed epidermis, primary human keratinocytes (KCs) and immortalized human melanoma cells are seeded onto the basal membrane (papillary side) of the fibroblast-repopulated DED (day 4). KCs and melanoma cells are cultured sub-merged for 3 days, to allow KCs proliferation and distribution of cancer cells in the epidermal layer. Subsequently, differentiation of KCs is achieved by culturing the organotypic model for additional 7 days, at the air-liquid interphase (day 7). When a fully developed epidermal layers is formed, freshly isolated, primary $CD1c^+$ DCs are injected into the dermal compartment (day 14). The 3D skin melanoma model is cultured air-exposed for further 2 days, thus for a total culture period of 16 days (Fig 1a). In order to mimic melanoma growth in the skin model, we co-cultured KCs with BLM melanoma cells, at different KC-to-tumor cell ratios. Immunohistochemistry

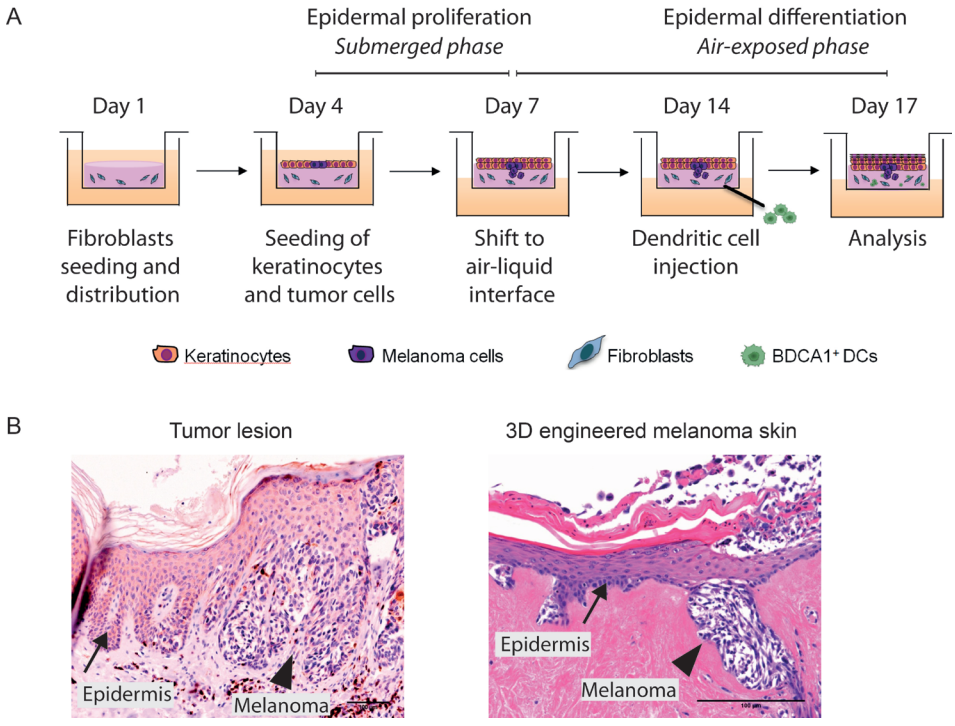

Figure 1. 3D Skin melanoma model displays morphological features of human melanoma. **A** Schematic representation of the generation of human skin melanoma organotypic model. **B** Histological comparison of tissue sections obtained from primary tumor (left) and skin melanoma model (right). Hematoxylin and eosin staining. Scale bar 100µm.

analysis of model tissue sections and comparison to primary human tumor biopsies showed that extensive proliferation of melanoma cells, as observed at low KC:tumor cell ratios, negatively affected the morphology of the epidermal layer. Co-seeding large amounts of fast-diving melanoma cells with epidermal cells, in fact, caused the tumor cells to outnumber KCs, thereby affecting KC differentiation and preventing the formation of the five characteristic epidermal strata (Suppl. Fig 1b). The optimal cell seeding concentration, defined as the amount of KCs and melanoma cells that preserves epidermal differentiation and morphology, while allowing proliferation of tumor cells, was found to be 25:1 (Fig 1b, Suppl. Fig 1b). Furthermore, we noticed that BLM cells, seeded on DEDs in a mixed KC-tumor cell suspension, spontaneously relocated in the basal layer of the epidermis, where they developed into tumor nests and infiltrate the underneath dermis (Fig 1b). Taken together, these observations show that the 3D skin melanoma mimics the growth of tumor cells, closely resembling morphological features of malignancy-associated human skin.

Melanoma model supports DC survival and motility

Human CD1c$^+$ DCs, pre-labeled with a cell tracking dye (CFSE or PKH), were injected into the dermal compartment of a fully differentiated melanoma skin model (day 14; Fig 1a). Distribution and migration of CD1c$^+$ DCs was monitored for up to 48 hours with advanced imaging techniques. In order to confirm the presence of fluorescently-labeled CD1c$^+$ DCs in the dermis, melanoma skin models were imaged with an inverted epifluorescence microscope, approximately 2h after DC injection (Fig 2 a, b). First, we identified the area in the dermis in which the DCs were injected, which appeared as a cloud of fluorescent cells (Fig 2a, left). Next, we measured the extension (depth or z-volume) of the dermal region in which we could find CD1c$^+$ DCs and scanned the whole area that contained the fluorescent cells (Fig 2b, middle). In order to monitor DC distribution through the dermal compartment over time, we repeated the analysis 48 hours after DC injection (Fig 2a, right and Fig 2b). We observed that the region of the dermis containing DCs was more extensive after 48h (97.29±11.06), as compared to 2h average (154.7±14.97) after injection, thus suggesting that DCs disseminated across a broad area over time (Fig 2b). We thus predicted that DCs actively migrated throughout the dermal layer. We used live two-photon microscopy to confirm motility and assess longevity of CD1c$^+$ DCs in our melanoma skin model (Fig 2c-g). Combination of fluorescent signal (for live-cell visualization) with second harmonic generation (SHG, elicited by collagen fiber bundles) delivers information on the 3D anatomy of the dermal tissue. Collagen fibers were organized in heterogeneous networks, including randomly arranged loose collagen fibers and aligned and more compacted collagen bundles (Fig 2c). We sought to confirm that DCs survive in our model despite the absence of serum, which would normally be administered to culture media to ensure survival of immune cells cultured *in vitro*. Using a

Figure 2. CD1c$^+$ DCs actively migrate through the dermal compartment of skin melanoma model. In order to analyze fluorescently-labeled CD1c$^+$ DCs distribution over time, skin models were imaged with an inverted epifluorescence microscope, 2h and 48h after DC injection. **A** Schematic representation of image acquisition and analysis. Scale bar 1mm. **B** Comparison of dermal areas (Z-volumes) containing DCs at 2h and 48h. Matched color symbols indicate differences in Z-volumes in the same skin model, analyzed at two different time points (n=4). **C** PKH26 and second harmonic generation (SHG) signals of multiphoton images, acquired with excitation wavelength (λ) of 950nm. PKH26 signal indicates CD1c$^+$ DCs; SHG was generated by collagen bundles. **D** Representative time points during time-lapse recording of skin model at 2h, 24h and 48h after DC injection. **E-G** Time-lapse microscopy and single cell tracking of DCs showed motility, with (F) median velocity of 3μm/min over 24h. (G) DCs showed characteristic amoeboid migration. **H** Representative time points during time-lapse recording of melanoma ▶

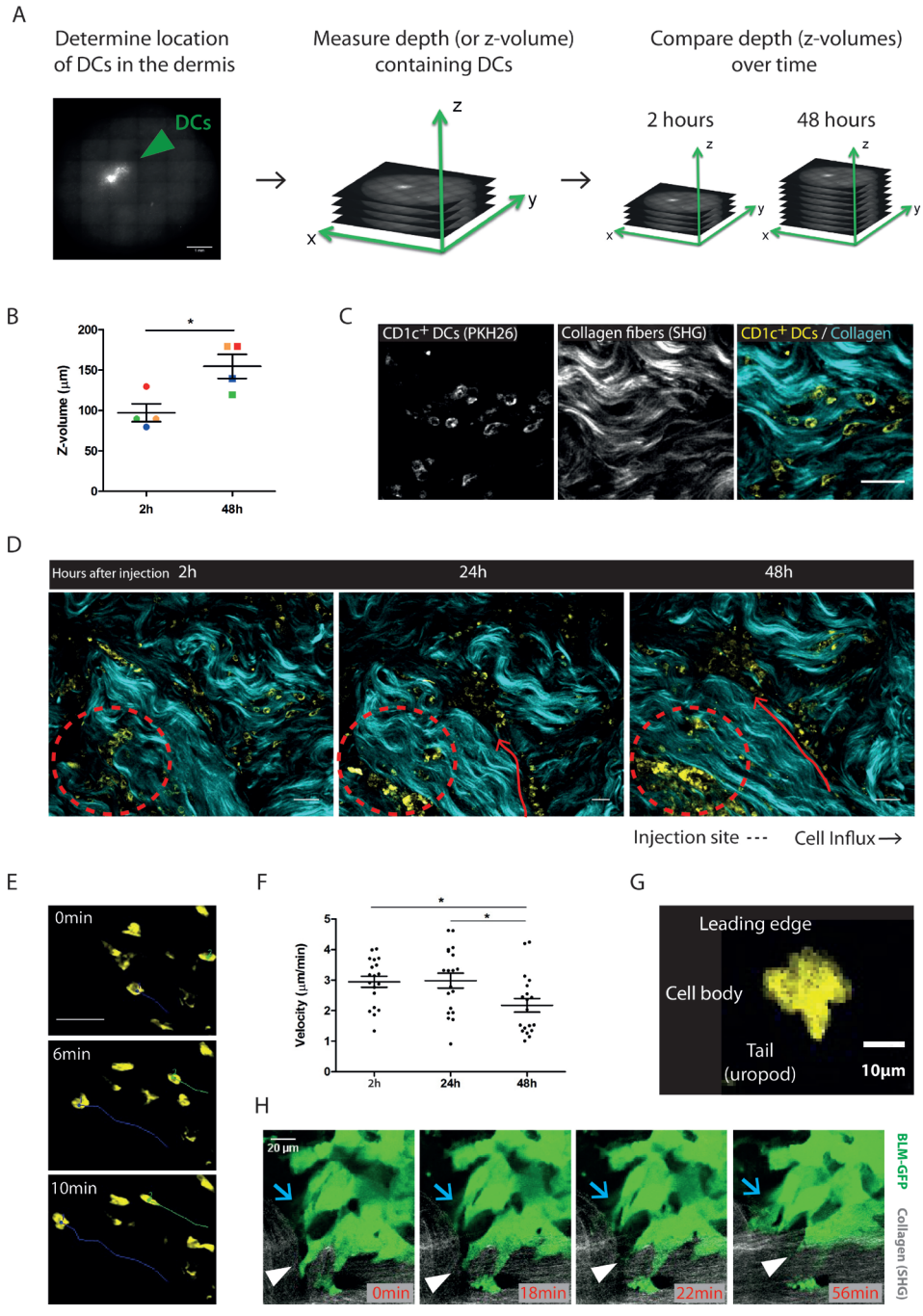

▶ BLM cells expressing GFP [λ (excitation) = 950nm]. BLM cells showed high cellular dynamics (protrusion, *blue arrow* and retraction, *white arrowhead*). Scale bars, 50µm (unless otherwise indicated). Statistical significance was determined by *t*-test, *p < 0.05.

time-lapse setting with 120sec time interval between individual scans, areas were imaged at 2, 24 and 48 hours after CD1c$^+$ DC injection, for approximately 2 consecutive hours (Fig 2d). Single-cell tracking and time-lapse recording revealed motile DCs, moving along and into collagen networks, maintaining median velocities of 3 μm/min for over a period of 24 hours (Fig 2e, f). Over time, the average velocity reduced to approximately 2 μm/min (Fig 2f). Occasionally, small clusters of 2-3 DCs were observed to migrate interconnected, with the leading cells opening the way for other DCs (not shown). Trafficking CD1c$^+$ DCs adopted a typical "hand mirror shape", characteristic of amoeboid migration. DCs displayed a leading edge, consisting of multiple dendrites that intercalated between tissue structures, followed by the cell body containing the nucleus, and a posterior tail (uropod) (Fig 2g). Additionally, we observed that melanoma BLM cells, expressing the fluorescent protein GFP (hereafter referred to as BLM-GFP), were confined by collagen fiber bundles and showed intense membrane dynamics, appreciated as protrusive and retractive activity (Fig 2h). Altogether, these findings demonstrate that the biological composition of the 3D melanoma skin organotypic model supports survival of CD1c$^+$ DCs as well as melanoma cells.

CD1c$^+$ DCs directly interact with tumor cells and ingest tumor-derived particles

Immunohistochemistry end point analysis of fixed models revealed that DCs in the dermal compartment were in close association with non-immune cells (Fig 3a). Live imaging and tracking of DC-tumor cell interactions was performed by two-photon imaging of the melanoma skin models (Fig 3b, c). We observed multiple CD1c$^+$ DCs directly interacting with BLM-GFP cells. Dynamic DC-tumor cell interactions were followed over at least 20min (Fig 3b). DCs in the skin model encountered and shortly interacted with live tumor cells. We repeatedly observed that prolonged interactions and stable cell engagement were established between DCs and tumor-associated cellular microparticles (or blebs) (Fig 3c). Microparticles were released into the ECM by BLM-GFP cells and the blebs themselves retained the cytoplasmic fluorophore, GFP. We also captured images of sampling and engulfment of tumor-derived particles by DCs (Fig 3b,c). Uptake of GFP-containing tumor fragment by CD1c$^+$ DCs was imaged by live two-photon microscopy as early as a few hours after immune cell injection. Taken together, these observations clearly indicate that melanoma skin models represent a promising and valuable platform for accurate investigation of cellular interplay and function, in an *in vivo*-like skin tissue architecture.

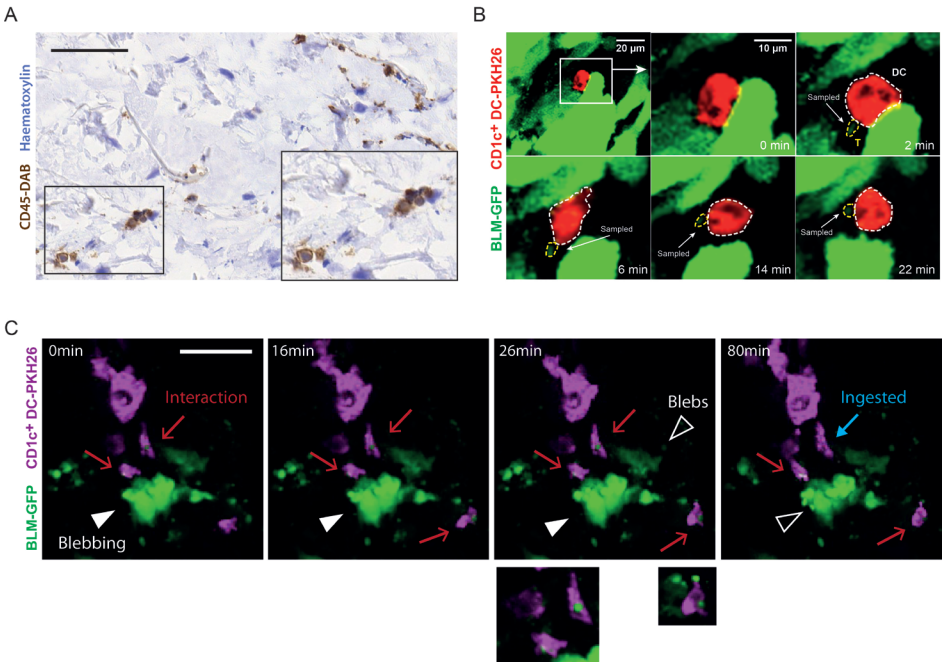

Figure 3. Visualization of CD1c⁺ DCs-tumor cell interaction and uptake of tumor-fragments. **A** Section of 3D melanoma skin model showing immunohistochemical staining for CD45. In brown (DAB) CD45 positive DCs, in close proximity to non-immune (CD45 negative) cells. Hematoxylin counterstaining, original magnification 20X. **B, C** Representative time points during time-lapse recording of DC (PKH26)-tumor cell (GFP) interaction [λ (excitation) = 950nm]. (B) DC sensed and sampled tumor-derived particle (abbreviation: T, tumor fragment). (C) Prolonged interaction of DCs with tumor-derived fragments. Tumor cells showed intense membrane dynamics and blebbing. Scale bars, 50µm (unless otherwise indicated).

Discussion

The tissue microenvironment is increasingly recognized to influence a broad range of events involved in maintaining homeostasis and regulating host response to disease, such as tumors [21, 22]. Both conventional *in vitro* and *in vivo* studies have largely contributed to our understanding of the mechanisms regulating tumor development and progression. However, our knowledge in many aspects of the immunobiology of human cancer is still poor.

We here established an *in vitro* human 3D engineered melanoma skin model that closely recreates, in a controlled and titrated system, the *in vivo* complexity of the melanoma microenvironment. The advantage of our model, with respect to existing co-culture cell systems, relies on the possibility of bringing different

cell types together in an *in vivo*-like tissue context. This is in fact the first model that places in a non synthetic, human-derived extracellular matrix (ECM), the key components of the epidermal, stromal and immune compartments of the tumor microenvironment (TME). Moreover, our organotypic model provides a new platform that allows real-time, 4 dimensional (X,Y,Z, time) direct observation of melanoma interactions with the colonized tissue, in a human setting.

IHC examination of our model showed that the melanoma skin model displayed the morphological features of malignancy-associated human skin. We showed that melanoma cells, co-seeded with epidermal cells on a fibroblast-repopulated DED, spontaneously relocated in the deepest layer of the epidermis, the *stratum basale*. This observation is particularly interesting as it indicates that, different cell types retain their unique characteristics and adapt to each other when cultured in a multi-cellular environment. In human skin, in fact, normal melanocytes are located in the *stratum basale*. Upon malignant transformation, melanocytes escape from the growth control exerted by epidermal cells and acquire extensive proliferative potential and migratory ability, eventually resulting in dermal invasion and distant metastases [13, 23].

Stromal cells, such as fibroblasts, are key cellular components of the TME [24]. Fibroblasts can influence proliferation and invasive potential of melanoma cells, as well as conferring tumor resistance to chemotherapy [24, 25]. Previous work also demonstrated that incorporation of fibroblasts into skin models significantly improved epidermal morphogenesis and doubled the life span of skin models to up to 6 weeks of culture[26]. Different approaches have been described to incorporate stromal cells in the dermal compartment of HSEs. These include (a) culturing fibroblasts for a few (at least 3) weeks to allow deposition of ECM components and (b) centrifugal seeding of stromal cells onto acellular DEDs [26, 27]. For development of skin melanoma models we adapted the centrifugal seeding method previously described [26]. This approach offers the advantage of considerably reducing the time required to obtain a fibroblast-populated dermis, and guarantees reproducible seeding efficiency and homogeneous distribution of fibroblasts into DEDs [28].

Onset of an effective anti-tumor immune response requires dendritic cells (DCs) to be at the right place at the right time [29]. Nearly all steps, from antigen capture to activation and effector cell function, depend upon DC positioning and migration in peripheral and lymphoid tissues. Within peripheral tissues, such as skin, DCs are the sentinels that interact with malignant cells and eventually capture tumor material [30]. The two main DC populations found in the skin are the epidermal Langerhans cells and the dermal $CD1c^+$ DCs [31-33]. Isolation of DC subsets from the skin is a complex procedure, which requires extensive handling and manipulation. Moreover, it is limited by the availability of skin tissue and the relatively low amounts of DCs that can be obtained. The dermal $CD1c^+$ DC population is mirrored in the blood by circulating $CD1c^+$ DCs [34]. Therefore,

blood CD1c$^+$ DCs represent a suitable model for dermal DCs in human skin models. Imaging analysis of our melanoma skin model showed that, 72 hours after the injection of fluorescently labeled CD1c$^+$ DCs, the dermal area occupied by DCs was bigger than the area measured immediately after DC injection. This suggest that the DCs moved from the injection site over time. However, fluorescent end-point imaging studies provide a static view on dynamic processes, such as migration, and can only give indirect insights into positioning mechanisms. Time-lapse second generation harmonic (SHG), suitable for collagen visualization combined with fluorescence microscopy, allows visualization of 3D topography of tissue structures and delivers insights into DC migration in skin models. In 3D environments, DCs employ amoeboid migration [35, 36]. In contrast to the slow (less than 1μm/min), proteolysis-dependent mesenchymal movement of tumor and stromal cells; amoeboid modes are fast (up to 10μm/min for DCs and 5μm/min for monocytes), independent of adhesive interactions with tissues and preserve tissue structure [37].

We recently reported that CD1c$^+$ DCs, co-cultured *in vitro* with viable melanoma BLM cells, ingested tumor-derived blebs or fragments (Chapters 2 and 3 of this thesis). Uptake of tumor fragments *in vitro*, as opposed to membrane binding, was demonstrated by culturing CD1c$^+$ DCs and BLM-GFP at 37°C *vs* 4°C. Consistently, we here observed that BLM cells released fluorescently detectable particles in the ECM. In addition, we extended previous observations by showing that CD1c$^+$ DCs were able to actively take up GFP$^+$-tumor particles in 3D settings. Previous work suggested that these tumor-derived blebs favor cell-to-cell communication and are therefore implicated in cancer progression, tumor invasion and metastasis, as well as anti-tumor drug resistance [9, 10, 38, 39]. Alternatively, these particles can be taken up by APCs, function as antigen carriers and mediate anti-tumor immunity [40]. Notably, CD1c$^+$ DCs were also frequently found interacting with viable tumor cells. However, during the many hours of imaging, we never observed phagocytosis of intact tumor cells, thus suggesting that tumor-derived particles might be the main source of tumor-ingested material.

In summary, this novel 3D organotypic model mimics the complex melanoma TME and allows live investigation of CD1c$^+$ DCs migration and function in an *ex vivo*-like tissue. Our model has the potential to provide new insights into the mechanisms that underlie melanoma growth and may help the identification of candidate genes and molecules involved in this disease-relevant process.

Author contribution

SDB, SVH and CGF conceived the study. SDB designed, performed, analyzed the experiments and wrote the manuscript. GJB provided help and support with multiphoton image acquisition. SVH, EHB and CGF critically revised the manuscript. All authors approved the final version of the manuscript.

References

1. Hanahan D, Weinberg Robert A. Hallmarks of Cancer: The Next Generation. Cell 2011; 144:646-74.
2. Hanahan D, Weinberg RA. The Hallmarks of Cancer. Cell 2000; 100:57-70.
3. Gross S, Walden P. Immunosuppressive mechanisms in human tumors: Why we still cannot cure cancer. Immunology Letters 2008; 116:7-14.
4. Miller AJ, Mihm MC. Melanoma. New England Journal of Medicine 2006; 355:51-65.
5. Smalley KSM, Lioni M, Herlyn M. Life ins't flat: Taking cancer biology to the next dimension. In Vitro Cellular & Developmental Biology - Animal; 42:242-7.
6. Yamada KM, Cukierman E. Modeling Tissue Morphogenesis and Cancer in 3D. Cell 2007; 130:601-10.
7. Davis MM. Immunology Taught by Humans. Science translational medicine 2012; 4:117fs2-fs2.
8. Pampaloni F, Reynaud EG, Stelzer EHK. The third dimension bridges the gap between cell culture and live tissue. Nat Rev Mol Cell Biol 2007; 8:839-45.
9. Mazzoleni G, Di Lorenzo D, Steimberg N. Modelling tissues in 3D: the next future of pharmaco-toxicology and food research? Genes & Nutrition 2009; 4:13-22.
10. Hill DS, Robinson NDP, Caley MP, Chen M, O'Toole EA, Armstrong JL, Przyborski S, Lovat PE. A Novel Fully Humanized 3D Skin Equivalent to Model Early Melanoma Invasion. Molecular Cancer Therapeutics 2015; 14:2665-73.
11. Meier F, Nesbit M, Hsu M-Y, Martin B, Van Belle P, Elder DE, Schaumburg-Lever G, Garbe C, Walz TM, Donatien P, et al. Human Melanoma Progression in Skin Reconstructs : Biological Significance of bFGF. The American Journal of Pathology 2000; 156:193-200.
12. Li L, Fukunaga-Kalabis M, Herlyn M. The Three-Dimensional Human Skin Reconstruct Model: a Tool to Study Normal Skin and Melanoma Progression. Journal of Visualized Experiments : JoVE 2011:2937.
13. Hsu M-Y, Meier FE, Nesbit M, Hsu J-Y, Van Belle P, Elder DE, Herlyn M. E-Cadherin Expression in Melanoma Cells Restores Keratinocyte-Mediated Growth Control and Down-Regulates Expression of Invasion-Related Adhesion Receptors. The American Journal of Pathology 2000; 156:1515-25.
14. Syed DN, Chamcheu J-C, Khan MI, Sechi M, Lall RK, Adhami VM, Mukhtar H. Fisetin inhibits human melanoma cell growth through direct binding to p70S6K and mTOR: findings from 3-D melanoma skin equivalents and computational modeling. Biochemical pharmacology 2014; 89:349-60.
15. Eves P, Katerinaki E, Simpson C, Layton C, Dawson R, Evans G, Mac Neil S. Melanoma invasion in reconstructed human skin is influenced by skin cells – investigation of the role of proteolytic enzymes. Clinical & Experimental Metastasis; 20:685-700.
16. Gibot L, Galbraith T, Huot J, Auger FA. Development of a tridimensional microvascularized human skin substitute to study melanoma biology. Clinical & Experimental Metastasis 2012; 30:83-90.
17. Van Kilsdonk JWJ, Bergers M, Van Kempen LCLT, Schalkwijk J, Swart GWM. Keratinocytes drive melanoma invasion in a reconstructed skin model. Melanoma Research 2010; 20:372-80.
18. Hirt C, Papadimitropoulos A, Mele V, Muraro MG, Mengus C, Iezzi G, Terracciano L, Martin I, Spagnoli GC. "In vitro" 3D models of tumor-immune system interaction. Advanced Drug Delivery Reviews 2014; 79–80:145-54.

19. Tjabringa G, Bergers M, van Rens D, de Boer R, Lamme E, Schalkwijk J. Development and Validation of Human Psoriatic Skin Equivalents. The American Journal of Pathology 2008; 173:815-23.
20. van den Bogaard EH, Tjabringa GS, Joosten I, Vonk-Bergers M, van Rijssen E, Tijssen HJ, Erkens M, Schalkwijk J, Koenen HJPM. Crosstalk between Keratinocytes and T Cells in a 3D Microenvironment: A Model to Study Inflammatory Skin Diseases. Journal of Investigative Dermatology 2014; 134:719-27.
21. Quail DF, Joyce JA. Microenvironmental regulation of tumor progression and metastasis. Nat Med 2013; 19.
22. Chen F, Zhuang X, Lin L, Yu P, Wang Y, Shi Y, Hu G, Sun Y. New horizons in tumor microenvironment biology: challenges and opportunities. BMC Medicine 2015; 13:1-14.
23. Bonaventure J, Domingues MJ, Larue L. Cellular and molecular mechanisms controlling the migration of melanocytes and melanoma cells. Pigment Cell & Melanoma Research 2013; 26:316-25.
24. Bhowmick NA, Neilson EG, Moses HL. Stromal fibroblasts in cancer initiation and progression. Nature 2004; 432:332-7.
25. Commandeur S, Sparks SJ, Chan H-L, Gao L, Out JJ, Gruis NA, van Doorn R, el Ghalbzouri A. In-vitro melanoma models: invasive growth is determined by dermal matrix and basement membrane. Melanoma Research 2014; 24:305-14.
26. El Ghalbzouri A, Lamme E, Ponec M. Crucial role of fibroblasts in regulating epidermal morphogenesis. Cell and Tissue Research; 310:189-99.
27. El Ghalbzouri A, Commandeur S, Rietveld MH, Mulder AA, Willemze R. Replacement of animal-derived collagen matrix by human fibroblast-derived dermal matrix for human skin equivalent products. Biomaterials 2009; 30:71-8.
28. Roh JD, Nelson GN, Udelsman BV, Brennan MP, Lockhart B, Fong PM, Lopez-Soler RI, Saltzman WM, Breuer CK. Centrifugal Seeding Increases Seeding Efficiency and Cellular Distribution of Bone Marrow Stromal Cells in Porous Biodegradable Scaffolds. Tissue Eng 2007; 13:2743-9.
29. Spel L, Boelens J-J, Nierkens S, Boes M. Antitumor immune responses mediated by dendritic cells: How signals derived from dying cancer cells drive antigen cross-presentation. Oncoimmunology 2013; 2:e26403.
30. Yanofsky VR, Mitsui H, Felsen D, Carucci JA. Understanding Dendritic Cells and Their Role in Cutaneous Carcinoma and Cancer Immunotherapy. Clinical and Developmental Immunology 2013; 2013:624123.
31. Zaba LC, Fuentes-Duculan J, Steinman RM, Krueger JG, Lowes MA. Normal human dermis contains distinct populations of CD11c(+)BDCA-1(+) dendritic cells and CD163(+)FXIIIA(+) macrophages. The Journal of Clinical Investigation 2007; 117:2517-25.
32. Zaba LC, Krueger JG, Lowes MA. Resident and "inflammatory" dendritic cells in human skin. The Journal of investigative dermatology 2009; 129:302-8.
33. Ochoa MT, Loncaric A, Krutzik SR, Becker TC, Modlin RL. "Dermal dendritic cells" comprise two distinct populations: CD1+ dendritic cells and CD209+ macrophages. The Journal of investigative dermatology 2008; 128:2225-31.
34. Haniffa M, Shin A, Bigley V, McGovern N, Teo P, See P, Wasan Pavandip S, Wang X-N, Malinarich F, Malleret B, et al. Human Tissues Contain CD141(hi) Cross-Presenting Dendritic Cells with Functional Homology to Mouse CD103(+) Nonlymphoid Dendritic Cells. Immunity 2012; 37:60-73.

35. Heuzé ML, Vargas P, Chabaud M, Le Berre M, Liu Y-J, Collin O, Solanes P, Voituriez R, Piel M, Lennon-Duménil A-M. Migration of dendritic cells: physical principles, molecular mechanisms, and functional implications. Immunological Reviews 2013; 256:240-54.
36. Roediger B, Ng LG, Smith AL, de St Groth BF, Weninger W. Visualizing dendritic cell migration within the skin. Histochemistry and Cell Biology 2008; 130:1131-46.
37. Friedl P, Wolf K. Tumour-cell invasion and migration: diversity and escape mechanisms. Nat Rev Cancer 2003; 3:362-74.
38. Lee TH, D'Asti E, Magnus N, Al-Nedawi K, Meehan B, Rak J. Microvesicles as mediators of intercellular communication in cancer—the emerging science of cellular 'debris'. Seminars in Immunopathology 2011; 33:455-67.
39. Muralidharan-Chari V, Clancy JW, Sedgwick A, D'Souza-Schorey C. Microvesicles: mediators of extracellular communication during cancer progression. Journal of Cell Science 2010; 123:1603-11.
40. Zeelenberg IS, van Maren WWC, Boissonnas A, Van Hout-Kuijer MA, Den Brok MHMGM, Wagenaars JAL, van der Schaaf A, Jansen EJR, Amigorena S, Théry C, et al. Antigen Localization Controls T Cell-Mediated Tumor Immunity. The Journal of Immunology 2011; 187:1281-8.

Supplementary material

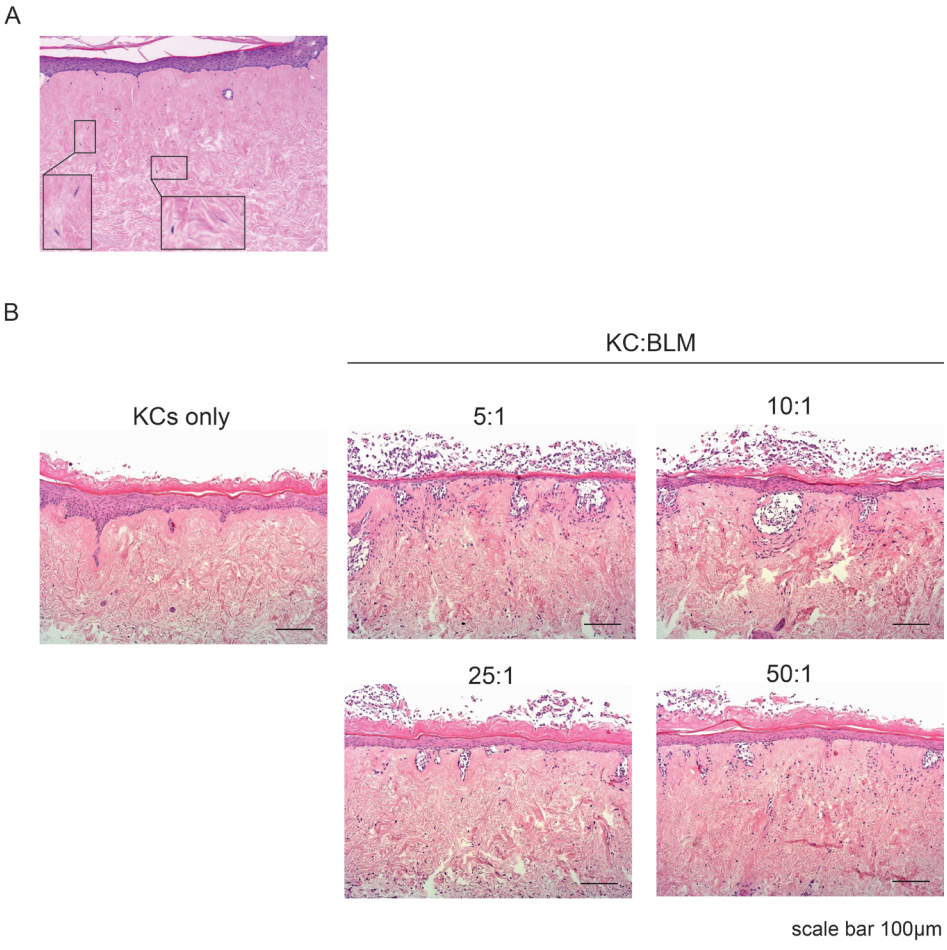

Supplementary Figure 1. A Representative image of fibroblast distribution through the dermal compartment of a 3D model of normal skin (keratinocytes, KC only). **B** Hematoxylin and eosin staining of melanoma skin models with different KC:melanoma BLM cell ratio.

CHAPTER 5

Multispectral imaging for highly accurate analysis of Tumor Infiltrating Lymphocytes in primary melanoma

Angela Vasaturo #[1], **Stefania Di Blasio #**[1], Dagmar Verweij[1,2], Willeke A.M. Blokx[2], J. Han van Krieken[2], I. Jolanda M. de Vries [1,3], Carl G. Figdor[1]

 # Equal contribution

[1]Department of Tumor Immunology (Radboud Institute for Molecular Life Sciences), [2]Pathology and [3]Medical Oncology, Radboud university medical center, Nijmegen, the Netherlands.

Published in the form of short report: Histopathology. 2016 Aug 29. epub ahead of print

Abstract

The quality and quantity of the infiltration of immune cells into tumor tissues has substantial impact on patients' clinical outcome and is associated with response to immunotherapy. Therefore, the precise analysis of tumor-infiltrating lymphocytes (TIL) is becoming an important additional pathological biomarker. Analysis of TILs is usually performed semi-quantitatively by pathologists on H&E stained or immunostained tissue sections. However, automated quantification outperforms semi-quantitative approaches and is becoming the standard. Due to the presence of melanin pigment this approach is seriously hampered in melanoma, because the spectrum of melanin lies close to that of commonly used immunohistochemical stains.

Here, we successfully apply a novel multispectral imaging technique to enumerate T cells in human primary melanomas. This microscopy technique combines imaging with spectroscopy to obtain both, quantitative expression data and tissue distribution of different cellular markers. We show that multispectral imaging allows complete and accurate analysis of TILs, successfully avoiding melanin pigments, in whole slide primary melanoma lesions, which could otherwise not be accurately detected by conventional digital image methodologies.

Our study highlights the potency of multispectral imaging to accurately assess immune cell infiltrates including those in notoriously difficult tissues, such as pigmented melanomas. Quantification of tumor infiltration by different immune cell types is crucial in the search for new biomarkers to predict patient responses to immunotherapies. Our findings show that this innovative microscopy technique is an important extension of the armamentarium in melanoma research.

Introduction

Melanoma is a potentially lethal skin cancer generating from the malignant transformation of melanocytes, the melanin-producing cells in the skin[1,2]. Although development of successful strategies remains a challenge, the past decade uncovered encouraging advances in melanoma management[3,4]. Perhaps the biggest improvement in melanoma therapy comes from immunotherapeutic approaches, in particular immunomodulatory monoclonal antibodies (mAbs). Immunomodulatory mAbs target molecules ('checkpoints') that are crucial in regulating immune responses and keeping tumor progression under control[3,4]. In particular, immune checkpoint regulators CTLA-4 and PD-1 have been extensively studied[3,4]. Clinical trials using ipilimumab (anti-CTLA-4 mAb) and/or nivolumab or pembrolizumab (anti-PD-1 mAbs) have recently reported durable clinical responses and increased overall survival (OS)[5-8]. Nonetheless, costs and toxicity associated with immune checkpoint inhibition, urge for the development of biomarkers for predicting the efficacy of the treatment and disease outcome, in patients treated with immunotherapy[9]. The availability of predictive biomarkers is of extreme importance to further advance this field of cancer immunotherapy.

The crucial role of the patient's own immune system on clinical outcome is demonstrated by the immunological characterization of the tumor microenvironment (TME)[10,11]. Immune cells can infiltrate the core (center) of the tumor or remain located in peritumoral areas. The analysis of type, location and density of tumor-infiltrating immune cell components is referred to as "immune contexture"[12]. Immunohistochemical (IHC) evaluation of this immune contexture resulted in the identification of immune cell types that can be either beneficial or harmful to patients[13-15]. For example, high-density infiltration of lymphocytes in the tumor core, in particular $CD8^+$ effector T cells, positively correlates with survival of patients suffering from melanoma or other cancer types[16-19].

So far, density and location of TILs have been estimated by tissue IHC of limited areas of the sample, by independent histopathologic reviews. The total amount of infiltrating immune cells is generally calculated by multiplying the number of cells counted in one region by the entire surface of the tumor[14]. Others take advantage of the use of semi-automated digital image analysis. This method is based on mathematical algorithms that can recognize and quantify cells of interest within the tumor area. Although relatively accurate, this methodology is extremely time-consuming and in the case of melanoma fail because of the melanin pigment[20,21]. As this pigment is also produced by a substantial part of melanomas, it creates a high background in bright-field IHC stains[22]. This melanin signal can obscure tumor-infiltrating immune cells or even generate false positive signals, resulting in

inaccurate, under- / over- estimated TIL counts when a digital approach is used. An established technique for the study of immune infiltrates is melanin bleaching with strong oxidants[23,24]. Although this technique can give satisfactory results in many cases, certain antigens (such as CD3 and CD45RO) and the tissue itself can be partially destroyed. Besides, conventional chromogens used for antibody detection (i.e. DAB) are also affected by the intense oxidative procedure, thus making the analyses less accurate[25,26]. The use of a red chromogen in the immunostaining of melanocytic lesions, if limited to tumor markers, can partially overcome this problem[27], however it remains not optimal for immune cells detection. Recent advances in the field of tissue imaging resulted in the development of multispectral imaging applied to whole-slide tissue sections[28]. This novel technique combines imaging with spectroscopy, thereby allowing both quantification and tissue distribution of multiple cellular markers in the entire tissue section. Here, we exploit multispectral imaging for linear spectral unmixing of melanin pigmentation in human primary melanoma biopsies and demonstrate that melanin unmixing allows for highly accurate quantification of $CD3^+$ T lymphocytes infiltrating a tumor lesion, which could otherwise not be detected by conventional digital image analysis because of melanin blurring the images. By comparing quantitative assessment of $CD3^+$ T cells, by semi-automated and our fully automated image analysis, we show that using traditional approaches melanin pigments lead to significant overestimation of T cell counts in primary pigmented lesions. We believe that our innovative spectral unmixing technique will be of great value in melanoma research, and may contribute to the identification of new biomarkers crucial for clinical management of melanoma patients.

Materials and Methods

Patients

We obtained tissue sections of 23 primary cutaneous melanomas of patients who were enrolled in our dendritic cell vaccination studies at the Radboud university medical center (Nijmegen, the Netherlands) and were available at our hospital. The studies were approved by the appropriate Medical Ethical Review Board, and written informed consent was obtained from all patients.

Immunohistochemistry

Slides of 4-µm thickness were cut from formalin-fixed, paraffin-embedded (FFPE) primary melanoma tissue blocks. The slides were deparaffinized, after which antigen retrieval followed using 10 mM citrate buffer (Skytek, Utah, United States, pH 6.0) for 10 min at 96°C. After this pre-treatment, the slides were placed in an Autostainer 480

(Thermo scientific, labvision). At first, during the automated procedure, endogenous peroxidase was blocked using 3% hydrogen peroxidase (EMD Millipore corporation, Darmstadt, Germany) in methanol (EMD Millipore corporation, Darmstadt, Germany) followed by primary antibody incubation (anti-CD3, Thermo Scientific, dilution: 1/40) for 60 min at room temperature. Next, incubation with Brightvision poly-HRP-anti Ms/Rb/Rt IgG (Immunologic BV, Duiven, Netherlands, Dilution: 1/2) was performed for 30 min at room temperature followed by a visualization step with the Vector Nova Red substrate kit (Vector laboratories, Burlingame, United States) for 7 min, at room temperature. Between each step, samples were rinsed using PBS (klinipath, Duiven, Netherlands, dilution: 1/10). After visualization, the slides were manually counterstained with haematoxylin and enclosed with Quick-D mounting medium (Klinipath).

Manual digital analysis

Whole tissue slides were digitally scanned at high resolution by the automated scanner Pannoramic 250 (Pannoramic P250, 3DHistech Ltd, Budapest, Hungary). The bright-field images were analyzed using the open source-imaging platform, Fiji (imageJ 64 Bit for Windows). After manual drawing of the tumor and stroma regions, original bright-field images were converted into a "binary", black and white, 8-bit image. In order to discriminate objects of interest from the background, a threshold range was set. Thus, all objects in the image, whose pixel values are above the threshold, were shown in white; whereas objects in the background, having pixel values lying below the threshold, were displayed as black regions. The resulting binary image is further processed to separate (segment) cells clustered together, which would misrepresent the final result. Hence, segmented images were analyzed and single cells counted, by using the automatic particle counting plug-in. Each cell detected was outlined and the output image overlaid on a duplicate of the original bright-field image, in order to visually verify the success of the algorithm.

Spectral library generation for melanin unmixing

Images of single stained tissues and unstained tissue were used to extract the spectrum of each chromogen and of tissue melanin pigmentation, respectively, with Nuance Multispectral Imaging System (Version 3.0.2, PerkinElmer Inc). The chromogens used were haematoxylin for nuclear staining and nova red (Vector laboratories, Burlingame, United States) for $CD3^+$ T cells. The extracted spectra built a so called spectral library which was used to enable the quantitative separation, or unmixing, of the stained markers into its own channel/image, thus removing cross-talk between chromogens and interfering tissue pigmentation.

Tissue imaging and quantitative digital analysis

Whole tissue slides were imaged using Vectra Intelligent Slide Analysis System (Version 2.0.8, PerkinElmer Inc.) in an automated manner. A selection of 10 to 15 representative original multispectral images was loaded into an advanced user-trainable morphologic image analysis software, (InForm Version 2.1, PerkinElmer Inc.) which utilizes sophisticated machine learning to allow the user to train it to recognize and find morphologic regions of the tissue which then allow the determination of which cells are, for instance, in the tumor and which are in the stromal regions (fig S1). The analysis software also utilizes the multimarker, multispectral data to calculate per-cell and per-cellular-compartment (i.e., nuclear, cytoplasmic, and membrane) optical intensity values to score cell positivity for the specific marker used as described before[33,34].

All the settings applied to the training images were saved within an algorithm allowing batch analysis of multiple original multispectral images of the same tumor. A separate algorithm was generated per single patient applying the same settings for cell segmentation and positivity score but with different training for tissue segmentation due to the numerous morphological differences between and within tumors, which is very common in melanoma.

Statistics

Significance between groups is established using T test performed in Graphpad Prism.

Results

Semi-automated digital image analysis of T cell infiltrates in human primary melanoma is affected by the presence of melanin pigmentation.

Tissue sections obtained from 23 primary melanoma excisions were stained for IHC evaluation of CD3 positive ($CD3^+$) T cells in order to investigate the distribution of tumor-infiltrating lymphocytes in primary human melanomas (Fig. 1 and 2). Analysis of the tumor areas was accomplished by applying a semi-automated algorithm, consisting of four main steps: (I) color threshold, (II) cell segmentation, (III) cell counting, and (IV) overlaying of the resulting mask with the original image (Fig. 1B-F). In melanoma tissue sections though, the presence of melanin affects IHC quantification, due to its high background signal often indistinguishable from brown or red chromogens, like DAB and nova red (Fig.2A). Another limitation of the semi-automated algorithm is the difficulty in efficiently separating groups of cells, from single cells. Clusters of cells are then erroneously reported as a single cell (independent of the size of the cell cluster), thus seriously affecting the end results

of the analysis. In the examples shown in figures 2B and 2C, where CD3$^+$ T cells are stained with nova red, the semi-automated algorithm incorrectly identifies melanin pigments as cells positive for the specific immunohistochemical marker used and fails segmenting clusters of T cells.

Unmixing of melanin and cellular signal components to generate a spectral library

To overcome the above-mentioned limitations in the assessment of immune infiltrates in pigmented tumors, we used a multispectral imaging system that combines imaging with spectroscopy. We observed that different tumors synthesize melanin with varying intensities and distinct spectral characteristics (Fig. 3A, B and C). In particular, in our cohort of patients we could identify three different spectra of melanin. One of the three measured melanin spectra showed a strong overlap with

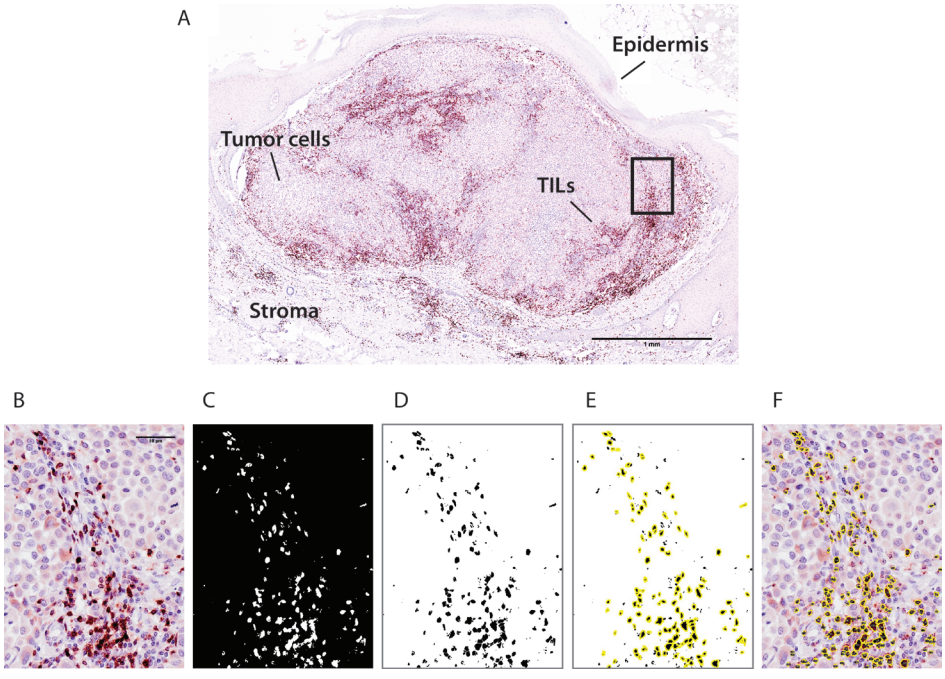

Figure 1. Overview of the semi-automated image analysis process for the assessment of T cell density in primary human melanoma. Section of human primary cutaneous melanoma showing immunohistochemical staining for CD3. In red CD3 positive (CD3$^+$) T lymphocytes. Hematoxylin counterstaining, original magnification 20X (A). Zoom-in on tumor region indicated in the original image A (B). Output image after applying an image color thresholding (C), segmentation (D) and cell counting in yellow (E) by using the imaging software Fiji. Processed image after superimposing the segmented image with cell borders marked in yellow on the original bright-field image (F). Scale bar 1mm.

the spectrum of the nova red chromogen (Fig. 3F) and therefore was responsible of the failure of the semi-automated algorithm in the quantification of true positive cells, especially in the tumor area. We combined the melanin spectra with the ones of heamatoxylin and nova red in a so-called "spectral library" (Fig 3F), which was then applied to all of the acquired bright field images. This resulted in new images (Fig 4), where the brown melanin signals could be distinguished from the true nova red signal and therefore not quantified as positive in the T cells positivity score.

Comparison of T cell density assessment performed by semi-automated or multispectral analysis

The density of $CD3^+$ T lymphocytes was quantified in both, intratumoral (lymphocytes infiltrating the melanoma cell nests) and peritumoral regions (lymphocytes surrounding the tumor deposits) of primary cutaneous melanoma. Intratumoral and peritumoral regions were defined by fully-automated trainable tissue segmentation, based on morphological features (Fig S1). Furthermore, nuclear staining allowed the efficient separation (segmentation) of cell clusters, which were then properly assessed. The 23 primary tumors analyzed showed a variable level of melanin pigmentation, both in terms of pigment intensity and content. The percentage of pigmented tumor cells was manually scored, resulting in 14 highly pigmented

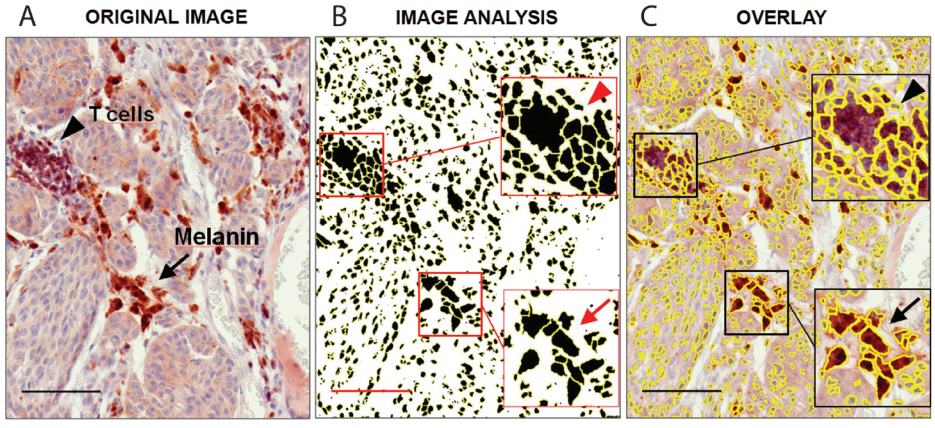

Figure 2. Semi-automated image analysis of highly pigmented melanoma. Assessment of the presence of $CD3^+$ T lymphocytes in highly pigmented melanoma tumor using semi-automated image analysis. Original immunohistochemical image of human melanoma, containing clusters of infiltrating $CD3^+$ T cells (nova red, arrowhead) and brown melanin pigments (arrow) (A). Output image of semi-automated algorithm for image analysis and cell count (B). Overlay of output and original multispectral image (C). The image processing presents some limitations (see zoom-in): T cells in cluster cannot be efficiently separated (top, arrowhead) and melanin pigments originate false positives (bottom, arrow) (B, C). Scale bars 50µm.

melanomas (>50% pigmented tumor cells) and 9 melanomas, which showed between 5% and 20% of pigmented tumor cells. T cell density was assessed using both our semi-automated algorithm and fully-automated multispectral analysis (Suppl. Table I) (Fig 5A-F). Our results clearly show that the T cell density in highly pigmented tumor was significantly higher using conventional analysis, as compared to multispectral approach (Fig. 5G). This difference, however, was not significant in tumors with low melanin pigmentation (Fig 5H). These findings suggest that linear spectral unmixing of melanin from chromogens with spectra close to one of the melanin spectra (such as nova red and DAB) is crucial in the assessment of T cell density, particularly in highly pigmented melanomas (14 out of 23 patients). In some

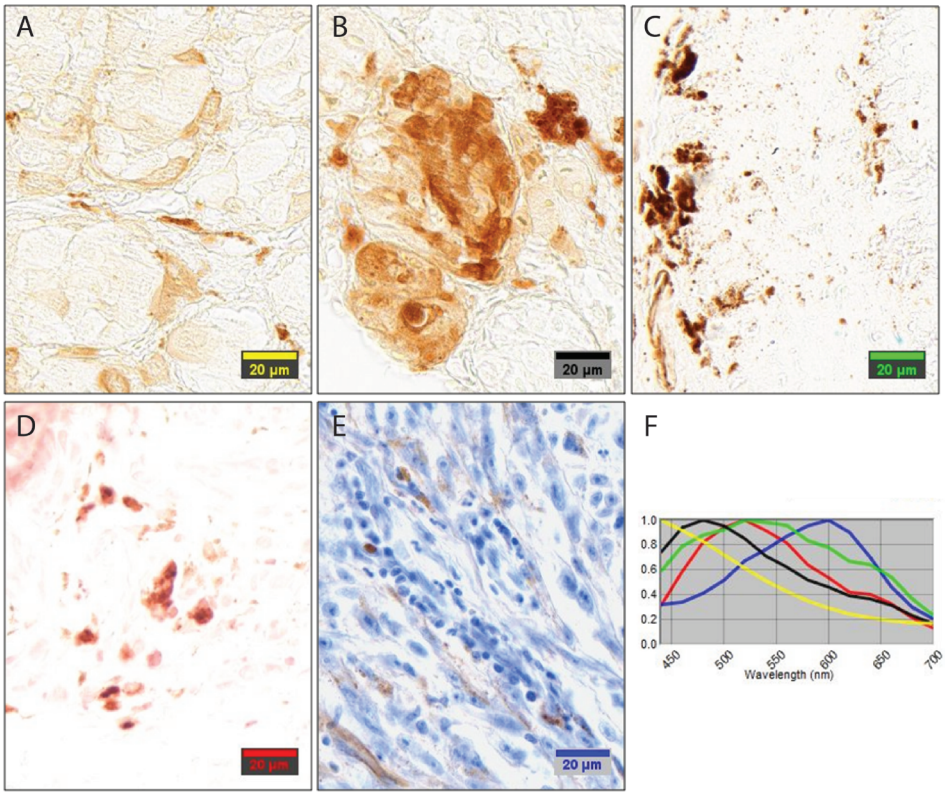

Figure 3. Spectral unmixing in human melanoma tumors reveals different spectra of melanin pigmentation. Representative immunohistochemical images of cellular components and melanin pigments used to build a spectral library for image analysis of TILs in melanomas. Three differently pigmented melanin samples (A, B, C), CD3-nova red positive T lymphocytes D), haematoxylin staining of nuclei (E). A spectral library of nova red (red) and haematoxylin (blue) and 3 different Melanin (green, black and yellow) was built in Nuance software using single stained or unstained human melanoma tissues respectively (F). Scale bar 20µm.

tumors, T cell density was slightly higher when quantified by the automated software (T cells count in Fig 5 E and F, Suppl. Table I). This was mainly due to a more accurate cell segmentation where all the cells are detected and clusters are correctly split.

Discussion

Analysis of location, type and density of the immune infiltrate and their correlation with clinical outcome is of crucial importance in cancer research[11,13,14,29]. Nowadays, the assessment of T cell density in solid tumors is usually investigated with traditional IHC analysis and bright-field microscopy[14]. Here, we compare two different digital imaging approaches to estimate the amount of TILs in the tumoral and peritumoral area of melanoma primary lesions.

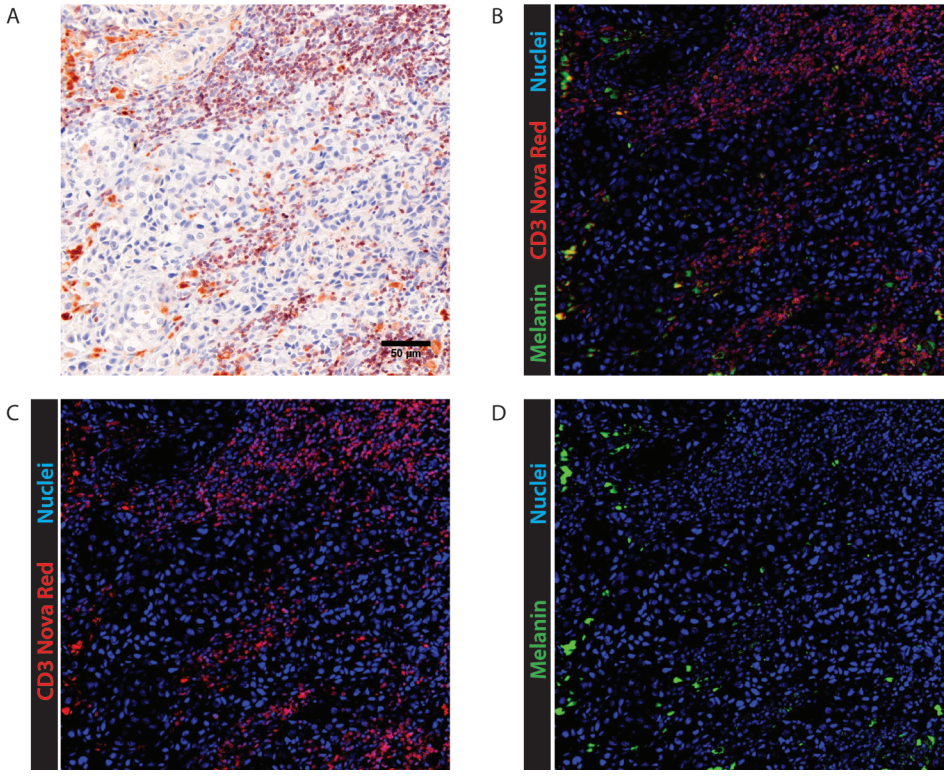

Figure 4. Melanin unmixing reveals T cell infiltrates in melanoma tumor. Melanin unmixing allows visualization of infiltrating T lymphocytes in melanoma tumor. Original colored image of human melanoma (A). Composite pseudo-fluorescent image containing both melanin (in green) and $CD3^+$-nova red T cells (in red) (B). Pseudo-fluorescent images of (C) unmixed $CD3^+$-nova red T cells and (D) melanin. Nuclei are shown in blue (haematoxylin staining). Scale bar 50µm.

At first, we developed and tested a semi-automated digital image approach, which was expected to represent a useful tool to assess T cell density in tumor areas. Unfortunately, we observed that accuracy, which is of eminent importance for proper interpretation of IHC results, was still far from perfect. Especially in melanoma samples that contained dark brown melanin pigments in the tumor area, a large portion of the immune cells were obscured therefore hampering IHC measurements[22]. This because different colors in bright-field images are

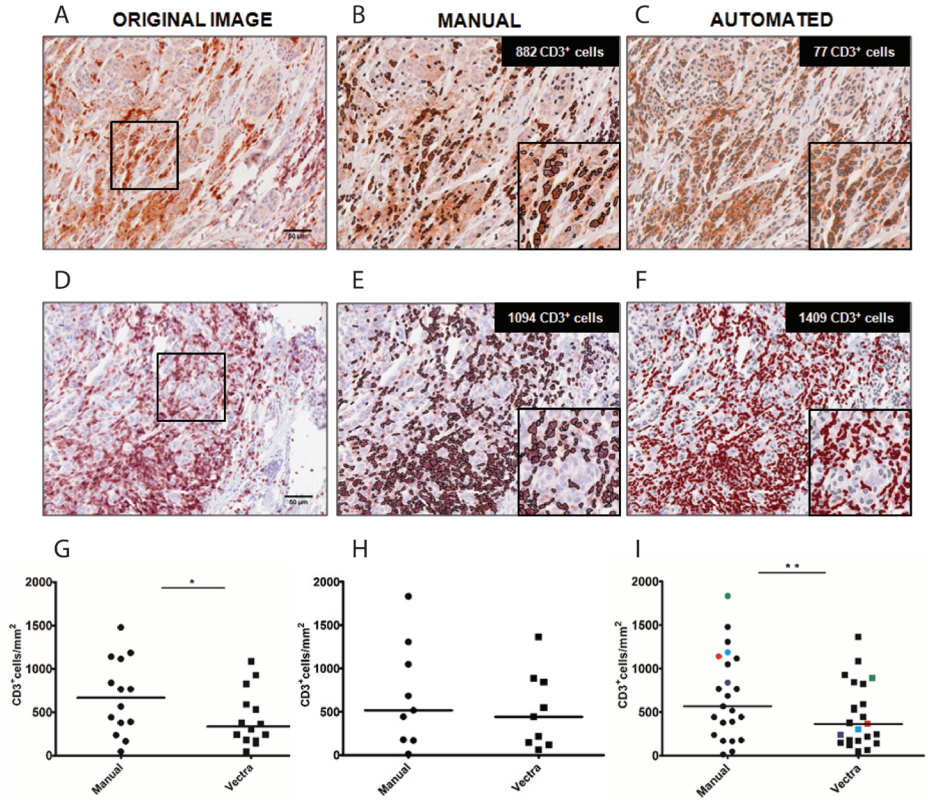

Figure 5. Comparison of manual and automated cell count in pigmented and non-pigmented melanoma. Comparison of the quantitative assessment of CD3⁺ T lymphocytes in human primary melanomas performed by manual image software Fiji (B, E) or fully automated Vectra/InForm platform (C, F). For tumor with more than 50% of cells pigmented (A-C) the absolute CD3⁺ T cell counts are significantly higher using the manual (B) compared to the automated (C) analysis, because of false positives due to melanin pigmentation. In tumors with no or low pigmentation (D-F), the CD3⁺ T cells counts are comparable in manual (E) *vs* automated (F) analysis. Dot plots of CD3⁺ T lymphocytes enumeration for pigmented (G) *vs*. non-pigmented (H) melanomas and the combination of the two groups (I). Matched color symbols indicate differences in T cell counts in the same tumor, obtained with manual or automated analysis (I). Scale bars 50μm.

perceived as a mixture of the RGB (red, green, blue) channels and routinely used imaging software solutions are not able to discriminate between the single color components. Consequently, melanin was detected in all three channels, at different intensities[20,30]. In addition, conventional red and brown chromogens used for IHC staining generate signals that are analogous to the background signal caused by melanin pigments can also lead to overestimation of the amount of T cells infiltrating the tumor, resulting in false positive counts.

Based on these findings we next applied techniques that were able to discriminate between the melanin and red and brown chromogens used for IHC staining. We found that multispectral imaging and linear spectral melanin unmixing to quantitatively assess the density of CD3+ T lymphocytes infiltrating human primary cutaneous melanoma could effectively overcome the limits of the conventional semi automated algorithm[22,28]. A major advantage of multispectral over conventional bright-field imaging is the possibility to clearly separate emission spectra of each chromogen present in the tissue section. Likewise, the spectrum of melanin, which otherwise distorts the nova red chromogen signal, can now be unmixed from the original multispectral image. Our findings demonstrate major differences in T cells densities dependent on the two methods described. Conventional analysis leads to overestimation of T cell infiltration and therefore to possible misinterpretation of the data. This is of special importance when comparing different groups of melanoma patients exhibiting dissimilar degrees of tissue pigmentation.

Furthermore, the presence of immune pigmented cells, such as melanophages, also challenges the quantification of TILs making it difficult to distinguish them from $CD3^+$ tumor-infiltrating T cells especially when localized in close proximity[31]. In our melanoma biopsies, melanin pigments specifically co-localized with melanoma cells and not with melano-macrophages (data not shown) suggesting that the three distinct melanin spectra detected are not a result of enzymatic processing by melanophages, but are a specific characteristic of malignant melanocytes.

Finally, tissue segmentation often also encounters difficulties with conventional approaches: stroma located between tumor clusters is difficult to exclude from the tumor area using manual definition of the tumor area (data not shown). The tissue trainable automated image analysis software allows precise tissue segmentation, where even stromal tissue and T cells located in between tumor clusters could clearly be distinguished and thus excluded from the tumor tissue. Furthermore, T cell clusters were accurately segmented based on nuclear staining and typical cell size, thereby overcoming additional limitations of semi-automated analyses.

In conclusion, our study highlights the potency of multispectral imaging to accurately assess immune cell infiltrates including those in notoriously difficult tissues, such as highly pigmented melanomas. By using this innovative microscopy

technique, we recently showed that the density of pre-existing lymphocytes inside the tumor and at the tumor margin is an accurate predictor of survival for metastatic melanoma patients receiving DC vaccination[32]. Therefore, we strongly believe that this approach is an important addition to the armamentarium in melanoma research, where the assessment of tumor infiltration is crucial in the search for new biomarkers to predict patient responses to immunotherapies.

Aknowledgments

This work was supported by a KWO Grant, KUN2009-4402 from the Dutch Cancer Society. CGF received an NWO Spinoza award and ERC Advanced Grant PATHFINDER (269019). IJMdV received NWO Vici Grant 016.140.655.

Author contribution

AV and CGF conceived the study. AV and DV performed the experiments and analyzed the data. WAMB assisted with image interpretation. SDB and AV wrote the manuscript. All authors revised and approved the final version of the manuscript.

References

1. Miller, A. J. & Mihm, M. C. Melanoma. *New England Journal of Medicine* **355**, 51-65, doi:doi:10.1056/NEJMra052166 (2006).
2. Palmieri, G., Capone, M., Ascierto, M. *et al.* Main roads to melanoma. *Journal of Translational Medicine* **7**, 86 (2009).
3. Ascierto, M. L., Melero, I. & Ascierto, P. A. Melanoma: From Incurable Beast to a Curable Bet. The Success of Immunotherapy. *Frontiers in Oncology* **5**, 152, doi:10.3389/fonc.2015.00152 (2015).
4. Niezgoda, A., Niezgoda, P. & Czajkowski, R. Novel Approaches to Treatment of Advanced Melanoma: A Review on Targeted Therapy and Immunotherapy. *BioMed Research International* **2015**, 851387, doi:10.1155/2015/851387 (2015).
5. Larkin, J., Chiarion-Sileni, V., Gonzalez, R. *et al.* Combined Nivolumab and Ipilimumab or Monotherapy in Untreated Melanoma. *New England Journal of Medicine* **373**, 23-34, doi:doi:10.1056/NEJMoa1504030 (2015).
6. Johnson, D. B., Peng, C. & Sosman, J. A. Nivolumab in melanoma: latest evidence and clinical potential. *Therapeutic Advances in Medical Oncology* **7**, 97-106, doi:10.1177/1758834014567469 (2015).
7. Hodi, F. S., O'Day, S. J., McDermott, D. F. *et al.* Improved Survival with Ipilimumab in Patients with Metastatic Melanoma. *New England Journal of Medicine* **363**, 711-723, doi:doi:10.1056/NEJMoa1003466 (2010).
8. Robert, C., Schachter, J., Long, G. V. *et al.* Pembrolizumab versus Ipilimumab in Advanced Melanoma. *New England Journal of Medicine* **372**, 2521-2532, doi:doi:10.1056/NEJMoa1503093 (2015).
9. Karagiannis, P., Fittall, M. & Karagiannis, S. N. Evaluating Biomarkers in Melanoma. *Frontiers in Oncology* **4**, 383, doi:10.3389/fonc.2014.00383 (2014).
10. Gajewski, T. F., Schreiber, H. & Fu, Y.-X. Innate and adaptive immune cells in the tumor microenvironment. *Nature immunology* **14**, 1014-1022, doi:10.1038/ni.2703 (2013).
11. Fridman, W. H., Pagès, F., Sautès-Fridman, C. & Galon, J. The immune contexture in human tumours: impact on clinical outcome. *Nat Rev Cancer* **12**, 298-306 (2012).
12. Galon, J., Fridman, W.-H. & Pagès, F. The Adaptive Immunologic Microenvironment in Colorectal Cancer: A Novel Perspective. *Cancer Research* **67**, 1883-1886, doi:10.1158/0008-5472.can-06-4806 (2007).
13. Ribas, A., Comin-Anduix, B., Economou, J. S. *et al.* Intratumoral Immune Cell Infiltrates, FoxP3, and Indoleamine 2,3-Dioxygenase in Patients with Melanoma Undergoing CTLA4 Blockade. *Clinical Cancer Research* **15**, 390-399, doi:10.1158/1078-0432.ccr-08-0783 (2009).
14. Erdag, G., Schaefer, J. T., Smolkin, M. E. *et al.* Immunotype and Immunohistologic Characteristics of Tumor-Infiltrating Immune Cells Are Associated with Clinical Outcome in Metastatic Melanoma. *Cancer Research* **72**, 1070-1080, doi:10.1158/0008-5472.can-11-3218 (2012).
15. Ladányi, A. Prognostic and predictive significance of immune cells infiltrating cutaneous melanoma. *Pigment Cell & Melanoma Research* **28**, 490-500, doi:10.1111/pcmr.12371 (2015).

16. Mahmoud, S. M. A., Paish, E. C., Powe, D. G. *et al.* Tumor-Infiltrating CD8+ Lymphocytes Predict Clinical Outcome in Breast Cancer. *Journal of Clinical Oncology* **29**, 1949-1955, doi:10.1200/jco.2010.30.5037 (2011).
17. Kmiecik, J., Poli, A., Brons, N. H. C. *et al.* Elevated CD3+ and CD8+ tumor-infiltrating immune cells correlate with prolonged survival in glioblastoma patients despite integrated immunosuppressive mechanisms in the tumor microenvironment and at the systemic level. *Journal of Neuroimmunology* **264**, 71-83, doi:http://dx.doi.org/10.1016/j.jneuroim.2013.08.013 (2013).
18. Berghoff, A. S., Ricken, G., Widhalm, G. *et al.* Tumour-infiltrating lymphocytes and expression of programmed death ligand 1 (PD-L1) in melanoma brain metastases. *Histopathology* **66**, 289-299, doi:10.1111/his.12537 (2015).
19. Ahmadzadeh, M., Johnson, L. A., Heemskerk, B. *et al.* Tumor antigen–specific CD8 T cells infiltrating the tumor express high levels of PD-1 and are functionally impaired. *Blood* **114**, 1537-1544, doi:10.1182/blood-2008-12-195792 (2009).
20. van der Laak, J. A. W. M., Pahlplatz, M. M. M., Hanselaar, A. G. J. M. & de Wilde, P. C. M. Hue-saturation-density (HSD) model for stain recognition in digital images from transmitted light microscopy. *Cytometry* **39**, 275-284, doi:10.1002/(sici)1097-0320(20000401)39:4<275::aid-cyto5>3.0.co;2-8 (2000).
21. Woo, J., Liss, M., Muldong, M. *et al.* Tumor infiltrating B-cells are increased in prostate cancer tissue. *Journal of Translational Medicine* **12**, 30 (2014).
22. Ito, S. & Wakamatsu, K. Quantitative Analysis of Eumelanin and Pheomelanin in Humans, Mice, and Other Animals: a Comparative Review. *Pigment Cell Research* **16**, 523-531, doi:10.1034/j.1600-0749.2003.00072.x (2003).
23. Mäkitie, T., Tarkkanen, A. & Kivelä, T. Comparative immunohistochemical oestrogen receptor analysis in primary and metastatic uveal melanoma. *Graefe's Arch Clin Exp Ophthalmol* **236**, 415-419, doi:10.1007/s004170050099 (1998).
24. Mäkitie, T., Summanen, P., Tarkkanen, A. & Kivelä, T. Tumor-Infiltrating Macrophages (CD68+ Cells) and Prognosis in Malignant Uveal Melanoma. *Investigative Ophthalmology & Visual Science* **42**, 1414-1421 (2001).
25. Orchard, G. E. & Calonje, E. The Effect of Melanin Bleaching on Immunohistochemical Staining in Heavily Pigmented Melanocytic Neoplasms. *The American Journal of Dermatopathology* **20**, 357-361 (1998).
26. Shen, H. & Wu, W. Study of Melanin Bleaching After Immunohistochemistry of Melanin-containing Tissues. *Applied Immunohistochemistry & Molecular Morphology* **23**, 303-307, doi:10.1097/pai.0000000000000075 (2015).
27. Jiang, K., Brownstein, S., Lam, K., Burns, B. & Farmer, J. USefulness of a red chromagen in the diagnosis of melanocytic lesions of the conjunctiva. *JAMA Ophthalmology* **132**, 622-629, doi:10.1001/jamaophthalmol.2013.8216 (2014).
28. Feng, Z., Puri, S., Moudgil, T. *et al.* Multispectral imaging of formalin-fixed tissue predicts ability to generate tumor-infiltrating lymphocytes from melanoma. *Journal for ImmunoTherapy of Cancer* **3**, 47 (2015).
29. Rahbar, M., Naraghi, Z. S., Mardanpour, M. & Mardanpour, N. Tumor-Infiltrating CD8+ Lymphocytes Effect on Clinical Outcome of Muco-Cutaneous Melanoma. *Indian Journal of Dermatology* **60**, 212-212, doi:10.4103/0019-5154.152571 (2015).
30. Zhao, L. & Josiane, Z. Skin image illumination modeling and chromophore identification for melanoma diagnosis. *Physics in Medicine and Biology* **60**, 3415 (2015).

31. Piras, F., Colombari, R., Minerba, L. *et al.* The predictive value of CD8, CD4, CD68, and human leukocyte antigen-D-related cells in the prognosis of cutaneous malignant melanoma with vertical growth phase. *Cancer* **104**, 1246-1254, doi:10.1002/cncr.21283 (2005).
32. Vasaturo, A., Halilovic, A., Bol, K. F. *et al.* T cell landscape in a primary melanoma predicts the survival of patients with metastatic disease after their treatment with dendritic cell vaccines. *Cancer Research*, doi:10.1158/0008-5472.can-15-3211 (2016).
33. Mansfield, J. R. Cellular context in epigenetics: quantitative multicolor imaging and automated per-cell analysis of miRNAs and their putative targets. *Methods* **52**, 271-280, doi:10.1016/j.ymeth.2010.10.001 (2010).
34. Stack, E. C., Wang, C., Roman, K. A. & Hoyt, C. C. Multiplexed immunohistochemistry, imaging, and quantitation: A review, with an assessment of Tyramide signal amplification, multispectral imaging and multiplex analysis. *Methods* **70**, 46-58, doi:http://dx.doi.org/10.1016/j.ymeth.2014.08.016 (2014).

Supplementary material

Suppl. Table I. Comparison of tumor T cell density by manual *vs* automated analysis

	Manual		Vectra	
Study number	Area (mm²)	Number CD3/mm²	Area (mm²)	Number CD3/mm²
1	63,08	444,0869	123,4401	149,2609
2	4,451	1478,319	25,64852	826,894
3	1,486	1833,109	3,220092	890,401
4	10,412	1115,636	12,74008	1086,342
5	100,972	567,2167	84,48246	929,516
6	16,155	389,6626	58,31399	177,8837
7	20,276	517,9523	64,70396	443,3608
8	9,082	1185,312	18,65365	306,2196
9	26,471	47,0326	95,50739	48,28947
10	47,969	378,6195	95,40543	591,1332
11	18,562	1048,917	15,0673	1366,469
12	13,26	1306,071	45,32296	843,2178
13	12,19	442,2888	30,57088	244,2098
14	11,68	1140,154	17,66768	364,7105
15	12,213	11,95447	10,82412	63,42938
16	6,214	765,5294	6,099012	530,2608
17	5,715	685,3893	4,872096	548,5977
18	117,01	169,4129	209,8617	221,1044
19	2,655	766,4783	5,794596	377,4328
20	7,145	236,9489	9,157	144,4622
21	7,669	177,9893	6,812928	122,349
22	24,744	838,8296	21,0258	241,3278
23	48,948	165,9516	27,21056	170,6309

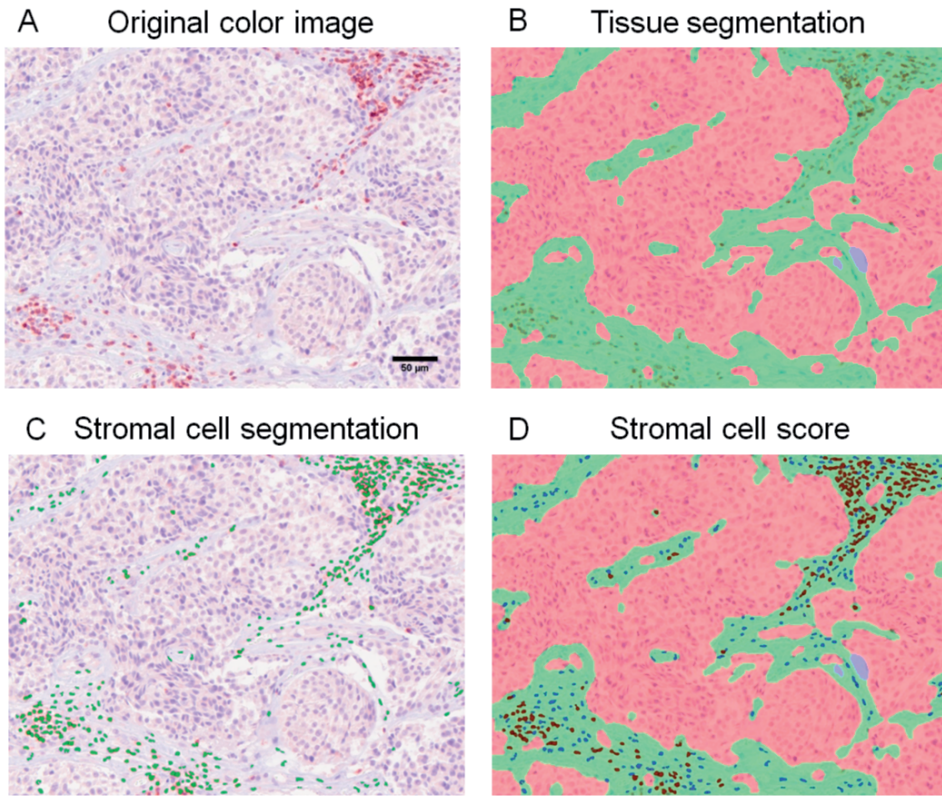

Suppl. Figure 1. Fully-automated digital image analysis of primary melanoma on the Vectra/ Inform platform. Original colored image of a primary human melanoma (A). Trainable tissue segmentation function of the inform software used to automatically identify tumor region (red) and stromal region (green) mainly based on morphological features (B). Nuclear cell segmentation (green nuclei) exclusively in the stromal compartment (C). Automated CD3 positivity score in the stromal region (red nuclei in the green stromal segmented tissue). Scale bar 50µm.

CHAPTER 6

Summary, discussion and future perspectives

Summary

The immune system can be divided into two separate but interlocked arms: the innate and the adaptive immune response. Bridging of those two arms is orchestrated by antigen presenting cells (APCs). In the context of anti-tumor immunity, APCs detect the presence of malignant cells. Sensing of "danger" triggers capture of tumor material by APCs and clearance of the threat. Subsequently, APCs prime adaptive immune cells against the tumor, which eventually results in a durable and highly specific response against malignant cells. It is conceptually established that dendritic cells (DCs) are the sentinel APCs of the immune system. The ability of DCs to sense signs of danger, and efficiently communicate these to the adaptive immune cells, determines the fate of anti-tumor immunity. Success of this communication hinges upon the activation status of DCs. Defective or impaired DC activation facilitates tolerance towards cancer cells, while fully functional DCs strongly promote cytotoxic T cell activation.

In order to grow and survive, tumors employ several strategies to escape immune surveillance. Growing knowledge on the immunosuppressive mechanisms that accompany tumor progression indicates that they result in a suppressive tumor microenvironment (TME), which inhibits innate and adaptive immune responses on several levels. In terms of DC function, the TME is the main artificer of the defective activation of DCs. Indeed, malignant cells directly interfere with DC basic functions and modulate expression of DC phenotypic markers, as well as secretion of cytokines and chemokines. In addition, the tumor influences the behavior of normal neighboring stromal and immune cells. This, in turn, generates a habitat that favors tumor growth and dissemination, while being hostile towards the activation of effective anti-tumor immune responses. The goal of anti-cancer therapy is to destroy the tumor. In order to achieve this, the immunosuppressive networks of the TME need to be tackled, either by destroying cancer cells (conventional chemotherapy) or by "releasing the breaks" on the immune system (immunotherapeutic strategies).

The first objective of this thesis was to gain more insights into the impact of tumor-driven immunosuppression on human naturally-occurring DCs; and to study two distinct anti-cancer strategies that have the potential to restore DC activation.

In this thesis we have introduced the relatively new insights that show that the efficacy of chemotherapy is in part dependent on the immune system. A lot of effort has been devoted into increasing our understanding of the molecular parameters that govern the beneficial effects of chemotherapy-induced immunogenic cell death

(ICD). Yet, little is known about the immune cells that detect tumor cells undergoing ICD. In fact, the role human naturally occurring DC subsets, such as $CD1c^+$ and $CD16^+$ myeloid (mDCs) and plasmacytoid (pDCs) DCs, in the context of ICD had never been studied. In **Chapter 2**, we highlighted the unique ability of human $CD1c^+$ DCs to mediate anti-tumor immune responses, upon induction of ICD by platinum compounds. We showed that, treatment of different human tumor cell lines with clinically relevant doses of oxaliplatin (OXP) or cisplatin (CDDP), caused a form of cell death consistent with ICD. This confirmed the ability of OXP to induce ICD on tumor cells of different origins, and expanded the list of ICD-inducers to include the "platinum-sister compound", CDDP. Platinum-treated tumor cells exposed the pro-phagocytic signal, calreticulin (CRT). Exposure of CRT mediated tumor cell uptake by human DC subsets, as confirmed by peptide-binding blocking assays. Interestingly, uptake of tumor material by DCs was not abrogated by blocking of the CRT receptor, CD91; pointing towards the involvement of other receptors in mediating binding of CRT. We next showed that sensing of the "ICD-signals" (HSPs, ATP and HMGB1) contributed to the induction of maturation of mDCs and pDCs. Finally, we reported that, although all DC subsets were able to mature upon interaction with platinum-treated tumor cells, only $CD1c^+$ DCs effectively stimulated proliferation of T cells. These novel findings suggest functional specialization between human naturally occurring DC subsets, in response to the induction of ICD by chemotherapeutic drugs.

The tumor-DCs interplay markedly suppresses maturation and function of DCs. As reported in **Chapter 3**, co-culture of DC and tumor cells resulted in a down-modulation of the surface expression of co-stimulatory molecules (CD80, CD86) and major histocompatibility class (MHC) I and II molecules. This was accompanied by reduced secretion of the pro-inflammatory cytokine TNF-α, as well as increased production of the anti-inflammatory cytokine IL-10; which ultimately resulted in impaired induction of T cell proliferation by DCs. Blockade of the inhibitory CD47/SIRPα signaling pathway has shown therapeutic efficacy in various preclinical models of malignancies. This beneficial effect relies upon the ability of APCs to take up tumor material and induce adaptive immunity [1]. Phagocytosis is regulated by the balance between pro-phagocytic and anti-phagocytic cues provided by target cells [2]. Evidence shows that the dominant "eat me" signal CRT is counterbalanced by the "don't eat me" tag given by CD47 [3]. In Chapter 3 we reported that increased uptake of tumor material by human $CD1c^+$ DCs was determined by the binding of blocking moAbs against CD47. The uptake of tumor fragments induced DC maturation and counteracted tumor-driven suppression of DCs. In addition, previous studies demonstrated that anti-CD47-mediated tumor clearance by phagocytic

cells *in vivo,* was enhanced in the presence of immunogenic stimuli, derived from cells undergoing immunogenic apoptosis. Although in our settings, combination of platinum treatment with anti-CD47 moAbs did not augment phagocytosis by DCs, we could observe upregulation of the phenotypic marker CD86. In summary, our observations not only expand the knowledge on the role of naturally-occurring DCs in the context of tumor-mediated immunosuppression; but they also provide a rationale for further investigation of the potential cooperation of conventional chemotherapy with immunotherapy.

In multiple parts of this thesis, we have underscored the concept that, the cell biological context and the heterotypic crosstalk within the TME are key determinants of the multi-step process that controls effective activation of anti-tumor immunity. Because of the lack of physiological complexity of two-dimensional (2D) cell monolayers, another part of this work aimed at exploring novel techniques that will contribute to our understanding of the complexity of in vivo tissues.

Chapter 4 covers the development of a three-dimensional (3D) organotypic model of human skin melanoma to analyze DC-tumor cross talk in a 3D environment. Skin is characterized by a defined molecular composition and stiffness and by the presence of physical interfaces, which are difficult to faithfully reproduce using collagen matrices. The use of a human-derived dermal component provides the correct space and guidance, and acts as a physical barrier by the basement membrane, facilitating or restricting cell motility and interaction. Moreover, an *in vitro* model for melanoma model offers the advantage of modulating the local cellular environment, in a controllable and reproducible way, by titrating cell types and numbers; whilst ensuring the survival of all cell types involved. Furthermore, this reconstructed 3D environment provides a potential platform to study migration and invasion of cancer cells into surrounding tissues, assess the contribution of other relevant cells of the tissue in cancer development, as well as investigate regulation of DC functional properties within the local TME. In this respect, we show that DCs efficiently migrated along the extracellular meshwork and interacted with invasive tumor cells (found grouped in clusters or as single cells in the dermis), which finally resulted in engulfment of tumor material by DCs. In summary, malignant and non-malignant cells retain their basic functions (such as tumor cell invasion; DC migration and uptake), when cultured within this multicellular reconstitution of human melanoma skin tissue. Our observations indicate that this skin melanoma model can be exploited to gather insights into the dynamics of the TME; and it has multiple advantages over conventional monolayer co-cultures by the presence of physiological complexity.

During the past decade, different types of immunotherapies became available for the treatment of various tumors, including melanoma. Despite long-term therapeutic benefit in a distinct number of patients, there are still some challenges ahead, mostly associated with high costs, potential toxicity and suboptimal efficacy of immunotherapeutic strategies. Therefore, there is an urgent need to identify early biomarkers that predict potential efficacy of immunotherapy. The quantification of cells of the innate and adaptive immune system that infiltrate tumors is crucial in this search. Late advances in the field of cancer immunology have shown that infiltration of immune cells, such as $CD3^+$ lymphocytes, within the TME may impact the induction of tumor-specific immune responses. Chapter 5 highlights the potency of multispectral imaging (MSI) to accurately assess immune cell infiltrates, including those in notoriously difficult tissues such as pigmented melanomas. The innovative MSI technique combines imaging with spectroscopy, to obtain accurate information about quantitative expression data and tissue distribution of different cell types within the TME. With respect to melanoma, the presence of dark melanin pigments in the tumor area can often obscure immune cells and/or lead to false positive cell classification, both cases hampering analysis and quantification of immune cell composition. In this chapter, we have compared two different T cell quantification methodologies and demonstrate that multispectral unmixing of tissue images overcomes this difficulty, thereby facilitating a very accurate enumeration of tumor infiltrating T lymphocytes in melanomas.

Discussion and future perspectives

Immunogenic cell death

Cell death, as a byproduct of tissue renewal and cell turnover, occurs continuously in the human body through apoptosis. In principle, cell death and damage are processes that alert the immune system; as an exception, the process of apoptosis involves a series of morphological changes that are immunologically silent. Apoptosis is characterized by membrane integrity and disintegration of the cell into apoptotic bodies, which are efficiently cleared by neighboring cells. Therefore, apoptosis does not lead to activation of the adaptive immune response and subsequent adverse autoimmune reactions. By contrast, cells succumbing to necrosis, undergo plasma membrane disruption and leakage of cellular content into the intercellular space. This results in inflammatory immune responses [4]. Although the equation "apoptosis equals immunologically-silent cell death" has been taught in textbooks for decades, recent studies have demonstrated that this assumption is an incorrect generalization. Rather, apoptosis seems to occur through a non-uniform series of molecular and biochemical events; meaning that distinct pathways may lead to cell death and induce stimulus-specific cellular alterations, before the cells adopt the classical morphological characteristics of apoptosis [5].

Highly proliferative tumor cells exist in a continuous state of stress, and cell death is a common feature [6]. However, physiological death of malignant cells, or chemotherapy-induced cell death in general, do not overcome the immunosuppressive nature of the TME. Only when tumor cells succumb to a defined subset of cytotoxic agents, does their demise have the potential to trigger highly specific anti-tumor immunity [7,8]. Thus, subcutaneous injection of chemotherapy-treated tumor cells in mice with a functional immune system (and in the absence of any adjuvants), activates a specific anti-tumor immune response, which protects the animal from a subsequent challenge with viable tumor cells of the same origin [9]. Moreover, studies using immunocompetent *versus* immunodeficient mice revealed that treatment with certain chemotherapeutic drugs are more effective in eradicating tumors in the presence of an intact immune system [10,11]. In other words, functional innate and adaptive immune components are an essential contribution to the beneficial therapeutic outcome of chemotherapy, highlighting the clinical relevance of ICD.

Chemotherapy induces ICD

The immunostimulatory activity of certain chemotherapeutic drugs, including some platinum-based agents, was recently recognized[12,13, 107]. As presented in this thesis (**Chapters 2 and 3**), treatment of tumor cells with OXP or CDDP favors the release of 'danger' signals, or damaged-associated molecular patterns (DAMPs), which

function as immunological adjuvants on DCs. OXP and CDDP are alkylating agents that exert their cytotoxic effect by binding genomic DNA in the nucleus and forming crosslinks with DNA strands. The result of such adducts stops DNA synthesis and repair, thus leading to cell death. Despite sharing similar mechanisms of action, OXP and CDDP have different immunogenic potential. OXP causes a cellular response that culminates with endoplasmic reticulum (ER) stress and exposure of intracellular ER-associated DAMPs, like CRT and HSPs. Unresolved ER stress eventually leads to protein degradation, disruption of mitochondrial permeability and ultimately cell death [14,15]. By contrast, CDDP was never considered an ICD inducer as it fails to provoke ER stress; unless it is co-administered with an ER stressor, such as tunicamycin [10,16,17]. Curiously, it has recently been reported that CDDP can promote CRT exposure by a - yet to be identified - mechanism that involves binding of chemokines, such as IL-8, to their GPCR receptors [18]. This consolidates our findings that suggest a role for CDDP as ICD inducer, and demonstrates that numerous details on the molecular events that define immunogenicity remain to be defined.

The "key-lock paradigm" in DC activation

A crucial question is how the immune system can effectively distinguish between different cell death modalities. A possible explanation is provided by the mechanisms that lead to CRT exposure. We briefly explained that prolonged ER stress causes translocation of intracellular molecules to the outer leaflet of the plasma membrane. This means that upregulation of surface CRT can be detected not only upon immunogenic cell death, but also in later stages of apoptosis (also called secondary necrosis). Although the details are not fully understood yet, it seems that pre-apoptotic exposure of CRT (as it happens upon ICD induction) relies upon the concomitant translocation of the ER-associated molecule ERp57, as demonstrated by abrogation of CRT surface expression in ERp57$^{-/-}$ cells [19]. In contrast, exposure of CRT occurring at later time points is independent on ERp57. This suggests that, the defined temporal sequence and the combination of immunogenic events are decisive to provide the security tokens to gain access to the initiation of a productive anti-tumor response [20]. In this analogy, only the correct key-set (DAMPs) can open the locks (receptors), which make the way to DC maturation.

In vivo depletion of DCs abrogates tumor-specific immune cell activation, confirming that DCs are necessary for mounting effective immune responses against dying tumor cells following ICD [9,21]. However, the presence of DCs per se is not sufficient to trigger T cell priming against tumor-associated antigens (TAA) [22]. The immunostimulatory effect of CDDP *in vivo*, as evidenced by increased co-stimulatory molecule expression (CD80, CD86) on myeloid DCs, and subsequent induction of TAA-specific cytotoxic T cells, was abolished in mice lacking CD80 and CD86 on APCs [22].

The multistep process that leads to DC maturation consists of (at least) three defined parameters involving ICD-related DAMPs, released by dying tumor cells, and their specific receptors on DCs: recruitment, engulfment, activation. DCs need to be recruited to the proximity of dying tumor cells, they have to take up tumor antigens and then respond to activating stimuli to undergo phenotypical maturation and functional activation. If all these three steps are taken, DCs will merge the signals emanated by ICD-DAMPs and converge them into one command for launching an immune response. Absence of one or more of these 'danger' signals abrogates DC maturation and effective activation of the immune system. Accordingly, addition of recombinant CRT is not sufficient to dictate cellular immunogenicity and induce DC maturation [23]. Although decisive for uptake, CRT does not provide maturation signals, which have to come from other cellular factors. CDDP-treatment of tumor cells *in vitro,* indirectly induces DC maturation, through the stimulatory activity of DAMPs, such as HMGB1 [24,25]. The binding of HMGB1 to its receptor, TLR4, seems to modulate DC function by inhibiting processing of tumor-antigens. Thus, *tlr4*$^{-/-}$ DCs fail to perform cross presentation to CD8^{+} T cells, *in vivo* [21]. Interestingly, absence of TLR4 does not affect expression of co-stimulatory molecule on DCs in response to HMGB1 stimulation. This suggests that additional locks might match the same key to unlocking phenotypical DC maturation [21,25].

In other words, if the delivery of three different types of 'danger' signals (recruitment, engulfment, activation) is undoubtedly required for DC activation, there seem to be multiple 'key-lock combinations' that may act in concert to induce effective anti-tumor responses. In Chapter 2 we show that addition of blocking antibodies directed against CRT significantly reduced dying tumor-cell uptake by myeloid DCs. However, blockade of the most described CRT receptor, CD91, failed to impair tumor cell engulfment; pointing to the existence of additional players for CRT recognition. Previous studies indicated the scavenger receptor class-A (SR-A, also known as CD204) and the scavenger receptor expressed by endothelial cell-1 (SREC-I) as additional CRT-receptors. However, it must be noted the evidence is limited to a small number of observations, mostly based on competition studies that showed that binding of soluble CRT to APCs was efficiently competed by the addition of the scavenger receptor ligand, fucoidan [26,27]. In addition, recombinant expression of SREC-I in macrophages augmented recognition of CRT, further supporting SREC-I function in ecto-CRT binding [27]. Our microarray analysis on primary DCs revealed differences in expression levels for SR-A and SREC-I between DC subsets. Both receptors, show high expression on human CD1c^{+} DCs while the expression on CD16^{+} DCs and pDCs is much lower. Although different receptors have been proposed to bind ecto-CRT, the actual contribution of each receptor to apoptotic cell engulfment have not yet been fully elucidated.

Human innate effector cells in ICD

Although many of the molecular characteristics that define immunogenic key-lock systems are being identified, our understanding at the level of the responding innate effectors, such as phagocytes, is still far from complete. This is due to the fact that, evidence of central role of DCs as main mediators of ICD is mostly based on studies performed with murine APCs or with human monocytes or moDCs. The findings presented in Chapter 2 propose, for the first time that, in the context of platinum-induced ICD, induction of a T cell response relies on the critical contribution of certain DC subsets. In fact, we show that $CD1c^+$ DCs are more efficient than $CD16^+$ DCs and pDCs in stimulating ICD-mediated T cell proliferation. Further investigation should include studies on other naturally occurring DC subsets in humans, including tissue-resident and other blood circulating DCs. $CD141^+$ DCs in humans and its murine equivalent $CD8\alpha^+$ DCs were described to be endowed with potent ability to prime tumor antigen specific immune responses [28,29,30]. Hence, it would be crucial to also understand the role of this DC population in ICD-responses. Unveiling the molecular pathways, activated upon engagement of receptors on DCs by ICD-DAMPs, is pivotal to understand whether these key-lock interactions can be exploited to increase the efficacy of immunogenic inducers, and to develop new strategies for cancer therapy.

CD47 in the tumor microenvironment limits anti-tumor immunity

Initially described as a regulator of cell clearance in physiological conditions for circulating erythrocytes, CD47 was soon reported to be widely expressed on nearly every cell type in the body and, most intriguingly, to be markedly upregulated on malignant cells [31]. It became clear that overexpression of CD47 on tumor cells delivers an inhibitory message to both innate and adaptive immune cells, with the final effect of weakening the host immune system against cancer. Hence, CD47 is considered an adverse prognostic factor. Accordingly, analysis of immune infiltrate in mice revealed that high expression of CD47 in the TME is inversely correlated with T cell infiltrates; whereas blockade of CD47 enhances $CD8^+$ T cell migration in the tumor and subsequently augments T cell-dependent, intra-tumoral granzyme B activity that induces death of malignant cells [32].

CD47 on tumor cells

The most studied role of CD47 is linked to its ability to regulate immune evasion. Thus, blockade of CD47 *in vivo* restored macrophage-mediated immune surveillance, by reducing the ability of CD47 on tumor cells to engage SIRPα

on tumor-associated macrophages [33]. Both *in vitro* and *in vivo* studies provided evidence that CD47/SIRPα pathway has a negative effect on uptake by APCs [34-36]. As discussed in **Chapter 3**, CD47 on melanoma cells blocks uptake of tumor material by human macrophages, moDCs and the naturally-occurring DC subset, $CD1c^+$ DCs and subsequently inhibits DC maturation and expression of co-stimulatory molecules. We therefore investigated the effect of CD47 blockade in co-cultures of tumor cells and DCs. Analysis of phagocytosis, by both flow cytometry and fluorescence microscopy, showed that addition of the anti-CD47 blocking antibody B6H12, yielded significant increase of uptake relative to IgG control or non-blocking anti-CD47 antibody, 2D3. Similarly to what we observed during time-lapse imaging of the reconstructed melanoma microenvironment (**Chapter 4**), DCs do not take up whole tumor cells, but rather engulf tumor particles. Besides impairing DC maturation, ligation of SIRPα with CD47-Fc fusion protein was shown to abrogate the migration of murine Langerhans cells (LCs) *in vivo* and *in vitro,* in response to inflammatory stimuli [37]. Moreover, it is proposed that, the downstream inhibitory signaling delivered to macrophages or DCs via SIRPα engagement, induces the formation of "giant cells", generated by the fusion of the tumor cell with phagocyte. As described for melanoma cells fused with macrophages, this cell-to-cell fusion may favor tumor dissemination and metastasis [38]. Although this mechanism remains controversial for the lack of proof of concept *in vivo*, it is certainly intriguing and may be not be completely excluded.

One of the additional names by which we identify CD47 is "integrin-associated protein (IAP)". CD47 was initially shown to associate with α-integrins (in particular $\alpha_3\beta_V$) and together regulate neutrophil transmigration through the endothelium, during inflammatory responses [39]. Likewise, CD47 on lymphoma cells stimulates malignant cell migration through a tight cooperation with $\alpha_4\beta_1$ integrins [40]. Accordingly, the $\alpha_V\beta_3$ integrin (vitronectin receptor)-dependent migration of melanoma, prostate cancer and ovarian cancer cells was markedly reduced by the addition of neutralizing antibodies against CD47 [41].

The first identified endogenous ligand for CD47 was thrombospondin-1 (TSP-1). TSP-1 is a calcium binding protein and participates in multiple biological processes [42]. High levels of TSP-1 are commonly found in stromal fibroblasts and endothelial cells within tumors [43,44]. Binding of TSP-1 to CD47 induces activation of the downstream signaling pathway PI3K/Akt, which has been reported either to induce apoptosis or to enhance proliferation and survival of malignant astrocytoma cells [45,46]. These observations are somewhat paradoxical and thus far, the molecular basis of CD47-induced programmed cell death/survival are not fully understood. Further investigation on the mechanisms regulating therapeutic resistance in cancer cells, suggested that TSP-1/CD47 interaction may (either directly or indirectly)

mediate tumor sensitivity to anti-cancer therapy. In human prostate cancer or gastric cancer cells, activation of the drug-resistance gene, taxol-resistant gene 1 (Txr1) and expression of Txr1 protein, dramatically down-regulated TSP-1. Lack of TSP-1 in turn, conferred resistance to taxol and OXP [47]. Indication of the involvement of CD47 signalling was given by stimulation of CD47 with exogenous administration of TSP-1 or anti-CD47 moAbs, reverting drug resistance and increasing cellular sensitivity to taxanes [47].

CD47 on immune cells

Professional APCs, such as monocytes, macrophages and DCs, co-express SIRPα and CD47. Therefore, in a complex cellular environment as found within the TME, APCs can be stimulated either by SIRPa-engagement (blocking of phagocytosis and inhibition of DC maturation and migration), or by CD47-binding to its cognate receptors and ligands.

Expression of CD47 on DCs mediates a series of complex – yet not fully understood – cellular mechanisms that regulate DC activation and migration. Blocking of CD47 on murine LCs suppressed the expression of CD80 and CD86, and significantly affected migration of LCs from the epidermis into the draining lymphnode, following treatment with the proinflammatory cytokine TNF-α [48] Accordingly, absence of CD47 on myeloid DCs of skin in mice, impaired skin DC migration, trafficking to secondary lymphoid organs and T-cell priming, both at steady state and under inflammatory conditions [49,50] Altogether, these observations suggest that CD47 expression is required on DCs for efficient DC trafficking.

By contrast, CD47 may also reduce the efficacy of immune responses by inducing tolerance towards the tumor. In particular, activation of CD47, by tumor-secreted TSP-1 or anti-C47 moAbs, inhibits DC maturation and function, observed as down-modulation MHC molecules and co-stimulatory molecules, inhibition of pro-inflammatory cytokine (IL12, TNFα and IL6) secretion and impaired T- cell stimulation by DCs [50]. Moreover, it seems that CD47 stimulation may induce clearance of DCs by triggering programmed cell death [51].

CD47 expression was also reported on T cells where, upon binding of TSP-1, it serves as a self-control negative regulator of inflammation and activation of Th1 responses [52,53]. This effect seems to be in part dependent on the inhibition of the autocrine activating function of hydrogen sulfide signaling in T cells [54-56]. As a result, T cells become hyporesponsive or anergic [57]. Additionally, CD47/TSP signaling triggers the conversion of naïve or memory $CD4^+CD25^+$ T cells into regulatory T cells (Tregs) in response to inflammation [58]. Moreover, TSP-1/CD47 interaction on T cells has been described to cause profound inhibition of the nitric oxide/cGMP signaling, which in turn regulates several death/survival pathways [59].

In conclusion, given the broad expression of CD47 and its role in regulating multiple cellular processes, it represents a potential target for therapeutic blockade in cancer patients. In fact, treatment with CD47 blocking antibodies, which can inhibit both SIRPα and TSP1 binding to CD47, could directly modulate innate as well as adaptive anti-tumor immunity.

Combining immunotherapy with strategies that increase tumor immunogenicity

Phagocytosis requires the coordinated expression of "eat me" signals and disruption of "don't eat me" signals. In **Chapter 3** we exploited the possibility of inducing immunogenic pro-phagocytic signals (such as CRT), while blocking the most potent anti-phagocytic signal described to date, CD47. We show that either addition of anti-CD47 moAbs to live cells or platinum treatment alone enhanced tumor uptake by DCs. However, combining chemotherapy with CD47 blockade did not potentiate phagocytosis. Many factors might be responsible for the lack of a synergistic effect. The significant ICD-induced upregulation of surface CRT might dominate over the targeting of CD47 with blocking antibodies, which may in turn be insufficient to warrant induction of cellular engulfment. A second possible explanation may be that, upon induction of apoptosis, CD47 alters its plasma membrane distribution. In particular, CD47 on dying cells redistributes into patches that were described to decrease its ability to engage SIRPα [60]. Additionally, in situ competition with other CD47 ligands, such as integrins or TSP-1, might compromise CD47 availability for the binding of blocking moAbs.

In this regard, it is worth mentioning that upon ICD induction, TSP-1 is actively secreted into the extracellular matrix, where it serves as an "eat me" signal, in addition to CRT. TSP-1 functions as a bridging molecule between apoptotic and phagocytic cells. In particular, TSP-1 binds to APCs via the multi-molecular, TSP-1/CD36/αv-integrins (αvβ3 or αvβ5) complex and triggers the formation of protein complexes that increase APC phagocytic ability. [61-64]. In support of these findings, blockade of any one of the elements involved in the TSP-1/CD36/$\alpha_v\beta_3$ complex, resulted in abrogated phagocytosis of dying cells by human macrophages[62,63].

Despite the lack of a synergistic effect between ICD and CD47 blockade on tumor cell uptake by $CD1c^+$ DCs, we reported a potential effect on DC maturation when chemotherapy was administered before anti-CD47 blocking antibodies. In support of our observation, *in vivo* administration of chemotherapy before, but not after, treatment with anti-CD47 moAbs promoted tumor cell death, which in turn enhanced engulfment of tumor cells by APCs and enabled processing and cross-presentation of tumor antigens to $CD8^+$ T cells. Interestingly, this study underscored

the fact that cross-prime of cytotoxic T cells, in the presence of CD47 blocking agents and chemotherapy-treatment, was almost exclusively depended on DCs rather than macrophages [65].

In this thesis, we have extensively discussed the ability of chemotherapeutic drugs to induce ICD. Additionally, other therapeutic modalities, including radiation therapy, have been reported to act as ICD inducers, and showed therapeutic potential in combination with CD47 blockade [7]. In particular, blockade of CD47 or its deficiency, in combination with ionizing radiation (IR) resulted in increased radiation sensitivity of implanted melanoma or squamous carcinoma cells, which eventually caused delay in tumor growth, *in vivo*. This effect was associated with enhanced blood flow, improved tumor oxygenation and increased infiltration of cytotoxic lymphocytes [66,67]. Moreover, CD47 blockade seems to provide radioprotection of normal soft tissue, bone marrow and tumor-infiltrating leukocytes, by activation of pro-survival mechanisms regulating autophagy [67]. In other words, while immunogenic apoptosis, as a result of chemo- or radiation therapy, is an important contributor of anticancer immune responses; the combination of ICD induction with moAbs, targeting malignant cells, may further increase the therapeutic effect of these strategies. Thus, if further investigation confirms safety for host cells in the tumor stroma, in combination with damage to tumor cells caused by treatment, this approach may shed light on new complementary combination strategies for future trials.

Modelling cancer in 3D

Albeit informative for basic aspects of cancer biology, two-dimensional (2D) culture systems are a poor copy of the *in vivo* cellular environment, as they do not accurately mimic the meshwork of human tissues. *In vivo,* cells face complex and structurally heterogeneous 3D tissue architectures and are exposed to a multitude of cellular and extracellular matrix (ECM) parameters, which influence tumor growth and the ability of stromal and immune cells to orchestrate immune responses locally. Chapter 4 presents an *in vitro* 3D organotypic skin model of melanoma, which will serve as a model of malignancy to deepen our understanding of the drivers of cancer and immune evasion.

Three exciting facets summarize the potential of our *in vitro* 3D model for tumor-immunology research. Firstly, the ability of ensuring the correct geometry and spatial distribution of cells. Secondly, the capacity to experimentally manipulate each component of the TME. Thirdly, the possibility to investigate normal and malignant cell regulation within the local TME, and how this changes during cancer related inflammation as opposed to steady state.

Possibilities and challenges

Tumor growth and dissemination

Tumor cell invasion into adjacent tissues is a key step of cancer dissemination that leads to metastases. 3D cancer models offer the unique possibility to investigate such processes, which would be otherwise impossible in conventional cell cultures. Melanoma cell lines, obtained from different stages of tumor progression, show characteristic invasive behavior when cultured in 3D skin reconstructs. Thus, cells derived from radial growth phase (RGP) lesions, characterized by limited invasiveness, form nests in the epidermis and leave the BM intact; whereas cells from vertical growth phase (VGP) invade the dermal compartment [68,69]. Researchers have also shown that dermal invasion, mediated by the proteolytic activity of matrix metalloproteinases (MMPs), is strictly dependent on the interaction of melanoma cells with keratinocytes [70]. Metastatic melanoma cell lines, unable to degrade the BM and migrate through the dermis when cultured alone on DEDs, actively invaded in the presence of adjacent normal epidermal cells. In our model, we tested the growth behaviors of a panel of established metastatic melanoma cell lines. Interestingly we observed that the BLM melanoma cell line formed tumor nests at the epidermal-dermal junction and invaded the dermis mostly as single cells; while a distinct cell line, Mel-624, proliferated forming larger and more compact groups of cells and invaded as a bulk of malignant cells (data not shown).

Conventional anti-cancer therapy

Organotypic cancer models are valuable platforms to unravel mechanisms of resistance to targeted anti-cancer therapies. Studies have shown that growing cells in 3D confers resistance to chemotherapy, as compared to cells grown in 2D monolayers. One of the possible reasons is that the drug penetration through multicellular structures is heterogeneous. The quiescent population sequestered on the inside of the cellular cluster is less exposed to the drug than the cells on the outside of the cluster and will likely remain protected from the drug. If therapy is halted too early, these protected cells may be able to re-enter the cell cycle and recapitulate a tumor that was shrunk but not completely killed [71-73]. In addition to this, 3D cell cultures profoundly affect gene expression and likely influence regulation of genes involved in drug resistance [74]. Hence, 3D models offer the opportunity to validate multi-drug therapy regimens *in vitro,* before proceeding to pre-clinical testing and ultimately clinical trials. This may greatly improve the understanding of cancer biology, eliminate poor drug candidates and reveal new physiologically relevant targets that might have been missed in 2D studies. Surely, there are certain aspects of efficacy and toxicity that will always require evaluation in animal models prior to human clinical trials.

In this view, investigation of ICD-related mechanisms, induced by chemotherapy or radiation therapy, may greatly benefit from a 3D approach that includes tumor, stromal and immune compartments. We attempted to exploit this aspect and performed preliminary experiments to test whether chemotherapy treatment would affect skin morphology and tumor growth. We observed that increasing drug dosage and treatment duration augments cancer cell death, preeminently in compact tumor clusters, without dramatically disturbing normal tissue cells (data not shown). *In vivo* studies reported that DAMP release upon CDDP treatment favored the intra-tumor recruitment of inflammatory APCs (macrophages and DCs) [22,75]. Therefore, it would be of particular relevance using our model to evaluate the effect of ICD on the local environment (that includes not only immune cells, but also epidermal cells and fibroblasts), in order to understand how this influences DC responses.

Immunotherapy targeting cellular checkpoints

In Chapter 4 we showed that DCs encounter tumor cells, sense their presence and efficiently take up tumor material. This process may likely influence their phenotype and activation status, as suggested by our co-culture experiments performed in conventional 2D cultures (described in Chapter 3). Conceivably, the local TME also plays a role in shaping DC behavior. Thus, as a desirable follow-up it would be to crucial to confirm our 2D data in a more complex 3D system. Next, we may further explore the addition of moAbs targeting inhibitory molecules on tumor cells, such as the "don't eat me" signal CD47. Alternatively, we could exploit the use of newly developed moAbs targeting the CD47 receptor, SIRPα on DCs [76]. Because CD47 is a ubiquitous molecule, broadly expressed on non-malignant and malignant cells, targeting SIRPα in our 3D model might be more informative than employing moAbs against CD47. This would provide deeper understanding of the role of CD47-SIRPα interactions in the context of DC function.

The 3D skin melanoma model, as presented in this thesis, was generated using a combination of primary human factors (dermis, KCs, Fbs, DCs) and cell lines (melanoma cell lines). This seems comprehensible as the primary goal of our study was to prove feasibility, reproducibility and applicability of the 3D tissue reconstruction into distinct aspects of cancer research. Nevertheless, our 3D organotypic model may also become a useful tool to study tumor-associated effects on the adaptive immune system. The integration of adaptive immune cells within a reconstructed TME requires extra care, particularly in the context of human leukocyte antigen (HLA) matching. For this reason, during the time of completion of this thesis, we have been exploring the possibility of taking the model to the next level and attempted to inoculate tumor and stromal components derived from tumor biopsies. This will be followed by the addition of immune cells, isolated from the same patient. The

model may therefore become extremely relevant to investigate mechanisms that regulate checkpoint inhibition by immunotherapy, such as those related to the use of anti-CTLA-4 or anti-PD-1 moAbs in melanoma treatment.

Discovery of new biomarkers for immunotherapy

T cell-mediated anti-tumor immunity can be exploited therapeutically in several ways, including cell-based immunotherapy (such as DC vaccination strategies and adoptive T cell transfer) and antibody-based immunotherapy (such as anti-CTLA-4 or anti-PD-1). These therapeutic approaches have shown significant success in a number of patients. However, we still do not understand why some patients respond very well to immunotherapy, while others do not. The discovery of cellular and molecular biomarkers that can predict clinical benefit of distinct anti-tumor therapies is, therefore, a crucial need. As recently reported by our group, accurate analysis of density and distribution of T cell infiltrates in primary melanomas, assessed by the multispectral imaging approach presented in **Chapter 5**, can be a potential biomarker for treatment selection. In particular, the presence of large numbers of $CD3^+$ T cells inside the primary tumor, as compared to peritumoral regions, correlates with long survival of metastatic melanoma patients who received DC vaccination, even several years after primary tumor resection [77]. As mentioned earlier in this thesis, the fate of clinical efficacy of anti-cancer treatments can be mostly attributed to a complex - yet not fully understood - TME. By supporting a heterogeneous growth of cells in 3D and offering the possibility to manipulate the local tumor environment, our organotypic model of melanoma could be used to explore the role of key cellular and molecular components that determine the induction of anti-tumor immunity. This will greatly contribute to our growing knowledge about the TME, and especially how it can be manipulated in a therapeutic setting, ultimately supporting future biomarker identification for personalized anti-cancer therapy.

References

1. Vonderheide, R. H. CD47 blockade as another immune checkpoint therapy for cancer. *Nat Med* **21**, 1122-1123, doi:10.1038/nm.3965 (2015).
2. Chao, M. P., Majeti, R. & Weissman, I. L. Programmed cell removal: a new obstacle in the road to developing cancer. *Nat Rev Cancer* **12**, 58-67 (2012).
3. Chao, M. P. *et al.* Calreticulin is the dominant pro-phagocytic signal on multiple human cancers and is counterbalanced by CD47. *Science translational medicine* **2**, 63ra94, doi:10.1126/scitranslmed.3001375 (2010).
4. Kanduc, D. *et al.* Cell death: Apoptosis versus necrosis (Review). *Int J Oncol* **21**, 165-170 (2012).
5. Green, D. R., Ferguson, T., Zitvogel, L. & Kroemer, G. IMMUNOGENIC AND TOLEROGENIC CELL DEATH. *Nature reviews. Immunology* **9**, 353, doi:10.1038/nri2545 (2009).
6. Krysko, D. V. *et al.* Immunogenic cell death and DAMPs in cancer therapy. *Nat Rev Cancer* **12**, 860-875, doi:http://www.nature.com/nrc/journal/v12/n12/suppinfo/nrc3380_S1.html (2012).
7. Inoue, H. & Tani, K. Multimodal immunogenic cancer cell death as a consequence of anticancer cytotoxic treatments. *Cell death and differentiation* **21**, 39-49, doi:10.1038/cdd.2013.84 (2014).
8. Hato, S. V., Khong, A., de Vries, I. J. & Lesterhuis, W. J. Molecular pathways: the immunogenic effects of platinum-based chemotherapeutics. *Clinical cancer research : an official journal of the American Association for Cancer Research* **20**, 2831-2837, doi:10.1158/1078-0432.ccr-13-3141 (2014).
9. Casares, N. *et al.* Caspase-dependent immunogenicity of doxorubicin-induced tumor cell death. *The Journal of Experimental Medicine* **202**, 1691-1701, doi:10.1084/jem.20050915 (2005).
10. Tesniere, A. *et al.* Immunogenic death of colon cancer cells treated with oxaliplatin. *Oncogene* **29**, 482-491, doi:http://www.nature.com/onc/journal/v29/n4/suppinfo/onc2009356s1.html (2009).
11. Zitvogel, L., Galluzzi, L., Smyth, Mark J. & Kroemer, G. Mechanism of Action of Conventional and Targeted Anticancer Therapies: Reinstating Immunosurveillance. *Immunity* **39**, 74-88, doi:http://dx.doi.org/10.1016/j.immuni.2013.06.014 (2013).
12. Kroemer, G., Galluzzi, L., Kepp, O. & Zitvogel, L. Immunogenic cell death in cancer therapy. *Annual review of immunology* **31**, 51-72, doi:10.1146/annurev-immunol-032712-100008 (2013).
13. Schiavoni, G. *et al.* Cyclophosphamide Synergizes with Type I Interferons through Systemic Dendritic Cell Reactivation and Induction of Immunogenic Tumor Apoptosis. *Cancer Research* **71**, 768 (2011).
14. Sano, R. & Reed, J. C. ER stress-induced cell death mechanisms. *Biochimica et biophysica acta* **1833**, 10.1016/j.bbamcr.2013.1006.1028, doi:10.1016/j.bbamcr.2013.06.028 (2013).
15. Xu, C., Bailly-Maitre, B. & Reed, J. C. Endoplasmic reticulum stress: cell life and death decisions. *Journal of Clinical Investigation* **115**, 2656-2664, doi:10.1172/JCI26373 (2005).
16. Martins, I. *et al.* Restoration of the immunogenicity of cisplatin-induced cancer cell death by endoplasmic reticulum stress. *Oncogene* **30**, 1147-1158, doi:http://www.nature.com/onc/journal/v30/n10/suppinfo/onc2010500s1.html (2011).
17. Bezu, L. *et al.* Combinatorial Strategies for the Induction of Immunogenic Cell Death. *Frontiers in Immunology* **6**, 187, doi:10.3389/fimmu.2015.00187 (2015).

18. Sukkurwala, A. Q. *et al.* Immunogenic calreticulin exposure occurs through a phylogenetically conserved stress pathway involving the chemokine CXCL8. *Cell Death Differ* **21**, 59-68, doi:10.1038/cdd.2013.73 (2014).
19. Panaretakis, T. *et al.* The co-translocation of ERp57 and calreticulin determines the immunogenicity of cell death. *Cell Death Differ* **15**, 1499-1509, doi:http://www.nature.com/cdd/journal/v15/n9/suppinfo/cdd200867s1.html (2008).
20. Tesniere, A. *et al.* Immunogenic cancer cell death: a key-lock paradigm. *Current Opinion in Immunology* **20**, 504-511, doi:http://dx.doi.org/10.1016/j.coi.2008.05.007 (2008).
21. Apetoh, L. *et al.* Toll-like receptor 4-dependent contribution of the immune system to anticancer chemotherapy and radiotherapy. *Nat Med* **13**, 1050-1059, doi:10.1038/nm1622 (2007).
22. Beyranvand Nejad, E. *et al.* Tumor Eradication by Cisplatin Is Sustained by CD80/86-Mediated Costimulation of CD8⁺ T Cells. *Cancer Research* **76**, 6017 (2016).
23. Bak, S. P., Amiel, E., Walters, J. J. & Berwin, B. CALRETICULIN REQUIRES AN ANCILLARY ADJUVANT FOR THE INDUCTION OF EFFICIENT CYTOTOXIC T CELL RESPONSES. *Molecular immunology* **45**, 1414-1423, doi:10.1016/j.molimm.2007.08.020 (2008).
24. Di Blasio, S. *et al.* Human CD1c(+) DCs are critical cellular mediators of immune responses induced by immunogenic cell death. *Oncoimmunology* **5**, e1192739, doi:10.1080/2162402X.2016.1192739 (2016).
25. Beyranvand Nejad, E. *et al.* http://www.w3.org/1999/xhtml">Tumor Eradication by Cisplatin Is Sustained by CD80/86-Mediated Costimulation of CD8⁺ T Cells</div&gt. *Cancer Research* **76**, 6017 (2016).
26. Berwin, B. *et al.* Scavenger receptor-A mediates gp96/GRP94 and calreticulin internalization by antigen-presenting cells. *The EMBO journal* **22**, 6127-6136, doi:10.1093/emboj/cdg572 (2003).
27. Berwin, B., Delneste, Y., Lovingood, R. V., Post, S. R. & Pizzo, S. V. SREC-I, a Type F Scavenger Receptor, Is an Endocytic Receptor for Calreticulin. *Journal of Biological Chemistry* **279**, 51250-51257, doi:10.1074/jbc.M406202200 (2004).
28. Tel, J. *et al.* Human plasmacytoid dendritic cells efficiently cross-present exogenous Ags to CD8+ T cells despite lower Ag uptake than myeloid dendritic cell subsets. *Blood* **121**, 459-467, doi:10.1182/blood-2012-06-435644 (2013).
29. Broz, M. *et al.* Dissecting the Tumor Myeloid Compartment Reveals Rare Activating Antigen Presenting Cells, Critical for T cell Immunity. *Cancer cell* **26**, 638-652, doi:10.1016/j.ccell.2014.09.007 (2014).
30. Bracci, L., Schiavoni, G., Sistigu, A. & Belardelli, F. Immune-based mechanisms of cytotoxic chemotherapy: implications for the design of novel and rationale-based combined treatments against cancer. *Cell Death and Differentiation* **21**, 15-25, doi:10.1038/cdd.2013.67 (2014).
31. Olsson, M., Bruhns, P., Frazier, W. A., Ravetch, J. V. & Oldenborg, P.-A. Platelet homeostasis is regulated by platelet expression of CD47 under normal conditions and in passive immune thrombocytopenia. *Blood* **105**, 3577-3582, doi:10.1182/blood-2004-08-2980 (2005).
32. Soto-Pantoja, D. R. *et al.* CD47 in the tumor microenvironment limits cooperation between anti-tumor T cell immunity and radiation therapy. *Cancer research* **74**, 6771-6783, doi:10.1158/0008-5472.CAN-14-0037-T (2014).
33. Tseng, D. *et al.* Anti-CD47 antibody–mediated phagocytosis of cancer by macrophages primes an effective antitumor T-cell response. *Proceedings of the National Academy of*

Sciences of the United States of America **110**, 11103-11108, doi:10.1073/pnas.1305569110 (2013).
34. Barclay, A. N. & van den Berg, T. K. The Interaction Between Signal Regulatory Protein Alpha (SIRPα) and CD47: Structure, Function, and Therapeutic Target. *Annual Review of Immunology* **32**, 25-50, doi:10.1146/annurev-immunol-032713-120142 (2014).
35. Willingham, S. B. *et al.* The CD47-signal regulatory protein alpha (SIRPa) interaction is a therapeutic target for human solid tumors. *Proceedings of the National Academy of Sciences of the United States of America* **109**, 6662-6667, doi:10.1073/pnas.1121623109 (2012).
36. Oldenborg, P.-A. CD47: A Cell Surface Glycoprotein Which Regulates Multiple Functions of Hematopoietic Cells in Health and Disease. *ISRN Hematology* **2013**, 614619, doi:10.1155/2013/614619 (2013).
37. Fukunaga, A. *et al.* Src Homology 2 Domain-Containing Protein Tyrosine Phosphatase Substrate 1 Regulates the Migration of Langerhans Cells from the Epidermis to Draining Lymph Nodes. *The Journal of Immunology* **172**, 4091-4099, doi:10.4049/jimmunol.172.7.4091 (2004).
38. Pawelek, J. M. Viewing Malignant Melanoma Cells as Macrophage-Tumor Hybrids. *Cell Adhesion & Migration* **1**, 2-6 (2007).
39. Liu, Y. *et al.* The Role of CD47 in Neutrophil Transmigration: INCREASED RATE OF MIGRATION CORRELATES WITH INCREASED CELL SURFACE EXPRESSION OF CD47. *Journal of Biological Chemistry* **276**, 40156-40166, doi:10.1074/jbc.M104138200 (2001).
40. Yoshida, H. *et al.* Integrin-associated protein/CD47 regulates motile activity in human B-cell lines through CDC42. *Blood* **96**, 234 (2000).
41. Shahan, T. A., Fawzi, A., Bellon, G., Monboisse, J.-C. & Kefalides, N. A. Regulation of Tumor Cell Chemotaxis by Type IV Collagen Is Mediated by a Ca2+-dependent Mechanism Requiring CD47 and the Integrin αVβ3. *Journal of Biological Chemistry* **275**, 4796-4802, doi:10.1074/jbc.275.7.4796 (2000).
42. Magnetto, S. *et al.* CD36 mediates binding of soluble thrombospondin-1 but not cell adhesion and haptotaxis on immobilized thrombospondin-1. *Cell Biochemistry and Function* **16**, 211-221, doi:10.1002/(SICI)1099-0844(199809)16:3<211::AID-CBF788>3.0.CO;2-Z (1998).
43. Streit, M. *et al.* Overexpression of Thrombospondin-1 Decreases Angiogenesis and Inhibits the Growth of Human Cutaneous Squamous Cell Carcinomas. *The American Journal of Pathology* **155**, 441-452 (1999).
44. Hawighorst, T. *et al.* Thrombospondin-2 plays a protective role in multistep carcinogenesis: a novel host anti-tumor defense mechanism. *The EMBO journal* **20**, 2631 (2001).
45. Rath, G. M. *et al.* Thrombospondin-1 C-terminal-derived peptide protects thyroid cells from ceramide-induced apoptosis through the adenylyl cyclase pathway. *The International Journal of Biochemistry & Cell Biology* **38**, 2219-2228, doi:http://dx.doi.org/10.1016/j.biocel.2006.07.004 (2006).
46. Sick, E. *et al.* Activation of CD47 receptors causes proliferation of human astrocytoma but not normal astrocytes via an Akt-dependent pathway. *Glia* **59**, 308-319, doi:10.1002/glia.21102 (2011).
47. Lih, C.-J., Wei, W. & Cohen, S. N. Txr1: a transcriptional regulator of thrombospondin-1 that modulates cellular sensitivity to taxanes. *Genes & Development* **20**, 2082-2095, doi:10.1101/gad.1441306 (2006).
48. Yu, X. *et al.* Engagement of CD47 Inhibits the Contact Hypersensitivity Response Via the Suppression of Motility and B7 Expression by Langerhans Cells. *Journal of Investigative Dermatology* **126**, 797-807, doi:http://dx.doi.org/10.1038/sj.jid.5700176 (2006).

49. Van, V. Q. *et al.* Expression of the self-marker CD47 on dendritic cells governs their trafficking to secondary lymphoid organs. *The EMBO journal* **25**, 5560-5568, doi:10.1038/sj.emboj.7601415 (2006).
50. Demeure, C. E. *et al.* CD47 Engagement Inhibits Cytokine Production and Maturation of Human Dendritic Cells. *The Journal of Immunology* **164**, 2193-2199, doi:10.4049/jimmunol.164.4.2193 (2000).
51. Johansson, U. & Londei, M. Ligation of CD47 During Monocyte Differentiation into Dendritic Cells Results in Reduced Capacity for Interleukin-12 Production. *Scandinavian Journal of Immunology* **59**, 50-57, doi:10.1111/j.0300-9475.2004.01354.x (2004).
52. Bouguermouh, S. *et al.* CD47 Expression on T Cell Is a Self-Control Negative Regulator of Type 1 Immune Response. *The Journal of Immunology* **180**, 8073-8082, doi:10.4049/jimmunol.180.12.8073 (2008).
53. Lamy, L. *et al.* Interactions between CD47 and Thrombospondin Reduce Inflammation. *The Journal of Immunology* **178**, 5930-5939, doi:10.4049/jimmunol.178.9.5930 (2007).
54. Li, Z., He, L., Wilson, K. E. & Roberts, D. D. Thrombospondin-1 Inhibits TCR-Mediated T Lymphocyte Early Activation. *The Journal of Immunology* **166**, 2427-2436, doi:10.4049/jimmunol.166.4.2427 (2001).
55. Kaur, S. *et al.* Heparan Sulfate Modification of the Transmembrane Receptor CD47 Is Necessary for Inhibition of T Cell Receptor Signaling by Thrombospondin-1. *The Journal of biological chemistry* **286**, 14991-15002, doi:10.1074/jbc.M110.179663 (2011).
56. Miller, T. W., Kaur, S., Ivins-O'Keefe, K. & Roberts, D. D. Thrombospondin-1 is a CD47-dependent endogenous inhibitor of hydrogen sulfide signaling in T cell activation. *Matrix biology : journal of the International Society for Matrix Biology* **32**, 316-324, doi:10.1016/j.matbio.2013.02.009 (2013).
57. Avice, M.-N., Rubio, M., Sergerie, M., Delespesse, G. & Sarfati, M. Role of CD47 in the Induction of Human Naive T Cell Anergy. *The Journal of Immunology* **167**, 2459-2468, doi:10.4049/jimmunol.167.5.2459 (2001).
58. Grimbert, P. *et al.* Thrombospondin/CD47 Interaction: A Pathway to Generate Regulatory T Cells from Human CD4+CD25− T Cells in Response to Inflammation. *The Journal of Immunology* **177**, 3534-3541, doi:10.4049/jimmunol.177.6.3534 (2006).
59. Isenberg, J. S. *et al.* CD47 Is Necessary for Inhibition of Nitric Oxide-stimulated Vascular Cell Responses by Thrombospondin-1. *Journal of Biological Chemistry* **281**, 26069-26080, doi:10.1074/jbc.M605040200 (2006).
60. Gardai, S. J. *et al.* Cell-surface calreticulin initiates clearance of viable or apoptotic cells through trans-activation of LRP on the phagocyte. *Cell* **123**, 321-334, doi:10.1016/j.cell.2005.08.032 (2005).
61. Fadok, V. A., Warner, M. L., Bratton, D. L. & Henson, P. M. CD36 Is Required for Phagocytosis of Apoptotic Cells by Human Macrophages That Use Either a Phosphatidylserine Receptor or the Vitronectin Receptor (αvβ3). *The Journal of Immunology* **161**, 6250-6257 (1998).
62. Savill, J., Dransfield, I., Hogg, N. & Haslett, C. Vitronectin receptor-mediated phagocytosis of cells undergoing apoptosis. *Nature* **343**, 170-173 (1990).
63. Moodley, Y. *et al.* Macrophage Recognition and Phagocytosis of Apoptotic Fibroblasts Is Critically Dependent on Fibroblast-Derived Thrombospondin 1 and CD36. *The American Journal of Pathology* **162**, 771-779, doi:http://dx.doi.org/10.1016/S0002-9440(10)63874-6 (2003).

64. Krispin, A. *et al.* Apoptotic cell thrombospondin-1 and heparin-binding domain lead to dendritic-cell phagocytic and tolerizing states. *Blood* **108**, 3580-3589, doi:10.1182/blood-2006-03-013334 (2006).
65. Liu, Y. & Cao, X. Intratumoral dendritic cells in the anti-tumor immune response. *Cell Mol Immunol* **12**, 387-390, doi:10.1038/cmi.2014.130 (2015).
66. Maxhimer, J. B. *et al.* Radioprotection in Normal Tissue and Delayed Tumor Growth by Blockade of CD47 Signaling. *Science translational medicine* **1**, 3ra7-3ra7, doi:10.1126/scitranslmed.3000139 (2009).
67. Soto-Pantoja, D. R. *et al.* CD47 deficiency confers cell and tissue radioprotection by activation of autophagy. *Autophagy* **8**, 1628-1642, doi:10.4161/auto.21562 (2012).
68. Meier, F. *et al.* Human Melanoma Progression in Skin Reconstructs : Biological Significance of bFGF. *The American Journal of Pathology* **156**, 193-200 (2000).
69. Eves, P. *et al.* Melanoma invasion in reconstructed human skin is influenced by skin cells – investigation of the role of proteolytic enzymes. *Clinical & Experimental Metastasis* **20**, 685-700, doi:10.1023/B:CLIN.0000006824.41376.b0 (2003).
70. Van Kilsdonk, J. W. J., Bergers, M., Van Kempen, L. C. L. T., Schalkwijk, J. & Swart, G. W. M. Keratinocytes drive melanoma invasion in a reconstructed skin model. *Melanoma Research* **20**, 372-380, doi:10.1097/CMR.0b013e32833d8d70 (2010).
71. Perche, F. & Torchilin, V. P. Cancer cell spheroids as a model to evaluate chemotherapy protocols. *Cancer Biology & Therapy* **13**, 1205-1213, doi:10.4161/cbt.21353 (2012).
72. Chitcholtan, K., Asselin, E., Parent, S., Sykes, P. H. & Evans, J. J. Differences in growth properties of endometrial cancer in three dimensional (3D) culture and 2D cell monolayer. *Experimental Cell Research* **319**, 75-87, doi:http://dx.doi.org/10.1016/j.yexcr.2012.09.012 (2013).
73. Syed, D. N. *et al.* Fisetin inhibits human melanoma cell growth through direct binding to p70S6K and mTOR: findings from 3-D melanoma skin equivalents and computational modeling. *Biochemical pharmacology* **89**, 349-360, doi:10.1016/j.bcp.2014.03.007 (2014).
74. Luca, A. C. *et al.* Impact of the 3D Microenvironment on Phenotype, Gene Expression, and EGFR Inhibition of Colorectal Cancer Cell Lines. *PLOS ONE* **8**, e59689, doi:10.1371/journal.pone.0059689 (2013).
75. Ma, Y. *et al.* Anticancer Chemotherapy-Induced Intratumoral Recruitment and Differentiation of Antigen-Presenting Cells. *Immunity* **38**, 729-741, doi:http://dx.doi.org/10.1016/j.immuni.2013.03.003 (2013).
76. Zhao, X. W. *et al.* CD47–signal regulatory protein-α (SIRPα) interactions form a barrier for antibody-mediated tumor cell destruction. *Proceedings of the National Academy of Sciences* **108**, 18342-18347, doi:10.1073/pnas.1106550108 (2011).
77. Vasaturo, A. *et al.* T-cell Landscape in a Primary Melanoma Predicts the Survival of Patients with Metastatic Disease after Their Treatment with Dendritic Cell Vaccines. *Cancer Research* **76**, 3496 (2016).

CHAPTER 7

Nederlandse samenvatting
Riassunto in italiano

Nederlandse samenvatting

Onze afweer bestaat uit twee verschillende onderdelen: Het aangeboren immuunsysteem en het adaptieve immuunsysteem. Deze systemen zijn verbonden door het functioneren van antigen presenterende cellen (APCs). In het aangeboren immuunsysteem tasten APCs hun directe omgeving af voor pathogenen of, in de context van kanker, maligne cellen. Wanneer bepaalde signalen van dreiging herkent worden, nemen APCs tumormateriaal op via fagocytose. Vervolgens, in het adaptieve systeem, activeren APCs andere immuuncellen (T lymfocyten), resulterend in langdurige bescherming tegen kankercellen. De dendritische cel (DC) staat bekend als een professionele APC en is, in de context van kanker, centraal voor de herkenning en verwijdering van tumormateriaal. Succes van een anti-tumor respons hangt logischerwijs samen DC functionaliteit. Wanneer activiteit van DCs wordt verzwakt leidt dit tot immuun tolerantie voor kankercellen, terwijl functionele DCs T lymfocyten kunnen instrueren om kankercellen onschadelijk te maken.

Tumorprogressie gaat vaak gepaard met verscheidene mechanismes die het immuunsysteem onderdrukken waardoor de tumor detectie en destructie voorkomt. Zodoende vormt zich een tumor micro-omgeving (TME, uit het Engels: tumor microenvironment) die immunologisch onderdrukt wordt en waarin verschillende immuuncellen, waaronder DCs, verzwakt zijn. In de TME interfereren kankercellen direct met DC functie waardoor expressie van specifieke DC markers wordt gemoduleerd en secretie van ontstekings moleculen wordt verlaagd. Daarnaast beïnvloed de tumor ook de werking van gezonde cellen in het omliggende weefsel. Dit leidt tot een omgeving die tumorprogressie en metastase bevordert terwijl een mogelijke immuun respons onderdrukt wordt.

Het doel van anti-kanker behandelingen is om de tumor te vernietigen. Om dit doel te bereiken zal het onderdrukte immuunsysteem vrij gemaakt moeten worden. Dit kan enerzijds via vernietiging van de kankercellen (met conventionele chemotherapie) of door immunologische remmen los te laten (immuuntherapie).

Het eerste doel van dit proefschrift was het verkrijgen van meer inzicht op het effect van immuun onderdrukking op humane DCs; en op twee verschillende kanker therapieën die, in potentie, DC functie zouden kunnen herstellen.

In dit proefschrift demonstreren we dat effectiviteit van chemotherapie gedeeltelijk afhankelijk is van ons immuunsysteem. Veel onderzoek is verricht naar moleculaire parameters die gunstig zijn voor chemotherapie geïnduceerde immunogene celdood (ICD, uit het Engels: immunogenic cell death). Niettemin is er weinig bekend over immuuncellen die tumorcellen herkennen die ICD ondergaan. Sterker

nog, de rol van humane circulerende DC subsets, zoals CD1c$^+$ en CD16$^+$ myeloide (mDCs) en plasmacytoide (pDCs) DCs, is in de context van ICD nooit bestudeerd. In Hoofdstuk 2 belichten we het unieke vermogen van humane CD1c$^+$ DCs om anti-tumor reacties op te wekken na inductie van ICD met platinum drugs. We stelden vast dat behandeling van verschillende tumorcellijnen met een klinisch relevante dosis van oxaliplatin (OXP) of cisplatin (CDDP) celdood veroorzaakt die consistent is met ICD. Deze waarneming bevestigt het vermogen van OXP om ICD op tumorcellen van verschillende afkomst te bewerkstellingen en voegt CDDP toe aan de lijst van ICD drugs. Behandeling van kankercellen met platinum drugs brengt calreticulin (CRT) tot expressie. Blootstelling van CRT zorgde voor fagocytose van tumorcellen door humane DC subsets. Opvallend was dat opname van tumormateriaal door DCs niet stopte na blokkade van de CRT receptor CD91. Deze waarneming suggereert dat naast CD91 ook andere receptoren betrokken zijn in CRT interactie. Daarnaast demonstreerden we dat detectie van de ICD signalen (HSPs, ATP and HMGB1) bijdragen aan mDC en pDC maturatie. Ten slotte hebben we vastgesteld dat, hoewel alle DC subsets matureren na contact met platinum behandelde tumorcellen, alleen CD1c$^+$ DCs effectief T-cel vermenigvuldiging stimuleren. Deze nieuwe bevindingen suggereren een specialisatie van specifieke humane DC subsets in reactie op ICD door chemotherapie.

De interactie tussen tumorcellen en DCs interfereert met DC functie. In Hoofdstuk 3 resulteerde celkweek van DCs met tumorcellen in een verminderde expressie van co-stimulatoire moleculen (CD80, CD 86) en het major histocompatibility complex (MHC) I en II. Dit ging gepaard met een verminderde secretie van het pro-inflammatoire cytokine TNF-α en verhoogde secretie van het anti-inflammatoire cytokine IL-10. Deze veranderingen leidden uiteindelijk tot een verzwakte inductie van T-cel proliferatie door DCs.

Blokkade van de remmende CD47/SIRPα signaaltransductie heeft therapeutische effectiviteit in verschillende pre-klinische tumormodellen. Dit voordelige effect hangt af van het vermogen van APCs om tumormateriaal op te nemen en het adaptieve immuunsysteem te activeren. Fagocytose wordt gereguleerd door een balans van tussen pro- en anti-fagocytose signalen van defecte cellen. Data laat zien dat het dominante ''eat me'' signaal CRT wordt tegengewerkt door het "don't eat me" signaal van CD47. In Hoofdstuk 3 beschrijven we dat blokkering van CD47 zorgt voor een verhoogde opname van tumormateriaal door humane CD1c$^+$ DCs. De opname van tumorfragmenten induceerde DC activiteit en ging immunosupressie tegen. Daarnaast hebben *in vivo* studies gedemonstreerd dat blokkade van CD47 in combinatie met immunogene stimuli leidt tot een verbeterde anti-tumor respons. Hoewel in onze studie de combinatie van platinum behandeling met anti-CD47 antilichamen het fagocyterende vermogen van DCs niet veranderde, observeerden

we wel een verhoging van de co-stimulatoire marker CD86. De waarnemingen in hoofdstuk 3 vergroten onze kennis van de rol van DCs in de context van immuun onderdrukking door tumoren, en geven een rationaal voor verder onderzoek naar combinatie tussen chemo- en immunotherapie.

DC activiteit wordt beïnvloedt door een complex proces waarin twee factoren een belangrijke rol spelen; cel-cel contacten en de celbiologische context waarin de DCs zich bevinden. Gezien deze complexiteit moeilijk te vangen is in conventionele 2D modellen, hebben we een innovatief 3D huidmodel ontwikkeld om immuniteit in melanoom te bestuderen.

Hoofdstuk 4 omschrijft de ontwikkeling van een 3D organotypisch model van de humane melanoom om interacties tussen DCs tumorcellen in een 3D structuur te bestuderen. De huid wordt gekarakteriseerd door een moleculaire compositie, een rigide organisatie en aanwezigheid van fysieke barrière, welke moeilijk na te bootsen in een collageen matrix. Het gebruik van dermale componenten van humane herkomst zorgt voor een correcte ruimtelijke indeling en voorziet een fysieke barrière via het basale membraan waarin celmigratie en cel-cel interacties worden bevorderd. Daarnaast biedt dit model de mogelijkheid om lokaal gecontroleerd de cellulaire omgeving te moduleren, waarbij celdood tot een minimum wordt beperkt. Tevens biedt een gereconstrueerde 3D micro-omgeving een potentieel platform om migratie en invasie van kankercellen in omringend weefsel te bestuderen, de bijdrage van stromacellen in kanker progressie te analyseren en DC functie in de TME te onderzoeken. Via dit model demonstreren we dat DCs efficiënt migreren langs het extracellulaire netwerk, interactie vormen met maligne tumorcellen waardoor DCs tumormateriaal opnemen. Verder hebben we vastgesteld dat maligne en gezonde cellen hun basis functies behouden in dit huidmodel voor melanoom. Samenvattend suggereren onze waarnemingen dat het huidmelanoom model superieur is over huidige modellen en ingezet kan worden om complexe processen in de TME te bestuderen.

In het laatste decennium zijn verschillende immuuntherapieën beschikbaar gemaakt voor behandeling van verschillende tumoren, inclusief melanoom. Ondanks dat deze behandelingen therapeutisch effectiviteit hebben in een aanzienlijk deel van de patiënten, zijn er nog veel obstakels die overwonnen moeten worden. Zo zijn de huidige therapieën duur, potentieel cytotoxisch en suboptimaal. Daarom is de vraag naar biomarkers die in een vroeg stadium effectiviteit van een bepaalde immunotherapie kunnen voorspellen hoog. Het kwantificeren van immuuncellen die tumoren infiltreren is een belangrijke factor in de zoektocht naar nieuwe

biomarkers. Recent onderzoek in het veld van tumor immunologie demonstreerde dat infiltratie van immuuncellen, zoals $CD3^+$ T-lymfocyten, binnen de TME invloed hebben op de inductie van tumor specifieke immuunreactie. **Hoofstuk 5** behandelt de potentie van multispectral imaging (MSI) om accuraat immuuncel infiltraten the karakteriseren, ook in weefsel wat karakterisatie voorheen bemoeilijkte. De innovatieve MSI techniek combineert imaging met spectroscopy om kwantitatief de expressie en distributie van verschillende celtypen in de TME te bepalen. In melanoom interfereren donkere melanine pigmenten met de juiste karakterisatie van verschillende celtypes van het immuunsysteem. In dit hoofdstuk, hebben we twee methodes toegepast om T cel infiltratie te kwantificeren en stelden we vast dat gebruik van unmixing in multispectral imaging leidde tot een accurate vaststelling van infiltrerende T lymfocyten in melanoom.

Riassunto in italiano

Il sistema immunitario è l'insieme delle nostre naturali armi di difesa ed è costituito da due "armate", distinte tra loro ma strettamente interconnesse: quella del sistema immunitario innato e quella dell'adattivo. Queste due armate sono coordinate dalle cellule che presentano l'antigene (APCs, dall'inglese: antigen presenting cells). A seguito dell'insorgenza del tumore, le APCs percepiscono la minaccia e rilevano la presenza di cellule maligne. Ciò fa scattare la cattura (fagocitosi) di materiale derivante dalle cellule tumorali (antigeni tumorali) da parte delle APCs e ne stimola l'attivazione. Le APCs, così attivate, istruiscono le cellule del sistema immunitario adattivo a riconoscere il tumore. Il successo di questa azione culmina con la stimolazione di una risposta immunitaria durevole ed altamente specifica che distrugge le cellule maligne.

Grazie a queste peculiari caratteristiche, le cellule dendritiche (DCs, dall'inglese dendritic cells), un tipo specifico di APCs, sono definite le sentinelle del sistema immunitario. L'efficienza con la quale le cellule dendritiche percepiscono i segnali di pericolo e li comunicano all'armata del sistema adattivo, determina il destino della risposta anti-tumorale. Questa efficienza dipende dal loro stato di attivazione: un'attivazione parziale o difettosa delle cellule dendritiche genera uno stato di tolleranza verso le cellule maligne; al contrario, cellule dendritiche funzionali favoriscono l'eliminazione del tumore, da parte delle cellule T linfocitarie del sistema adattivo.

Tuttavia, al fine di sfuggire alla sorveglianza immunitaria e sopravvivere, le cellule tumorali si servono di strategie definite immunosoppressive, ossia che sopprimono la risposta immunitaria. Lo studio di queste strategie ha fatto luce sull'esistenza di un micro-ambiente (o habitat) tumorale, che è stato dimostrato essere il principale artefice della mancata attivazione delle cellule dendritiche. Nel micro-ambiente tumorale le cellule maligne possono, da una parte, interferire direttamente con le principali funzioni delle cellule dendritiche; dall'altra, modulare il comportamento di altre cellule sane che si trovano in prossimità. In questo modo, il tumore genera un habitat favorevole per la propria crescita ed ostile verso l'attivazione di risposte immunitarie efficaci. L'intento delle terapie oncologiche è quindi quello di distruggere le cellule tumorali (come nella chemioterapia convenzionale) ed annientare i meccanismi immunosoppressivi che impediscono un'adeguata azione anti-tumorale (attraverso l'immunoterapia).

I primi obiettivi di questa tesi sono stati quelli di studiare l'attività immunosoppressiva delle cellule tumorali a danno delle cellule dendritiche, e verificare la potenzialità di due distinte strategie anti-tumorali di rispristinarne la corretta attivazione.

L'efficacia della chemioterapia dipende, in parte, dalla presenza di un sistema immunitario funzionale. Gli agenti chemioterapici esercitano la loro azione causando la morte delle cellule tumorali, che in alcuni casi può avere caratteristiche immunogeniche (ICD, dall'inglese immunogenic cell death), ossia che stimola una risposta immunitaria. I parametri molecolari che determinano l'effetto benefico della ICD sono stati al centro di molti studi nell'ultimo decennio. Tuttavia, resta ancora da capire quali sono le principali cellule immunitarie che, a seguito del trattamento con farmaci chemioterapici, rilevano le cellule tumorali danneggiate. In particolare, il ruolo delle sentinelle del sistema immunitario – le cellule dendritiche – in questo contesto non è mai stato delineato. Nel Capitolo 2, abbiamo confrontato diverse classi di cellule dendritiche presenti nel sangue: le mieloidi, $CD1c^+$ DCs e $CD16^+$ DCs, e le plasmacitoidi, pDCs; evidenziando la capacità unica delle $CD1c^+$ DCs di mediare una risposta immunitaria anti-tumorale, a seguito dell'induzione di ICD. Abbiamo riportato che, il trattamento di diverse linee cellulari tumorali umane, con dosi clinicamente rilevanti di agenti chemioterapici a base di platino, quali l'oxaliplatino (OXP) o il cisplatino (CDDP), causa una forma di morte cellulare compatibile con ICD. Le cellule tumorali che subiscono ICD espongono sulla loro superficie la molecola calreticulina (CRT), che funge da segnale "eat me" (trad. "mangiami") riconosciuto dalle cellule immunitarie. La presenza della CRT facilita la cattura delle cellule tumorali da parte delle cellule dendritiche, come confermato dall'utilizzo di peptidi bloccanti che interferiscono con questa interazione. Abbiamo inoltre dimostrato che, i segnali rilasciati dalle cellule tumorali in risposta alla ICD (HSP, ATP e HMGB1) contribuiscono alla maturazione delle cellule dendritiche. Nonostante l'avvenuta maturazione di tutte le classi di cellule dendritiche osservate nello studio, solo le $CD1c^+$ DCs sono in grado di stimolare la proliferazione delle cellule T linfocitarie. Questi nuovi risultati suggeriscono una specializzazione funzionale delle diverse classi di cellule dendritiche, in risposta al trattamento chemioterapico che causa ICD.

L'interazione tra le cellule tumorali e le cellule dendritiche ha un effetto drammatico sull'attivazione e sulla funzionalità delle sentinelle del sistema immunitario. Come descritto nel Capitolo 3, la presenza di cellule tumorali causa una diminuzione dell'espressione di marcatori di superficie, quali le molecole co-stimolatorie (CD80, CD86) ed il complesso maggiore di istocompatibilità (MHC, dall'inglese: major histocompatibility complex). Questa modulazione è accompagnata da una ridotta secrezione della citochina pro-infiammatoria TNF-α, e dall'aumento della produzione della citochina anti-infiammatoria IL-10. Il risultato di tali cambiamenti è un'alterazione nella capacità delle cellule dendritiche di stimolare la proliferazione delle cellule T linfocitarie.

Il blocco della via di segnalazione inibitoria mediata dalla proteina di membrana CD47 ha mostrato efficacia terapeutica in vari modelli murini di tumori maligni. Il vantaggio di questa strategia si basa sulla possibilità di ripristinare la cattura (fagocitosi), da parte delle cellule dendritiche, di materiale derivante dalle cellule maligne e stimolare così l'immunità adattativa. La fagocitosi è regolata dal bilanciamento tra segnali pro-fagocitici ed anti-fagocitici, forniti dalle cellule bersaglio. Sulle cellule tumorali, il segnale "eat me" (trad. "mangiami"), generato dalla molecola CRT (descritta nel capitolo 2), è controbilanciato dal segnale "don't eat me" (trad. "non mangiarmi"), fornito dalla molecola CD47.

Nel capitolo 3 abbiamo riportato che il blocco del segnale "don't eat me", CD47, attraverso l'utilizzo di specifici anticorpi monoclonali, aumenta la cattura di antigeni tumorali da parte delle cellule dendritiche, $CD1c^+$ DCs. Il potenziamento della fagocitosi stimola a sua volta la maturazione delle cellule dendritiche e contrasta l'immunosoppressione provocata dal tumore. Studi su modelli animali hanno dimostrato che l'effetto del blocco del segnale "don't eat me", CD47, può essere ulteriormente potenziato dal trattamento chemioterapico, che induce morte tumorale ed è accompagnato dall'espressione del segnale "eat me", CRT. La combinazione di queste due strategie anti-tumorali non ha mostrato un aumento della fagocitosi da parte delle $CD1c^+$ DCs; tuttavia, abbiamo riportato un aumento dell'espressione del marcatore di maturazione, CD86. Non solo queste osservazioni ampliano le nostre conoscenze sul ruolo delle cellule dendritiche nel contesto dell'immunosoppressione mediata dal tumore; ma forniscono anche una base razionale per approfondire lo studio della cooperazione tra la chemioterapia convenzionale e le nuove strategie oncologiche basate sull'immunoterapia.

In questa tesi abbiamo sottolineato più volte il concetto che, il contesto biologico del micro-ambiente tumorale e la comunicazione tra le cellule, sono determinanti chiave del processo che controlla l'attivazione della risposta anti-tumorale. A causa della mancanza di complessità fisiologica che caratterizza le colture cellulari in monostrato bi-dimensionale (2D), un'altra parte di questo lavoro è stata dedicata ad esplorare nuove tecniche, che contribuiranno alla nostra comprensione della complessità dei tessuti in vivo.

Il Capitolo 4 descrive lo sviluppo di un modello tri-dimensionale (3D) di tumore della pelle: il melanoma cutaneo. Questo modello permette di osservare e studiare la comunicazione tra cellule maligne e cellule sane, in un micro-ambiente tumorale molto simile al tessuto umano.

La pelle è caratterizzata da una composizione molecolare definita e dalla presenza di interfacce fisiche, che sono difficili da riprodurre fedelmente utilizzando

matrici di collagene. L'utilizzo di una componente dermica di derivazione umana fornisce lo spazio e l'orientamento corretto. Inoltre, la membrana basale agisce come una barriera fisica che favorisce o limita la motilità e l'interazione cellulare. Un ulteriore vantaggio di questo modello di melanoma cutaneo *in vitro* è dato dalla possibilità di modulare l'ambiente cellulare locale, in modo controllabile e riproducibile, titolando quantità e tipologie cellulari, e garantendo nel contempo la sopravvivenza di tutti i tipi di cellule coinvolte. Questo modello rappresenta una piattaforma sulla quale studiare la migrazione e l'invasione delle cellule tumorali nei tessuti circostanti, il contributo di altre cellule sane nello sviluppo del tumore, nonché indagare la regolazione delle proprietà funzionali delle cellule dendritiche all'interno del micro-ambiente tumorale. A questo proposito, abbiamo osservato che le cellule dendritiche, dopo aver migrato lungo il reticolo extracellulare, interagiscono con le cellule maligne e le catturano. Ciò indica che il nostro modello 3D di melanoma cutaneo può essere sfruttato per studiare nel dettaglio le intricate dinamiche cellulari del micro-ambiente tumorale, ed offre molteplici vantaggi rispetto agli approcci convenzionali di culture 2D monostrato, che mancano della complessità fisiologica tipica dei tessuti umani.

Nell'ultimo decennio, le strategie immunoterapiche hanno trovato applicazione per il trattamento di diverse forme tumorali, tra cui il melanoma cutaneo. Nonostante il beneficio terapeutico osservato in molti pazienti, alcune sfide restano ancora da affrontare. Queste sono associate a costi elevati, ad una potenziale tossicità e al rischio di una mancata risposta terapeutica. Pertanto, vi è un urgente bisogno di identificare biomarcatori precoci che possano aiutare a predire l'efficacia della terapia. Un aspetto fondamentale in tal senso è la quantificazione delle cellule del sistema immunitario che infiltrano i tumori. I recenti progressi nel campo della immunologia oncologica hanno dimostrato che l'infiltrazione di cellule immunitarie, come le cellule T linfocitarie, all'interno del micro-ambiente tumorale può influenzare la stimolazione di specifiche risposte immunitarie anti-tumorali. Il Capitolo 5 mette in evidenza il vantaggio della diagnostica per immagini multispettrali (MSI, dall'inglese: multispectral imaging), per valutare con precisione gli infiltrati cellulari in tessuti notoriamente difficili, come il melanoma pigmentato. La tecnica innovativa MSI combina l'imaging con la spettroscopia, al fine di ottenere informazioni quantitative e qualitative accurate, circa la distribuzione di diversi tipi di cellule all'interno del micro-ambiente tumorale. Il melanoma cutaneo è spesso caratterizzato dalla presenza di pigmenti scuri di melanina che possono oscurare la presenza di cellule immunitarie o falsarne la classificazione, in entrambi i casi ostacolando l'analisi e la quantificazione della composizione cellulare del tessuto. In questo capitolo, abbiamo confrontato due diverse metodologie di quantificazione delle cellule T linfocitarie

nel melanoma, la "classica" diagnostica per immagini e l'innovativa tecnica MSI. LE nostre osservazioni hanno dimostrato che, il principio di separazione degli spettri di un'immagine, sul quale si basa la tecnica MSI, risolve le difficoltà legate all'analisi classica e permette in tal modo un'enumerazione estremamente accurata della componente T linfocitaria che infiltra il melanoma.

CHAPTER 8

Acknowledgments

Curriculum vitae

List of publications

List of abbreviations

Acknowledgments

And as we are coming to an end, I would like to dedicate the epilogue of this book to all the people I met along the way, and who have -directly or indirectly- contributed to make this journey possible.

First of all, my enormous gratitude goes to my promotors and co-promotors. Dear **Carl**, a long time has passed since I was intimidated every time I had a meeting with you! I remember our first skype conference to discuss the project. While waiting for your call, I spent a good half an hour in front of the computer to practice my most professional attitude! I was immediately fascinated by your charisma, your openness and your ability to see the thousands facets of science. I appreciated the way you conducted me along the vicissitudes of my PhD, the freedom you gave me to shape my project, but also your reliable guidance when I felt disoriented and my motivation was at risk. Thanks Carl, for being an example as a researcher and as a supervisor and for your ability to care for "your" people also beyond work. Many times, I had the feeling you exactly knew what was going through my mind, without the need of me speaking it out loud. I still wonder whether you have spies in the lab that keep you informed about us all!

Dear **Jolanda**, it has been great working with you. Thanks for your precious advices and suggestions over many aspects of this –all but easy- project. You are a beautiful example of how hard work and positive attitude can take us anywhere we want. Congratulations on your last success with including the DC vaccination in the basic health care insurance. I wish you all the best for your career!

Dear **Stanley**, my daily scientific supporter! Things were not always easy, but looking back I am grateful for your presence and supervision: I have learnt so much from you! This work would have certainly not been possible without your help! You were always understanding and reachable, especially during the last hectic period of completion of this thesis. Thanks for finding time for me at impossible hours and during weekends! You have a great scientific mind and I admire how you manage to deal with stressful situations in the calmest way possible! I wish you all the best in your career, as well as in your personal life, and I really hope we will stay in touch!

Dear **Ellen**, you introduced me into the wonderful world of three-dimensional cell culture. I appreciated all the tips & tricks and your valuable suggestions, both on the experimental part and during the finalization of this thesis. I hope our collaboration will soon become fruitful and we can toast over a great publication together! Dear

Prof. Schalkwijk, dear Joost, thank you for welcoming me at the Department of Dermatology and for believing in this project. Special thanks goes to all the people of the dermatology lab who helped me out, answered my questions, shared protocols and reagents, and always welcomed me with their warmest smile! Hanna, Diana and Ivonne, dank jullie wel! Hanna, good luck with your finishing up your thesis!

I arrived in Nijmegen for the first time in February 2011, to perform a research internship as part of my master's studies. I had no clue how to pronounce the name of this town, nor how to safely cycle under pouring rain, while carrying three grocery bags. Nevertheless, at the very moment I met you, **Alessandra**, I knew that coming to Nijmegen was amongst the best decisions of my life! Dear Alessandra, what can I say more that I have not told you already?! You are my scientific muse! I really enjoyed working with you as a student. You have a contagious enthusiasm and your passion for science is admirable. You convinced me to pursue this journey, and your support and encouraging words made the difference! I am glad you are part of my thesis committee…I could not think of a best way to end this adventure! Grazie mille! Di tutto!! Congratulations on your achievements and best of luck at the lead of Cell Biology! Next to Alessandra, other people contributed to make my internship unforgettable. **Ben**, **Koen**, **Marjolein**, **Christina**, **Joost** and **Inge**...thank you all guys, for immediately making me feel part of the group! After more than five years, my calendar still reminds me every Monday that I should join the sub-group meeting at 2pm sharp!

I would like to continue this jump into memories with acknowledging all the people that actively devoted their time and energy to performing the magnificent work described in this book! :P

Irene, the "first recruit" for the 3D melanoma project. Although your time in Nijmegen was (too) short, the long days at work gave us the opportunity to get to know each other and enjoy our Dutch lives outside the lab. I had promised I would have come visit you in Trento, or anywhere else you were, but I did not stick to my words…I take this opportunity to renew the (self)invitation and hope you are still willing to walk me around!

Tijtske and **Rob**, thank you for your help and precision with cell sorting, and for always making time for those urgent experiments that "otherwise my project is screwed!". You are great!

Nienke, thanks for offering a hand with the huge experiment for the ICD paper and helping with the beautiful figures for the review and this introduction. Good luck with your project, you are doing great! No worries!

Sonja and **Kuntal**, thanks for the nice microarray data picture in the ICD manuscript! I wish you all the best in your professional and personal lives! **Gert-Jan**, I am grateful for your support with the multi-photon microscope. I seriously would have not been able to handle such a machine without your patience and professionality!

Annemiek dB, my trusted provider of cell lines! You saved my experiments multiple times when my cells did not want to behave! **Jeanette**, my utje-mate for the most part of my PhD. You helped me with protocols and new techniques, and any questions I had. Thanks for accepting (and not complaining about) the Italian flavour Angela and I gave to the utje, and for all our laughs and silly moments! **Inge**, your accuracy and dedication made it working with you an enjoyable experience. Thanks for your crucial help in many steps and good luck with the other challenging projects you are currently working on!

Mark, **Anne**, **Altuna** and **Dagmar,** thanks for all the sectioning – staining – imaging – analysing, that created some of the beautiful microscopy pictures in this thesis. Thanks Mark for having a final look at the Nederlanse samenvatting! But most of all, thanks for the fun time and for pushing me "om Nederlands te praten". Ik beloof het!

Thanks **Angela** for the time we shared at the TIL, as colleagues and friends. I learnt a lot from you and your rich microscopy experience! Most of the new techniques I approached would have been much more difficult without your help! I am glad you finally realized your dream to live as a Parisian! Good luck with everything, and enjoy yourself in the most romantic city of Europe!

Marcella! Marci, the newest recruit of the "3D army", and surely the best I could have hoped for! Over the past 9 months we have been together almost 24/7, no kidding! You got the whole "Di Blasio deal" when you moved to Nijmegen: living, working, having meetings&coffees together! Of course, it could have gone wrong… but in reality, it turned out to be "perfetto"! I have gotten to know you as I honest, superfunny, brilliant scientist, and –most importantly- a reliable friend. I will miss you, but I am sure you will achieve anything you wish and deserve in Italy!

I obviously would like to praise my fantastic students, **Laura**, **Diede** and **Inge**. It has been a pleasure working with you and sharing some of the manuscripts in this book. Having contributed, at least for a small part, to your professional development is something that really makes me proud of. Success, ladies!

I also had the pleasure to collaborate and share publications with skilled collaborators, Prof. **Han van Krieken** and Dr. **Willeke A.M. Blokx**. I would like to warmly thank you for the professionality with which you contributed to my thesis.

I now would like to spend some thankful words for the other colleagues that animated the 5th floor.

Simone, my favourite German lady! You were a naïve, fresh PhD student when I first met you. We immediately became friends. And, with the enthusiasm that characterizes PhDs in their first few months, we thought we could conquer the scientific world (and win the Noble Prize within the following five years). Well…we must say that the initial enthusiasm encountered some obstacles along the way, but we never missed the occasion to celebrate our achievements and the most important life steps. Meeting you was one of the best things this journey brought into my life! Ich habe dich lieb, bella! I wish you nothing but the best! PS: You never know!

Dear **Pauline**, **Mika** and **Ghaith**. Awesome colleagues (I know Pauline, you hate this definition!) but above all good friends! It has been great travelling with you to Mallorca, Paris, Marseille and Pescara. The moments we shared together are amongst the most beautiful memories of the past five years. Let's keep on building countless memories in the future!...Time to plan a trip to the UK?!

Dear **Arie** (and Liset), it has been a pleasure visiting you in Sanur, in Bali. What a wonderful place! You make me so jealous every time you come back to Nijmegen so relaxed and sun-tanned! You are always very cheerful, when we bump into each other in the corridors or at the coffee table...I really enjoy our short, but joyful conversations!

The TIL is known as one of the most social and party-oriented departments of the RIMLS. Indeed, no TIL'ler has never been disappointed! If I had to name all the people I have shared at least a funny moment with, I would have to list you ALL! **TIL'lers** and **ex-TIL'lers**, you are the soul of this lab and it has been amazing working, lunching, partying, laughing with you!

Bedankt! Thanks! Gracias! Danke! Grazie! 谢谢! Tak! Tack! Gràcies!
Спасибо! Dziękuję! Teşekkür ederim! Merci! !كل اركش

And then you, **Bas**! You specifically asked me to dedicate three pages of "laudatie" only to you! I hope you do not mind if, for the sake of time (mine and of the reader), I will be concise...Grazie bello! For the spark you bring into my everyday life, for the simplicity of you at my side, and for tolerating the "Italian drama" that sometimes

I simply cannot hold back! And above all, a gigantic praise for the endless evenings you spent translating my English summary into Dutch! In conclusion, I would like to cite one of your self-compliments: "Yes Bas, you are to me the brightest star in the sky"!!

A few more people had a huge role in ensuring my survival here: the **International Gang**. Simone, Niccolò, Rocìo, Antoine, Angela, Davide, Pedro (Pedrito!!), Cindy, Anchel, Vicky, Brooke, Mariam, Benny, Till, Bart, Philipp, Ganesh, Sip, Andrè, Olga, Nuria, Pedro, Pavel, Katia. And again, Dora (I love the cover of this thesis!!), Marco, Daniel, Cosimo and many others…I have discovered fascinating worlds in each and everyone of you. You made my years guys!!!

Grazie Davide, per aver condiviso con me buona parte di questo cammino. Per i tuoi consigli, la tuà genuinità e la capacità di vedere sempre il lato bello delle cose.

Un grazie speciale a tutti i miei amici di sempre, a quelli che "la distanza non ha cambiato nulla" ed ogni volta ritrovarsi é la cosa piú naturale del mondo. Grazie per le volte che mi avete chiesto di spiegarvi cosa diavolo stavo facendo e per aver condiviso le mie piccole soddisfazioni professionali, seppur da lontano. Vi voglio un mondo di bene e sono strafelice che qualcuno di voi sia riuscito ad essere qui oggi!

Concludo questo monologo, con il ringraziamento piú grande alla mia famiglia. Sicuramente, i miei fans numero uno! Dedico questo lavoro a voi, per il supporto, l'entusiasmo e la fiducia con la quale siete riusciti a riempire la distanza fisica che ci separa. Siete la mia forza ed il mio modello. Non avrei potuto desiderare di meglio!

Stefania

Curriculum vitae

Stefania Di Blasio was born on November 8th, 1985 in Pesaro (Italy). She grew up in Pescara (Italy), where she attended a science-oriented high school. Stefania continued her education at the Faculty of Medical Biotechnology of the University of l'Aquila "Università degli Studi de l'Aquila". At the end of the second year, Stefania moved to the University of Abertay Dundee (Scotland), within the framework of the EU articulation scheme for talented students, where she completed her studies and obtained her BSc degree in Biomedical Sciences in 2008. Following graduation, Stefania went back to Italy and enrolled in a master's program of the Faculty of Biological Sciences of University of Camerino "Università degli Studi di Camerino". During that time, she became passionate about immunology and moved to the Radboud University Medical Center in Nijmegen (The Netherlands), to perform a research internship at the Department of Tumor Immunology, under the supervision of Prof. Dr. Alessandra Cambi. Her research, investigating the immunomodulatory effects of Omega-3 and Omega-6, two classes of poly-unsaturated fatty acids (PUFAs), on maturation and functional activation of monocyte-derived dendritic cells, yielded the results required for the completion of her master thesis. Immediately after having obtained her MSc diploma with a *summa cum laude* in 2012, Stefania started her PhD at the Department of Tumor Immunology, in collaboration with the Department of Dermatology, of the Radboud University Medical Center in Nijmegen (The Netherlands); under the supervision of Dr. Stanleyson V. Hato, Prof. Dr. Carl G. Figdor, Prof. Dr. I. Jolanda M. de Vries and Dr. Ellen H. van den Bogaard. During her PhD, Stefania studied the cross talk between tumor cells and immune cells, and developed a novel three dimensional organotypic model of human melanoma, to explore the immunosuppressive mechanisms arising within the tumor microenvironment. Her findings are presented in this thesis. Stefania followed several courses and seminars, and supervised three undergraduate students. She obtained several travel grants to attend international conferences, where talks and poster presentations were given about her work. Moreover, she was awarded with two poster prizes at the NVVI meeting (The Netherlands, 2014) and EMIM conference (France, 2015). Stefania is currently continuing her project as a post-doctoral research fellow at the Department of Tumor Immunology, under the supervision of Prof. Dr. Carl G. Figdor and Prof. Dr. I. Jolanda M. de Vries.

List of publications

Di Blasio S, Stolk DA, de Haas N, Figdor CG, Hato SV. Tumor-dendritic cell interplay in cancer: immunogenic DAMPs and their receptors. *Submitted.* Review.

Vasaturo A[#], **Di Blasio S**[#], Verweij D, Blokx WA, van Krieken JH, de Vries IJ, Figdor CG. Multispectral imaging for highly accurate analysis of tumour-infiltrating lymphocytes in primary melanoma. Histopathology. 2016 Aug 29. (PMID:27571246)

Di Blasio S, Wortel IM, van Bladel DA, de Vries LE, Duiveman-de Boer T, Worah K, de Haas N, Buschow SI, de Vries IJ, Figdor CG, Hato SV. Human $CD1c^+$ DCs are critical cellular mediators of immune responses induced by immunogenic cell death. Oncoimmunology. 2016 Aug 3;5(8):e1192739. (PMID:27622063)

Tel J, Koornstra R, de Haas N, van Deutekom V, Westdorp H, Boudewijns S, van Erp N, **Di Blasio S**, Gerritsen W, Figdor CG, de Vries IJ, Hato SV. Preclinical exploration of combining plasmacytoid and myeloid dendritic cell vaccination with BRAF inhibition. J Transl Med. 2016 Apr 14;14:88. (PMID:27075584)

Vasaturo A[#], **Di Blasio S**[#], Peeters DG, de Koning CC, de Vries JM, Figdor CG, Hato SV. Clinical Implications of Co-Inhibitory Molecule Expression in the Tumor Microenvironment for DC Vaccination: A Game of Stop and Go. Front Immunol. 2013 Dec 3;4:417. Review. (PMID:24348481)

[#] *Equal contribution*

List of abbreviations

2D		Two-dimensional
3D		Three-dimensional
λ		Lambda (indicating wavelength)
Ab		Antibody
Ag		Antigen
APC		Antigen Presenting Cell
ATP		Adenosine triphosphate
BM		Basal membrane
CD		Cluster of differentiation
CDDP		cis-diamino-dichloro-platinum (II), Cisplatin
CFSE		5(6)-Carboxyfluorescein diacetate N-succinimidyl ester
CRT		Calreticulin
CTC		Circulating tumor cell
CTLA-4		Cytotoxic T lymphocyte-associated antigen-4
DAB		3,3'-Diaminobenzidine
DAMP		Damage associated molecular patterns
DC		Dendritic Cell
	inflDC	Inflammatory Dendritic Cell
	mDC	Myeloid Dendritic Cell
	moDC	Monocyte-derived Dendritic Cell
	moLC	Monocyte-derived Langerhans cell
	pDC	Plasmacytoid Dendritic Cell
DED		De-epidermised dermis
ECM		Extracellular matrix
ELISA		Enzyme-linked immunosorbent assay
ER		Endoplasmic reticulum
Fb		Fibroblast
FFPE		formalin-fixed, paraffin-embedded
GFP		Green fluorescent protein
GM-CFS		Granulocyte-macrophage colony-stimulating factor
GPCR		G-protein coupled receptor
H&E		haematoxylin and eosin
HLA		Human leukocyte antigen
HMGB1		High Mobility Group Box 1
HSE		Human skin equivalent
HSP		Heat shock protein
IAP		Integrin-associated protein

ICD	Immunogenic Cell Death
IFN	Type I interferon
Ig	Immunoglobulin
IHC	Immunohistochemistry
IL	Interleukin
IR	Ionizing radiation
ITIM	Immunoreceptor-based inhibition motif
KC	Keratinocyte
LC	Langerhans cell
MDSC	Myeloid-derived suppressor cell
MHC	Major Histocompatibility Complex
MLR	Mixed Lymphocyte Reaction
MM	Metastatic melanomas
MMP	Matrix metalloprotease
moMf	Monocyte-derived macrophage
MSI	Multispectral imaging
NK cell	Natural killer cell
OXP	Oxaliplatin
OS	Overall survival
PBL	Peripheral Blood Leukocyte
PBMC	Peripheral Blood Mononuclear Cell
PD-1	Programmed cell death-1
PD-L1	PD-ligand 1
PD-L2	PD-ligand 2
PRR	Pattern recognition receptors
P2R	Purinergic class 2 receptor
RGP	Radial growth phase
RBC	Red blood cell
SHG	Second harmonic generation
SHP	SRC homology 2 domain-containing phosphatase
SIRPα	Signal regulatory protein alpha
SR-A	Scavenger receptor class-A
SREC-I	Scavenger receptor expressed by endothelial cell-1
STAT	Signal transducer and activator of transcription
TAA	Tumor-associated antigens
TAM	Tumor-associated macrophage
TCR	T cell receptor
TGF	Transforming growth factor
Th	T helper

TIL	Tumor infiltrating lymphocyte
TLR	Toll-Like Receptor
TME	Tumor microenvironment
TNFα	Tumor necrosis factor alpha
TSP-1	Thrombospondin-1
Treg	Regulatory T cell
VEGF	Vascular endothelial growth factor
VGP	Vertical growth phase